# BRAIN-REGION-SPECIFIC CONTRIBUTIONS OF FOXP1 TO AUTISM AND INTELLECTUAL DISABILITY PHENOTYPES

Daniel John Araujo

APPROVED BY SUPERVISORY COMMITTEE:

Amelia J. Eisch, Ph.D. (Chair)

_____

Genevieve Konopka, Ph.D. (Mentor)

_____

Craig M. Powell, M.D., Ph.D.

_____

Lenora J. Volk, Ph.D.

_____

Jiang Wu, Ph.D.

_____

## DEDICATION

I would like to thank my thesis advisor Dr. Genevieve Konopka who has always pushed me to strive for excellence in my work. It's been an honor to study neuroscience under her supervision and she will serve as an example for the rest of my scientific career. I would like to thank my wife Sarah Teresita Vega for her unwavering love and patience. Sarah has been my best friend for the past nine years and her encouragement has allowed me to face any challenge with grit. I also thank my thesis committee members for all of their suggestions on how to improve my research. I would like to thank Dr. Timothy Raabe and Dr. Nancy Street for their continuous support of both my undergraduate and graduate career. Finally, I dedicate this dissertation to my grandparents George Cuellar Araujo and Margarita Salinas Araujo who raised my two siblings and me. Any success I've had in life belongs to them.

# BRAIN-REGION-SPECIFIC CONTRIBUTIONS OF FOXP1 TO AUTISM AND INTELLECTUAL DISABILITY PHENOTYPES

By

DANIEL JOHN ARAUJO, B.S.

DISSERTATION

Presented to the Faculty of the Graduate School of Biomedical Sciences at

The University of Texas Southwestern Medical Center

In Partial Fulfillment of the Requirements for the Degree of

DOCTOR OF PHILOSOPHY

The University of Texas Southwestern Medical Center

Dallas, Texas

August 11, 2017

BRAIN-REGION-SPECIFIC CONTRIBUTIONS OF FOXP1 TO AUTISM AND INTELLECTUAL DISABILITY PHENOTPES

Publication No. _____

Daniel John Araujo, B.S.

The University of Texas Southwestern Medical Center, 2017

Supervising Professor: Genevieve Konopka, Ph.D.

## ABSTRACT

Mutations and deletions in the transcription factor *FOXP1* are causative for severe forms of autism spectrum disorder (ASD) that are often comorbid with intellectual disability (ID). FOXP1 is enriched throughout the brain, with strong expression in the pyramidal neurons of the neocortex, the CA1/CA2 subfields of the hippocampus, and the medium spiny neurons of the striatum. Understanding the role that FOXP1 plays within these brain regions could allow for management of ASD and ID symptoms. This

doctoral dissertation leverages multidisciplinary techniques and *Foxp1* mutant mouse models to ascertain the role of Foxp1 in the brain and its contribution to specific ASD- and ID-relevant phenotypes. In the first chapter of this dissertation, I review the literature on the characteristics, demographics, and shared genetic underpinnings of ASD and ID and I review the work linking FOXP1 to these disorders. Afterwards, I describe the regional transcriptome regulated by Foxp1 within the brain and I correlate alterations in the gene expression profile of the striatum with deficits in communication (**Chapter 2**). Briefly, I utilized RNA-sequencing performed on *Foxp1* heterozygous knockout animals to uncover the genes regulated by Foxp1 within the neocortex, hippocampus, and striatum. I also recorded the early postnatal ultrasonic vocalizations (USVs) of these animals and I was able to correlate changes in the properties of striatal medium spiny neurons with deficits in USV production. Next, I move onto using a *Foxp1* conditional knockout ($Foxp1^{cKO}$) mouse model to ascertain the contributions of Foxp1 in the neocortex and the hippocampus to ASD and ID-related behaviors (**Chapter 3**). In brief, I show that total loss of *Foxp1* in the pyramidal neurons of the neocortex and the CA1/2 hippocampal subfields results in social communication deficits as well as hyperactivity and anxiety-like behaviors. I also show that $Foxp1^{cKO}$ mice display gross impairments in hippocampal-based spatial-learning tasks and I correlate these deficits with alterations in the expression of genes involved in hippocampal physiology and synaptic plasticity. In my final chapter (**Chapter 4**), I consider the implications that these data have on our understanding of the role that Foxp1 plays within the brain and I suggest research strategies to answer the new questions that my findings have

generated. I also discuss the implications that this research has on our understanding of ASD and ID pathophysiology in general and I recommend future directions for work focused on managing these disorders.

## TABLE OF CONTENTS

## PRIOR PUBLICATIONS

**Research**

Usui, N., **Araujo, D.J.**, Kulkarni, A., Ellegood, J., Co, M., Ellegood, J., Harper, M., Torimui, K., Lerch, J.P., Konopka, G. Foxp1 regulation of neonatal vocal and motor behaviors via cortical development. ***Submitted to Genes and Development*** **for peer-review.**

**Araujo, D.J.**, Toriumi, K., Escamilla, C.O., Kulkarni, A., Anderson, A.G., Harper, M., Usui, N., Ellegood, J., Lerch, J.P., Birnbaum, S.G., Tucker, H.O., Powell, C.M., and Konopka, G. Foxp1 in forebrain pyramidal neurons controls gene expression required for spatial learning and synaptic plasticity. ***Re-submitted to The Journal of Neuroscience*** **for peer-review.**

**Araujo, D.J.***, Anderson, A.G.*, Berto, S., Runnels, W., Harper, M., Ammanuel, S., Rieger, M.A., Huang, H.C., Rajkovich, K., Loerwald, K.W., Dekker, J.D., Tucker, H.O., Dougherty, J.D., Gibson, J.R., Konopka, G. FoxP1 orchestration of ASD-relevant signaling pathways in the striatum. **Genes and Development** 29, 2081-2096 (2015). *These authors contributed equally to this work.

Macrini, T.E., Coan, H.B., Levine, S.M., Lerma, T., Saks, C.D., **Araujo, D.J.**, Bredbenner, T.L., Coutts, R.D., Nicolella, D.P., Havill, L.M. Reproductive status and sex show strong effects on knee OA in a baboon model. **Osteoarthritis and Cartilage** 21, 839-848 (2013).

**Opinion/Resource**

**Araujo, D.J.**, Nevarez, Andres. The Grassroots Movement to Diversify STEM. **SACNAS News** 18, No.1, 21-23 (2015).

## LIST OF FIGURES

## LIST OF TABLES

## LIST OF DEFINITIONS

**Autism Spectrum Disorder:** a group of heterogeneous neurodevelopmental disorders characterized by social communication deficits and repetitive/stereotypic behaviors and/or interests

**Chromatin Immunoprecipitation Followed by DNA-Sequencing:** a technique combining chromatin-based immunoprecipitation and DNA-sequencing that is used to identify direct DNA targets of transcription factors and other DNA-binding proteins

**Gene Ontology Enrichment Analysis:** a bioinformatics technique used to determine statistically-enriched categories of gene products within ChIP-seq and RNA-seq datasets

**Intellectual Disability:** a neurodevelopmental disorder characterized by below average IQs and impairments in intellectual reasoning and skills necessary for everyday functioning

**Long-term Potentiation:** a process by which excitatory synapses are strengthened in response to stimulation

**RNA-sequencing:** a technique used to identify differentially expressed RNA transcripts within certain cell and tissue populations

**Ultrasonic Vocalizations:** isolation calls produced by early postnatal rodent pups in response to separation from their mother and/or their nest

**Weighted Gene Co-expression Network Analysis:** a bioinformatics technique performed on gene expression (RNA-sequencing) datasets to identify networks of genes whose expression changes are correlated with one another

## LIST OF ABBREVIATIONS

**ADHD:** attention-deficit hyperactivity disorder

**ASD:** autism spectrum disorder

**ChIP-seq:** chromatin immunoprecipitation followed by DNA sequencing

**CTX:** neocortex

**D1+:** Drd1a receptor positive

**D2+:** Drd2 receptor positive

**DEG:** differentially expressed gene

**DVD:** developmental verbal dyspraxia

**FKH:** forkhead domain

**FMRP:** Fragile-X mental retardation protein

**FXS:** Fragile-X syndrome

**GMD:** gross motor delay

**GO:** gene ontology

**HIP:** hippocampus

**hNP:** human neural progenitor

**ID:** intellectual disability

**LTP:** long-term potentiation

**MSN:** medium spiny neuron

**MWM:** Morris water maze

**NDD:** neurodevelopmental disorder

**NGS:** next generation sequencing

**OCD:** obsessive-compulsive disorder

**qRT-PCR/qPCR:** quantitative reverse transcriptase PCR

**RNA-seq:** RNA-sequencing

**SFARI:** Simmons Foundation Autism Research Initiative

**SLI:** severe language impairment

**STR:** striatum

**USV:** ultrasonic vocalization

**WES:** whole-exome sequencing

**WGCNA:** weighted gene co-expression network analysis

# CHAPTER ONE:

# INTRODUCTION

## OVERVIEW

Autism spectrum disorder denotes a set of neurodevelopmental disorders, which hinder the quality of life for both affected individuals and their families. Autism is often comorbid with intellectual disability, another illness that can negatively impact the functions necessary for daily life. Susceptibility to these two conditions is in large part driven by common genetic factors. These shared risk genes are often expressed during early brain development and their expression patterns are tightly controlled by transcription factors. In order to understand the overarching mechanisms underlying autism and intellectual disability, the Konopka laboratory has concentrated on studying transcription factors with which the two disorders are genetically associated. Concentrating on transcription factors could allow for novel insights into the underlying disease mechanisms of autism and intellectual disability and open the door for new therapeutics for the two conditions. FOXP1 is a transcription factor that is widely expressed throughout the mouse and human brain and heterozygous perturbations to the coding region of *FOXP1* are causative for severe forms of autism, which are often comorbid with intellectual disability. This dissertation focuses on addressing two main questions: 1) what are the gene targets of FOXP1 in both the rodent brain and human neurons? and 2) what, if any, are the brain-region-specific contributions of FOXP1 to autism- and intellectual disability-related phenotypes? The first part of my dissertation details my efforts at understanding the gene

targets of Foxp1 within distinct regions of the brain by studying a patient-relevant heterozygous *Foxp1* knockout mouse model **(Chapter 2)**. The second part of my dissertation describes my work on characterizing a conditional homozygous *Foxp1* knockout mouse to identify the contributions of neocortical and hippocampal Foxp1 to specific autism and intellectual disability phenotypes **(Chapter 3)**. Finally, the third part of my dissertation reviews the implications of this research and suggests future experiments to answer newly arisen questions on the role of FOXP1 in the brain **(Chapter 4)**. In order to have a complete understanding of the results presented in this dissertation, this introductory chapter will provide background information on a broad range of topics. Specifically, this introduction will provide background on autism spectrum disorder and intellectual disability, the shared mechanisms between these disorders, and the evidence supporting the involvement of FOXP1 in their pathogenesis.

## AUTISM SPECTRUM DISORDER AND INTELLECTUAL DISABILITY

### Clinical Features of Autism Spectrum Disorder

The term “autism” (derived from the Greek word αὐτός (“self”)) was coined by the psychiatrist Paul Eugen Bleuler to designate the emotionally withdrawn and detached behaviors he noticed in schizophrenic adults (Bleuler, 1912). Afterwards, Hans Asperger borrowed the term to define a new condition in children, with features distinct from those observed by Bleuler, that he termed “autistic psychopathy” (now called “Asperger’s Syndrome”) (Asperger, 1944). However, our modern usage of the word comes from the work of Leo Kanner who reported on what he called “infantile autism” in a small cohort of

children (Kanner, 1943). Similar to Asperger, Kanner described these children as having a condition that "[differed] in many respects from all other known instances of childhood schizophrenia" (Kanner, 1943). Kanner suggested what made the children unique was that they had "shown their extreme aloneness from the very beginning of life" (Kanner, 1943). Moreover, Kanner went on to say, "We must then assume that these children have come into the world with [an] innate inability to form the usual, biologically provided affective contact with people […]" (Kanner, 1943). Kanner's hypothesis that infantile autism was "innate" would eventually lay the groundwork for what defines modern autism research: the search for neurobiological underpinnings that can be leveraged to predict and treat occurrences of the disorder.

Today, autism is no longer thought to be one disorder. Indeed, the Diagnostic and Statistical Manual of Mental Disorders, 5$^{th}$ Edition (DSM-5), currently uses the term "autism spectrum disorder (ASD)" to denote a collection of heterogeneous neurodevelopmental disorders (NDDs) that are characterized by two core symptoms: 1) disruptions in social communication and 2) repetitive/restricted behaviors and interests (American Psychiatry Association, 2013). This definition is an umbrella term and it encompasses several distinct disorders including autism, Asperger's syndrome, pervasive developmental disorder not otherwise specified, and childhood disintegrative disorder (American Psychiatry Association, 2013). Social communication deficits in ASD entail but are not limited to loss of eye contact, improper body language, and muted facial expressions (Fakhoury, 2015; Park et al., 2016). Repetitive/restricted behaviors and

interests vary wildly but can include spinning, finger tapping, self-injury, and preoccupation with certain objects and routines (Leekam et al., 2011; Park et al., 2016).

The Autism and Developmental Disabilities Monitoring (ADDM) Network currently estimates that the incidence of ASD in children 8 years of age is 1 in 68 in the United States (Christensen et al., 2016). ASD is more prevalent in males than females (at 4:1) with symptom type but not severity also being sexually dimorphic (e.g., males exhibit more externalized symptoms than females) (Werling and Geschwind, 2013). The increased prevalence of ASD in males compared to females suggests that unique biological mechanisms conferring risk to males and/or protection to females are at play (Robinson et al., 2013; Werling and Geschwind, 2013). The prevalence of ASD has risen in recent decades but this rise has been largely explained by improved diagnostic criteria and increased public awareness for the condition (Prior, 2003; Park et al., 2016). However, given the variety of behaviors associated with ASD, which can differ in their intensity from patient to patient, early diagnosis remains challenging. In fact, while practiced physicians are able to diagnose ASD by 2-3 years of age, the average age for diagnosis is above 5 years (Shattuck et al., 2009; Maenner et al., 2013).

Thus, the current state of ASD research presents an inherent challenge: researchers treat ASD as a single condition when trying to understand its biological architecture but as a group of conditions when assessing its clinical presentation.

**Clinical Features of Intellectual Disability**

Previously known as “mental retardation,” intellectual disability (ID) has been observed since at least the time of the Egyptian Papyrus Ebers (circa 1550 BC) (Harris, 2006). Research on ID, and neuropsychiatric conditions in general, became a feature of mainstream genetics when Fragile-X syndrome (FXS) and Down syndrome, two well-known syndromes that produce the disorder, were determined to have specific, genetic causes (Mefford et al., 2012; Vissers et al., 2016). Similar to ASD research, work on ID is currently focused on identifying liable neurobiological processes in an attempt to develop improved therapies and treatments. Lastly, as described below, the clinical presentation of ID is far more stereotypical and ascertainable than that of ASD.

There are currently two accepted sets of diagnostic criteria for ID. One set comes from the DSM-5 and it defines ID by: 1) deficits in intellectual functioning and 2) deficits in adaptive functioning (American Psychiatry Association, 2013). Deficits in intellectual functioning can affect reasoning, abstract thinking, and planning (American Psychiatry Association, 2013). Deficiencies in intellectual functioning are usually detected by an IQ score of 70 or below as well as a clinical assessment (American Psychiatry Association, 2013). Deficits in adaptive functioning can influence social skills, communication, and personal independence (at work and home) (American Psychiatry Association, 2013). Deficiencies in adaptive functioning are assessed by a variety of standardized tests as well as a clinical evaluation (American Psychiatry Association, 2013).

The other set of diagnostic criteria for ID is detailed in the definitional manual (*Intellectual Disability: Definition, Classification, and Systems of Supports* – 11$^{th}$ Edition) published by the American Association on Intellectual and Developmental Disabilities

(AAIDD). The two main criteria set forth in the AAIDD's definitional manual (impairments in intellectual functioning and impairments in adaptive behaviors) are analogous to those specified in the DSM-5 with a slightly different grouping of symptoms (American Association on Intellectual and Developmental Disabilities, 2010). The AAIDD and the DSM-5 also agree that ID is a NDD, as it manifests before 18 years of age. The average age for diagnosis with ID is 3 to 3.5 years with males being diagnosed slightly earlier than females (Bailey et al., 2009). At a ratio of 1.4:1, the prevalence of ID amongst males is only slightly higher than that seen in females (Bryson et al., 2008; Nicholas et al., 2008; Postorino et al., 2016; Vissers et al., 2016).

**Overlapping Demographics Between ASD and ID**

It has long been recognized that a considerable subset of ASD patients often present with ID (Postorino et al., 2016). However, estimates of the number of ASD cases that are comorbid for ID range widely from approximately 20% to 70% (Fombonne, 2003; Keen and Ward, 2004; Chakrabarti and Fombonne, 2005; de Bildt et al., 2005; Oliveira et al., 2007; Bolte et al., 2009; Matson and Shoemaker, 2009; Charman et al., 2011; Carlsson et al., 2013; Miller et al., 2013; Christensen et al., 2016; Postorino et al., 2016). It must be stressed that such studies are often concerned with determining the prevalence of ASD and not necessarily the co-occurrence of ID with ASD (Postorino et al., 2016). Reports on the comorbidity rates between the two disorders are also hampered by the finding that diagnosing ASD is often confounded by the presence of ID (Polyak et al., 2015). This latter observation may represent a broad trend for the re-categorization of ID

as ASD by practicing physicians (Polyak et al., 2015). Interestingly, females with ASD are at a greater risk for ID than males with ASD (Werling and Geschwind, 2013; Christensen et al., 2016). Therefore, the high prevalence of ASD in males compared to females is greatest when ID is not considered (Bryson et al., 2008; Nicholas et al., 2008; Fombonne, 2009; Werling and Geschwind, 2013; Postorino et al., 2016). Together, these observations support the notion that ASD and ID are often conflated with one another in the clinical setting.

Traits that are often comorbid with ASD and ID include hyperactivity, epilepsy, altered sleep patterns, aggression, anxiety, and abnormal sensory perception **(Figure 1.1)** (McGrother et al., 2006; Engel-Yeger et al., 2011; Ageranioti-Belanger et al., 2012; Fakhoury, 2015; Park et al., 2016). Symptoms shared by ASD and ID often vary in severity and can be more or less common within patient subsets. These are also secondary traits and therefore not necessary for diagnosing either illness. When included, secondary symptoms represent another roadblock for proper diagnosis for both disorders.

**Genetics of ASD and ID**

ASD and ID have a strong genetic component (de la Torre-Ubieta et al., 2016; Vissers et al., 2016). Estimates of the heritability of ASD range from 30 to 90% (Rosenberg et al., 2009; Hallmayer et al., 2011; Gaugler et al., 2014; Sandin et al., 2014; Chen et al., 2015; De Rubeis and Buxbaum, 2015; de la Torre-Ubieta et al., 2016; Mullins et al., 2016). Recent evidence has shown that intelligence is at least partially heritable and it has been linked to the effects of various genes (Plomin and Deary, 2015; Sniekers

et al., 2017). Still, there is a scarcity of primary studies on the heritability of ID itself performed on the scale as those focused on ASD (Reichenberg et al., 2016; Vissers et al., 2016). Nevertheless, the overlapping characteristics of ASD and ID suggest that there are genetic factors common to both disorders.

The first study to identify a genetic basis for ID came in 1943 when James Purdon Martin and Julia Bell found FXS to be X-linked (Martin and Bell, 1943). Afterwards, in 1959, Jérôme Lejeune determined that Down syndrome is produced by an additional, third copy of chromosome 21 (either in part or whole) (Lejeune et al., 1959). This report was followed up by investigators who in 1991 revealed that a CGG expansion in the gene encoding Fragile-X mental retardation protein (or FMRP, an RNA-binding protein that regulates the translation of genes involved in synaptic function) is causal for FXS (Pieretti et al., 1991; Verkerk et al., 1991).

Advances in the study of ID motivated researchers to initially employ linkage studies on multiplex families (pedigrees with several affected people) (Mefford et al., 2012; Geschwind and State, 2015; Vissers et al., 2016). By utilizing linkage studies, investigators hoped to classify segments of chromosomal material (and therefore specific gene coding regions) that are shared by those with the same neuropsychiatric disorders (Mefford et al., 2012; Geschwind and State, 2015; Vissers et al., 2016). Ultimately, researchers were able to uncover the causes of several ID syndromes (Vissers et al., 2016) such as Angelman syndrome (produced by silencing of *UBE3A*) (Buiting, 2010), Prader-Willi syndrome (caused by deletions of *NDN* and *SNRPN*) (Buiting, 2010) and Smith-Magenis syndrome (produced by deletions of *RAI1*) (Elsea and Girirajan, 2008;

Vissers et al., 2016). Additionally, it is now known that Down syndrome represents the most ID cases (6 to 8%) while FMRP is the most commonly mutated gene in ID (representing 0.5% of cases) (Vissers et al., 2016).

The level of success seen in genetic research focused on ID was not reproduced in linkage studies concentrated on ASD (Geschwind and State, 2015). We now know that this failure was due to the fact that these analyses did not contain the statistical power needed to produce replicable results (Geschwind and State, 2015). Moreover, with subsequent use of genome-wide association studies (used to detect single nucleotide polymorphisms between patient populations) it was determined that the complexity seen in ASD genetics is due to two main classes of mutations: 1) rare variants with large effect sizes and 2) common variants with small effect sizes (Geschwind and State, 2015).

The advent of next-generation sequencing (NGS) in the early 2000s allowed geneticists to catalog entire genomes on a time-scale that was previously inaccessible. NGS has since provided deep insights into the genomic underpinnings of ASD that could not be adequately captured by previous efforts (Geschwind and State, 2015; de la Torre-Ubieta et al., 2016). For example, large duplications or deletions of chromosomal regions (known as copy number variations or CNVs) are currently recognized as contributing to 5-7% of ASD cases (Geschwind and State, 2015; de la Torre-Ubieta et al., 2016). By integrating the results of NGS studies, researchers have been able to identify specific chromosomal loci that are associated with ASD (Geschwind and State, 2015). NGS has also allowed for the documentation of single-nucleotide variants (SNVs) in specific genes that produce ASD (Geschwind and State, 2015; de la Torre-Ubieta et al., 2016).

Interestingly, many of the genetic alterations associated with ASD are *de novo* meaning that they are not carried by either parent and that they instead arise either in a parent's germline or over the course of an embryo's development (Geschwind and State, 2015; de la Torre-Ubieta et al., 2016). FXS and tuberous sclerosis complex (caused by mutations in *TSC1* or *TSC2*) contribute to the most ASD cases (1.9% and 0.9%, respectively) (de la Torre-Ubieta et al., 2016). However, single-gene mutations are predicted to explain no more than 5% of all ASD cases (de la Torre-Ubieta et al., 2016). Lastly, NGS has yielded similar advancements with regards to understanding the role of CNVs and SNVs in ID (Vissers et al., 2016). This cache of information has provided investigators the opportunity to compare the genetic architecture underlying the two disorders.

There is a large overlap of ID-risk genes with ASD-risk genes (Vissers et al., 2016). Shared genes between the two disorders code for proteins with diverse biological functions such as chromatin modification (e.g., *AR1D1B*, *CDH2*, and *CDH8*), cellular adhesion (e.g., *CNTNAP2* and *NRXN1*), and kinase signaling (e.g., *CAMK2A*, *CAMK2B*, and *DYRK1A*) (Mullins et al., 2016). A major feature of both ASD and ID genetics is a disruption in numerous genes encoding proteins involved in synaptic function (Zoghbi and Bear, 2012). Because synapse-related genes are all necessarily expressed throughout the brain, this finding is able to explain how disparate mutations could lead to a similar clinical presentation (Zoghbi and Bear, 2012). Lastly, many of the genes associated with ASD and ID are enriched during early brain development (Geschwind and State, 2015; de la Torre-Ubieta et al., 2016; Mullins et al., 2016). Certain transcription factors

coordinate the spatial and temporal expression patterns of ASD- and ID-risk genes. Therefore, studying transcription factors that are themselves genetically associated with ASD and ID could allow for an improved understanding of the neurodevelopmental mechanisms at risk in these disorders.

## EVIDENCE SUPPORTING A ROLE FOR *FOXP1* IN ASD AND ID

### FOXP1 as a Transcription Factor

Forkhead Box P1 (FOXP1) **(Figure 1.2)** is a transcription factor enriched in the developing brain and which is recognized as a high-confidence ASD- and ID-risk gene (Bacon and Rappold, 2012; Iossifov et al., 2014; Sanders et al., 2015). FOXP1 belongs to the FOX family of transcription factors (made up of subfamilies FOXA-FOXS), which is defined by the presence of the forkhead (FKH) domain (Lalmansingh et al., 2012; Lam et al., 2013). The FKH region allows FOX proteins to make physical contact with DNA and thus regulate transcription (Lalmansingh et al., 2012; Lam et al., 2013). The FKH domain gets its name from the "forked head" phenotype seen in *Drosophila melanogaster* that is produced by the loss of the *forkhead* gene (*FOXA1* in humans) (Weigel et al., 1989; Hannenhalli and Kaestner, 2009). The FKH domain is approximately 100 amino acids in length and it is highly conserved amongst the FOX proteins (Lalmansingh et al., 2012).

The members of the FOXP subfamily (FOXP1-4) are involved in various biological processes including organ development, immune system functioning, and vocal communication (Hannenhalli and Kaestner, 2009; Lalmansingh et al., 2012). The FKH domain of the FOXP subfamily is uniquely shortened (to roughly 90 amino acids) and,

unlike what is seen in the other FOX subfamilies, it is positioned towards the C-terminus (Lalmansingh et al., 2012; Lam et al., 2013). Other domains found in the FOXP protein subfamily include a zinc-finger domain, a leucine-zipper domain, and a transrepression domain (Lalmansingh et al., 2012; Lam et al., 2013). With the exception of FOXP3, which cannot interact with FOXP1/2/4 due to its divergence from them, the FOXP proteins are able to homodimerize and heterodimerize with one another both *in vitro* and *in vivo* (Li et al., 2004; Sin et al., 2015; Mendoza and Scharff, 2017). I have also been able to demonstrate that Foxp1 and Foxp2 are able to interact in the early postnatal mouse striatum **(Figure 1.3)**. Because of their shortened FKH domain, it appears that dimerization is necessary for these proteins to stably interact with DNA (Li et al., 2004; Lalmansingh et al., 2012). Dimerization amongst FOXP proteins is mediated by the leucine zipper domain (Li et al., 2004). The dimerization of FOXP proteins (known as "domain-swapping") involves the production of a "winged-helix" conformation in which two FKH regions fold over each other and allow for the bridging of two DNA molecules (Stroud et al., 2006; Bandukwala et al., 2011; Chu et al., 2011; Lalmansingh et al., 2012). Finally, because the FKH domain is highly conserved (at about 85%) between the FOXP proteins, the diversity in this subfamily stems from the flanking regions (Lalmansingh et al., 2012).

FOXP1 was first identified in 1993 as part of a screen carried out in B-cells and was originally named glutamine (Q)-rich factor 1 (QRF1) (Li and Tucker, 1993; Koon et al., 2007). QRF1 was eventually renamed FOXP1 after the human gene was cloned (Banham et al., 2001; Koon et al., 2007) in accordance with the nomenclature developed for FOX transcription factors (Kaestner et al., 2000). The FOX transcription factors are

governed by a specific naming system, which uses uppercase for primate proteins (e.g., FOXP1), title case for rodent proteins (e.g., Foxp1), and mixed case for proteins from all other species or collection of species (e.g., FoxP1) (Kaestner et al., 2000). FOXP1 is enriched throughout the body and it participates in orchestrating cardiomyocyte proliferation (Wang et al., 2004), the formation of the lungs and the esophagus (Shu et al., 2007; Li et al., 2012), and T cell and B cell development (Hu et al., 2006; Feng et al., 2010). There is also a wealth of literature describing *FOXP1* both as an oncogene and as a tumor suppressor gene (Koon et al., 2007; Brown et al., 2008; Feng et al., 2012; Lam et al., 2013; Brown et al., 2016; Xiao et al., 2016). Indeed, alterations in the expression of *FOXP1* are associated with improved and worsened prognostic outcomes for different types of cancer (Koon et al., 2007; Lam et al., 2013; Xiao et al., 2016).

Members of the NuRD complex (a chromatin-remodeling protein complex) interact with FOXP1 in the recruitment of HDACs (which silence gene expression) (Chokas et al., 2010). Additionally, FOXP1 is able to interact with CtBP and the SMRT protein complex (both transcriptional co-repressors), which are also able to recruit HDACs (Li et al., 2004; Lam et al., 2013). Consequently, FOXP1 has classically been thought of as a transcriptional repressor (Wang et al., 2003; Lalmansingh et al., 2012). Still, there is some evidence to suggest that the FOXP proteins, including FOXP1 itself, can act as transcriptional activators (Spiteri et al., 2007; Sagardoy et al., 2013). To address this question directly, I have combined chromatin immunoprecipitation followed by DNA-sequencing (ChIP-seq) and RNA-sequencing (RNA-seq) analyses in human neural progenitors as well as RNA-seq analysis in a patient-relevant heterozygous *FOXP1*

knockout mouse model. With the resultant data sets, I have shown that FoxP1 is able to act as a transcriptional repressor and activator in the control of region-specific transcriptional profiles in the brain **(Chapter 2)**.

### *FOXP1* as a High-Confidence ASD- and ID-Risk Gene

The first piece of evidence tying FOXP1 to NDDs came from a patient displaying gross motor delay (GMD) and delayed speech who was found to harbor a large deletion in chromosome 3 that included the *FOXP1* gene (Pariani et al., 2009; Bacon and Rappold, 2012). However, this deletion also included three other genes (*GPR27*, *PROK2*, and *EIF4E3*), which confounded interpretations (Pariani et al., 2009; Bacon and Rappold, 2012). A deletion impacting only *FOXP1* was then identified in an individual displaying GMD and severe speech delay (Carr et al., 2010; Bacon and Rappold, 2012). But again, the behavioral symptoms shown by this patient could not be entirely attributed to loss of *FOXP1* because this individual also presented with a type I Chiari malformation (a type of cerebellar malformation) (Carr et al., 2010; Bacon and Rappold, 2012). Shortly following this report, a karyotyping study uncovered three mutations exclusively in *FOXP1* within three patients diagnosed with GMD, severe language impairment (SLI), and ID (Horn et al., 2010; Bacon and Rappold, 2012). This signified the first time that disruptions to *FOXP1* were demonstrated to be causative for ID (Horn et al., 2010; Bacon and Rappold, 2012). Afterwards, researchers performing a microarray-based screen of ID cases observed a deletion impacting only *FOXP1* in an individual presenting with ID and SLI (Hamdan et al., 2010; Bacon and Rappold, 2012). They also observed a nonsense

mutation affecting only *FOXP1* in an individual presenting with SLI, ID, and ASD (Hamdan et al., 2010; Bacon and Rappold, 2012). Thus, conclusive links to both ASD and ID were established for FOXP1.

Motivated by the aforementioned findings, a series of case-reports have continued to connect mutations and deletions in *FOXP1* to ASD, ID, and NDDs in general **(Table 1.1)**. Whole-exome sequencing (WES) performed on 20 families detected a premature stop codon caused by a frameshift insertion in a patient with hyperactivity, speech impairments, and ASD (O'Roak et al., 2011; Bacon and Rappold, 2012). Whole-genome-sequencing then detailed a chromosomal translocation in a patient with ASD, delays in speech acquisition, and GMD (Bacon and Rappold, 2012; Talkowski et al., 2012). However, the two afformentioned studies were confounded by disruptions in other genes (*CNTNAP2* and *ANK3*, respectively) (O'Roak et al., 2011; Bacon and Rappold, 2012; Talkowski et al., 2012). Next, a large deletion in chromosome 3 that included *FOXP1* was observed in a person with ASD, speech delay, and motor impairments (Palumbo et al., 2013). Following this, a large intragenic deletion exclusively affecting *FOXP1* was identified in an individual afflicted with ID (Le Fevre et al., 2013). Then, a missense mutation was isolated in a person exhibiting ID, SLI, and ASD through WES (Srivastava et al., 2014). Afterwards, a person diagnosed with GDD and speech impairments was revealed to carry a mutation in *FOXP1* but the clinical features could not be completely ascribed to this gene because a mutation in *PRKAA1* was also uncovered (Song et al., 2015). Subsequently, a case report detailed a two-base pair deletion that yields a premature stop codon in *FOXP1* in a patient exhibiting ID, attention-deficit hyperactivity

disorder (ADHD), obsessive-compulsive disorder (OCD), ASD, anxiety, and SLI (Lozano et al., 2015). A follow-up account described the responses of this individual to pharmaceutical treatments including methylphenidate (for ADHD), sertraline (for anxiety), as well as clomipramine and aripiprazole (both for OCD) (Cohen, 2017). Lastly, WES uncovered three missense mutations in three separate individuals diagnosed with ID, abnormal sensory processing, speech and language deficiencies, and autistic features (Sollis et al., 2016).

*FOXP1* has also been implicated in ASD and ID via recent, high-profile sequencing projects. Specifically, WES performed on 2,517 ASD families revealed frameshift and nonsense mutations in *FOXP1* to be causal for the disorder (Iossifov et al., 2014). Another study, relying on improved analysis of results from previous sequencing efforts as well as data from a new cohort, was able to identify 71 genomic loci that are associated with an increased risk for ASD, and one of these included *FOXP1* (Sanders et al., 2015). Additionally, WES carried out on 1,133 people with severe, undiagnosed NDDs were able to identify four genetic perturbations to *FOXP1* (Deciphering Developmental Disorders, 2015). Most recently, sequencing of 208 candidate genes in over 11,700 cases of ASD, ID and developmental disorders, found eleven people with gene-disrupting mutations solely impacting *FOXP1* (Stessman et al., 2017).

The genetic perturbations influencing *FOXP1* discussed so far are all *de novo*, heterozygous in nature (homozygous disruptions are presumably lethal), and frequently produce a severe form of ASD that is often comorbid with ID (Le Fevre et al., 2013; Lozano et al., 2015; Vissers et al., 2016). However, one study has found increased

*FOXP1* expression in lymphoblastoid cell lines derived from ASD patients (Chien et al., 2013). Therefore, the importance of *FOXP1* dosage to the reported symptoms still remains to be determined and I consider this in my discussion **(Chapter 4)**.

As demonstrated above, an important characteristic of almost all the reports on *FOXP1* mutations and deletions is the presence of SLI and speech impairments (Bacon and Rappold, 2012; Le Fevre et al., 2013). These deficits have helped create a recognizable phenotype associated with *FOXP1* loss (Bacon and Rappold, 2012; Le Fevre et al., 2013). Because these disturbances do not occur in the absence of other deficiencies, they may represent secondary features of decreased intellectual functioning rather than an independent disruption of communication itself (Bacon and Rappold, 2012). Thus, it is difficult to say whether or not these deficits are due to either ID or ASD (Bacon and Rappold, 2012). Nevertheless, this highlights a critical role for FOXP1 in the acquisition and expression of language (Bacon and Rappold, 2012; Le Fevre et al., 2013; Konopka and Roberts, 2016).

Taken together, these observations indicate that FOXP1 plays a role in controlling broad neurological processes such as cognitive ability, impulse control, sensory processing, social communication development, and the acquisition of motor skills (Bacon and Rappold, 2012; Le Fevre et al., 2013). Disturbances in these processes contribute to both the core and peripheral symptoms of ASD and ID.

## KNOWN FUNCTIONS OF FOXP1 WITHIN THE BRAIN

### Neuronal Functions of Foxp1 *in vitro* and *in vivo*

The impact of heterozygous loss of *FOXP1* on cognitive, social, and linguistic abilities has encouraged investigators to study the neuronal functions of this transcription factor (Bacon and Rappold, 2012; Golson and Kaestner, 2016). There are nine FoxP1 isoforms in humans and four in mice (Wang et al., 2003; Brown et al., 2008). FoxP1 isoforms show cell-type and time-point-specific enrichment (Shu et al., 2001; Wang et al., 2003; Brown et al., 2008; Brown et al., 2016; Garaud et al., 2017; van Keimpema et al., 2017). Foxp1A and Foxp1D are the murine isoforms of Foxp1 that show brain-specific expression (Wang et al., 2003) and they are observable by embryonic day 14.5 (E14.5) (Ferland et al., 2003). *FOXP1* is present in the human fetal brain as early as 8 weeks of gestation but it is unclear which isoform(s) this represents (Teramitsu et al., 2004; Saito et al., 2011; Onorati et al., 2014; Precious et al., 2016).

Foxp1 is highly enriched within the mouse neocortex, hippocampus, and striatum (Ferland et al., 2003; Tamura et al., 2004; Hisaoka et al., 2010). Foxp1 expression is largely restricted to the projection neurons, but not the interneurons, of these regions (Ferland et al., 2003; Tamura et al., 2004; Hisaoka et al., 2010; Precious et al., 2016). Within the pyramidal neurons of the neocortex, Foxp1 is enriched throughout layers III-VIa (Ferland et al., 2003; Hisaoka et al., 2010). Foxp1 expression in the pyramidal neurons of the hippocampus is mostly constrained to the *Cornu Ammonis* areas 1 and 2 (CA1/2) (Ferland et al., 2003). The medium spiny neurons (MSNs) of the striatum express the highest levels of Foxp1 in the brain (Ferland et al., 2003; Tamura et al., 2004; Heiman et al., 2008; Precious et al., 2016). Foxp1 shows sparse expression in other brain regions including the olfactory bulb, the thalamus, the hypothalamus, and the amygdala (Ferland

et al., 2003). Foxp1 has been proposed to function in neuroglia such as astrocytes and oligodendrocytes (Surmeli et al., 2011; Tang et al., 2012; Freeman and Rowitch, 2013) but there is no direct evidence that it is expressed in either cell-type (Precious et al., 2016). On the other hand, microglia (the brain's resident immune cells) express detectable levels of *Foxp1* mRNA and their levels increase upon treatment with pro-inflammatory molecules (Tang et al., 2012). Stimulation with gonadal hormones can affect FoxP1 expression (Takayama et al., 2008; Shigekawa et al., 2011) but there are conflicting reports as to whether or not this translates into sexually-dimorphic expression in the brain (Bowers et al., 2013; Bowers et al., 2014; Frohlich et al., 2017).

Owing to its robust expression in MSNs, the brain-specific role of Foxp1 has been most thoroughly investigated in the striatum. Indeed, the first report to look at the role of Foxp1 within the brain employed genome-wide expression arrays and ChIP-seq on cultured MSNs overexpressing Foxp1 (Tang et al., 2012). This study found an MSN transcriptome characterized by altered expression of genes involved in immune signaling, neuronal development, and Huntington's disease-relevant pathways (Tang et al., 2012). Moreover, this article recapitulated these findings *in vivo* by using microarrays on a Huntington's disease mouse model with striatal *Foxp1* over-expression (Tang et al., 2012).

Use of a *Nestin.Cre* line (which targets neuronal and glial precursor cells in the brain) has demonstrated that mice with homozygous deletion of *Foxp1* throughout the brain display delayed striatal development and ASD- and ID-like phenotypes such as decreased sociability, hyperactivity, stereotypic/repetitive behaviors, impaired learning

and memory, and increased anxiety (Bacon et al., 2014). Microarray-based expression analysis performed on the striatum of these whole-brain *Foxp1* knockout mice discovered dysregulation of genes involved in chromatin assembly and cellular division (Bacon et al., 2014). Whole-brain *Foxp1* conditional knockout animals also possess decreased hippocampal CA1 neuron excitability (Bacon et al., 2014). Finally, FoxP1 regulates striatal differentiation by controlling the expression of the MSN-marker DARPP-32 and thus FoxP1 can be used as indicator of successful MSN transplantation (Precious et al., 2016).

Given the wide distribution of Foxp1 in the pyramidal neurons of the neocortex, attention has also been paid to the function of this transcription factor in neocortical development. Knocking down neocortical *Foxp1* mRNA results in impaired axonal development, irregular multipolar-to-bipolar shape conversion both *in vitro* and *in vivo*, and abnormal neocortical patterning (Li et al., 2015). These observations are concordant with the finding that FOXP1 is required for dendritic morphogenesis in neocortical neurons (Rocca et al., 2017). Regulation of dendritic development in neocortical neurons is dependent upon SUMOylation (a ubiquitin-like post-translational modification) of FOXP1 and the subsequent recruitment of CtBP (Rocca et al., 2017).

Over the last several years, there has been a marked improvement in our understanding of the neuronal mechanisms governed by FoxP1. Based on the work accomplished so far, FoxP1 appears to be involved in distinct processes within different regions of the brain. Proper expression of Foxp1 seems to be especially critical for MSN identity and striatal development (Bacon et al., 2014; Precious et al., 2016). Thus, there has been a focus on the striatal-dependent behavior of vocalization/speech production in

relation to altered *Foxp1* levels (Bacon and Rappold, 2012; Konopka and Roberts, 2016). Such efforts are vital for understanding the mechanisms behind the SLI phenotype that repeatedly accompanies heterozygous loss of *FOXP1* (Bacon and Rappold, 2012; Konopka and Roberts, 2016).

**FoxP1 and FoxP2 in the Regulation of Vocal Communication**

FOXP2 is a paralog of FOXP1 and mutations in the *FOXP2* gene produce a condition known as developmental verbal dyspraxia (DVD) (Lai et al., 2001; MacDermot et al., 2005). DVD is a disorder affecting the coordination of facial muscles involved in speech control (Fisher and Scharff, 2009). DVD has been phenocopied in the isolation-based ultrasonic vocalizations (USVs) of rodent pups with altered *Foxp2* expression (Shu et al., 2005; French et al., 2007; Enard et al., 2009; Bowers et al., 2013) and alterations to USV production have been correlated with altered physiological and morphological properties in MSNs (Enard et al., 2009; Vernes et al., 2011). Moreover, mouse models of Huntington's and Parkinson's disease, conditions characterized by striatal degeneration, also produce abnormal USVs (Kurz et al., 2010; Pietropaolo et al., 2011; Grant et al., 2014). Foxp2 is co-expressed with Foxp1 in the striatum (Ferland et al., 2003; Frohlich et al., 2017) and these proteins are able to heterodimerize and homodimerize with one another **(Figure 1.3)** (Li et al., 2004; Sin et al., 2015; Mendoza and Scharff, 2017). Therefore, the role of FoxP1 in controlling striatal-based USVs has been of particular interest to researchers for some time (Bacon and Rappold, 2012). Consequently, I was the first to show that proper Foxp1 expression is necessary for this behavior **(Chapter 2)**.

Following this study, a report demonstrated that loss of *Foxp1* leads to sex-specific changes in USV production (Frohlich et al., 2017).

Finally, as stated above, full-brain conditional loss of *Foxp1* results in a plethora of ASD- and ID-like behaviors (Bacon et al., 2014). However, more in-depth analyses of the behavioral consequences caused by specific disruptions in these processes are needed. To address this question, I took advantage of a *Foxp1* conditional knockout (*Foxp1*$^{cKO}$) mouse with ablation of *Foxp1* specifically in the pyramidal neurons of the neocortex and hippocampus. I have shown that this loss of *Foxp1* is sufficient to produce ASD- and ID-relevant behaviors such as decreased sociability, hyperactivity, and gross impairments in learning and memory tasks. I have also correlated the learning and memory deficits with altered hippocampal physiology and transcriptional signatures **(Chapter 3)**.

## QUESTIONS ADDRESSED IN THIS THESIS

### Chapter 2

1. What are the region-specific gene targets of Foxp1 within the mouse brain?
2. Does heterozygous loss of *Foxp1* influence the production of mouse USVs?
3. Does heterozygous loss of *Foxp1* differentially influence murine MSN subtypes?
4. How conserved are Foxp1 targets between human and mouse neurons?

### Chapter 3

1. Is loss of *Foxp1* in the pyramidal neurons of the neocortex and hippocampus sufficient to produce ASD- and ID-like behaviors in mice?
2. What are the transcriptional and physiological changes associated with the learning and memory deficits caused by loss of *Foxp1* in the mouse hippocampus*?*

### Chapter 4

1. Is Foxp1 expression in striatal neurons necessary and sufficient for proper USV production?
2. Is it possible to disentangle the gene targets between Foxp1 and Foxp2 heterodimers and Foxp1 and Foxp2 homodimers?
3. Can we disentangle the contributions of neocortical and hippocampal *Foxp1* to the behavioral phenotypes of $Foxp1^{cKO}$ mice?
4. Are the behaviors caused by loss of forebrain *Foxp1* developmental in origin?

5. Are the phenotypes exhibited by *Foxp1*$^{cKO}$ mice dose-dependent?

6. Are *Foxp1* mutant mice models of ASD and ID in general?

## FIGURES FOR CHAPTER ONE

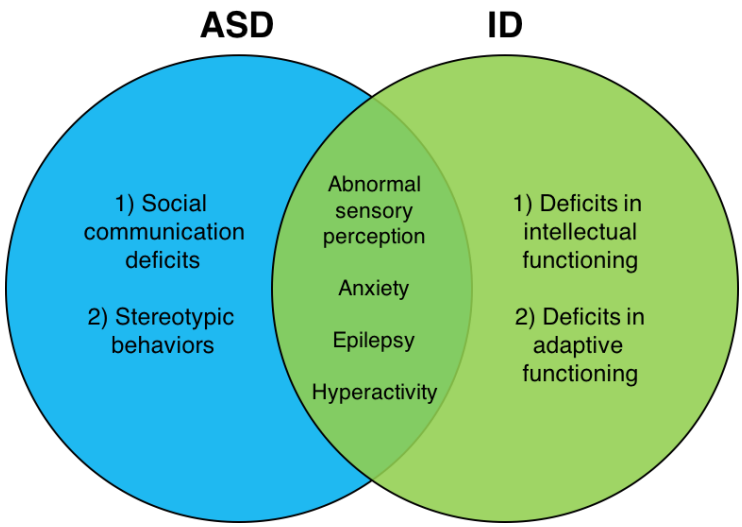


**Figure 1.1. Distinct and overlapping clinical characteristics of ASD and ID.** ASD and ID are each defined by two unique core symptoms. However, ASD and ID often present with overlapping secondary symptoms.


**Figure 1.2. Diagram of FOXP1.** A simplified schematic of the transcription factor FOXP1 highlighting important functional domains. The forkhead domain allows the protein to make stable contacts with DNA. The leucine zipper is required for homodimerization as well as heterodimerization with other FOXP proteins. FKH, forkhead domain; polyQ, poly-glutamine segment; LZ, leucine zipper domain, TR; transrepression domain; ZF, zinc finger domain.

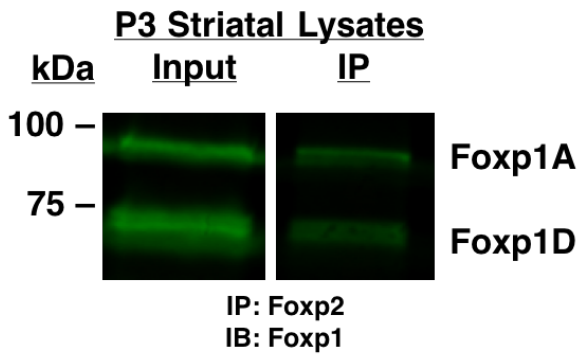


**Figure 1.3. Co-immunoprecipitation of Foxp1 with Foxp2 in the mouse brain.** Representative image showing co-immunoprecipitation of Foxp1 isoforms A and D with Foxp2 in the postnatal day 3 (P3) mouse striatum. Immunoblotting (IB) for Foxp1 (Foxp1 antibody (rabbit, 1:5000) (Spiteri et al., 2007)) was carried out after immunoprecipitation (IP) of Foxp2 (Foxp2 antibody (goat, 20 uL/IP), Santa Cruz) was performed on pooled (3 animals/pool) P3 striatal protein lysates.

# TABLES FOR CHAPTER ONE

**Table 1.1. Literature connecting *FOXP1* to NDDs.**

| Reference | Study Design | Sex | Reported *FOXP1* Disruption or Main Conclusion | Reported IQ | Reported Clinical Presentation |
|---|---|---|---|---|---|
| Pariani et al., 2009 | Case report with microarray analysis | Male | 785 Kb deletion (exons 1-11 deleted along with *GPR27*, *PROK2*, and *EIF4E3*) | Data Not Available (N/A) | Speech delay (SD) and gross motor delay (GMD) |
| Carr et al., 2010 | Case report with microarray analysis | Male | 1.1 Mb deletion (exons 4-21 deleted) | N/A | Severe SD, GMD, Chari I malformation, and epileptiform discharges |
| Horn et al., 2010 | Karyotyping screen on 1,523 individuals with intellectual disability | Male | 498 Kb deletion (exons 7-21 deleted) | < 50 (non-verbal) | Intellectual disability (ID), GMD, global developmental delay (GDD), and SD |
| | | Female | 659 Kb deletion (exons 5-21 deleted) | < 50 (non-verbal) | Intellectual disability (ID), GMD, GDD, and SD |
| | | Male | 1.0 Mb deletion (exons 6-21 deleted) | 50 (non-verbal) | Intellectual disability (ID), GMD, GDD, and SD |
| Hamdan et al., 2010 | Microarray-based screen on 245 nonsyndromic ID and/or ASD cases | Female | 390 Kb deletion (exons 4-14 deleted) | 58 (non-verbal) | ID, SLI, anxiety, and social withdrawal |
| | | Male | c.1573C>T nonsense mutation (predicted to result in a p.R525X variant) | 48 (non-verbal) | ID, ASD, SLI, and hyperactivity |
| O'Roak et al., 2011 | WES screen of 20 ASD children and their families | Male | Single base pair insertion (+A), leading to a frameshift (predicted to result in a p.Ala339Ser*fs**4 protein variant); an inherited *CNTNAP2* mutation also present | 34 (non-verbal) | ASD, ID, and language delay |
| Talkowski et al., 2012 | Whole-genome sequencing study on 38 patients with NDDs | N/A | Chromosomal translocation (3;10)(p13;q21.2), resulting in reduced *FOXP1* expression; *ANK3* also affected by the same chromosomal translocation | N/A | GMD, SD, and spina bifida occulta |

| | | | | | |
|---|---|---|---|---|---|
| Palumbo et al., 2013 | Case report with microarray analysis | Male | 1.0 Mb deletion (exons 4-21 deleted) | N/A | ASD, ID, GMD, EEG anomalies, and speech delay |
| Le Fevre et al., 2013 | Case report with microarray analysis | Male | 190 Kb deletion (exons 6-13 deleted) | N/A | GMD, SD, GDD, and ID |
| Srivastava et al., 2014 | Whole-exome sequencing (WES) on 78 individuals with NDDs | N/A | c.1600T>C substitution, leading to a missense mutation (predicted to result in a p.W534R variant) | N/A | ID, SLI, autistic features, and MRI abnormalities |
| Iossifov et al., 2014 | WES on 2,517 families with at least one child with ASD | Male | Nonsense mutation resulting from a G>A substitution | 64 (non-verbal) | ID and ASD |
| | | Male | Single base pair insertion (+T) leading to a frameshift mutation | 34 (non-verbal) | ID and ASD |
| Song et al., 2015 | Case report with WES | Female | Singe base pair substitution T>C, resulting in a missense mutation | N/A | Severe SD and GDD |
| The Deciphering Developmental Disorders Study, 2015 | WES and microarray analysis on 1,133 with severe, undiagnosed NDDs | N/A | 4 perturbations affecting *FOXP1,* including a missense mutation (G>A), a nonsense mutation (Q/*), a splice donor variant (C>T), and an initiator codon variant | N/A | NDDs (undiagnosed) |
| Sanders et al., 2015 | Whole-genome sequencing on 2,591 families with at least one child with ASD (in addition to reanalysis of previous ASD sequencing efforts) | N/A | *FOXP1* locus is associated with an increased ASD risk | N/A | ASD |
| Lozano et al., 2015 | Case report with WES | Female | c.1267_1268delGT base pair deletions, resulting in a p.V423H*fs**37 variant | 54 (total) | ASD, ID, and SLI |
| Sollis et al., 2016 | Case report with WES | Male | c.1393A>G missense mutation, resulting in a p.R465G variant | 50-80 (task dependent) | ID, GDD, autistic features, attention deficit hyperactivity disorder (ADHD), and sensory processing disorder |
| | | Male | c.1540C>T missense mutation, resulting in a p.R514C variant | 53 (total) | GDD, ID, speech and language impairments, ADHD, and GMD |

| | | | | | |
|---|---|---|---|---|---|
| | | Female | c.1317C>G missense mutation, resulting in a p.Y439* variant | N/A | Developmental delays, ID, autistic features, anxiety, and aggression |
| Stessman et al., 2017 | Sequencing of 208 candidate genes within a cohort of >11,730 ASD, ID, and developmental disorder cases | Mixed | 11 total gene disrupting mutations affecting *FOXP1* | 48 (non-verbal/average for 2 individuals) | ASD, ID, and/or presentation with seizures |

## REFERENCES FOR CHAPTER ONE


Ageranioti-Belanger S, Brunet S, D'Anjou G, Tellier G, Boivin J, Gauthier M (2012) Behaviour disorders in children with an intellectual disability. Paediatr Child Health 17:84-88.

American Association on Intellectual and Developmental Disabilities (2010), 11th Edition. Washington, DC, USA: American Association on Intellectual and Developmental Disabilities.

American Psychiatry Association (2013) Diagnostic and Statistical Manual of Mental Disorders: DSM-5, 5th Edition. Arlington, Virginia, USA: American Psychiatry Association.

Asperger H (1944) The "autistic psychopathy" in childhood. Arch Psychiat Nerven 117:76-136.

Bacon C, Rappold GA (2012) The distinct and overlapping phenotypic spectra of FOXP1 and FOXP2 in cognitive disorders. Human genetics 131:1687-1698.

Bacon C, Schneider M, Le Magueresse C, Froehlich H, Sticht C, Gluch C, Monyer H, Rappold GA (2014) Brain-specific Foxp1 deletion impairs neuronal development and causes autistic-like behaviour. Molecular psychiatry.

Bailey DB, Jr., Raspa M, Bishop E, Holiday D (2009) No change in the age of diagnosis for fragile x syndrome: findings from a national parent survey. Pediatrics 124:527-533.

Bandukwala HS, Wu Y, Feuerer M, Chen Y, Barboza B, Ghosh S, Stroud JC, Benoist C, Mathis D, Rao A, Chen L (2011) Structure of a domain-swapped FOXP3 dimer on DNA and its function in regulatory T cells. Immunity 34:479-491.

Banham AH, Beasley N, Campo E, Fernandez PL, Fidler C, Gatter K, Jones M, Mason DY, Prime JE, Trougouboff P, Wood K, Cordell JL (2001) The FOXP1 winged helix transcription factor is a novel candidate tumor suppressor gene on chromosome 3p. Cancer Res 61:8820-8829.

Bleuler E (1912) The theory of schizophrenic negativism. J Nerv Ment Dis 39:133-+.

Bolte S, Dziobek I, Poustka F (2009) Brief report: The level and nature of autistic intelligence revisited. J Autism Dev Disord 39:678-682.

Bowers JM, Perez-Pouchoulen M, Edwards NS, McCarthy MM (2013) Foxp2 mediates sex differences in ultrasonic vocalization by rat pups and directs order of maternal retrieval. The Journal of neuroscience : the official journal of the Society for Neuroscience 33:3276-3283.

Bowers JM, Perez-Pouchoulen M, Roby CR, Ryan TE, McCarthy MM (2014) Androgen modulation of Foxp1 and Foxp2 in the developing rat brain: impact on sex specific vocalization. Endocrinology 155:4881-4894.

Brown PJ, Ashe SL, Leich E, Burek C, Barrans S, Fenton JA, Jack AS, Pulford K, Rosenwald A, Banham AH (2008) Potentially oncogenic B-cell activation-induced smaller isoforms of FOXP1 are highly expressed in the activated B cell-like subtype of DLBCL. Blood 111:2816-2824.

Brown PJ, Gascoyne DM, Lyne L, Spearman H, Felce SL, McFadden N, Chakravarty P, Barrans S, Lynham S, Calado DP, Ward M, Banham AH (2016) N-terminally truncated FOXP1 protein expression and alternate internal FOXP1 promoter usage in normal and malignant B cells. Haematologica 101:861-871.

Bryson SE, Bradley EA, Thompson A, Wainwright A (2008) Prevalence of autism among adolescents with intellectual disabilities. Can J Psychiatry 53:449-459.

Buiting K (2010) Prader-Willi syndrome and Angelman syndrome. Am J Med Genet C Semin Med Genet 154C:365-376.

Carlsson LH, Norrelgen F, Kjellmer L, Westerlund J, Gillberg C, Fernell E (2013) Coexisting disorders and problems in preschool children with autism spectrum disorders. ScientificWorldJournal 2013:213979.

Carr CW, Moreno-De-Luca D, Parker C, Zimmerman HH, Ledbetter N, Martin CL, Dobyns WB, Abdul-Rahman OA (2010) Chiari I malformation, delayed gross motor skills, severe speech delay, and epileptiform discharges in a child with FOXP1 haploinsufficiency. European journal of human genetics : EJHG 18:1216-1220.

Chakrabarti S, Fombonne E (2005) Pervasive developmental disorders in preschool children: confirmation of high prevalence. The American journal of psychiatry 162:1133-1141.

Charman T, Pickles A, Simonoff E, Chandler S, Loucas T, Baird G (2011) IQ in children with autism spectrum disorders: data from the Special Needs and Autism Project (SNAP). Psychol Med 41:619-627.

Chen JA, Penagarikano O, Belgard TG, Swarup V, Geschwind DH (2015) The emerging picture of autism spectrum disorder: genetics and pathology. Annu Rev Pathol 10:111-144.

Chien WH, Gau SS, Chen CH, Tsai WC, Wu YY, Chen PH, Shang CY, Chen CH (2013) Increased gene expression of FOXP1 in patients with autism spectrum disorders. Molecular autism 4:23.

Chokas AL, Trivedi CM, Lu MM, Tucker PW, Li S, Epstein JA, Morrisey EE (2010) Foxp1/2/4-NuRD interactions regulate gene expression and epithelial injury response in the lung via regulation of interleukin-6. The Journal of biological chemistry 285:13304-13313.

Christensen DL, Baio J, Van Naarden Braun K, Bilder D, Charles J, Constantino JN, Daniels J, Durkin MS, Fitzgerald RT, Kurzius-Spencer M, Lee LC, Pettygrove S, Robinson C, Schulz E, Wells C, Wingate MS, Zahorodny W, Yeargin-Allsopp M, Centers for Disease C, Prevention (2016) Prevalence and Characteristics of Autism Spectrum Disorder Among Children Aged 8 Years--Autism and Developmental Disabilities Monitoring Network, 11 Sites, United States, 2012. MMWR Surveill Summ 65:1-23.

Chu YP, Chang CH, Shiu JH, Chang YT, Chen CY, Chuang WJ (2011) Solution structure and backbone dynamics of the DNA-binding domain of FOXP1: insight into its domain swapping and DNA binding. Protein Sci 20:908-924.

Cohen SL, R.; Kolevzon, A.; Hagerman, R. J. (2017) Medication Treatment in an Adolescent Female with *FOXP1* Mutation. SRL Neurol Dis 1:001-005.

de Bildt A, Sytema S, Kraijer D, Minderaa R (2005) Prevalence of pervasive developmental disorders in children and adolescents with mental retardation. J Child Psychol Psychiatry 46:275-286.

de la Torre-Ubieta L, Won H, Stein JL, Geschwind DH (2016) Advancing the understanding of autism disease mechanisms through genetics. Nat Med 22:345-361.

De Rubeis S, Buxbaum JD (2015) Recent advances in the genetics of autism spectrum disorder. Curr Neurol Neurosci Rep 15:36.

Deciphering Developmental Disorders S (2015) Large-scale discovery of novel genetic causes of developmental disorders. Nature 519:223-228.

Elsea SH, Girirajan S (2008) Smith-Magenis syndrome. European journal of human genetics : EJHG 16:412-421.

Enard W et al. (2009) A humanized version of Foxp2 affects cortico-basal ganglia circuits in mice. Cell 137:961-971.

Engel-Yeger B, Hardal-Nasser R, Gal E (2011) Sensory processing dysfunctions as expressed among children with different severities of intellectual developmental disabilities. Res Dev Disabil 32:1770-1775.

Fakhoury M (2015) Autistic spectrum disorders: A review of clinical features, theories and diagnosis. Int J Dev Neurosci 43:70-77.

Feng J, Zhang X, Zhu H, Wang X, Ni S, Huang J (2012) High expression of FoxP1 is associated with improved survival in patients with non-small cell lung cancer. Am J Clin Pathol 138:230-235.

Feng X, Ippolito GC, Tian L, Wiehagen K, Oh S, Sambandam A, Willen J, Bunte RM, Maika SD, Harriss JV, Caton AJ, Bhandoola A, Tucker PW, Hu H (2010) Foxp1 is an essential transcriptional regulator for the generation of quiescent naive T cells during thymocyte development. Blood 115:510-518.

Ferland RJ, Cherry TJ, Preware PO, Morrisey EE, Walsh CA (2003) Characterization of Foxp2 and Foxp1 mRNA and protein in the developing and mature brain. The Journal of comparative neurology 460:266-279.

Fisher SE, Scharff C (2009) FOXP2 as a molecular window into speech and language. Trends in genetics : TIG 25:166-177.

Fombonne E (2003) Epidemiological surveys of autism and other pervasive developmental disorders: an update. J Autism Dev Disord 33:365-382.

Fombonne E (2009) Epidemiology of pervasive developmental disorders. Pediatr Res 65:591-598.

Freeman MR, Rowitch DH (2013) Evolving concepts of gliogenesis: a look way back and ahead to the next 25 years. Neuron 80:613-623.

French CA, Groszer M, Preece C, Coupe AM, Rajewsky K, Fisher SE (2007) Generation of mice with a conditional Foxp2 null allele. Genesis 45:440-446.

Frohlich H, Rafiullah R, Schmitt N, Abele S, Rappold GA (2017) Foxp1 expression is essential for sex-specific murine neonatal ultrasonic vocalization. Human molecular genetics 26:1511-1521.

Garaud S, Roufosse F, De Silva P, Gu-Trantien C, Lodewyckx JN, Duvillier H, Dedeurwaerder S, Bizet M, Defrance M, Fuks F, Bex F, Willard-Gallo K (2017) FOXP1 is a regulator of quiescence in healthy human CD4+ T cells and is constitutively repressed in T cells from patients with lymphoproliferative disorders. Eur J Immunol 47:168-179.

Gaugler T, Klei L, Sanders SJ, Bodea CA, Goldberg AP, Lee AB, Mahajan M, Manaa D, Pawitan Y, Reichert J, Ripke S, Sandin S, Sklar P, Svantesson O, Reichenberg A, Hultman CM, Devlin B, Roeder K, Buxbaum JD (2014) Most genetic risk for autism resides with common variation. Nature genetics 46:881-885.

Geschwind DH, State MW (2015) Gene hunting in autism spectrum disorder: on the path to precision medicine. Lancet Neurol.

Golson ML, Kaestner KH (2016) Fox transcription factors: from development to disease. Development 143:4558-4570.

Grant LM, Richter F, Miller JE, White SA, Fox CM, Zhu C, Chesselet MF, Ciucci MR (2014) Vocalization deficits in mice over-expressing alpha-synuclein, a model of pre-manifest Parkinson's disease. Behavioral neuroscience 128:110-121.

Hallmayer J, Cleveland S, Torres A, Phillips J, Cohen B, Torigoe T, Miller J, Fedele A, Collins J, Smith K, Lotspeich L, Croen LA, Ozonoff S, Lajonchere C, Grether JK, Risch N (2011) Genetic heritability and shared environmental factors among twin pairs with autism. Archives of general psychiatry 68:1095-1102.

Hamdan FF, Daoud H, Rochefort D, Piton A, Gauthier J, Langlois M, Foomani G, Dobrzeniecka S, Krebs MO, Joober R, Lafreniere RG, Lacaille JC, Mottron L, Drapeau P, Beauchamp MH, Phillips MS, Fombonne E, Rouleau GA, Michaud JL (2010) De novo mutations in FOXP1 in cases with intellectual disability, autism, and language impairment. American journal of human genetics 87:671-678.

Hannenhalli S, Kaestner KH (2009) The evolution of Fox genes and their role in development and disease. Nature reviews Genetics 10:233-240.

Harris JC (2006) Intellectual disability: understanding its development, causes, classification, evaluation, and treatment. New York, New York, USA: Oxford University Press.
Heiman M, Schaefer A, Gong S, Peterson JD, Day M, Ramsey KE, Suarez-Farinas M, Schwarz C, Stephan DA, Surmeier DJ, Greengard P, Heintz N (2008) A translational profiling approach for the molecular characterization of CNS cell types. Cell 135:738-748.
Hisaoka T, Nakamura Y, Senba E, Morikawa Y (2010) The forkhead transcription factors, Foxp1 and Foxp2, identify different subpopulations of projection neurons in the mouse cerebral cortex. Neuroscience 166:551-563.
Horn D et al. (2010) Identification of FOXP1 deletions in three unrelated patients with mental retardation and significant speech and language deficits. Human mutation 31:E1851-1860.
Hu H, Wang B, Borde M, Nardone J, Maika S, Allred L, Tucker PW, Rao A (2006) Foxp1 is an essential transcriptional regulator of B cell development. Nature immunology 7:819-826.
Iossifov I et al. (2014) The contribution of de novo coding mutations to autism spectrum disorder. Nature 515:216-221.
Kaestner KH, Knochel W, Martinez DE (2000) Unified nomenclature for the winged helix/forkhead transcription factors. Genes & development 14:142-146.
Kanner L (1943) Autistic Disturbances of Affective Contact. Nerv Child 2:217-250.
Keen D, Ward S (2004) Autistic spectrum disorder: a child population profile. Autism 8:39-48.
Konopka G, Roberts TF (2016) Insights into the Neural and Genetic Basis of Vocal Communication. Cell 164:1269-1276.
Koon HB, Ippolito GC, Banham AH, Tucker PW (2007) FOXP1: a potential therapeutic target in cancer. Expert Opin Ther Targets 11:955-965.
Kurz A, Wohr M, Walter M, Bonin M, Auburger G, Gispert S, Schwarting RK (2010) Alpha-synuclein deficiency affects brain Foxp1 expression and ultrasonic vocalization. Neuroscience 166:785-795.
Lai CS, Fisher SE, Hurst JA, Vargha-Khadem F, Monaco AP (2001) A forkhead-domain gene is mutated in a severe speech and language disorder. Nature 413:519-523.
Lalmansingh AS, Karmakar S, Jin Y, Nagaich AK (2012) Multiple modes of chromatin remodeling by Forkhead box proteins. Biochim Biophys Acta 1819:707-715.
Lam EW, Brosens JJ, Gomes AR, Koo CY (2013) Forkhead box proteins: tuning forks for transcriptional harmony. Nat Rev Cancer 13:482-495.
Le Fevre AK, Taylor S, Malek NH, Horn D, Carr CW, Abdul-Rahman OA, O'Donnell S, Burgess T, Shaw M, Gecz J, Bain N, Fagan K, Hunter MF (2013) FOXP1 mutations cause intellectual disability and a recognizable phenotype. American journal of medical genetics Part A 161A:3166-3175.
Leekam SR, Prior MR, Uljarevic M (2011) Restricted and repetitive behaviors in autism spectrum disorders: a review of research in the last decade. Psychol Bull 137:562-593.
Lejeune J, Gauthier M, Turpin R (1959) [Human chromosomes in tissue cultures]. C R Hebd Seances Acad Sci 248:602-603.
Li C, Tucker PW (1993) DNA-binding properties and secondary structural model of the hepatocyte nuclear factor 3/fork head domain. Proceedings of the National Academy of Sciences of the United States of America 90:11583-11587.
Li S, Weidenfeld J, Morrisey EE (2004) Transcriptional and DNA binding activity of the Foxp1/2/4 family is modulated by heterotypic and homotypic protein interactions. Molecular and cellular biology 24:809-822.
Li S, Wang Y, Zhang Y, Lu MM, DeMayo FJ, Dekker JD, Tucker PW, Morrisey EE (2012) Foxp1/4 control epithelial cell fate during lung development and regeneration through regulation of anterior gradient 2. Development 139:2500-2509.

Li X, Xiao J, Frohlich H, Tu X, Li L, Xu Y, Cao H, Qu J, Rappold GA, Chen JG (2015) Foxp1 regulates cortical radial migration and neuronal morphogenesis in developing cerebral cortex. PloS one 10:e0127671.

Lozano R, Vino A, Lozano C, Fisher SE, Deriziotis P (2015) A de novo FOXP1 variant in a patient with autism, intellectual disability and severe speech and language impairment. European journal of human genetics : EJHG 23:1702-1707.

MacDermot KD, Bonora E, Sykes N, Coupe AM, Lai CS, Vernes SC, Vargha-Khadem F, McKenzie F, Smith RL, Monaco AP, Fisher SE (2005) Identification of FOXP2 truncation as a novel cause of developmental speech and language deficits. American journal of human genetics 76:1074-1080.

Maenner MJ, Schieve LA, Rice CE, Cunniff C, Giarelli E, Kirby RS, Lee LC, Nicholas JS, Wingate MS, Durkin MS (2013) Frequency and pattern of documented diagnostic features and the age of autism identification. J Am Acad Child Adolesc Psychiatry 52:401-413 e408.

Martin JP, Bell J (1943) A Pedigree of Mental Defect Showing Sex-Linkage. J Neurol Psychiatry 6:154-157.

Matson JL, Shoemaker M (2009) Intellectual disability and its relationship to autism spectrum disorders. Res Dev Disabil 30:1107-1114.

McGrother CW, Bhaumik S, Thorp CF, Hauck A, Branford D, Watson JM (2006) Epilepsy in adults with intellectual disabilities: prevalence, associations and service implications. Seizure 15:376-386.

Mefford HC, Batshaw ML, Hoffman EP (2012) Genomics, intellectual disability, and autism. N Engl J Med 366:733-743.

Mendoza E, Scharff C (2017) Protein-Protein Interaction Among the FoxP Family Members and their Regulation of Two Target Genes, VLDLR and CNTNAP2 in the Zebra Finch Song System. Front Mol Neurosci 10:112.

Miller JS, Bilder D, Farley M, Coon H, Pinborough-Zimmerman J, Jenson W, Rice CE, Fombonne E, Pingree CB, Ritvo E, Ritvo RA, McMahon WM (2013) Autism spectrum disorder reclassified: a second look at the 1980s Utah/UCLA Autism Epidemiologic Study. J Autism Dev Disord 43:200-210.

Mullins C, Fishell G, Tsien RW (2016) Unifying Views of Autism Spectrum Disorders: A Consideration of Autoregulatory Feedback Loops. Neuron 89:1131-1156.

Nicholas JS, Charles JM, Carpenter LA, King LB, Jenner W, Spratt EG (2008) Prevalence and characteristics of children with autism-spectrum disorders. Ann Epidemiol 18:130-136.

O'Roak BJ, Deriziotis P, Lee C, Vives L, Schwartz JJ, Girirajan S, Karakoc E, Mackenzie AP, Ng SB, Baker C, Rieder MJ, Nickerson DA, Bernier R, Fisher SE, Shendure J, Eichler EE (2011) Exome sequencing in sporadic autism spectrum disorders identifies severe de novo mutations. Nature genetics 43:585-589.

Oliveira G, Ataide A, Marques C, Miguel TS, Coutinho AM, Mota-Vieira L, Goncalves E, Lopes NM, Rodrigues V, Carmona da Mota H, Vicente AM (2007) Epidemiology of autism spectrum disorder in Portugal: prevalence, clinical characterization, and medical conditions. Dev Med Child Neurol 49:726-733.

Onorati M, Castiglioni V, Biasci D, Cesana E, Menon R, Vuono R, Talpo F, Laguna Goya R, Lyons PA, Bulfamante GP, Muzio L, Martino G, Toselli M, Farina C, Barker RA, Biella G, Cattaneo E (2014) Molecular and functional definition of the developing human striatum. Nature neuroscience 17:1804-1815.

Palumbo O, D'Agruma L, Minenna AF, Palumbo P, Stallone R, Palladino T, Zelante L, Carella M (2013) 3p14.1 de novo microdeletion involving the FOXP1 gene in an adult patient with autism, severe speech delay and deficit of motor coordination. Gene 516:107-113.

Pariani MJ, Spencer A, Graham JM, Jr., Rimoin DL (2009) A 785kb deletion of 3p14.1p13, including the FOXP1 gene, associated with speech delay, contractures, hypertonia and blepharophimosis. European journal of medical genetics 52:123-127.
Park HR, Lee JM, Moon HE, Lee DS, Kim BN, Kim J, Kim DG, Paek SH (2016) A Short Review on the Current Understanding of Autism Spectrum Disorders. Exp Neurobiol 25:1-13.
Pieretti M, Zhang FP, Fu YH, Warren ST, Oostra BA, Caskey CT, Nelson DL (1991) Absence of expression of the FMR-1 gene in fragile X syndrome. Cell 66:817-822.
Pietropaolo S, Delage P, Cayzac S, Crusio WE, Cho YH (2011) Sex-dependent changes in social behaviors in motor pre-symptomatic R6/1 mice. PloS one 6:e19965.
Plomin R, Deary IJ (2015) Genetics and intelligence differences: five special findings. Molecular psychiatry 20:98-108.
Polyak A, Kubina RM, Girirajan S (2015) Comorbidity of intellectual disability confounds ascertainment of autism: implications for genetic diagnosis. Am J Med Genet B Neuropsychiatr Genet 168:600-608.
Postorino V, Fatta LM, Sanges V, Giovagnoli G, De Peppo L, Vicari S, Mazzone L (2016) Intellectual disability in Autism Spectrum Disorder: Investigation of prevalence in an Italian sample of children and adolescents. Res Dev Disabil 48:193-201.
Precious SV, Kelly CM, Reddington AE, Vinh NN, Stickland RC, Pekarik V, Scherf C, Jeyasingham R, Glasbey J, Holeiter M, Jones L, Taylor MV, Rosser AE (2016) FoxP1 marks medium spiny neurons from precursors to maturity and is required for their differentiation. Exp Neurol 282:9-18.
Prior M (2003) Is there an increase in the prevalence of autism spectrum disorders? J Paediatr Child Health 39:81-82.
Reichenberg A, Cederlof M, McMillan A, Trzaskowski M, Kapara O, Fruchter E, Ginat K, Davidson M, Weiser M, Larsson H, Plomin R, Lichtenstein P (2016) Discontinuity in the genetic and environmental causes of the intellectual disability spectrum. Proceedings of the National Academy of Sciences of the United States of America 113:1098-1103.
Robinson EB, Lichtenstein P, Anckarsater H, Happe F, Ronald A (2013) Examining and interpreting the female protective effect against autistic behavior. Proceedings of the National Academy of Sciences of the United States of America 110:5258-5262.
Rocca DL, Wilkinson KA, Henley JM (2017) SUMOylation of FOXP1 regulates transcriptional repression via CtBP1 to drive dendritic morphogenesis. Sci Rep 7:877.
Rosenberg RE, Law JK, Yenokyan G, McGready J, Kaufmann WE, Law PA (2009) Characteristics and concordance of autism spectrum disorders among 277 twin pairs. Arch Pediatr Adolesc Med 163:907-914.
Sagardoy A, Martinez-Ferrandis JI, Roa S, Bunting KL, Aznar MA, Elemento O, Shaknovich R, Fontan L, Fresquet V, Perez-Roger I, Robles EF, De Smedt L, Sagaert X, Melnick A, Martinez-Climent JA (2013) Downregulation of FOXP1 is required during germinal center B-cell function. Blood 121:4311-4320.
Saito T, Hanai S, Takashima S, Nakagawa E, Okazaki S, Inoue T, Miyata R, Hoshino K, Akashi T, Sasaki M, Goto Y, Hayashi M, Itoh M (2011) Neocortical layer formation of human developing brains and lissencephalies: consideration of layer-specific marker expression. Cereb Cortex 21:588-596.
Sanders SJ et al. (2015) Insights into Autism Spectrum Disorder Genomic Architecture and Biology from 71 Risk Loci. Neuron 87:1215-1233.
Sandin S, Lichtenstein P, Kuja-Halkola R, Larsson H, Hultman CM, Reichenberg A (2014) The familial risk of autism. JAMA : the journal of the American Medical Association 311:1770-1777.

Shattuck PT, Durkin M, Maenner M, Newschaffer C, Mandell DS, Wiggins L, Lee LC, Rice C, Giarelli E, Kirby R, Baio J, Pinto-Martin J, Cuniff C (2009) Timing of identification among children with an autism spectrum disorder: findings from a population-based surveillance study. J Am Acad Child Adolesc Psychiatry 48:474-483.

Shigekawa T, Ijichi N, Ikeda K, Horie-Inoue K, Shimizu C, Saji S, Aogi K, Tsuda H, Osaki A, Saeki T, Inoue S (2011) FOXP1, an estrogen-inducible transcription factor, modulates cell proliferation in breast cancer cells and 5-year recurrence-free survival of patients with tamoxifen-treated breast cancer. Horm Cancer 2:286-297.

Shu W, Yang H, Zhang L, Lu MM, Morrisey EE (2001) Characterization of a new subfamily of winged-helix/forkhead (Fox) genes that are expressed in the lung and act as transcriptional repressors. The Journal of biological chemistry 276:27488-27497.

Shu W, Lu MM, Zhang Y, Tucker PW, Zhou D, Morrisey EE (2007) Foxp2 and Foxp1 cooperatively regulate lung and esophagus development. Development 134:1991-2000.

Shu W, Cho JY, Jiang Y, Zhang M, Weisz D, Elder GA, Schmeidler J, De Gasperi R, Sosa MA, Rabidou D, Santucci AC, Perl D, Morrisey E, Buxbaum JD (2005) Altered ultrasonic vocalization in mice with a disruption in the Foxp2 gene. Proceedings of the National Academy of Sciences of the United States of America 102:9643-9648.

Sin C, Li H, Crawford DA (2015) Transcriptional regulation by FOXP1, FOXP2, and FOXP4 dimerization. J Mol Neurosci 55:437-448.

Sniekers S et al. (2017) Genome-wide association meta-analysis of 78,308 individuals identifies new loci and genes influencing human intelligence. Nature genetics.

Sollis E, Graham SA, Vino A, Froehlich H, Vreeburg M, Dimitropoulou D, Gilissen C, Pfundt R, Rappold GA, Brunner HG, Deriziotis P, Fisher SE (2016) Identification and functional characterization of de novo FOXP1 variants provides novel insights into the etiology of neurodevelopmental disorder. Human molecular genetics 25:546-557.

Song H, Makino Y, Noguchi E, Arinami T (2015) A case report of de novo missense FOXP1 mutation in a non-Caucasian patient with global developmental delay and severe speech impairment. Clin Case Rep 3:110-113.

Spiteri E, Konopka G, Coppola G, Bomar J, Oldham M, Ou J, Vernes SC, Fisher SE, Ren B, Geschwind DH (2007) Identification of the transcriptional targets of FOXP2, a gene linked to speech and language, in developing human brain. American journal of human genetics 81:1144-1157.

Srivastava S, Cohen JS, Vernon H, Baranano K, McClellan R, Jamal L, Naidu S, Fatemi A (2014) Clinical whole exome sequencing in child neurology practice. Ann Neurol 76:473-483.

Stessman HA et al. (2017) Targeted sequencing identifies 91 neurodevelopmental-disorder risk genes with autism and developmental-disability biases. Nature genetics.

Stroud JC, Wu Y, Bates DL, Han A, Nowick K, Paabo S, Tong H, Chen L (2006) Structure of the forkhead domain of FOXP2 bound to DNA. Structure 14:159-166.

Surmeli G, Akay T, Ippolito GC, Tucker PW, Jessell TM (2011) Patterns of spinal sensory-motor connectivity prescribed by a dorsoventral positional template. Cell 147:653-665.

Takayama K, Horie-Inoue K, Ikeda K, Urano T, Murakami K, Hayashizaki Y, Ouchi Y, Inoue S (2008) FOXP1 is an androgen-responsive transcription factor that negatively regulates androgen receptor signaling in prostate cancer cells. Biochem Biophys Res Commun 374:388-393.

Talkowski ME et al. (2012) Sequencing chromosomal abnormalities reveals neurodevelopmental loci that confer risk across diagnostic boundaries. Cell 149:525-537.

Tamura S, Morikawa Y, Iwanishi H, Hisaoka T, Senba E (2004) Foxp1 gene expression in projection neurons of the mouse striatum. Neuroscience 124:261-267.

Tang B, Becanovic K, Desplats PA, Spencer B, Hill AM, Connolly C, Masliah E, Leavitt BR, Thomas EA (2012) Forkhead box protein p1 is a transcriptional repressor of immune signaling in the CNS; implications for transcriptional dysregulation in Huntington disease. Human molecular genetics.

Teramitsu I, Kudo LC, London SE, Geschwind DH, White SA (2004) Parallel FoxP1 and FoxP2 expression in songbird and human brain predicts functional interaction. The Journal of neuroscience : the official journal of the Society for Neuroscience 24:3152-3163.

van Keimpema M, Gruneberg LJ, Schilder-Tol EJ, Oud ME, Beuling EA, Hensbergen PJ, de Jong J, Pals ST, Spaargaren M (2017) The small FOXP1 isoform predominantly expressed in activated B cell-like diffuse large B-cell lymphoma and full-length FOXP1 exert similar oncogenic and transcriptional activity in human B cells. Haematologica 102:573-583.

Verkerk AJ, Pieretti M, Sutcliffe JS, Fu YH, Kuhl DP, Pizzuti A, Reiner O, Richards S, Victoria MF, Zhang FP, et al. (1991) Identification of a gene (FMR-1) containing a CGG repeat coincident with a breakpoint cluster region exhibiting length variation in fragile X syndrome. Cell 65:905-914.

Vernes SC, Oliver PL, Spiteri E, Lockstone HE, Puliyadi R, Taylor JM, Ho J, Mombereau C, Brewer A, Lowy E, Nicod J, Groszer M, Baban D, Sahgal N, Cazier JB, Ragoussis J, Davies KE, Geschwind DH, Fisher SE (2011) Foxp2 regulates gene networks implicated in neurite outgrowth in the developing brain. PLoS genetics 7:e1002145.

Vissers LE, Gilissen C, Veltman JA (2016) Genetic studies in intellectual disability and related disorders. Nature reviews Genetics 17:9-18.

Wang B, Lin D, Li C, Tucker P (2003) Multiple domains define the expression and regulatory properties of Foxp1 forkhead transcriptional repressors. The Journal of biological chemistry 278:24259-24268.

Wang B, Weidenfeld J, Lu MM, Maika S, Kuziel WA, Morrisey EE, Tucker PW (2004) Foxp1 regulates cardiac outflow tract, endocardial cushion morphogenesis and myocyte proliferation and maturation. Development 131:4477-4487.

Weigel D, Jurgens G, Kuttner F, Seifert E, Jackle H (1989) The homeotic gene fork head encodes a nuclear protein and is expressed in the terminal regions of the Drosophila embryo. Cell 57:645-658.

Werling DM, Geschwind DH (2013) Sex differences in autism spectrum disorders. Curr Opin Neurol 26:146-153.

Xiao J, He B, Zou Y, Chen X, Lu X, Xie M, Li W, He S, You S, Chen Q (2016) Prognostic value of decreased FOXP1 protein expression in various tumors: a systematic review and meta-analysis. Sci Rep 6:30437.

Zoghbi HY, Bear MF (2012) Synaptic dysfunction in neurodevelopmental disorders associated with autism and intellectual disabilities. Cold Spring Harb Perspect Biol 4.

# CHAPTER TWO:

# FOXP1 ORCHESTRATION OF ASD-RELEVANT SIGNALING PATHWAYS IN THE STRIATUM

Adapted From: **Araujo, D.J.***, Anderson, A.G.*, Berto, S., Runnels, W., Harper, M., Ammanuel, S., Rieger, M.A., Huang, H.C., Rajkovich, K., Loerwald, K.W., Dekker, J.D., Tucker, H.O., Dougherty, J.D., Gibson, J.R., Konopka, G. FoxP1 orchestration of ASD-relevant signaling pathways in the striatum. **Genes and Development** 29, 2081-2096 (2015). *These authors contributed equally to this work.

## ABSTRACT

Mutations in the transcription factor *Forkhead Box P1* (*FOXP1*) are causative for neurodevelopmental disorders such as autism. However, the function of FOXP1 within the brain remains largely uncharacterized. Here, we identify the gene expression program regulated by FoxP1 in both human neural progenitor cells and the brains of patient-relevant heterozygous *Foxp1* knockout mice. We demonstrate a role for FoxP1 in the transcriptional regulation of autism-related pathways as well as genes involved in neuronal activity. We show that Foxp1 regulates the excitability of striatal medium spiny neurons and that reduction of Foxp1 correlates with defects in ultrasonic vocalizations. Finally, we demonstrate that FoxP1 has an evolutionarily conserved role in regulating pathways involved in striatal neuron identity through gene expression studies in human neural progenitors with altered FOXP1 levels. These data support an integral role for

FoxP1 in regulating signaling pathways vulnerable in autism and the specific regulation of striatal pathways important for vocal communication.

## INTRODUCTION

Autism spectrum disorder (ASD) denotes a group of heterogeneous neurodevelopmental conditions all characterized by diminished sociability, impaired communication, restricted interests, and stereotypic behaviors. While there is a strong genetic component to ASD, this is divided amongst several hundred genes each with only a small contribution to the prevalence of the disorder (Geschwind and State, 2015). Furthermore, many autism-risk genes are thought to exert their effects during early brain development (State and Sestan, 2012; Xu et al., 2014; Parikshak et al., 2015). Transcription factors play a key role in orchestrating the spatial and temporal gene expression patterns important for early brain development. Therefore, the identification of gene networks regulated by transcription factors implicated in ASD should provide broad insights into the developmental mechanisms at risk in autism.

The transcription factors FOXP1 and FOXP2 have been implicated in neurodevelopmental disorders such as ASD and developmental verbal dyspraxia (DVD), respectively (Bacon and Rappold, 2012). Forkhead box p1 (Foxp1) is a member of the Fox family of transcription factors, for which there is a designated protein nomenclature (uppercase for primates, title case for rodents, and mixed case for all other or collection of species) (Kaestner et al., 2000). Foxp1 is highly enriched within the developing and mature neocortex, hippocampus, and striatum (Ferland et al., 2003; Teramitsu et al.,

2004). Numerous studies have identified heterozygous deletions point mutations, and duplications of *FOXP1* as being causal for ASD (Bacon and Rappold, 2012). In particular, recent large-scale whole-exome sequencing efforts have identified recurrent *de novo* mutations in *FOXP1* to be associated with ASD (Iossifov et al., 2014). Therefore, understanding how FOXP1 functions within the brain should allow for key insights into the molecular pathways at risk in this disorder. Several reports have begun to elucidate a role for Foxp1 in the brain (Rousso et al., 2012; Tang et al., 2012) and recent work has shown that mice with brain-specific loss of *Foxp1* have altered hippocampal electrophysiology, striatal morphology, and diminished sociability (Bacon et al., 2014). However, the region-specific transcriptional profile of Foxp1 in the mouse brain, how well this profile is conserved in human-relevant *Foxp1* haploinsufficient models, and the behavioral consequences of disrupting these regional transcriptomes, remains unknown.

FOXP2 is a paralog of FOXP1 and mutations in the *FOXP2* gene lead to a number of brain and cognitive deficits including DVD (Fisher and Scharff, 2009; Bacon and Rappold, 2012). In addition to being able to heterodimerize with Foxp2, Foxp1 expression overlaps with Foxp2 expression in the GABAergic medium spiny neurons (MSNs) of the striatum, a brain region critically involved in human language, vocal imitation in zebra finches, and rodent ultrasonic vocalizations (USVs) (Ferland et al., 2003; Li et al., 2004; Teramitsu et al., 2004; Fisher and Scharff, 2009). Additionally, *Foxp2* mutant mice demonstrate disruptions in mouse USVs as well as alterations in the electrophysiological and projection properties of MSNs (Shu et al., 2005; Enard et al., 2009; Vernes et al., 2011; French et al., 2012). Given the role for both Foxp1 and Foxp2 in the striatum, we

hypothesized that Foxp1 regulates regional-gene expression patterns in the brain and that normal levels of Foxp1 are crucial for mouse vocalization behavior. To test this hypothesis, we took advantage of a heterozygous (*Foxp1*$^{+/-}$) mouse model and a human neural progenitor cellular model with altered expression of FOXP1. Using high-throughput sequencing technologies, we used these two systems to identify a conserved role for FoxP1 in regulating autism-risk genes. We show that Foxp1 differentially regulates the excitability of dopamine receptor 1 positive versus dopamine receptor 2 positive MSNs. We also demonstrate reduced USVs in *Foxp1*$^{+/-}$ mice, similar to that seen in *Foxp2*$^{+/-}$ mice (Shu et al., 2005). This similarity in behavioral phenotype is reflected at the genomic level as Foxp1-regulated genes in the striatum overlap with genes regulated by Foxp2 in the striatum. Finally, we find that FoxP1 regulates conserved pathways involved in striatal identity in both human and mouse. Taken together, these results suggest that FoxP1 plays a critical role in regulating striatal function and vocal communication, which, when disrupted, contributes to phenotypes characteristic of ASD.

## MATERIALS AND METHODS

### Mice

*Foxp1* heterozygous knockout (*Foxp1*$^{+/-}$) mice were backcrossed with C57BL/6J mice for at least 10 generations to obtain congenic animals. *Drd1a-tdTomato* line 6 and *Drd2-GFP* reporter mice were generously provided by Dr. Craig Powell and maintained on a C57BL/6J background. Mice were kept in the barrier facilities of the University of Texas Southwestern Medical Center under a 12 h light–dark cycle and given ad libitum access

to water and food. All studies with mice were approved by the University of Texas Southwestern Institutional Animal Care and Use Committee.

**hNP Cultures**

hNP cultures were purchased from Lonza and maintained as previously described (Konopka et al., 2012). hNPs were transduced with lentiviruses containing pLUGIP-FOXP1-3XFlag or pLUGIP-GFP (control) and harvested 3 days after transduction for downstream applications, including immunoblotting, qPCR, RNA-seq, and ChIP-seq.

**RNA Harvesting and qPCR**

RNA was purified from either hNPs or tissues dissected out from P47 male *Foxp1*$^{+/-}$ mice and littermate controls using an mRNeasy minikit (Qiagen) following the manufacturer's recommendations. qPCR was performed as previously described (Spiteri et al., 2007). All primer sequences are available on request.

**RNA-seq**

mRNA was isolated from total RNA samples using polyA selection. Four independent samples from each brain region or cell type per genotype were included for a total of 24 mouse samples and eight human samples. Samples were randomized, and barcoded libraries were generated following the manufacturer's instructions (Illumina). RNA-seq was performed by the McDermott Sequencing Core at the University of Texas Southwestern Medical Center on an Illumina HiSeq 2000 sequencer (Illumina). Stranded,

single-end 50-base-pair (bp) reads were generated for the hNP data, and stranded, paired-end 100-bp reads were generated for the mouse data.

**RNA-seq Data Analysis**

Reads were aligned to either hg19 or mm10 using TopHat (Trapnell et al., 2009) and Bowtie (Langmead et al., 2009). To obtain the gene counts, we used the HTSeq package (Anders et al., 2014), and the reads were normalized using the RPKM (reads per kilobase per million mapped reads) method (Mortazavi et al., 2008) implemented in the RSeQC package (Wang et al., 2012). For further analysis, we performed a sample-specific RPKM filtering considering genes with RPKM values of 0.5 in treatments or controls. EdgeR (Robinson et al., 2010) was used to detect the DEGs in each species. We applied a filter of FDR of $<0.05$ and absolute log fold change of $>0.3$ for both the human and mouse data sets. We then reconstructed the human and mouse co-expression networks using the R package WGCNA (Langfelder and Horvath, 2008). Modules were characterized using the biweight midcorrelation followed by signed network topology for both human and mouse data. Modules containing ≥30 genes were included in our analyses. For module visualization, we used the publically available VisANT software (Hu et al., 2013). To determine the reliability of the WGCNA module characterization and the DEGs, we performed a permutation test randomizing 1000 times the expression data associated with each gene, calculated the DEGs, and then applied the same module characterization. None of the permuted data showed similar module detection or different expression profiles compared with the observed data. We then considered the detected

modules, the detected DEGs, and the further gene overlaps significantly different from random expectation (permutation test, p=0.001). To infer the significance of the potential overlaps, we adapted a hypergeometric test. The resultant p-values were adjusted using the Benjamini-Hochberg FDR method (Benjamini and Hochberg, 1995).

**Foxp2 Microarray Analysis**

Data from project GSE13588 (Enard et al., 2009) were downloaded from Gene Expression Omnibus (GEO) (http://www.ncbi.nlm.nih.gov/geo). Only *Foxp2* heterozygous and matching control samples were selected for further analysis. Microarrays were analyzed using the R programming language and Bioconductor packages. We determined gene expression levels (robust multichip average (RMA) values) and MAS5 detection p-values from the probes using the "affy" library (Gautier et al., 2004). We considered the probe sets detected in at least one sample for a $p<0.05$. Differentially expressed probe sets were then determined adapting the f-test function implemented in the "multtest" library (Pollard et al., 2005). The resulting p-values were then adjusted with the Benjamini-Hochberg method. Probe sets were considered differentially expressed for an adjusted $p<0.05$.

**GO Analysis**

GO analysis was carried out using DAVID (http://david.abcc.ncifcrf.gov). A category containing at least three genes and a corrected p-value of <0.05 (Benjamini-Hochberg method) was considered significant.

**Antibodies**

The following antibodies were used for immunoblotting (IB), immunoprecipitation (IP), or immunocytochemistry (ICC): anti-β-tubulin (rabbit, 1:10,000; abcam, 6046 [IB]), anti-FLAG (mouse, 1:10,000 [IB/ICC], 10 μg [IP]; Sigma, F1804), anti-Foxp1 (rabbit, 1:5000 [IB], 1:1000 [ICC]) (Spiteri et al., 2007), anti-GAPDH (mouse, 1:5000; Millipore [IB]), and anti-Tuj1 (mouse, 1:1000 [ICC]; Covance, MMS-435P).

**ChIP-seq**

Fifty-million hNPs were used per experimental condition. Cells were fixed in 1% methanol-free formaldehyde for 10 min at room temperature and then quenched with glycine (125 mM final). Cells were washed twice in 1× cold PBS, resuspended in 10 mL of lysis buffer (50 mM HEPES-KOH at pH 7.5, 140 mM NaCl, 1 mM EDTA, 10% glycerol, 0.5% IGEPAL-CA630, 0.25% TritonX-100, 10 μL/mL protease inhibitor [PI] cocktail [Sigma], 7 μL/mL PMSF), and incubated for 10 min on ice. Pelleted cell nuclei were then resuspended in 1 mL of nucleus lysis buffer (200 mM NaCl, 1 mM EDTA, 0.5 mM EGTA, 10 mM Tris-HCl at pH 8.0, 10 μL/mL PI, 7 μL/mL PMSF) and incubated for 10 min on ice. Samples were sonicated in 300 μL of shearing buffer (1 mM EDTA, 0.5 mM EGTA, 10 mM Tris-HCl at pH 8.0, 0.1% SDS, 10 μL/mL PI, 7 μL/mL PMSF) using a Bioruptor (Diagenode) at 3-min intervals for a total of 12 min. Ten percent of volume from each sample was collected for input controls. One-hundred micrograms of precleared sheared chromatin and 1 μg of msFlag antibody were incubated overnight at 4°C while rotating. Magnetic IgG

Dynabeads (Invitrogen) were washed three times with 5 mg/mL BSA solution in PBS and then incubated with sheared chromatin/antibody solution for 2 hr at 4°C. Magnets were applied to samples at 4°C, and beads were washed with 500 $\mu$L of each of the following solutions supplemented with PI and rotated for 5 min at 4°C followed by magnetic separation: (1) low-salt wash buffer (0.1% SDS, 1% TritonX-100, 2 mM EDTA, 20 mM Tris-HCl at pH 8.0, 150 mM NaCl), (2) high-salt wash buffer (0.1% SDS, 1% TritonX-100, 2 mM EDTA, 20 mM Tris-HCl at pH 8.0, 500 mM NaCl), (3) LiCl wash buffer (0.25 M LiCl, 1% IGEPAL-CA630, 1% deoxycholic acid, 1 mM EDTA, 10 mM Tris-HCl at pH 8.0), and (4) TE buffer. After washes, beads were resuspended in elution buffer (50 mM Tris-HCl, 10 mM EDTA, 1% SDS) and incubated for 15 min at 65°C with vortexing every 2 min. Beads were magnetically separated, supernatant was collected, and cross-linking of all samples and inputs was reversed overnight at 65°C. DNA was purified using Qiagen MinElute columns and quantified using a Qubit Fluorometer. Sequencing was performed by the University of Texas Southwestern Medical Center McDermott Sequencing Core.

**ChIP-seq Data Analysis**

Reads were mapped to the human genome (hg19) using TopHat (Trapnell et al., 2009) and Bowtie (Langmead et al., 2009). The aligned reads were subsequently down-sampled according to the lowest number of reads detected, whereas the potential duplicated reads were removed using the Picard package (http://broadinstitute.github.io/picard). The uniquely mapped reads were then analyzed using MACS (Zhang et al., 2008) for the detection of potential peaks. PeakSplitter

(Salmon-Divon et al., 2010) was used to subdivide the larger peaks into smaller, more precise peaks using a height filtering of 0.7. The FOXP1 peaks were further compared with the GFP peaks applying a tag density ratio (TDR). For further analysis, we considered FOXP1 peaks with a TDR >2.0. The uncovered peaks were then annotated using the AnnotatePeaks function implemented in the HOMER package (Heinz et al., 2010).

**Immunoblotting**

Cellular lysates were obtained using lysis buffer containing 0.5% Nonidet P-40,1 mM PMSF, 0.1 mM $Na_3VO_4$, 50 mM NaF, 1 uM DTT, 2 $\mu$g/mL pepstatin, and 1 $\mu$g/mL leupeptin. Tissue samples were lysed in buffer containing 1% Igepal, 1 mM PMSF, 0.1 mM $Na_3VO_4$, 2 $\mu$g/mL pepstatin, and 1 $\mu$g/mL leupeptin. Protein concentrations were determined using a Bradford assay (Bio-Rad). A total of 35–45 $\mu$g of each sample was run and processed following standard protocols for both HRP-conjugated and fluorescent secondary antibodies.

**Immunocytochemistry**

hNPs were grown on glass coverslips and fixed with 4% PFA in PBS for 15 min and then washed with TBS at room temperature. Cells were permeabilized with TBS-T (0.4% Triton-X) for 15 min at room temperature and then washed with TBS at room temperature. Cells were treated with a blocking solution made of 3% normal donkey serum in TBS-T (0.2% Triton-X) for 30 min at room temperature. Cells were then incubated with primary

antibodies diluted in blocking solution overnight at 4°C. Afterward, cells were rinsed with TBS, treated with secondary antibodies diluted in blocking solution for 1 hr, and then rinsed with TBS, all at room temperature. Slides were imaged using a Zeiss Observer.Z1 inverted microscope and ZEN 2011 software.

**Electrophysiology Methods**

*Electrophysiology Recordings*

Acute brain slices were prepared from *Foxp1*$^{+/-}$ and *Foxp1*$^{+/+}$ mice crossed with either *Drd1a-tdTomato* or *Drd2-GFP* reporter mice (P17–P20) with the following procedure. Mice were anesthetized with 125 mg/kg ketamine and 25 mg/kg xylazine, and the brains were removed. Thalamocortical slices (Agmon and Connors, 1991) 300 $\mu$m thick were cut at ~4°C in dissection buffer, placed in ACSF for 30 min at 35°C, and slowly cooled over the next 30 min to 21°C. Whole-cell recordings were performed in the dorsal striatum, and cells were targeted with IR-DIC optics in an Olympus FV300 confocal microscope. Recordings were performed at 21°C. Data were collected with a 10-kHz sampling rate and a 3-kHz Bessel filter. Striatal neurons were identified by GFP or tdTomato fluorescence using confocal microscopy.

*Electrophysiology Solutions*

ACSF contained 126 mM NaCl, 3 mM KCl, 1.25 mM $NaH_2PO_4$, 2 mM $MgSO_4$, 26 mM $NaHCO_3$, 25 mM dextrose, and 2 mM $CaCl_2$. All slices were prepared in the following dissection buffer: 75 mM sucrose, 87 mM NaCl, 3 mM KCl, 1.25 mM $NaH_2PO_4$, 7 mM

$MgSO_4$, 26 mM $NaHCO_3$, 20 mM dextrose, 0.5 mM $CaCl_2$, and 1 mM kynurenate. All solutions were pH 7.4. ACSF was saturated with 95% $O_2$/5% $CO_2$. Unless stated otherwise, the pipette solution consisted of 130 mM K-Gluconate, 6 mM KCl, 3 mM NaCl, 10 mM HEPES, 0.2 mM EGTA, 4 mM ATP-Mg, 0.3 mM GTP-Tris, 14 mM phosphocreatine-Tris, and 10 mM sucrose. This was adjusted to pH 7.25 and 290 mOsm. The junction potential was ~10 mV and was not corrected.

**Ultrasonic Vocalization Recordings**

*Acquisition and Processing*

USVs were recorded from pups isolated from their dams at P4, P7, and P10. Pups were placed into clean plastic containers inside soundproof Styrofoam boxes and recorded for 3 min. Recordings were acquired using an UltraSoundGate condenser microphone (Avisoft Bioacoustics, CM16) positioned at a fixed height of 20 cm above the pups and were amplified and digitized (~20 dB gain, sampled at 16 bits, 250 kHz) using UltraSoundGate 416H hardware and Avisoft RECORDER software (Avisoft Bioacoustics). Sound spectrograms were prepared in MATLAB (50% overlapping, 512-point Hamming windows), resulting in 1.024-msec temporal resolution and 488.3-Hz spectral resolution. Spectrograms were band-pass filtered to 20–120 kHz and filtered for white noise. Positions of ultrasonic calls were determined automatically using a previously published method (Holy and Guo, 2005).

*Spectral and Temporal Measurements*

Vocalization behavior occurred in spurts of activity ("bouts") separated by longer pauses. To quantify bouts of vocalization, spectrograms were segmented using a pause length of ≥0.25 sec, which was chosen based on the empirical distribution of pause times between calls. All intercall pauses <0.25 sec represent constituents of the same bout of vocalization. The means of the dominant frequency ("mean frequency") as well as the duration time of individual calls were averaged over all calls by animal. The presence of instantaneous pitch jumps in calls was determined by a previously published method (Holy and Guo, 2005), and the fraction of all calls containing such jumps was determined for each animal. The trend slope (in hertz per millisecond) of calls lacking instantaneous pitch jumps was determined by linear regression, and slopes were averaged over all calls by animal.

*Statistical Analysis of Recordings*

Differences between genotypes on all measured features of vocalization were assessed using two-way analysis of variance, testing for main effects of genotype, day, and interaction of genotype by day. Post-hoc multiple comparisons were assessed using Sidak's procedure. Features of vocalization were considered independently.

**Postnatal Righting Reflexes**

Righting reflexes were assessed in P4, P7, and P10 *Foxp1*$^{+/-}$ and littermate control pups. In brief, pups were placed in a supine position on a clean, unobstructed surface, and the time taken to right onto all fours was measured using a stopwatch. A pup failed the test if

its time to right exceeded 1 min. In such cases, the time was scored as 60 sec. Each pup received one trial at each postnatal time point.

**Open Field Test**

The open field assay was performed on adult *Foxp1*$^{+/-}$ and littermate control mice by individually placing each animal in a 16-in × 16-in Plexiglass box and allowing them to explore the arena for 5 min. Videos of each mouse were obtained and scored for average velocity of movement and total distance moved using the EthoVision XT software package (Noldus).

**Rotarod Test**

Adult mice were placed on a textured drum within individual lanes of a Series 8 IITC Life Science rotarod. The drum was programed to accelerate from 4 to 40 rpm within a maximum time frame of 300 sec. Each mouse was positioned forward on the drum, and sensors detected the latency to fall, maximum revolutions per minute at fall, and total distance travelled for each mouse. Sensors were manually activated whenever a mouse made a full rotation holding onto the drum. Mice were tested for three consecutive days with four trials per day, separated by 20-min intervals.

**Grip Strength Test**

Forelimb and hindlimb grip strength was measured on adult mice using Chatillon Force Measurement equipment. Forelimbs or hindlimbs of each mouse were placed on a mesh

wire meter and pulled away from the wire at constant force. Five consecutive measurements were recorded for both hindlimbs and forelimbs and averaged for a final grip strength measurement for each mouse.

**Nesting Behavior**

Mouse nesting behavior was analyzed using a previously described approach (Deacon, 2006). Briefly, adult mice were individually housed overnight with 3 g of intact nesting material in a clean cage. After 16–18 hr, the amount of unused nesting material was weighed, and the nests formed were assessed, to generate a nest quality score of 1–5 for each mouse.

**Grooming Behavior**

Grooming behavior was assessed in adult mice by individually placing each mouse in a clean cage without nesting material and allowing them to habituate for 10 min. Afterward, grooming behaviors were recorded using an HDR-CX535 Handycam video camera (Sony), and videos were then manually scored based on the number of grooming bouts and total time spent grooming for 10 min.

**SHIRPA**

A modified SHIRPA behavioral screen from (Rogers et al., 1997) was performed on adult mice. First, mice were individually placed in a viewing jar for 5 min. During this time, mice were scored for (1) body position (inactive [0], active [1], or excessive activity [2]), (2)

tremors (absent [0] or present [1]), (3) palpebral closure (open [0] or closed [1]), (4) coat appearance (tidy and well-groomed coat [0] or irregularities/piloerection [1]), (5) skin color (blanched [0], pink [1], or deep red [2]), (6) whiskers (absent [1] or present [0]), (7) lacrimation (absent [0] or present [1]), (8) defecation (absent [0] or present [1]), (9) gait (fluid with 3-mm pelvic elevation [0] or lack of fluidity [1]), (10) tail elevation (dragging [0], horizontal elevation [1], or elevated tail [2]), and (11) startle response (none [0], Preyer reflex [1], or reaction in addition to Preyer reflex [2]). Mice were then transferred to a clean cage, and the following behaviors were recorded in or above this arena: (12) touch escape (no response [0], response to touch [1], or flees prior to touch [2]), (13) trunk curl (absent [0] or present [1]), (14) limb grasping (absent [0] or present [1]), (15) pinna reflex (absent [0] or present [1]), (16) corneal reflex (absent [0] or present [1]), (17) contact righting reflex (absent [0] or present [1]), (18) evidence of biting (none [0] or biting in response to handling [1]), (19) vocalizations (nonvocal [0] or audible in response to handling [1]), (20) positional passivity (struggles when held by tail [0], when held by neck [1], or laid supine [2] or no struggle [3]). Both pinna and corneal reflexes were tested with a 0.15-mm-diameter nylon filament from Touch Test Sensory Evaluators (Semmes-Weinstein Monofilaments).

**Other Statistics**

For qPCR, immunoblotting, electrophysiological, and behavioral assays, p-values were calculated with Student's t-test (two-tailed, type 2). F-values were calculated with two-way ANOVA followed by a Tukey post-hoc test for multiway comparison. Data were

assumed to be normally distributed. p-values for overlaps were calculated with a hypergeometric test using a custom-made R script. We obtained an independent background for population size (for humans, human protein-coding genes (20,389 genes) and BrainSpan-expressed genes (15,585 genes) (Kang et al., 2011), and for mice, Allen brain-expressed genes (13,600 genes) (Lein et al., 2007)). We used the protein-coding genes for background in the hypergeometric test used in Figure 2.5E. We used the BrainSpan-expressed genes for background in the hypergeometric test used in Figure 2.5F and Supplemental Figure 2.8. We used the Allen brain-expressed genes for background in the hypergeometric test used for Figure 2.1C and 2.2, A and D, and Supplemental Figure 2.2A. p-values were adjusted for multiple comparisons using the Benjamini-Hochberg FDR procedure when required. A two-way permutation test of 1000 was adapted to validate the overlaps. First, we randomized the external gene sets (for example, ASD or FMRP) by randomly selecting the same number of genes from an independent brain-expressed gene list (for humans, BrainSpan-expressed gene list; for mice Allen-expressed gene list) and subsequently calculating the overlap p-values. The second approach randomized the internal gene sets (for example, STR_DEG or hNP_DEG) by randomly selecting the same number of genes from RNA-seq-expressed genes and subsequently calculating the overlap p-values. Moreover, we adapted a permutation test to evaluate the detected DEGs, randomizing 1000 times the RNA-seq data and recalculating the DEGs. Analysis for RNA-seq, ChIP-seq, and microarrays were performed using custom-made R scripts implementing functions and adapting statistical designs comprised in the libraries used.

## Accession Numbers

The NCBI GEO accession number for the next-generation sequencing data reported in this study is GSE62718.

# RESULTS

## Foxp1 Gene Regulation Within Distinct Brain Regions

In order to assess the ASD-relevant role of Foxp1 within the brain, we took advantage of a *Foxp1* animal model. As *Foxp1* knockout mice are embryonic-lethal at embryonic day 14.5 (E14.5) due to a developmental heart defect (Wang et al., 2004) and as most patients with *FOXP1* mutations are haploinsufficient, we carried out analyses on *Foxp1* heterozygous (*Foxp1*$^{+/-}$) mice (Hu et al., 2006). We tested the specificity of an antibody recognizing FoxP1 using human neural progenitors (hNPs) with forced FOXP1 expression as well as whole brains from E13.5 *Foxp1* KO embryos. We identified expression of two Foxp1 isoforms (A and D), previously shown to be expressed in the mouse brain (Wang et al., 2003), both of which were absent in brain tissue from KO embryos (Supplemental Fig. 2.1A). Three brain regions relevant to ASD with substantial levels of Foxp1 expression are the striatum, hippocampus, and neocortex (Ferland et al., 2003; Maloney et al., 2013). We quantitatively determined an approximately 50% reduction in total Foxp1 protein levels (isoforms A and D) in the *Foxp1*$^{+/-}$ hippocampus or striatum compared to control littermates (Fig. 2.1A,B). Interestingly, neocortical expression of Foxp1 (either total protein or isoform-specific expression) was not reduced

to 50% in *Foxp1*$^{+/-}$ mice, suggesting a homeostatic up-regulation of Foxp1 in the neocortex of these animals (Fig. 2.1A,B and Supplemental Fig. 2.1B,C).

We ascertained potential transcriptional targets of Foxp1 *in vivo* using RNA sequencing (RNA-seq) in the hippocampus or striatum of *Foxp1*$^{-/+}$ mice and control littermates. To identify differentially expressed genes (DEGs), we filtered using a false discovery rate (FDR) of <0.05 and an absolute log fold change of ≥0.3 (Table 2.1). As a control, RNA-seq was also conducted in the neocortex and, not unexpectedly, we observed no significant changes in gene expression (data not shown).

**Foxp1 Regulation of ASD-Associated Pathways in the Striatum and Hippocampus**

To characterize the identified Foxp1 targets with respect to ASD etiology, we compared the list of Foxp1 DEGs with the current list of annotated ASD genes in the Simons Foundation Autism Research Initiative (SFARI) database (667 genes) (http://www.sfarigene.org). We found that *in vivo* Foxp1-regulated genes significantly overlap with ASD genes in both the hippocampus and striatum (Fig. 2.1C). The SFARI database stratifies genes based on the strength of their association with ASD, and when we removed the genes in categories #5 and #6 (hypothesized support and not supported, respectively) and repeated our analyses, we obtained a similar result (17 genes (p=0.057) for striatum and 39 genes (p=0.0001) for hippocampus, hypergeometric tests) (data not shown). Using qPCR, we confirmed 11 of 12 selected targets from the overlap between the *Foxp1*$^{+/-}$ striatal data set and the ASD genes in independent samples (Fig. 2.1D).

Mouse Foxp1 targets were further prioritized with respect to neurodevelopmental human diseases using weighted gene co-expression network analysis (WGCNA), which allows for the discovery of networks (or modules) of genes with high levels of co-expression (Supplemental Fig. 2.2A; (Zhang and Horvath, 2005; Oldham et al., 2008)). The top hub gene (or gene with the highest number of connections) in the striatal-associated MsM18 module is *Dpp10* (dipeptidyl peptidase) (Fig. 2.1E). *DPP10* is an ASD gene that encodes for a protein that regulates surface expression and properties of the potassium channel Kv4.2 (Marshall et al., 2008; Foeger et al., 2012). Of note, the gene encoding Kv4.2, *KCND2*, has also been implicated in ASD (Lee et al., 2014) and is highlighted within the MsM19 module (Supplemental Fig. 2.2C). We also observed and confirmed that *Dpp10* is increased and that *Kcnd2* is decreased in the striatum of *Foxp1*$^{+/-}$ mice (Fig. 2.1F).

Alteration of Kv4.2 function has been previously observed in a mouse model of Fragile X syndrome (FXS) (Gross et al., 2011), and Fragile X mental retardation protein (FMRP)-regulated genes have previously been shown to have significant genomic interactions with ASD-relevant pathways in human brain development (Parikshak et al., 2013). We therefore compared the mouse WGCNA modules with previously identified FMRP targets (Darnell et al., 2011) and found modules containing FMRP targets (MsM1, MsM6, MsM12, MsM14, and MsM23) (Supplemental Fig. 2.2A). While certainly interesting with regards to potential converging pathways, such enrichments need to be interpreted cautiously, as recent work has uncovered that FMRP targets tend to be over-represented in the brain (Ouwenga and Dougherty, 2015). Of particular interest, MsM14

correlates with genotype and contains a number of FMRP target genes, including the gene encoding FMRP (*Fmr1*) (Supplemental Fig. 2.2B), highlighting a potential direct role for coordination of disease-relevant genes in the striatum by Foxp1 and FMRP.

**Foxp1 Regulates Shared Targets with Foxp2 in the Striatum**

As previous work has implicated a role for the related transcription factor FoxP2 in striatal function, including altered MSN electrophysiology and morphology (Enard et al., 2009), and as the striatum is also one of the few brain regions where Foxp1 and Foxp2 have overlapping expression (Ferland et al., 2003), we compared the list of Foxp1 target genes in the striatum with published striatal Foxp2 targets in *Foxp2*$^{+/-}$ mice (Enard et al., 2009). We identified a significant overlap between Foxp1-regulated genes and previously published Foxp2 targets that are changing in the same direction across data sets with reduction of the respective transcription factors, indicating possible co-regulation of these targets (Fig. 2.2A). This overlap represents 12% of the total Foxp1 target genes identified in the striatum. Using independent samples, we confirmed six of these genes changing with Foxp1 expression in the striatum via qPCR (Fig. 2.2B). Within the *in vivo* WGCNA analysis, both Foxp1 and Foxp2 are co-expressed within the MsM3 module, which is enriched for striatal DEGs (Fig. 2.2C). Interestingly, within the MsM3 module, the gene encoding the dopamine receptor *Drd1a* is co-expressed with both *Foxp2* and *Foxp1* (Fig. 2.2C).

MSNs of the striatum are categorized as either $D_1^+$ (expressing the *Drd1a* receptor) or $D_2^+$(expressing the *Drd2* receptor) projection neurons, and these two subpopulations

of neurons are associated with opposing functions in the coordination of motor activity (Gerfen and Surmeier, 2011). To investigate whether disrupted Foxp1 signaling in the striatum would be expected to produce differential gene expression changes in $D_1^+$ versus $D_2^+$ MSNs, we overlapped our RNA-seq data set with published gene lists obtained from translating ribosome affinity purification of $D_1^+$ and $D_2^+$ MSNs (Maze et al., 2014). We found a significant enrichment of both Foxp1 and Foxp2 target genes within $D_1^+$ MSNs specifically (Fig. 2.2D). Although we found that the number of Foxp1 target genes is roughly equally distributed between genes enriched in both $D_1^+$ and $D_2^+$ MSNs (Fig. 2.2D), the number of Foxp2 target genes enriched in $D_1^+$ MSNs is almost twice the number of Foxp2 target genes enriched in $D_2^+$ MSNs (Heiman et al., 2008; Vernes et al., 2011; Maze et al., 2014). These results are in line with published data showing that Foxp2 is more enriched in $D_1^+$MSNs. Moreover, the overlapping targets of Foxp1 and Foxp2 going in the same direction are expressed only in $D_1^+$ MSNs, supporting coordinated regulation in these specific neurons. Interestingly, Foxp1-specific target genes that are enriched in $D_2^+$ MSNs include several genes involved in cation transport (e.g., *Atp1b1*, *Kcnk2*, *Htr7*, *Kcnip2*, and *Hrh3*) (Table 2). Together, these data support a role for Foxp1 and Foxp2 providing coordinated regulation of striatal signaling pathways and that this regulation may be differential between $D_1^+$ and $D_2^+$ MSNs in *Foxp1*$^{+/-}$ mice.

**Reduction of Foxp1 Leads to Differential Changes in the Excitability of MSNs**

Together with the co-regulation of genes by Foxp1 and Foxp2 (Fig. 2.2), the gene expression data indicated a role for FoxP1 in regulating genes coding for proteins

involved in both ion channel and neuronal activity, in particular within $D_2^+$ MSNs (Tables 2.1, 2.2). We therefore investigated the effect of reduced Foxp1 expression on neuronal activity within either $D_1^+$ or $D_2^+$ MSNs. At postnatal day 18 (P18), acute striatal slices were made from progeny of *Foxp1*$^{+/-}$ mice crossed with either *Drd1a-tdTomato*$^{+/-}$ or *Drd2-GFP*$^{+/-}$reporter mice (Gong et al., 2003; Ade et al., 2011) and whole-cell recordings of MSNs were carried out. $D_2^+$ ($GFP^+$) MSNs from *Drd2-GFP*$^{+/-}$*;Foxp1*$^{+/-}$ mice (Fig. 2.3A) exhibited significantly increased excitability, as indicated by the higher number of action potentials evoked for a given current step (Fig. 2.3B,C), an increase in input resistance (Fig. 2.3D), and a decrease in current threshold (Fig. 2.3E). We also observed no differences in resting potential (Fig. 2.3F), the action potential width (Fig. 2.3G), or the frequency of the spontaneous excitatory postsynaptic events (sEPSCs) of $D_2^+$ MSNs (Fig. 2.3H). Interestingly, we did observe a significant decrease in the amplitude of sEPSCs of these MSNs (Fig. 2.3I). Together, these data demonstrate that reduction of Foxp1 leads to increased excitability of $D_2^+$ MSNs in response to reduced Foxp1 expression.

Given the opposing functions traditionally associated with $D_1^+$ and $D_2^+$ MSNs (Gerfen and Surmeier, 2011) and the possibility for differential regulation of gene expression within $D_1^+$and $D_2^+$ MSNs in the *Foxp1*$^{+/-}$ mouse striatum (Fig. 2.2D), we asked whether the increased excitability of $D_2^+$ neurons due to Foxp1 loss was generalizable to all MSNs. Again, at P18, we carried out whole-cell recordings on MSNs from acute striatal slices. Although trending toward a decrease in excitability, $D_1^+$ ($tdTomato^+$) MSNs from *Drd1a-tdTomato*$^{+/-}$*;Foxp1*$^{+/-}$mice (Supplemental Fig. 2.3A) exhibited no significant change in their excitability compared with controls (Supplemental Fig. 2.3B,C). We also

found no significant increase in input resistance (Supplemental Fig. 2.3D) or current threshold (Supplemental Fig. 2.3E) and no significant difference in resting potential (Supplemental Fig. 2.3F) or action potential width with reduction of Foxp1 in these neurons (Supplemental Fig. 2.3G). Finally, we observed no changes in the frequency or amplitude (Supplemental Fig. 2.3H,I) of sEPSCs. These data indicate that haploinsufficiency of Foxp1 causes differential changes in the membrane excitability of $D_1^+$ and $D_2^+$ MSNs.

**Foxp1 Regulates Mouse USVs**

Huntington's and Parkinson's disease mouse models provide evidence for the involvement of MSNs in directing the production of USVs (Pietropaolo et al., 2011; Grant et al., 2014). Additionally, knockout of the *Drd2* receptor reduces the number of USVs produced by mouse pups (Curry et al., 2013). Because we uncovered a significant overlap between *Foxp1*$^{+/-}$ and *Foxp2*$^{+/-}$ striatal target genes as well as altered MSN excitability as a response to loss of Foxp1, we hypothesized that reduction of Foxp1 would lead to an altered USV phenotype similar to that seen in *Foxp2* mutant mice (Shu et al., 2005). To test this hypothesis, we examined the USVs of *Foxp1*$^{+/-}$ mouse pups in a maternal separation paradigm. Paralleling what has previously been seen in *Foxp2*$^{+/-}$ mice (Shu et al., 2005), we observed a significant decrease in both the number of times a *Foxp1*$^{+/-}$ mouse pup called ("bouts") (Fig. 2.4A) and the total number of calls (Fig. 2.4B) compared with littermate controls at P4 and P7 (see the Materials and Methods; Supplemental Fig. 2.4A for analysis details). Additionally, as a trend, the call

bouts and total number of calls produced by the *Foxp1*$^{+/-}$ mouse pups are reduced across all days (Fig. 2.4A,B). We also observed a significant decrease in the mean call frequency, as a trend across all days, in the *Foxp1*$^{+/-}$ mouse pups (Fig. 2.4C). Other parameters, such as average call duration and the fraction of calls with jumps, were not altered (Fig. 2.4D,E). Interestingly, we observed that the average slope of a call was significantly decreased in *Foxp1*$^{+/-}$ mice compared with controls (Fig. 2.4F). This result is the opposite of the increase in call slope exhibited by humanized *Foxp2* mice (Enard et al., 2009).

Differences in weight gain have been proposed to explain some variation seen in the postnatal USVs of transgenic mouse models (Scattoni et al., 2009). However, there were no significant differences in the weight gain of *Foxp1*$^{+/-}$ mice compared with controls (Supplemental Fig. 2.4B). To assess whether the vocalization deficits observed in the *Foxp1*$^{+/-}$ mice are secondary to a generalized impairment in striatal-mediated behaviors, we assessed locomotion in the open field test as well as rotarod performance, forelimb and hindlimb grip strength, nest building, and grooming behaviors in these animals (Supplemental Fig. 2.5). We also performed postnatal righting reflexes as part of an abbreviated SHIRPA battery to evaluate overall neurological function in these mice (see the Materials and Methods; Supplemental Figs. 2.5A, 2.6). In summary, we found that *Foxp1*$^{+/-}$mice display no differences in either the SHIRPA test, righting reflexes, nest building, rotarod performance, or grooming behaviors. Interestingly, *Foxp1*$^{+/-}$ mice do display hyperactivity in the open field test and decreased performance in the forelimb and hindlimb grip test. Together, these data suggest that wild-type levels of Foxp1 expression

are important for normal mouse vocal behavior but are not required for most striatal-based behaviors.

**FOXP1 Gene Regulation in Human Neural Cells**

In order to identify FoxP1 target genes that are most relevant to human brain development and ASD, we characterized the FOXP1 target genes in hNPs, which demonstrate a higher fidelity with *in vivo* brain transcriptomic data than either human embryonic stem cells or induced pluripotent stem cells (Konopka et al., 2012; Stein et al., 2014) and are genetically tractable using lentiviruses (Konopka et al., 2009). As undifferentiated hNPs do not express FOXP1 endogenously and given the current paucity of chromatin immunoprecipitation (ChIP)-grade antibodies against FoxP1, we ascertained direct FOXP1 targets by transducing hNPs with a lentivirus containing Flag-tagged FOXP1 or a GFP control virus (Fig. 2.5A). Forced expression of FOXP1 was limited to the nucleus (Fig. 2.5D).

To identify genome-wide direct targets of FOXP1, we conducted both RNA-seq and ChIP followed by DNA sequencing (ChIP-seq) in hNPs overexpressing FOXP1. Using the Flag tag on FOXP1, we identified >600 genes enriched for FOXP1 binding (Fig. 2.5B,E; Table 2.1). These directly bound targets are enriched for forkhead motifs (Supplemental Fig. 2.7; (Stroud et al., 2006)). Again, using RNA-seq, an FDR of <0.05, and an absolute log fold of ≥0.3, we uncovered >1500 DEGs within this cellular paradigm (Fig. 2.5E; Table 2.1). These DEGs are significantly enriched for gene ontology (GO) categories such as axon guidance, neuronal development, and neuronal differentiation,

and the overlap between both ChIP and RNA-seq data represents directly regulated FOXP1 targets in hNPs (Table 2.3). RNA-seq and ChIP-seq genes significantly overlap (Fig. 2.5E); however, because this overlap is significant yet small, these results suggest that the majority of gene regulation by FOXP1 occurs through indirect effects on signaling cascades, as might be expected for a transcription factor.

**FOXP1 Regulates ASD-Relevant Genes in hNPs**

To further characterize the identified hNP FOXP1 targets with respect to ASD etiology, we again compared the list of FOXP1 DEGs to the current list of annotated ASD genes in the SFARI database. We observed a significant overlap of FOXP1 targets and ASD genes (Fig. 2.5F). When we overlapped the list of hNP DEGs with the curated list of ASD genes (excluding genes in categories #5 and #6), we also obtained a significant overlap (48 genes, p=0.023, hypergeometric test) (data not shown). hNP DEGs that overlapped with the SFARI gene database were selected and confirmed within an independent hNP cell line using an independent measure of expression: qPCR (Fig. 2.5G). Previous work suggested that the members of the Foxp subfamily of forkhead transcription factors are primarily transcriptional repressors (Wang et al., 2003). However, we previously showed that the related transcription factor FOXP2 is also able to activate transcription (Spiteri et al., 2007). In line with those data, we found an almost equal representation of activated and repressed FOXP1 targets that overlap with ChIP-seq and ASD lists (Fig. 2.5H). Additionally, we also confirmed that FOXP1 directly binds within the first intron of *DPP10* and represses its expression in hNPs overexpressing FOXP1 (Fig. 2.5I,J).

Together with the results from the *Foxp1*$^{+/-}$ mice (Fig. 2.1F), this indicates that *Dpp10* is a conserved direct repressed target of FoxP1. Moreover, many genes overlapped with directional consistency between striatum and hNPs (12%) (Table 2.1).

Again, using WGCNA, we uncovered nine modules with first principal components correlating to FOXP1 expression (hNPM2, M3, M4, M6, M7, M13, M16, M20, and M21) (Supplemental Fig. 2.8). We then compared the hNP$^{FOXP1}$ RNA-seq data to recently reported co-expression modules derived from *in vivo* developing human brains (Parikshak et al., 2013). We found a significant overlap of DEGs in the hNP$^{FOXP1}$ data set with this report's M17 module (Table 2.1). The M17 module is one of three modules previously identified to contain a significant overlap with known ASD genes. We also compared the hNP$^{FOXP1}$ RNA-seq data with two other co-expression modules: asdM12 and asdM16 (derived from human brain tissue samples from ASD cases and controls), which were highly correlated with ASD disease status (Table 2.1; (Voineagu et al., 2011)). We found that many genes within these two modules were also found within the modules correlating to FOXP1 expression. Interestingly, *DPP10* is also present in asdM12, which further emphasizes its relevance to ASD etiology. Thus, the data from manipulation of FOXP1 expression in the *in vitro* system recapitulate identified genomic relationships from *in vivo* human brain data.

**Conserved Regulation of FoxP1 Targets Within the Striatum**

To further demonstrate the relevance of the *Foxp1*$^{+/-}$ mouse data with human biology and disease, we performed an analysis of module preservation (Langfelder et al., 2011)

between either the *Foxp1*$^{+/-}$ mouse hippocampal or striatal WGCNA data and the hNP WGCNA data. This approach allows one to determine how conserved gene co-expression relationships are between the two species. Interestingly, we found that there was significantly greater preservation of modules between the *Foxp1*$^{+/-}$ mouse striatal modules and the hNP modules than between the *Foxp1*$^{+/-}$ mouse hippocampal modules and the hNP modules (Fig. 2.6A). To examine whether any of the preserved human co-expression modules contain specific transcription factor-binding motifs, we used the ChIP enrichment analysis (ChEA) database, which contains experimental ChIP and ENCODE data sets (Lachmann et al., 2010). We found enrichment of FOXP2 motifs as well as other autism-related transcription factors (Fig. 2.6B). Finally, we used a recently developed tool—cell-specific expression analysis (Xu et al., 2014)—to examine within which brain regions and cellular populations the conserved FoxP1 targets are enriched. We found that DEGs down-regulated with loss of Foxp1 and up-regulated with overexpression of FOXP1 are enriched for striatal genes (Fig. 2.6C). In contrast, genes up-regulated with loss of Foxp1 and down-regulated with overexpression of FOXP1 are enriched for neocortical genes (Fig. 2.6D). Together, these data suggest that FoxP1 regulates conserved pathways in both humans and mice that are important in preserving MSN identity.

## DISCUSSION

Using unbiased genome-wide approaches in a patient-relevant *Foxp1*$^{+/-}$ mouse model and human neural cells, we uncovered a role for FoxP1 regulation of ASD-relevant genes.

We observed that Foxp1 regulates gene expression in a region-specific manner within the brain, with the hippocampus and the striatum of *Foxp1*$^{+/-}$ mice containing DEGs enriched for distinct ontological categories. We also uncovered altered neuronal excitability in distinct populations of MSNs as well as gross alterations in the postnatal USVs of *Foxp1*$^{+/-}$ mice. Last, we provide evidence that FoxP1 regulates evolutionarily conserved neuronal pathways within the striatum, which are important for striatal identity.

The inclusion of FMRP target genes within FoxP1-correlated modules suggests overarching brain mechanisms at risk in ASD pathophysiology. FMRP is an RNA-binding protein that is expressed throughout the brain and is involved in dendritic morphology and plasticity through the translational regulation of numerous genes that function at the synapse (Darnell and Klann, 2013). Deletions and mutations of the *FMR1* gene can lead to FXS, which is characterized by autistic traits and intellectual disability (Hernandez et al., 2009). We found an enrichment of genes encoding ion channels altered in both the human and rodent FoxP1 models. For example, *DPP10* is an ASD gene that is a conserved FoxP1 target (Figs. 2.1F, 2.5I,J). DPP10 functions to traffic surface expression of the KCND2 and KCND3 (or Kv4.2 and Kv4.3, respectively) potassium channels in neurons. We also uncovered activation of *Kcnd2* by FoxP1 (Fig. 2.1F). Moreover, *KCND2* is an FMRP target (Kim et al., 2005), rare variants and genetic association of *KCND2* have been reported in autism (Klassen et al., 2011; Lee et al., 2014), and impaired KCND2 function has been directly implicated in FXS (Gross et al., 2011). This convergence of Foxp1 downstream genes with FMRP-related genes suggests potential converging transcriptional and translational dysregulation in these disorders.

Relative to the entire brain, *Foxp1* is among the top 100 enriched genes in the striatum (Heiman et al., 2008). This striatal enrichment of *Foxp1* in the brain is greater than the comparative relative striatal expression of *Foxp2*. We showed significant overlaps between Foxp1 and Foxp2 gene targets in the striatum (in particular, $D_1^+$ MSN enriched genes) (Fig. 2.2A,D) and increased $D_2^+$ MSN excitability in *Foxp1*$^{+/-}$ mice (Fig. 2.3). Given that Foxp2 is preferentially expressed in $D_1^+$ MSNs (Vernes et al., 2011), we hypothesize that Foxp1 and Foxp2 may work in concert to differentially regulate neuronal excitability in these two populations of MSNs and therefore control striatal-based vocalizations. Therefore, the lack of alteration of $D_1^+$ MSN excitability in *Foxp1*$^{+/-}$ mice might be due to compensation by Foxp2, as supported by the overlapping target genes of Foxp1 and Foxp2 among $D_1^+$ MSN enriched genes. The identification of Foxp1-specific targets that are known to be involved in neuronal excitability within $D_2^+$ MSNs also supports the idea that differential gene regulation by Foxp1 in specific MSN subpopulations governs the observed neuronal and organismal phenotypes. For instance, Foxp1 may operate as a master regulator of genes important for overall neuronal function and activity in the striatum, with Foxp2 acting as a limiting factor for shared targets involved in vocalizations. This idea is bolstered by previous findings that *Fmr1* and *Foxp2* mutant mice exhibit increased striatal GABAergic transmission from and increased long-term depression in MSNs as well as decreased striatal volumes and deficits in postnatal USVs (Shu et al., 2005; Centonze et al., 2008; Enard et al., 2009; Roy et al., 2012; Ellegood et al., 2015). In addition, *Foxp2* levels are unchanged in the striatum of *Foxp1*$^{+/-}$ mice (Table 2.1) and do not appear to be significantly altered in either

MSN population specifically (data not shown), further suggesting that alterations in Foxp2/Foxp1 stoichiometry in $D_1^+$ MSNs could be driving our findings. Finally, the significant gene co-expression module preservation between the mouse striatal and hNP gene expression data supports the relevance of these mouse data to a human disorder such as ASD. Given the evolutionary distance between these two species and the developmental differences between hNPs and the adult mouse striatum, it is remarkable that these correlations were found. Therefore, such a finding is evidence for the robustness and relevance of these gene co-expression networks with respect to FoxP1 expression and function.

These data suggest a role for Foxp1 in regulating ASD risk genes in a region-specific manner within the brain. In particular, we demonstrate that Foxp1 plays an important role in regulating genes involved in striatal development and function. In this study, we also provide the first evidence that Foxp1 specifically contributes to vocal communication. It will be important to determine how these changes occur throughout development in further experiments. Since the *Foxp1*$^{+/-}$ mice used in this study were whole-body knockouts and because Foxp1 has been shown to regulate the development of a host of organ systems (Wang et al., 2004; Hu et al., 2006; Shu et al., 2007; Feng et al., 2010; Li et al., 2012), it cannot be entirely ruled out that the behavioral phenotypes displayed by these mice are secondary to the peripheral consequences of the knockout. Additionally, it should be noted that other brain regions besides the striatum, such as the neocortex, are known to both express Foxp1 and contribute to the production of USVs (Hisaoka et al., 2010; Sia et al., 2013). Moreover, while this study focused on a patient-

relevant model of FOXP1 function (namely, haploinsufficiency), at least one study has demonstrated increased *FOXP1* expression in lymphoblastoid cell lines from ASD patients (Chien et al., 2013). Therefore, the regional contribution and dosage-relevance of FoxP1 to the behavioral manifestations presented in this study remain to be determined.

## FIGURES FOR CHAPTER TWO

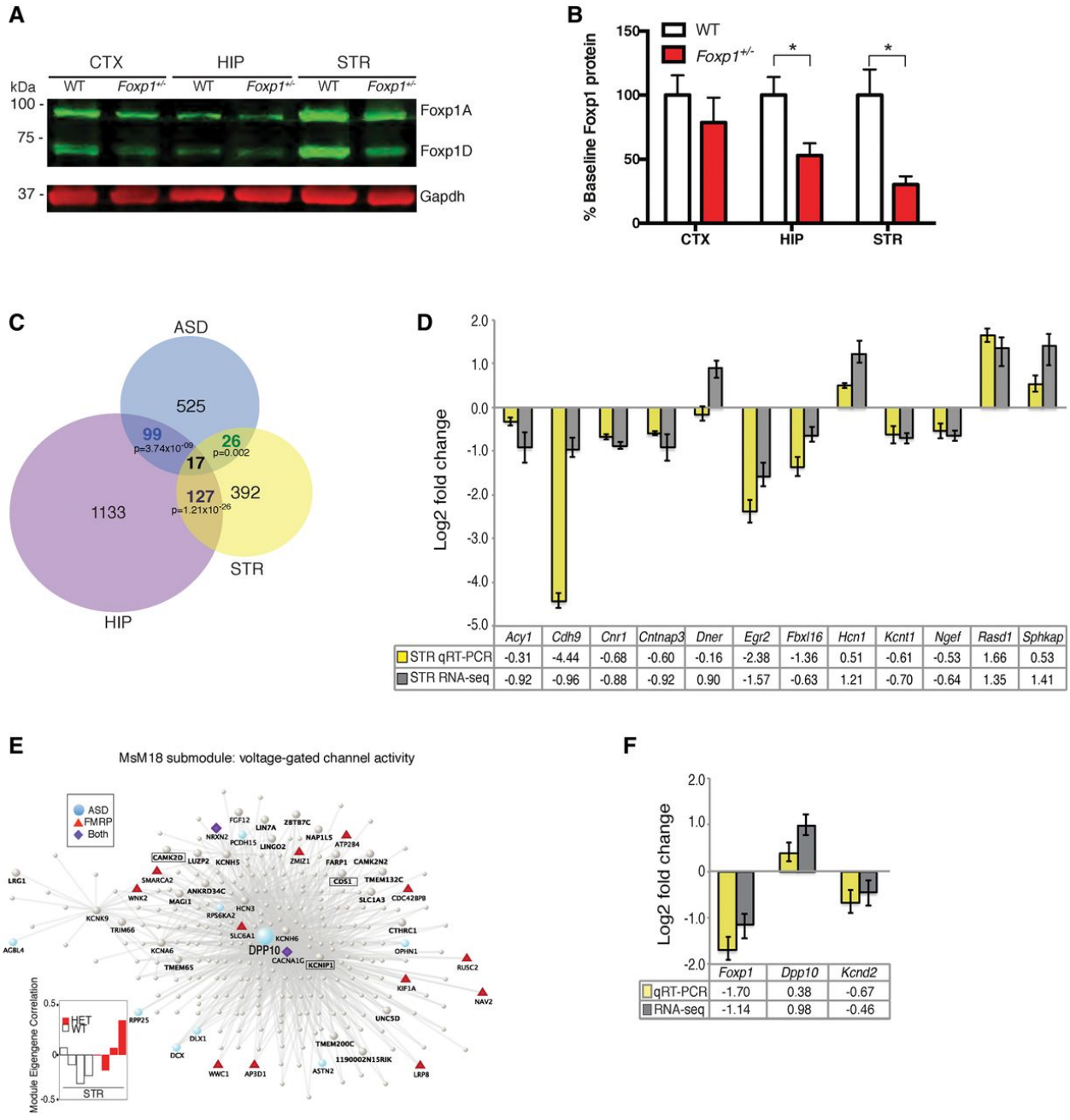


**Figure 2.1. Regulation of ASD genes by Foxp1 in the mouse brain.** (A) Representative immunoblot displaying reduced Foxp1 protein levels in the hippocampus (HIP) and striatum (STR), but not the neocortex (CTX), of *Foxp1*$^{+/-}$mice. GAPDH was used as a loading control. (B) Quantification of Foxp1 expression in adult *Foxp1*$^{+/-}$ mouse

brains. Data are represented as means (±SEM). n=4 mice per genotype for each region. *p=0.033 (hippocampus); *p=0.0163 (striatum), Student's t-test, compared with wild-type levels normalized to GAPDH. (C) Venn diagram showing overlaps between the differentially expressed genes (DEGs) in the mouse and ASD gene lists (144 genes between the hippocampus and striatum ($p=1.21x10^{-26}$), 116 genes between the hippocampus and ASD ($p=3.74\times10^{-9}$), and 43 genes between the striatum and ASD (p=0.002), hypergeometric test (p-values were adjusted using Benjamini-Hochberg FDR procedure)). (D) Confirmation of salient ASD-related gene targets in independent striatal samples from *Foxp1*$^{+/-}$mice using qPCR. Data are represented as means (±SEM). n=4 mice per genotype. With the exception of *Dner*, all qPCR values displayed are significant at $p<0.05$ (Student's t-test, compared with wild-type levels normalized to actin). (E) Visualization of a striatal-specific submodule (MsM18) that contains *Dpp10* (dipeptidyl peptidase) as a major hub gene. (F) qPCR confirmation of *Dpp10 and Kcnd2* activation in *Foxp1*$^{+/-}$mouse striatal samples. Data are represented as means (±SEM). n=4 mice per genotype. All qPCR values displayed are significant at $p<0.05$ (Student's t-test, compared with wild-type levels normalized to actin).

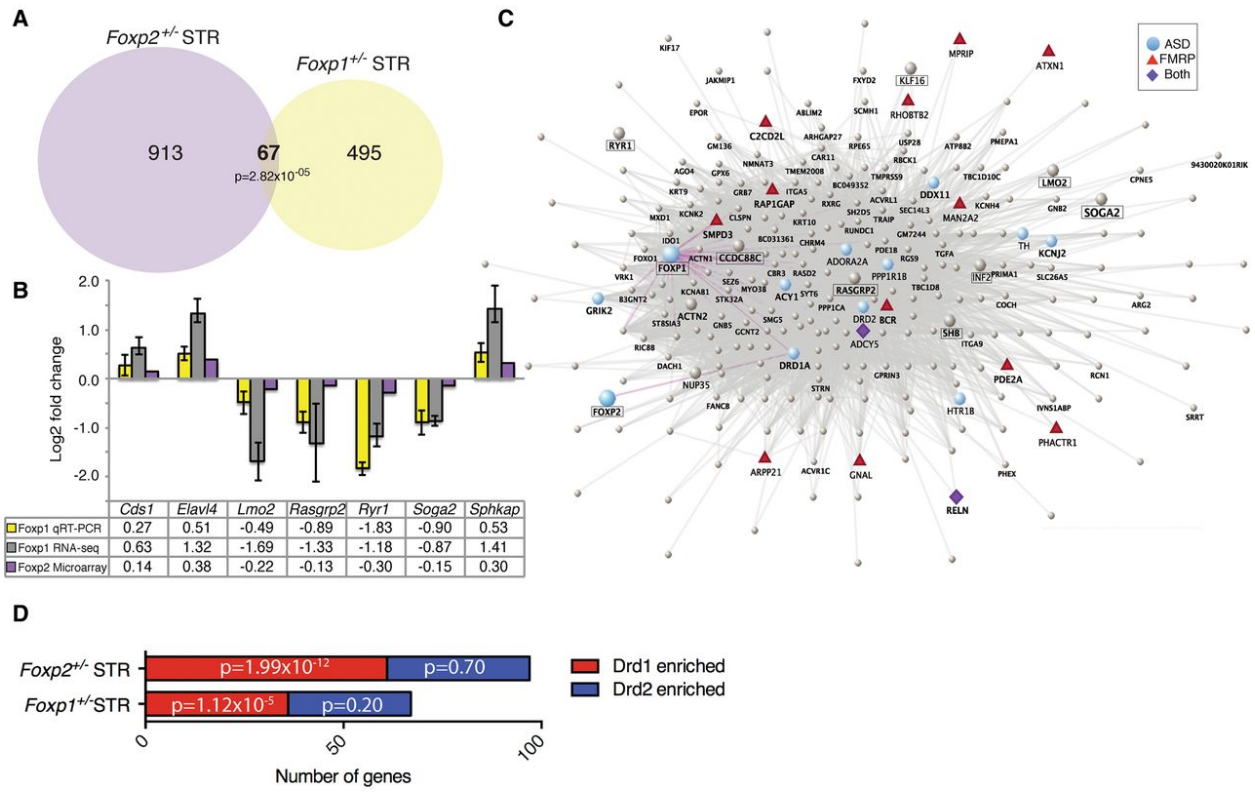


**Figure 2.2. Foxp1 and Foxp2 regulate overlapping targets within the striatum.** (A) Significant overlap of DEGs in the striatum of *Foxp1*$^{+/-}$and *Foxp2*$^{+/-}$ mice (67 genes between the *Foxp1*$^{+/-}$ and the *Foxp2*$^{+/-}$ striatal data sets ($p=2.82\times10^{-5}$), hypergeometric test). (B) qPCR confirmation of a subset of these genes in independent *Foxp1*$^{+/-}$ striatal samples. Data are represented as means (± SEM). n=3 mice per genotype. All qPCR values displayed are significant at $p<0.05$ (Student's t-test, compared with wild-type levels normalized to actin). (C) Visualization of the regionally specific striatal module MsM3 showing co-expression of both Foxp1 and Foxp2. Foxp1 and Foxp2 connections are highlighted in magenta. Genes in bold typeface indicate striatal DEGs, and boxed genes indicate Foxp1 and Foxp2 DEGs that overlap. (D) RNA-seq data from *Foxp1*$^{+/-}$ mice and microarray data from *Foxp2*$^{+/-}$ mice were overlapped with the most recently published list

of known enriched transcripts within $D_1^+$ or $D_2^+$ MSNs (Maze et al., 2014). Genes from both *Foxp1*$^{+/-}$ and *Foxp2*$^{+/-}$ mice significantly overlapped with $D_1^+$ MSN-enriched genes (36 genes $p=1.12\times10^{-5}$) and 61 genes ($p=1.99\times10^{-12}$), respectively, hypergeometric test). p-values for each overlap are shown within bar graphs.

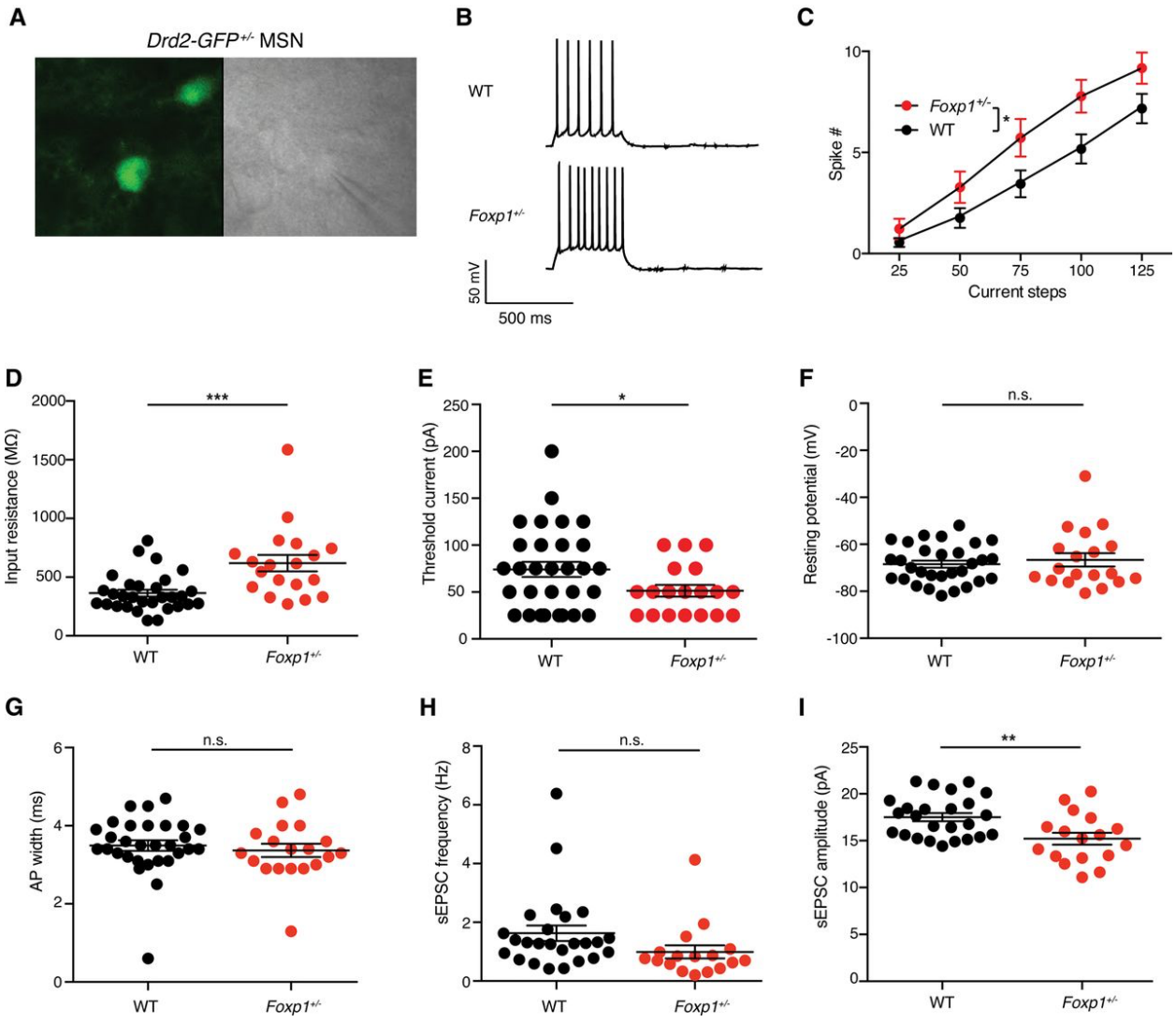


**Figure 2.3. $D_2^+$ MSNs of *Foxp1*$^{+/-}$ mice have increased excitability.** (A) Example image of a recorded GFP$^+$ ($D_2^+$) neuron. (B) Example recordings depicting spiking in response to a 125-pA current step in control and *Foxp1*$^{+/-}$ MSNs. (C) Firing rate versus input curves is significantly increased in *Foxp1*$^{+/-}$ MSNs. Data are represented as means (± SEM). n=18 wild-type cells and 29 *Foxp1*$^{+/-}$ cells. *p=0.040, two-way ANOVA with repeated measures for current step, compared between genotypes. (D) Input resistance is significantly increased *Foxp1*$^{+/-}$ MSNs. Data are represented as means (± SEM). n=19

wild-type cells and 30 *Foxp1*$^{+/-}$ cells. ***p=0.0004, Student's t-test, compared between genotypes. (E) The minimum, threshold current required for evoking an action potential is significantly decreased in *Foxp1*$^{+/-}$ MSNs. Data are represented as means (± SEM). n=19 wild-type cells and 30 *Foxp1*$^{+/-}$ cells. *p=0.049, Student's t-test, compared between genotypes. (F) Resting potential is not significantly changed in *Foxp1*$^{+/-}$ MSNs. Data are represented as means (± SEM). n=19 wild-type cells and 30 *Foxp1*$^{+/-}$ cells. p=0.53, Student's t-test, compared between genotypes. (G) Action potential width is not significantly altered in *Foxp1*$^{+/-}$ MSNs. Data are represented as means (± SEM). n=19 wild-type cells and 30 *Foxp1*$^{+/-}$ cells. p=0.57, Student's t-test, compared between genotypes. (H) Spontaneous EPSC frequency is not significantly changed in *Foxp1*$^{+/-}$ MSNs. Data are represented as means (± SEM). n=17 wild-type cells and 25 *Foxp1*$^{+/-}$ cells. p=0.091, Student's t-test, compared between genotypes. (I) Spontaneous EPSC amplitude is significantly decreased in *Foxp1*$^{+/-}$ MSNs. Data are represented as means (± SEM). n=17 wild-type cells and 25 *Foxp1*$^{+/-}$ cells. **p=0.004, Student's t-test, compared between genotypes.

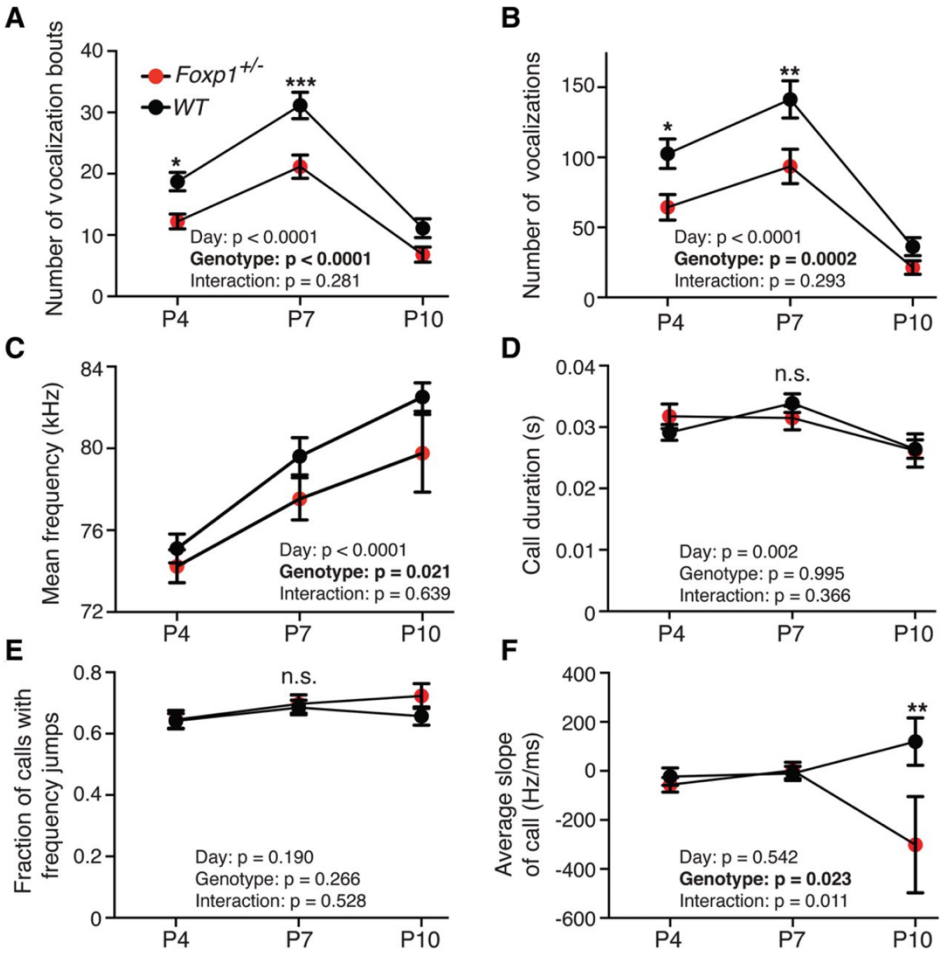


**Figure 2.4. *Foxp1* haploinsufficiency results in reduced mouse vocalizations.** (A) *Foxp1*$^{+/-}$ mouse pups exhibit a significantly reduced number of vocalization bouts. Data are represented as means (± SEM). n=57 wild-type pups and 34 *Foxp1*$^{+/-}$pups. *p=0.033 at P4; ***p=0.0003 at P7, two-way ANOVA with a Sidak multiple comparison test, compared between genotypes. (B) *Foxp1*$^{+/-}$ mouse pups exhibit fewer total numbers of USVs at P7. Data are represented as means (± SEM). n=57 wild-type pups and 34 *Foxp1*$^{+/-}$ pups. *p=0.038 at P4; **p=0.006 at P7, two-way ANOVA with a Sidak multiple comparison test, compared between genotypes. (C) As a trend, *Foxp1*$^{+/-}$ mouse pups exhibit a significant reduction in their mean call frequency across all days. Data are

represented as means (± SEM). n=57 wild-type pups and 34 *Foxp1*$^{+/-}$ pups. Two-way ANOVA with a Sidak multiple comparison test, compared between genotypes. (D) *Foxp1*$^{+/-}$ mice show no differences in average call duration. Data are represented as means (± SEM). n=57 wild-type pups and 34 *Foxp1*$^{+/-}$ pups. p=0.99, two-way ANOVA with a Sidak multiple comparison test, compared between genotypes. (E) *Foxp1*$^{+/-}$ mice show no difference in the fraction of calls with frequency jumps. Data are represented as means (± SEM). n=57 wild-type pups and 34 *Foxp1*$^{+/-}$ pups. p=0.27, two-way ANOVA with a Sidak multiple comparison test, compared between genotypes. (F) *Foxp1*$^{+/-}$ mice display a significant reduction in the average slope of a call at P10. Data are represented as means (± SEM). n=57 wild-type pups and 34 *Foxp1*$^{+/-}$ pups. **p=0.001, two-way ANOVA with a Sidak multiple comparison test, compared between genotypes. The main effects for genotype and postnatal day and the interactions between these two variables are reported at the bottom of each panel.

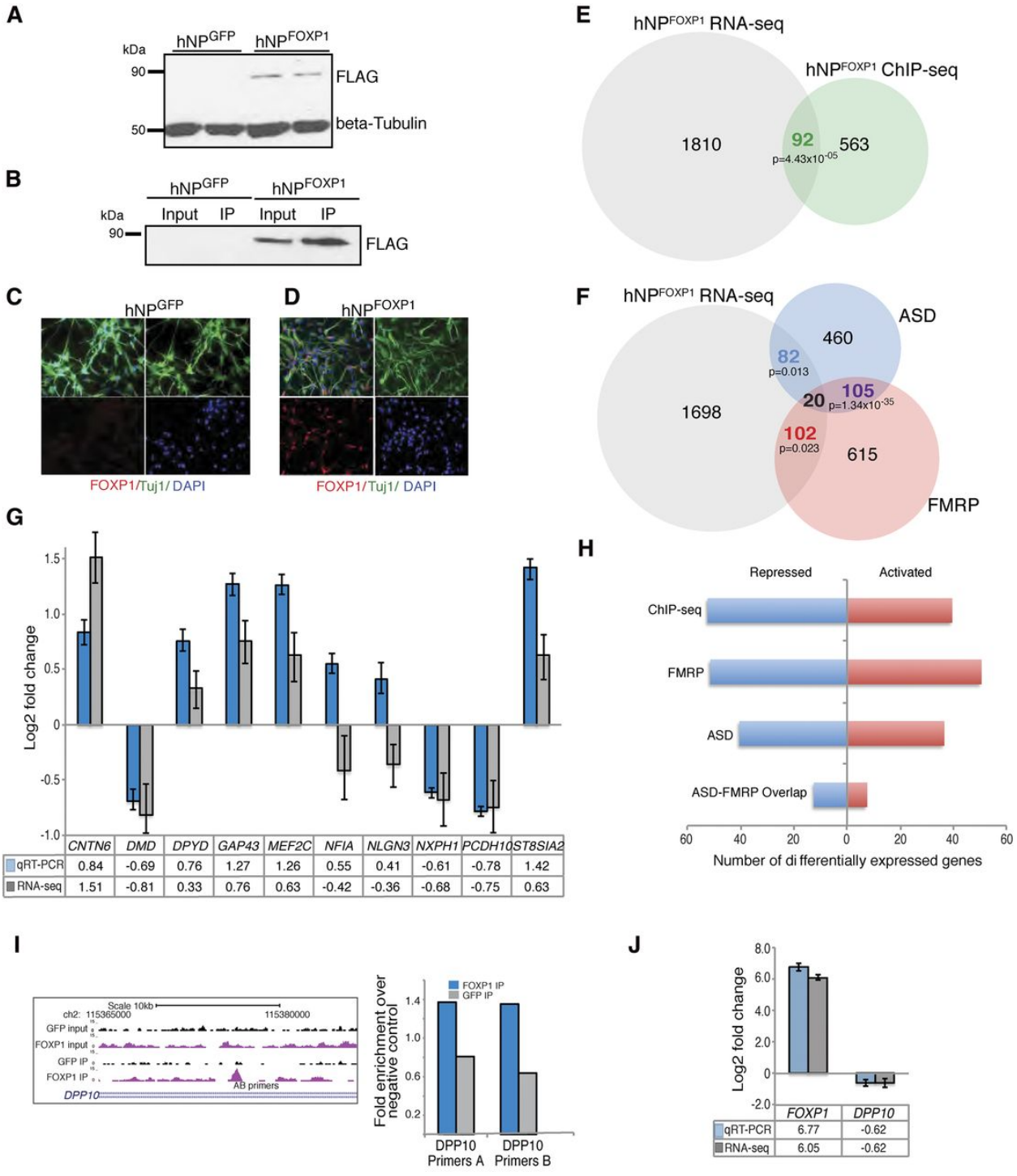


**Figure 2.5. Gene regulation by FOXP1 in human neural cells.** (A) Representative immunoblot depicting overexpression of FOXP-Flag signal in hNPs transduced with a FOXP1-Flag expression construct ($hNP^{FOXP1}$) but not in hNPs with a GFP expression

construct ($hNP^{GFP}$). β-Tubulin was used as a loading control. (B) Representative immunoblot confirming expression of FOXP1-Flag in input samples and enrichment of FOXP1-Flag during the immunoprecipitation (IP) portion of ChIP from $hNP^{FOXP1}$ lysates. (C,D) Representative images of $hNP^{GFP}$ and $hNP^{FOXP1}$ demonstrate that FOXP1 expression (red) in $hNP^{FOXP1}$ is restricted to the nucleus (DAPI, blue) and that FOXP1 is not expressed within neurites (Tuj1, green) and is absent in $hNP^{GFP}$. (E) Significant overlap between gene targets from RNA-seq and ChIP-seq (ChIP followed by DNA sequencing) performed on $hNP^{FOXP1}$ (92 genes between $hNP^{FOXP1}$ RNA-seq and $hNP^{FOXP1}$ ChIP-seq ($p=4.43\times10^{-5}$, hypergeometric test)). (F) Significant overlap among RNA-seq DEGs, ASD genes, and FMRP targets (102 genes between $hNP^{FOXP1}$ RNA-seq and ASD genes (p=0.013), 122 genes between $hNP^{FOXP1}$ RNA-seq and FMRP genes (p= 0.023), and 125 genes between ASD and FMRP genes ($p=1.34\times10^{-35}$), hypergeometric test (p-values were adjusted using Benjamini-Hochberg FDR procedure). (G) qPCR confirmation of a subset of these overlapping genes in independent $hNP^{FOXP1}$ samples. Data are represented as means (± SEM). n=4 samples per treatment. All qPCR values displayed are significant at $p<0.05$ (Student's t-test, compared with $hNP^{GFP}$ levels normalized to actin). (H) DEGs from these overlaps are equally represented among repressed and activated genes. (I, left panel) Human genome browser view showing the ChIP-seq result of enrichment of FOXP1 binding compared with GFP control. (I, right panel) ChIP-PCR confirmation of enriched binding of *DPP10* by FOXP1 in $hNP^{FOXP1}$ compared with $hNP^{GFP}$ using two separate primer pairs (DPP10 primers A and B) compared with control primers. Quantified data are represented as means (± SEM),

four samples per treatment. All qPCR values displayed are significant at $p<0.05$ (Student's t-test, compared with $hNP^{GFP}$ levels normalized to actin). (J) *DPP10* is repressed with FOXP1 overexpression in $hNP^{FOXP1}$ samples. Quantified data are represented as means (± SEM), four samples per treatment. All qPCR values displayed are significant at $p<0.05$ (Student's t-test, compared with $hNP^{GFP}$ levels normalized to actin).

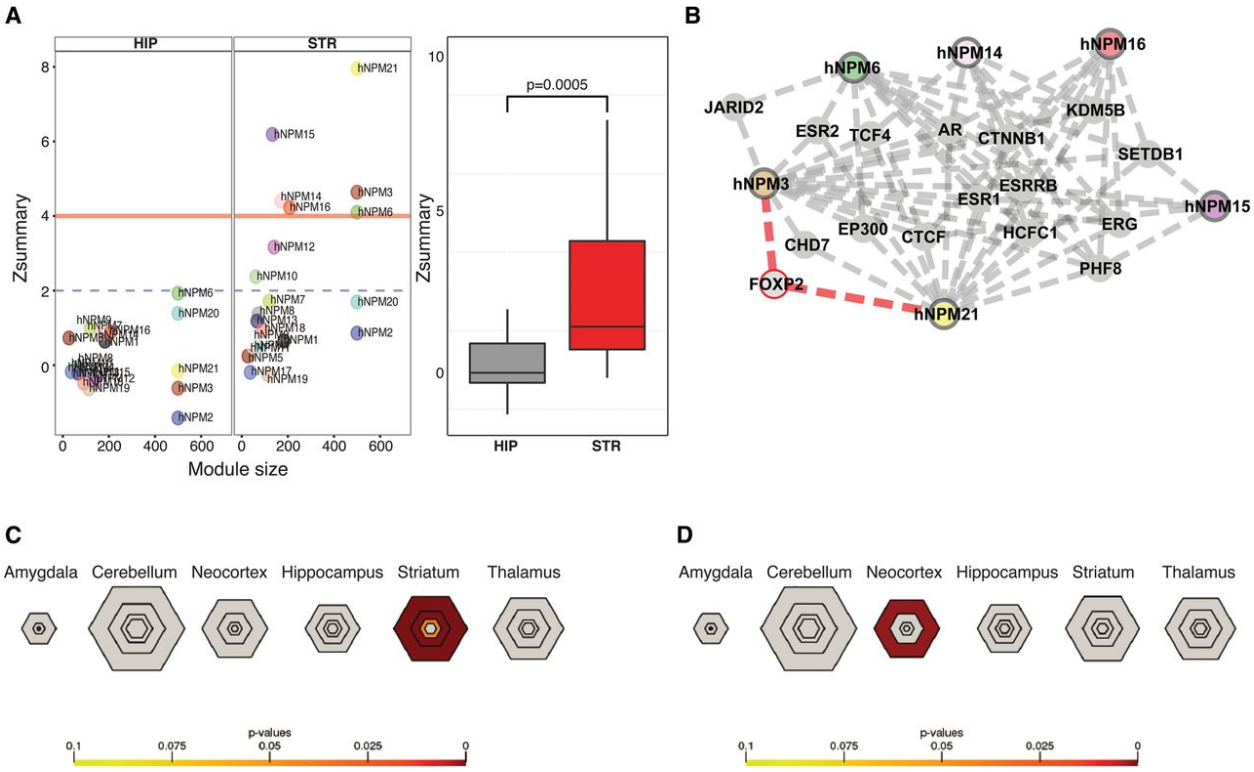


**Figure 2.6. Gene network preservation between mouse and human data sets.** (A) Module preservation analysis revealed that significantly more hNP modules are preserved in the striatum compared with the hippocampus. Zsummary scores >4 are well preserved, and those <2 are poorly preserved. (B) Genes in modules shared between humans and mice contain conserved binding sites for ASD-associated transcription factors, including FoxP2. (C) Genes down-regulated by loss of Foxp1 in mice and up-regulated by overexpression of FOXP1 in hNPs are enriched for striatal-associated genes. (D) Genes up-regulated by loss of Foxp1 in mice and down-regulated by overexpression of FOXP1 in hNPs are enriched for cortical genes. Briefly, hexagons are scaled to the stringency values of the specificity index thresholds (pSI), which ranks the region-specific enriched transcript gene lists from least specific to highly specific

transcripts; i.e., outer hexagons represent larger, less specific lists (pSI of 0.05), while inner hexagons represent shorter, highly specific lists (pSI of 0.001). Bonferroni-Hochberg (BH)-corrected p-values are shown.

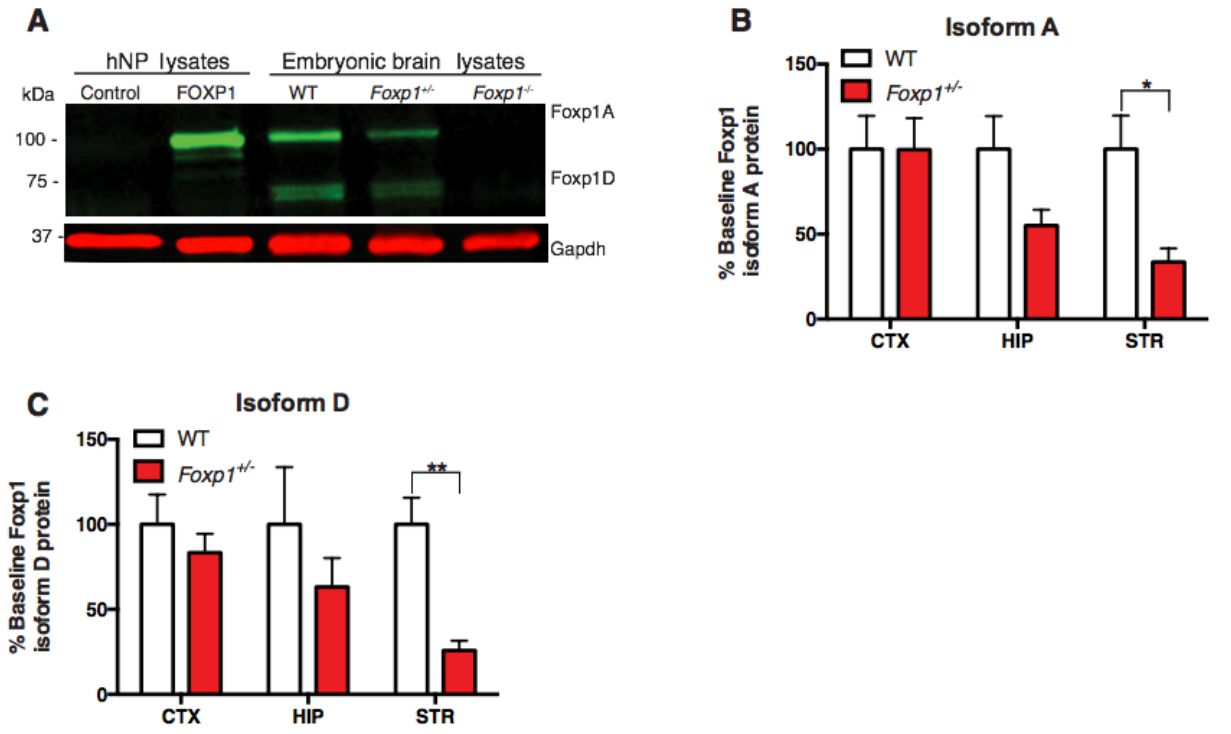


**Supplemental Figure 2.1. Immunoblot for Foxp1 demonstrating antibody specificity.** (A) hNP samples expressing FOXP1 and E13.5 mouse brain lysates from control and *Foxp1*$^{+/-}$ mice demonstrate expression whereas hNPs with GFP expression and brain lysate from *Foxp1* KO embryos do not demonstrate expression. (B) Foxp1A is significantly reduced only in the STR of *Foxp1*$^{+/-}$ mice. Data are represented as means (±SEM). n=4 mice/genotype for each region. *p=0.02, Student's t-test, compared to wildtype (WT) levels normalized to GAPDH. (C) Foxp1D is significantly reduced only in the STR of *Foxp1*$^{+/-}$ mice. Data are represented as means (±SEM). n=4mice/genotype for each region. *p=0.004, Student's t-test compared to WT levels normalized to GAPDH.

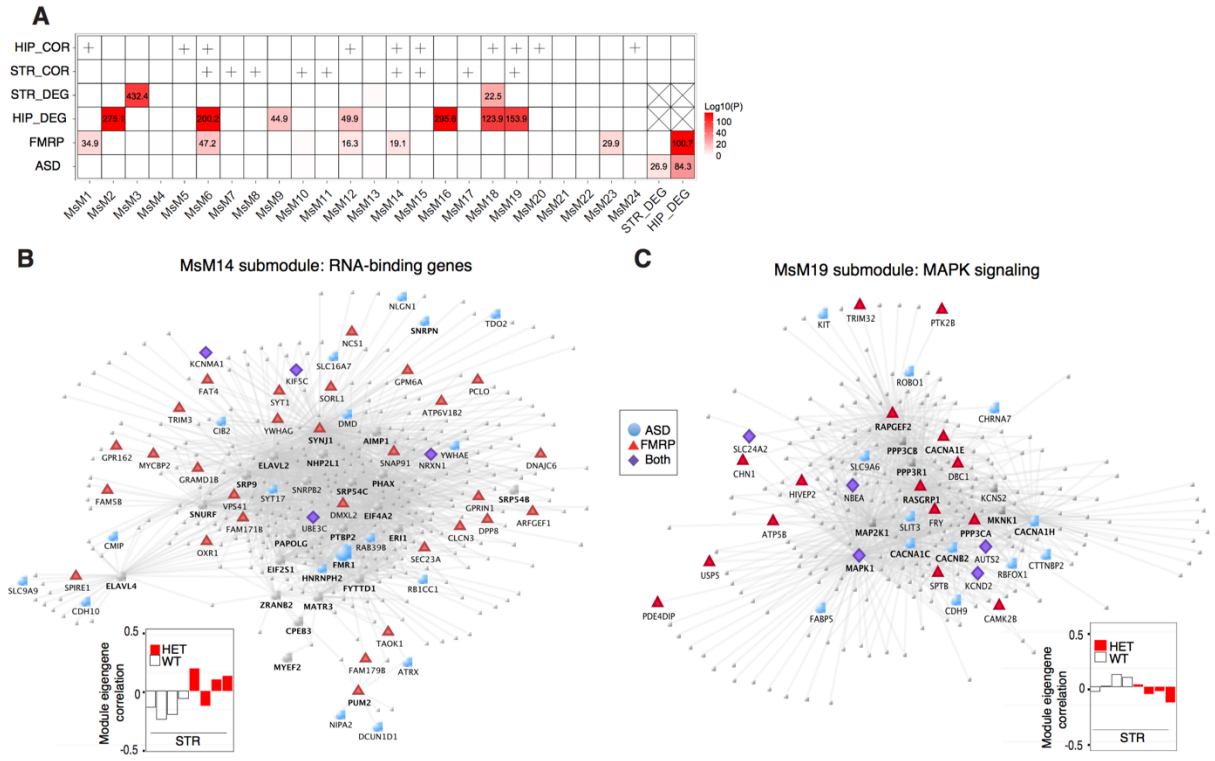


**Supplemental Figure 2.2. Overlaps between mouse WGCNA modules and DEGs.** (A) Heatmap displaying *Foxp1*$^{+/-}$ mouse RNA-seq WGCNA modules that contain significant enrichments of DEGs, ASD genes and/or FMRP targets. Plus signs indicate a genotype correlation of modules within specific brain regions. Log-transformed adjusted p-values from Benjamini-Hochberg false-discovery test (hypergeometric test). (B and C) Visualization of MsM19 containing genes significantly enriched in GO categories (using DAVD bioinformatics tool, http://david.abcc.ncifcrf.gov) for MAPK signaling (MsM19). Inserts: eigengene correlation plots show that genotype correlates negatively for MsM19 within the striatum.

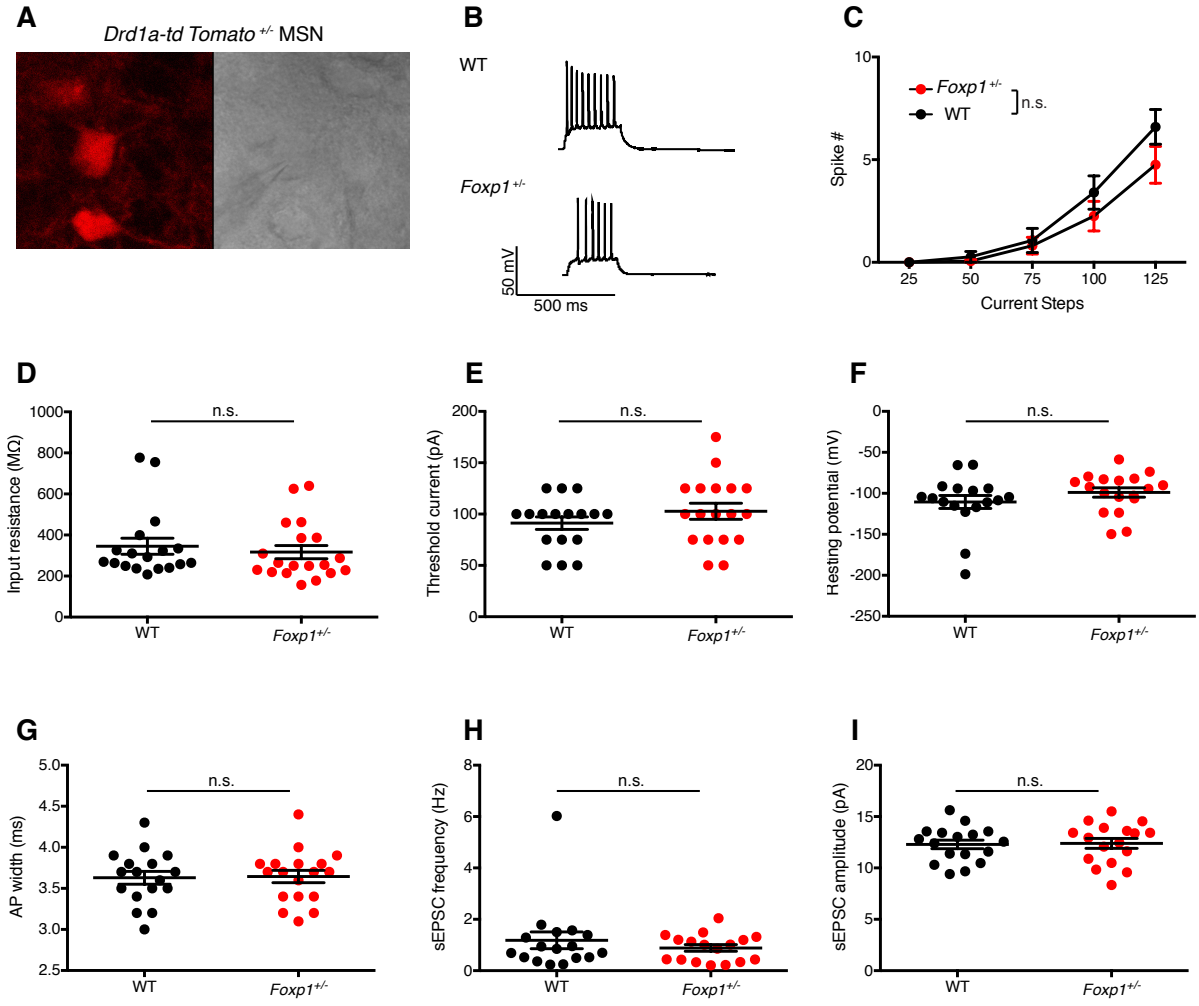


**Supplemental Figure 2.3. *Foxp1*$^{+/-}$ $D_1$+ MSNs have no change in in excitability.** (A) Example image of a recorded tdTomato+ ($D_1$+) neuron. (B) Example recordings depicting spiking in response to a 125 pA current step in control and *Foxp1*$^{+/-}$ MSNs. (C) Firing rate versus input curves are not significantly changed in *Foxp1*$^{+/-}$ MSNs. Data are represented as means (±SEM). n=15 WT cells, 16 *Foxp1*$^{+/-}$ cells. p=0.26, two-way ANOVA with repeated measures for current step compared between genotypes. (D) Input resistance is not significantly different in *Foxp1*$^{+/-}$ MSNs. Data are represented as means (±SEM). n=18 WT cells, 19 *Foxp1*$^{+/-}$ cells. p=0.58, Student's t-test compared between genotypes.

(E) The minimum threshold current required for evoking an action potential is not significantly altered in *Foxp1*$^{+/-}$ MSNs. Data are represented as means (±SEM). n=17 WT cells, 18 *Foxp1*$^{+/-}$ cells. p=0.25, Student's t-test compared between genotypes). (F) Resting potential is not significantly changed in *Foxp1*$^{+/-}$ MSNs. Data are represented as means (±SEM). n=17 WT cells, 18 *Foxp1*$^{+/-}$ cells. p=0.24, Student's t-test compared between genotypes. (G) Action potential width is not significantly altered in *Foxp1*$^{+/-}$ MSNs. Data are represented as means (±SEM). n=17 WT cells, 18 *Foxp1*$^{+/-}$ cells. p=0.89 (Student's t-test, compared between genotypes). (H) Spontaneous EPSC frequency is not significantly changed in *Foxp1*$^{+/-}$ MSNs. Data are represented as means (±SEM). n=17 WT cells, 17 *Foxp1*$^{+/-}$ cells. p=0.40, Student's t-test compared between genotypes. (I) Spontaneous EPSC amplitude is significantly decreased in *Foxp1*$^{+/-}$ MSNs. Data are represented as means (±SEM). n=17 WT cells, 17 *Foxp1*$^{+/-}$ cells. p=0.88, Student's t-test compared between genotypes.

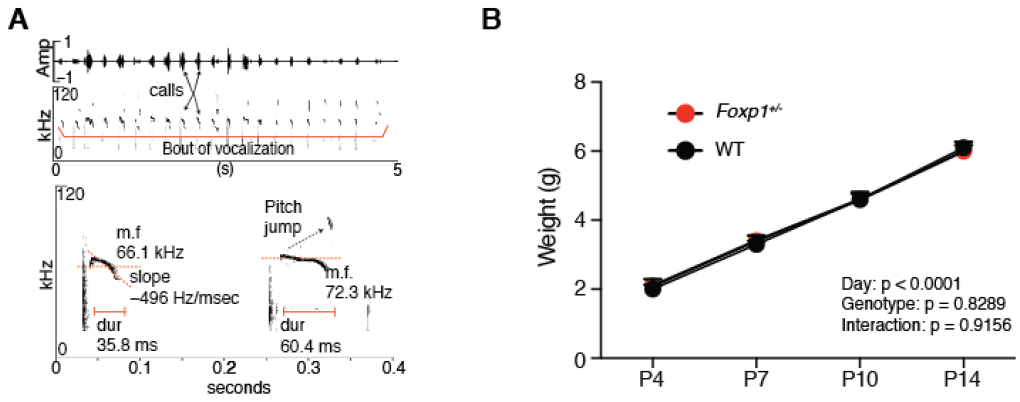


**Supplemental Figure 2.4. USV parameters and weight gain of *Foxp1*$^{+/-}$ mice.** (A) Illustration marking all major USV parameters measured including bouts, calls, mean frequency (m.f.), call duration (dur), slope, and jumps. (B) *Foxp1*$^{+/-}$ mice do not weigh significantly less than control littermates. Data are represented as means (±SEM). n=38 WT pups, 22 *Foxp1*$^{+/-}$ pups. p=0.83, two-way ANOVA with a Sidak multiple comparison test, compared between genotypes. The main effects for genotype and postnatal day, and the interactions between these two variables, are reported at the bottom of the panel.

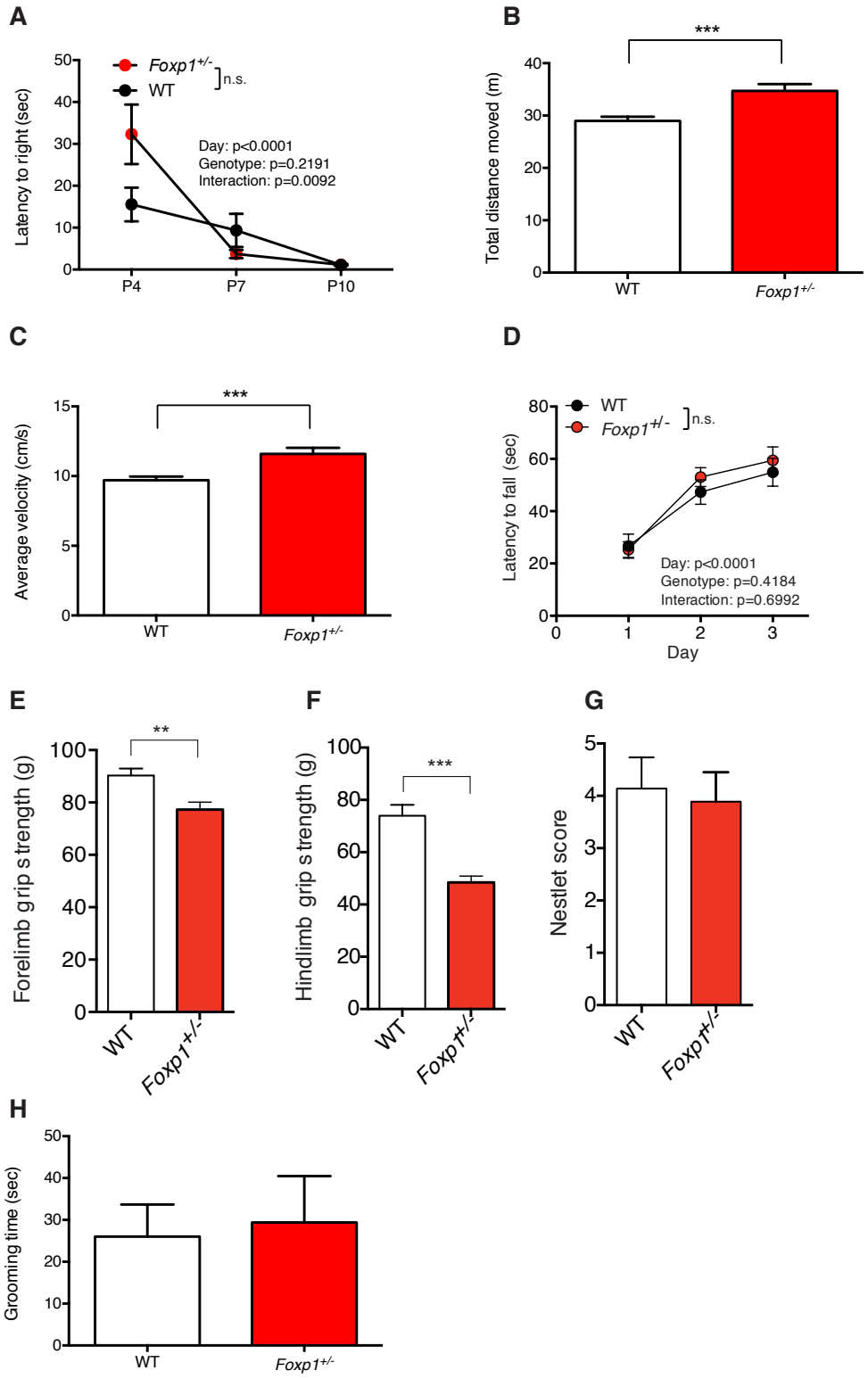
A
Latency to right (sec)
Foxp1+/-
WT
n.s.
Day: p<0.0001
Genotype: p=0.2191
Interaction: p=0.0092
P4
P7
P10
B
Total distance moved (m)
***
WT
Foxp1+/-
C
Average velocity (cm/s)
***
WT
Foxp1+/-
D
Latency to fall (sec)
WT
Foxp1+/-
n.s.
Day: p<0.0001
Genotype: p=0.4184
Interaction: p=0.6992
Day
E
Forelimb grip strength (g)
**
WT
Foxp1+/-
F
Hindlimb grip strength (g)
***
WT
Foxp1+/-
G
Nestlet score
WT
Foxp1+/-
H
Grooming time (sec)
WT
Foxp1+/-

**Supplemental Figure 2.5. Behavioral characterization of *Foxp1*$^{+/-}$ mice.** (A) Righting reflexes in *Foxp1*$^{+/-}$ pups at P4, P7, and P10. Data are represented as means (±SEM). n=11 *Foxp1*$^{+/-}$ pups, 15 WT pups. p=0.22, two-way ANOVA with a Sidak multiple comparison test compared between genotypes. (B and C) *Foxp1*$^{+/-}$ mice display hyperactivity in the open field test. (B) *Foxp1*$^{+/-}$ mice display increased total distance moved and (C) an increased average velocity in the open field test compared to WT mice. Data are represented as means (±SEM). n=27 *Foxp1*$^{+/-}$ mice, 39 WT mice. p=0.0006, p=0.0007, respectively, unpaired Student's t-test compared between genotypes. (C) *Foxp1*$^{+/-}$ mice do not exhibit deficits in motor coordination as measured by the latency to fall during the rotarod behavioral test. Data represented as means (±SEM) of 4 trials per day. n=9 *Foxp1*$^{+/-}$ mice, 7 WT mice, two-way ANOVA with a Sidak multiple comparison test compared between genotypes. (D) *Foxp1*$^{+/-}$ mice exhibit deficits in grip strength in both forelimbs and (E) hindlimbs. Data represented as means (±SEM). n=9 *Foxp1*$^{+/-}$ adults, 7 WT adults. **p=0.0058, ***p<0.0001, unpaired Student's t-test compared between genotypes. (F) *Foxp1*$^{+/-}$ mice show no difference in nesting behavior. Data represented as means (±SEM). n=9 *Foxp1*$^{+/-}$ mice, 7 WT mice. p=0.7667, unpaired Student's t-test compared between genotypes. (G) *Foxp1*$^{+/-}$ mice show no difference in grooming behavior. Data represented as means (±SEM). n=5 *Foxp1*$^{+/-}$ mice, 5 WT mice. p=0.81, unpaired Student's t-test compared between genotypes.

| Test | *Foxp1*$^{+/-}$ | WT | *p-value* |
|---|---|---|---|
| 1. Body position | 1 (±0) | 1 (±0) | NS |
| 2. Tremor | 0 (±0) | 0 (±0) | NS |
| 3. Palpebal closure | 0 (±0) | 0 (±0) | NS |
| 4. Coat appearance | 0.11 (±0.99) | 0 (±0) | NS |
| 5. Skin color | 1 (±0) | 1 (±0) | NS |
| 6. Whiskers | 0 (±0) | 0 (±0) | NS |
| 7. Lacrimation | 0 (±0) | 0 (±0) | NS |
| 8. Defecation | 0.22 (±0.44) | 0.57 (±0.53) | NS |
| 9. Gait | 0 (±0) | 0 (±0) | NS |
| 10. Tail elevation | 0 (±0) | 0 (±0) | NS |
| 11. Touch escape | 1.89 (±0.33) | 2 (±0) | NS |
| 12. Trunk curl | 0.22 (±0.44) | 0.14 (±0.38) | NS |
| 13. Limb grasping | 0.89 (±0.33) | 1 (±0) | NS |
| 14. Pinna reflex | 1 (±0) | 1 (±0) | NS |
| 15. Corneal reflex | 1 (±0) | 1 (±0) | NS |
| 16. Contact righting reflex | 0 (±0) | 0 (±0) | NS |
| 17. Evidence of biting | 0 (±0) | 0 (±0) | NS |
| 18. Vocalization (audible) | 0 (±0) | 0.14 (±0.38) | NS |
| 19. Startle response | 1 (±0) | 1 (±0) | NS |
| 20. Positional passivity | 0.78 (±0.83) | 0.43 (±0.53) | NS |

**Supplemental Figure 2.6. SHIRPA battery results.** *Foxp1*$^{+/-}$ mice underwent a modified SHIRPA behavioral screen and no differences were found between the 20 different categories tested. Individual tests were scored between 0-1, 0-2, or 0-3. Data represented as means (±SEM). n=9 *Foxp1*$^{+/-}$ mice, 7 WT mice.

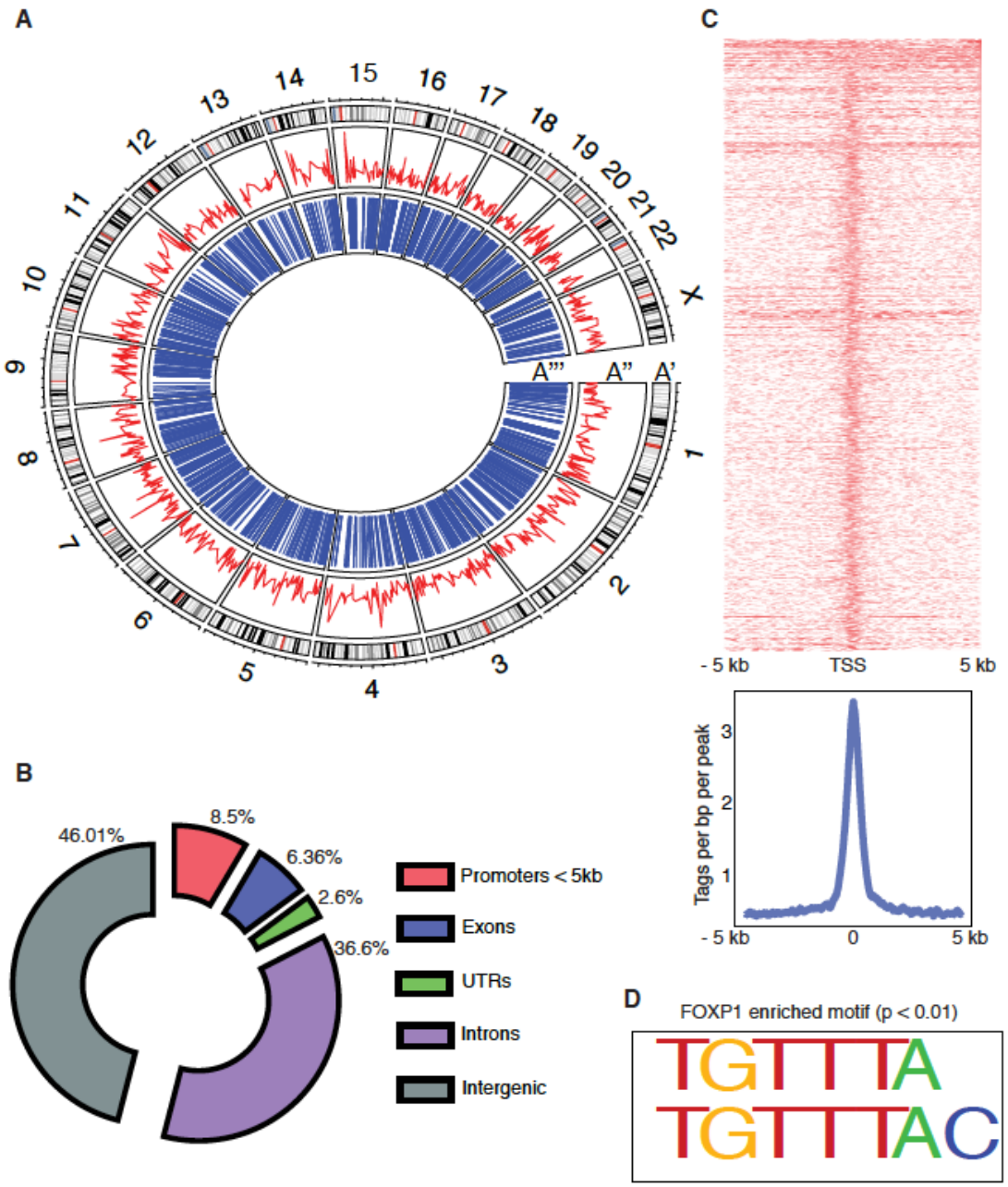


**Supplementary Figure 2.7. FOXP1 ChIP-seq characterization.** (A) Circular visualization of FOXP1 ChIP-seq. A' represents the chromosomal cytoband, A'' represents the FOXP1 peak height, and A''' represents the genomic distribution of FOXP1 binding sites. (B) Distribution of all FOXP1 binding site peaks in relation to gene structure.

(C) Heat map of FOXP1 ChIP-seq enrichment within gene promoters. Each row represents a 10-kb window extending 5kb upstream and 5kb downstream of the transcriptional start site (TSS). Bottom panel shows the average FOXP1 ChIP-seq enrichment across 5kb upstream and 5kb downstream of the TSS. (D) Enriched FOXP1 motifs within the detected peaks compared with GFP control.

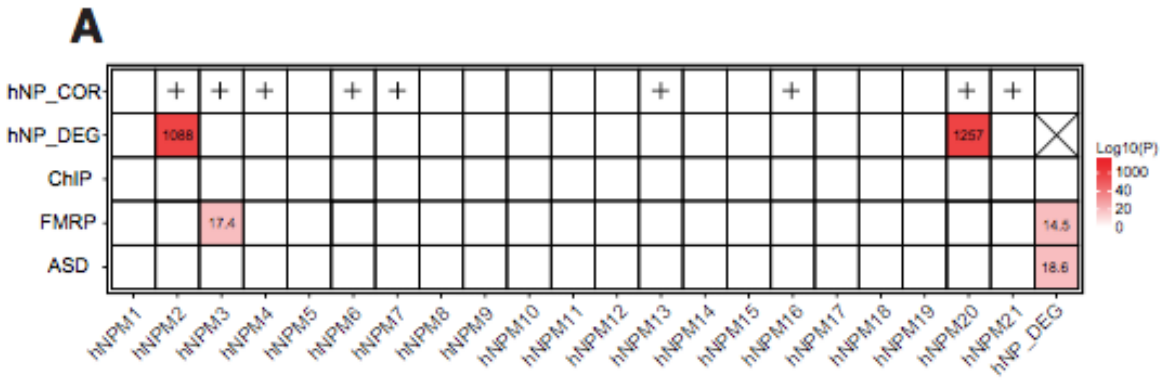


**Supplemental Figure 2.8. Overlaps between hNP WGCNA modules and DEGs.** (A) Heatmap displaying hNP$^{FOXP1}$ WGCNA modules that contain significant enrichments of DEGs, ASD genes. ASD scored genes, and/or FMRP targets. Log-transformed adjusted p-values from Benjamini-Hochberg false-discovery test (hypergeometric test). hNP_COR positive modules correlate with FOXP1 genotype. hNP_DEG indicates enrichment of FOXP1 differentially expressed genes.

# TABLES FOR CHAPTER TWO

**Table 2.1. DEGs in hNPs and *Foxp1*$^{+/-}$ mouse brains and ChIP targets in hNPs.**

| hNPs | | *Foxp1*$^{+/-}$ mouse | |
|---|---|---|---|
| **hNP ChIP targets** | **hNP DEGs** | ***Foxp1*$^{+/-}$ HIP DEGs** | ***Foxp1*$^{+/-}$ STR DEGs** |
| *ABCC1* | *A2M* | *1110008P14Rik* | *1190002N15Rik* |
| *ACADVL* | *AASS* | *1190002N15Rik* | *1700001O22Rik* |
| *ACTN2* | *ABCB1* | *1600029O15Rik* | *1700020I14Rik* |
| *ADAMTS1* | *ABCB6* | *1700007G11Rik* | *1700024P16Rik* |
| *ADRA1D* | *ABCB9* | *1700007K13Rik* | *1700040L02Rik* |
| *AGAP1* | *ABCC1* | *1700010I14Rik* | *1810041L15Rik* |
| *AGPAT4* | *ABCC4* | *1700012B09Rik* | *2310067B10Rik* |
| *AGPAT4-IT1* | *ABCC6* | *1700017B05Rik* | *3632451O06Rik* |
| *AGTPBP1* | *ABCC6P1* | *1700019D03Rik* | *6330409D20Rik* |
| *AGTR1* | *ABCC6P2* | *1700019G17Rik* | *9230009I02Rik* |
| *AKAP13* | *ABCD1* | *1700020I14Rik* | *9430020K01Rik* |
| *ALDH3A1* | *ABHD14A* | *1700024G13Rik* | *A830018L16Rik* |
| *ALG10B* | *ABL2* | *1700024P16Rik* | *A830082K12Rik* |
| *ANKRD11* | *ABR* | *1700026D08Rik* | *Abhd14a* |
| *ANKRD20A9P* | *ABRACL* | *1700048O20Rik* | *Abhd3* |
| *ANKRD30BP2* | *ABTB2* | *1700094D03Rik* | *Ablim2* |
| *ANO3* | *ACBD7* | *2010111I01Rik* | *Ace* |
| *ANXA1* | *ACD* | *2010204K13Rik* | *Acot5* |
| *AOAH* | *ACER3* | *2610020H08Rik* | *Acsl3* |
| *AP2B1* | *ACOT7* | *2610100L16Rik* | *Acsl4* |
| *ARAP2* | *ACP6* | *2610203C20Rik* | *Actn1* |
| *ARHGAP27* | *ACSBG1* | *2900026A02Rik* | *Actn2* |
| *ARL6IP1* | *ACSL4* | *3110035E14Rik* | *Acvr1* |
| *ASCC3* | *ACSS3* | *3110039M20Rik* | *Acvr1c* |
| *ASCL1* | *ACTA2* | *4833422C13Rik* | *Acvrl1* |
| *ASS1* | *ACTN2* | *4930539E08Rik* | *Acy1* |
| *ATP2B3* | *ACTR3B* | *4932411E22Rik* | *Adamtsl5* |
| *ATRN* | *ACYP2* | *4932418E24Rik* | *Adarb1* |
| *ATRNL1* | *ADA* | *4933409K07Rik* | *Adarb2* |
| *ATRX* | *ADAMTS1* | *4933412E12Rik* | *Adcy8* |
| *B3GALT2* | *ADAMTS12* | *4933426M11Rik* | *Adcyap1* |
| *BANK1* | *ADAMTS15* | *4933427D14Rik* | *Ago4* |
| *BFSP2* | *ADAMTS16* | *4933432I09Rik* | *AI593442* |
| *BHLHE22* | *ADAMTS19* | *5430417L22Rik* | *AK129341* |
| *BMPR1B* | *ADAMTS4* | *5930403L14Rik* | *Akap2* |
| *BOC* | *ADAMTS9* | *6030419C18Rik* | *Ampd2* |
| *BRD7P3* | *ADAMTSL1* | *6430411K18Rik* | *Amz1* |
| *BRF1* | *ADARB1* | *6430571L13Rik* | *Angptl4* |
| *C11orf82* | *ADCK3* | *6430573F11Rik* | *Ank1* |
| *C13orf45* | *ADCY1* | *6430584L05Rik* | *Ankrd29* |
| *C16orf82* | *ADCY2* | *6530402F18Rik* | *Ankrd34c* |
| *C16orf97* | *ADCY8* | *9030617O03Rik* | *Ano3* |
| *C19orf59* | *ADCY9* | *9230009I02Rik* | *Apln* |
| *C1orf229* | *ADCYAP1R1* | *9330182L06Rik* | *Arc* |
| *C1orf233* | *ADD3* | *9430021M05Rik* | *Arg2* |
| *C1orf87* | *ADM* | *9630033F20Rik* | *Arhgap10* |
| *C2CD4B* | *ADORA1* | *9830166K06Rik* | *Arhgap27* |
| *C3orf49* | *ADORA2B* | *A230065H16Rik* | *Arhgap33* |
| *C3orf55* | *ADRA1A* | *A330050F15Rik* | *Arhgdib* |

| | | | |
|---|---|---|---|
| *C3orf62* | *ADRBK2* | *A330070K13Rik* | *Arhgef15* |
| *C6orf10* | *ADSSL1* | *A4galt* | *Arid3b* |
| *C6orf123* | *AFF3* | *A730017C20Rik* | *Arid5b* |
| *C6orf170* | *AGER* | *A830018L16Rik* | *Arl4d* |
| *C6orf223* | *AGK* | *A930024E05Rik* | *Asap2* |
| *C6orf48* | *AGPAT9* | *Aak1* | *Asb11* |
| *C7orf62* | *AGT* | *Aard* | *Asic1* |
| *C7orf66* | *AHNAK* | *Abat* | *Asph* |
| *C9orf123* | *AHNAK2* | *Abi1* | *Asphd2* |
| *CAMSAP1* | *AHR* | *Acan* | *Atp10a* |
| *CAMTA1* | *AJAP1* | *Acap3* | *Atp1b1* |
| *CBLN2* | *AK4* | *Acot3* | *Atp6ap2* |
| *CBLN4* | *AK5* | *Acsl4* | *Atp8b2* |
| *CCDC102A* | *AKAP12* | *Acsl5* | *B2m* |
| *CCDC54* | *AKAP6* | *Actr3b* | *B3gnt2* |
| *CCDC57* | *ALAD* | *Acvr1c* | *Bbs9* |
| *CCL2* | *ALCAM* | *Adam11* | *BC031361* |
| *CCNY* | *ALDH1B1* | *Adam23* | *BC048546* |
| *CD226* | *ALDH1L1* | *Adamts3* | *BC049352* |
| *CDC42EP4* | *ALDH1L2* | *Adamts8* | *BC055324* |
| *CDH18* | *ALDH3A2* | *Adamts9* | *Bcat1* |
| *CDH23* | *ALDH3B1* | *Adamtsl1* | *Bcr* |
| *CDH8* | *ALDOA* | *Adck3* | *Bhlhe22* |
| *CDH9* | *ALOX5* | *Adcy7* | *Bhlhe40* |
| *CDK5RAP1* | *ALPK1* | *Adcy9* | *Btbd11* |
| *CDK7* | *ALPK2* | *Adcyap1r1* | *Btbd3* |
| *CDKAL1* | *ALPL* | *Add2* | *Bves* |
| *CENPJ* | *AMBN* | *Adora1* | *C2cd2l* |
| *CHAC2* | *AMIGO2* | *Adra1d* | *C530008M17Rik* |
| *CHD1* | *AMOTL1* | *Adra2a* | *C730002L08Rik* |
| *CHD3* | *AMY2B* | *Agap3* | *Cacna1h* |
| *CHEK2P2* | *ANGPTL1* | *Agbl5* | *Cadps* |
| *CHRM3* | *ANK1* | *Agfg2* | *Calb2* |
| *CHST2* | *ANK2* | *Agtpbp1* | *Calcoco1* |
| *CMAHP* | *ANK3* | *Ahi1* | *Camk2d* |
| *CNTN4-AS2* | *ANKDD1A* | *Ahnak* | *Camk2n2* |
| *CNTN5* | *ANKRD1* | *Ahr* | *Camkv* |
| *CNTN6* | *ANLN* | *AI115009* | *Car11* |
| *COL26A1* | *ANO1* | *AI854517* | *Cartpt* |
| *COX11* | *ANPEP* | *Ak4* | *Cav2* |
| *CPO* | *ANTXR2* | *Ak5* | *Cbln4* |
| *CPXM1* | *ANXA2* | *Ak7* | *Cbr3* |
| *CRH* | *ANXA2P2* | *Akap12* | *Ccdc136* |
| *CRYL1* | *AP1S3* | *Akap13* | *Ccdc141* |
| *CSF1R* | *APBA1* | *Akap9* | *Ccdc88c* |
| *CSTF3-AS1* | *APBA2* | *Akt3* | *Ccng1* |
| *CTF1* | *APCDD1* | *Aldoa* | *Ccno* |
| *CUL1* | *APCDD1L* | *Alk* | *Cd83* |
| *CUL4A* | *APIP* | *Alms1* | *Cdh12* |
| *CXCL13* | *APLN* | *Alox8* | *Cdh8* |
| *CXorf49* | *APOBEC3B* | *Amigo2* | *Cdh9* |
| *CXorf49B* | *APOBEC3C* | *Amotl1* | *Cdk14* |
| *CXXC11* | *APOL6* | *Ampd3* | *Cdkn1a* |
| *CXXC5* | *AQP1* | *Amph* | *Cds1* |
| *CYFIP2* | *AQP11* | *Amy1* | *Celf3* |
| *CYLD* | *AQP3* | *Angptl4* | *Cep128* |

| | | | |
|---|---|---|---|
| *CYP2A6* | *AQP4* | *Ankrd34b* | *Cep63* |
| *CYR61* | *ARAP2* | *Ankrd34c* | *Chdh* |
| *CYTH1* | *ARAP3* | *Ankrd44* | *Chrm4* |
| *DAB2IP* | *ARG2* | *Ankrd46* | *Cish* |
| *DAOA* | *ARHGAP10* | *Ankrd55* | *Clspn* |
| *DCAF8L1* | *ARHGAP19* | *Ankrd63* | *Cnr1* |
| *DCP2* | *ARHGAP26* | *Ankrd66* | *Cnst* |
| *DDX20* | *ARHGAP5-AS1* | *Ano1* | *Cntn3* |
| *DDX50* | *ARHGEF26* | *Ano2* | *Cntnap3* |
| *DEFB115* | *ARHGEF26-AS1* | *Ano3* | *Coch* |
| *DERA* | *ARHGEF37* | *Anxa11* | *Col11a2* |
| *DGKK* | *ARL4C* | *Anxa2* | *Cpne5* |
| *DIABLO* | *ARRB1* | *Ap1s2* | *Cpne7* |
| *DICER1* | *ARSE* | *Ap2a2* | *Crh* |
| *DIP2C* | *ARSI* | *Apold1* | *Crocc* |
| *DISC1* | *ASGR1* | *Arc* | *Crot* |
| *DKFZP586I1420* | *ASS1* | *Arg2* | *Crtac1* |
| *DLGAP1-AS3* | *ASXL3* | *Arhgap15* | *Csgalnact1* |
| *DLGAP1-AS5* | *ATG4A* | *Arhgap21* | *Cthrc1* |
| *DMD* | *ATIC* | *Arhgap25* | *Cux2* |
| *DNAH5* | *ATL2* | *Arhgap36* | *Cyr61* |
| *DNAJC14* | *ATP10B* | *Arhgap42* | *Dach1* |
| *DPP10* | *ATP10D* | *Arhgap6* | *Dbp* |
| *DPP6* | *ATP13A4* | *Arhgdib* | *Dcc* |
| *DPYD* | *ATP1A2* | *Arhgdig* | *Ddit4l* |
| *DPYD-AS1* | *ATP1B2* | *Arhgef17* | *Ddx11* |
| *DUSP22* | *ATP2B1* | *Arhgef25* | *Dgat2* |
| *ECE1* | *ATP2B4* | *Arhgef26* | *Dio2* |
| *ECT2* | *ATP5E* | *Arhgef28* | *Disp2* |
| *EDA* | *AURKA* | *Arhgef40* | *Dlgap1* |
| *EDN3* | *AVIL* | *Arhgef6* | *Dmkn* |
| *EEA1* | *AVPI1* | *Arid1b* | *Dnajc3* |
| *EFCAB4B* | *AXL* | *Arl15* | *Dner* |
| *EIF2B4* | *B2M* | *Arl4a* | *Dpp10* |
| *ELK2AP* | *B3GALT2* | *Arl5b* | *Dtnb* |
| *ELMO1* | *B3GALT4* | *Armcx3* | *Dusp1* |
| *ELTD1* | *B3GAT2* | *Arpc2* | *Dusp4* |
| *EML1* | *B3GNT2* | *Arpc4* | *Edil3* |
| *ENC1* | *B3GNT9* | *Arpp21* | *Efr3a* |
| *EPSTI1* | *B4GALT5* | *Asb11* | *Egr2* |
| *ERCC4* | *BACE2* | *Asph* | *Egr4* |
| *ERP27* | *BACH2* | *Asphd2* | *Ehbp1l1* |
| *ESM1* | *BAG2* | *Ass1* | *Elavl2* |
| *ETV3* | *BAG3* | *Astn2* | *Elavl4* |
| *FAM101A* | *BAI2* | *Atf6* | *Elfn1* |
| *FAM133CP* | *BAI3* | *Atg9b* | *Elovl4* |
| *FAM174A* | *BAMBI* | *Atp10a* | *Eml5* |
| *FAM189A1* | *BASP1* | *Atp2b1* | *Enah* |
| *FAM19A1* | *BBC3* | *Atp2b4* | *Endod1* |
| *FAM19A2* | *BBOX1* | *Atp6ap1l* | *Epha10* |
| *FAM27C* | *BCAM* | *Atp6v1a* | *Epha5* |
| *FAM41C* | *BCAN* | *Atp6v1c2* | *Epor* |
| *FAM81A* | *BCAT2* | *Atp6v1g2* | *Eps15* |
| *FAM83C* | *BCHE* | *Atrnl1* | *Eps8* |
| *FBXL14* | *BCL2L1* | *Auts2* | *Erf* |
| *FBXL7* | *BCL2L11* | *AW551984* | *Evc2* |

| | | | |
|---|---|---|---|
| *FBXO38* | *BCL2L12* | *B4galnt1* | *Exph5* |
| *FGD3* | *BCMO1* | *Bai2* | *F730043M19Rik* |
| *FLJ25363* | *BCYRN1* | *Baiap2* | *Fam105a* |
| *FLJ26245* | *BDH2* | *Baiap3* | *Fam107a* |
| *FLJ33581* | *BDNF* | *Bbox1* | *Fam132a* |
| *FLJ35282* | *BEAN1* | *BC005764* | *Fam150b* |
| *FLJ45079* | *BEND5* | *BC018242* | *Fam155a* |
| *FLJ46284* | *BEND6* | *BC048546* | *Fam160b2* |
| *FLRT2* | *BEST3* | *BC061194* | *Fam19a1* |
| *FMN1* | *BICC1* | *BC068157* | *Fam19a2* |
| *FOXN3* | *BIN1* | *BC089491* | *Fam222a* |
| *FOXP1* | *BMF* | *Bc1* | *Fam3c* |
| *FRMD3* | *BMP5* | *Bcl11a* | *Fam78a* |
| *FRMD4B* | *BMP8B* | *Bcl11b* | *Fam84b* |
| *FSD1L* | *BMPR1B* | *Bcl2* | *Fancb* |
| *FSHR* | *BNC2* | *Bdnf* | *Farp1* |
| *FUNDC2P2* | *BRICD5* | *Bex1* | *Fbln5* |
| *GAB1* | *BST1* | *Bex4* | *Fbxl16* |
| *GABRB2* | *BTBD11* | *Blnk* | *Fbxo32* |
| *GADL1* | *BTBD3* | *Brd9* | *Fbxo34* |
| *GAK* | *BTBD8* | *Bsn* | *Fcho1* |
| *GALNT10* | *BTG1* | *Btbd11* | *Fgf10* |
| *GALNT18* | *BTN2A2* | *Btbd3* | *Fgf12* |
| *GAP43* | *BTN3A1* | *C130060K24Rik* | *Fgf9* |
| *GAS7* | *BTN3A2* | *C130071C03Rik* | *Flna* |
| *GATA3* | *BTN3A3* | *C130074G19Rik* | *Flt3* |
| *GBE1* | *BZW2* | *C4b* | *Fmnl2* |
| *GLT1D1* | *C10orf107* | *Cables1* | *Foxo1* |
| *GLUD2* | *C10orf12* | *Cables2* | *Foxp1* |
| *GOLGA3* | *C10orf35* | *Cabp1* | *Frmpd1* |
| *GOLIM4* | *C11orf96* | *Cabp7* | *Fxyd2* |
| *GPR146* | *C12orf75* | *Cacna1a* | *Gabra1* |
| *GPR64* | *C15orf39* | *Cacna1c* | *Gabra3* |
| *GREB1L* | *C16orf45* | *Cacna1g* | *Gabrd* |
| *GRIA3* | *C16orf74* | *Cacna1h* | *Gabrg1* |
| *GRIK2* | *C18orf56* | *Cacna2d1* | *Gabrg2* |
| *GRIN2B* | *C18orf8* | *Cacna2d2* | *Galnt16* |
| *GRM7* | *C19orf18* | *Cacna2d3* | *Gcnt2* |
| *GSDMD* | *C1GALT1* | *Cacnb3* | *Gjb6* |
| *GTF2A2* | *C1orf110* | *Cacng4* | *Glra3* |
| *GUCA1C* | *C1orf21* | *Cacng5* | *Gm136* |
| *GYG2* | *C1orf226* | *Cadm2* | *Gm13629* |
| *GYG2P1* | *C1orf56* | *Cadm3* | *Gm20300* |
| *HAO1* | *C1orf94* | *Cadps2* | *Gm7244* |
| *HCN1* | *C1orf95* | *Calb2* | *Gmpr* |
| *HIF3A* | *C1QL2* | *Calm2* | *Gnai1* |
| *HIST4H4* | *C1QTNF1* | *Calm3* | *Gnas* |
| *HMBOX1* | *C1QTNF3* | *Camk1d* | *Gnb2* |
| *HMGXB4* | *C1QTNF6* | *Camk2a* | *Gnb5* |
| *HNRNPD* | *C1R* | *Camk2b* | *Gng4* |
| *HNRNPKP3* | *C1RL* | *Camk2d* | *Gpnmb* |
| *HPGD* | *C1S* | *Camk2n1* | *Gpr155* |
| *HS3ST1* | *C21orf2* | *Camk4* | *Gpr22* |
| *HS3ST5* | *C2CD2* | *Camkk1* | *Gprin3* |
| *HYI* | *C2orf72* | *Camta2* | *Gpx6* |
| *IAH1* | *C2orf80* | *Cap2* | *Grb7* |

| | | | |
|---|---|---|---|
| *IFI44* | *C3orf58* | *Capza2* | *Grik2* |
| *IGF2BP3* | *C3orf70* | *Car4* | *Gyk* |
| *IGFBP7* | *C4B_2* | *Car7* | *H2-DMa* |
| *IGSF1* | *C4orf19* | *Cartpt* | *Hapln1* |
| *IL1B* | *C5orf49* | *Cbln1* | *Hapln4* |
| *IL1RAPL1* | *C8orf4* | *Ccbe1* | *Hcn1* |
| *IL6ST* | *C8orf44* | *Ccdc108* | *Hcrtr2* |
| *IMPA2* | *C8orf56* | *Ccdc141* | *Hdac9* |
| *INO80D* | *CABLES1* | *Ccdc151* | *Hif3a* |
| *INPP5A* | *CACNA1A* | *Ccdc153* | *Homer2* |
| *INSIG2* | *CACNB4* | *Ccdc19* | *Hpca* |
| *INTU* | *CALB1* | *Ccdc3* | *Hrh3* |
| *IREB2* | *CALB2* | *Ccdc42* | *Hs3st1* |
| *IRX2* | *CALCRL* | *Ccdc65* | *Hspa12a* |
| *ITGB1* | *CALN1* | *Ccdc81* | *Hspa1a* |
| *ITPKB* | *CAMK2A* | *Ccnjl* | *Hspa1b* |
| *KAT5* | *CAMK2B* | *Ccsap* | *Hspa2* |
| *KCNH1* | *CAMK2N1* | *Cd109* | *Hspa5* |
| *KCNJ2* | *CAMK4* | *Cdc14a* | *Htr2a* |
| *KCNJ6* | *CAMKK1* | *Cdc40* | *Htr7* |
| *KCNK2* | *CAMKV* | *Cdc42ep3* | *Id2* |
| *KCNK9* | *CAPG* | *Cdc42se2* | *Ido1* |
| *KCNQ1OT1* | *CAPN2* | *Cdh13* | *Igf1* |
| *KCNU1* | *CAPN5* | *Cdh18* | *Igfn1* |
| *KCNV1* | *CAPS* | *Cdh22* | *Igsf3* |
| *KEL* | *CAPS2* | *Cdh24* | *Igsf9* |
| *KHDRBS3* | *CARD10* | *Cdh4* | *Il17rc* |
| *KIAA0430* | *CARHSP1* | *Cdh6* | *Ildr2* |
| *KIAA0947* | *CASP1* | *Cdh7* | *Inf2* |
| *KIF2B* | *CAV1* | *Cdh9* | *Isyna1* |
| *KIF4B* | *CBLN1* | *Cdhr3* | *Itga11* |
| *KLF6* | *CBLN4* | *Cdk14* | *Itga5* |
| *KLHDC9* | *CCBE1* | *Cdk18* | *Itga9* |
| *KLHL30* | *CCDC149* | *Cdkl2* | *Itpk1* |
| *KREMEN1* | *CCDC18* | *Cdkl4* | *Itpr1* |
| *L3MBTL4* | *CCDC28A* | *Cdkn1a* | *Ivns1abp* |
| *LAG3* | *CCDC71L* | *Cds1* | *Jag1* |
| *LAMB3* | *CCDC74A* | *Cecr6* | *Jakmip1* |
| *LCA5* | *CCDC77* | *Cgn* | *Jdp2* |
| *LHFPL1* | *CCDC80* | *Chgb* | *Junb* |
| *LHX2* | *CCDC85C* | *Chml* | *Kcna4* |
| *LHX4* | *CCL2* | *Chn1* | *Kcnab1* |
| *LHX9* | *CCNB1* | *Chn2* | *Kcnab3* |
| *LIMCH1* | *CCND1* | *Chrd* | *Kcnc2* |
| *LINC00052* | *CCRN4L* | *Chrdl1* | *Kcnd3* |
| *LINC00273* | *CD274* | *Chrm1* | *Kcnh4* |
| *LINC00293* | *CD276* | *Chrm2* | *Kcnh5* |
| *LINC00309* | *CD34* | *Chrm3* | *Kcnip1* |
| *LINC00461* | *CD38* | *Chrna7* | *Kcnip2* |
| *LINC00470* | *CD59* | *Chst1* | *Kcnip4* |
| *LINC00485* | *CD68* | *Chst11* | *Kcnj2* |
| *LINC00507* | *CD74* | *Cidea* | *Kcnj3* |
| *LINC00536* | *CD86* | *Cit* | *Kcnk2* |
| *LINC00578* | *CD9* | *Cited1* | *Kcnmb2* |
| *LINC00583* | *CD97* | *Cldn22* | *Kcnn2* |
| *LINC00609* | *CDC20* | *Cldn26* | *Kcns3* |

| | | | |
|---|---|---|---|
| *LINC00645* | *CDC42EP2* | *Clic4* | *Kcnt1* |
| *LINC00662* | *CDC42EP3* | *Clmp* | *Kctd17* |
| *LINC00669* | *CDCA2* | *Clstn2* | *Kif17* |
| *LINC00670* | *CDCA8* | *Clvs2* | *Klf16* |
| *LINGO2* | *CDH11* | *Cmtm8* | *Klhdc7a* |
| *LMOD2* | *CDH20* | *Cnih2* | *Klhdc8a* |
| *LOC100130000* | *CDH6* | *Cnksr2* | *Klhl1* |
| *LOC100130238* | *CDH8* | *Cnrip1* | *Kras* |
| *LOC100130480* | *CDKL1* | *Cntn4* | *Krt10* |
| *LOC100130744* | *CDKN1A* | *Cntn6* | *Krt12* |
| *LOC100131234* | *CDKN2B* | *Cntnap1* | *Krt9* |
| *LOC100132352* | *CEACAM1* | *Cntnap5c* | *Lancl3* |
| *LOC100169752* | *CEBPB* | *Col11a1* | *Laptm4b* |
| *LOC100190940* | *CEBPD* | *Col15a1* | *Lhfp* |
| *LOC100192426* | *CECR5-AS1* | *Col18a1* | *Lhx9* |
| *LOC100288069* | *CELF3* | *Col19a1* | *Lifr* |
| *LOC100288748* | *CENPW* | *Col23a1* | *Lin7a* |
| *LOC100288911* | *CEP135* | *Col25a1* | *Lingo2* |
| *LOC100505817* | *CEP19* | *Col26a1* | *Lingo3* |
| *LOC100505875* | *CEP250* | *Col27a1* | *Lipa* |
| *LOC100506207* | *CEP55* | *Col6a1* | *Lmo2* |
| *LOC100506895* | *CER1* | *Col9a2* | *Lonrf3* |
| *LOC100507205* | *CHAC2* | *Coro2b* | *Lpl* |
| *LOC100507217* | *CHADL* | *Cpeb1* | *Lrg1* |
| *LOC100507250* | *CHDH* | *Cplx1* | *Lurap1l* |
| *LOC100507651* | *CHEK1* | *Cplx2* | *Luzp2* |
| *LOC100508120* | *CHI3L1* | *Cpne4* | *Ly6c1* |
| *LOC283143* | *CHODL* | *Cpne5* | *Lypla1* |
| *LOC284294* | *CHRD* | *Cpne6* | *Lzts3* |
| *LOC284801* | *CHRDL1* | *Creg2* | *Mab21l1* |
| *LOC285074* | *CHRM4* | *Crhbp* | *Magi1* |
| *LOC285692* | *CHRNA7* | *Crispld1* | *Map3k6* |
| *LOC285762* | *CHRNA9* | *Crls1* | *Map7d2* |
| *LOC375295* | *CHST15* | *Crmp1* | *March1* |
| *LOC388813* | *CHST2* | *Crtac1* | *Matn2* |
| *LOC401397* | *CHST6* | *Cry1* | *Mctp2* |
| *LOC401557* | *CHST7* | *Crybb3* | *Me1* |
| *LOC440040* | *CHST9* | *Crygn* | *Megf11* |
| *LOC441204* | *CHSY3* | *Cryl1* | *Melk* |
| *LOC441666* | *CIITA* | *Crym* | *Mertk* |
| *LOC541471* | *CIRH1A* | *Csrnp1* | *Mgat4b* |
| *LOC643714* | *CITED1* | *Cthrc1* | *Mgat5b* |
| *LOC644649* | *CLASP2* | *Ctxn1* | *Mir365-1* |
| *LOC645166* | *CLCF1* | *Ctxn3* | *Mn1* |
| *LOC646214* | *CLCN5* | *Cuedc1* | *Mpped2* |
| *LOC646813* | *CLDN1* | *Cul7* | *Mreg* |
| *LOC649133* | *CLDN11* | *Cux1* | *Mxd1* |
| *LOC649395* | *CLDN15* | *Cxcl14* | *Mybpc1* |
| *LOC650226* | *CLDND1* | *Cxx1c* | *Mylk3* |
| *LOC654342* | *CLEC18B* | *Cxxc4* | *Myo16* |
| *LOC727915* | *CLIC1* | *Cyb5r1* | *Myo3b* |
| *LOC729121* | *CLIC6* | *Cyfip2* | *Myoc* |
| *LOC91948* | *CMTM7* | *Cyp26b1* | *Myom3* |
| *LPAL2* | *CMTM8* | *Cyp4f15* | *Nab2* |
| *LRBA* | *CNIH3* | *D430036J16Rik* | *Nap1l5* |
| *LRFN5* | *CNR1* | *D630023F18Rik* | *Napepld* |

| | | | |
|---|---|---|---|
| *LRIG1* | *CNTFR* | *Dab1* | *Ndst3* |
| *LRP1B* | *CNTN1* | *Dagla* | *Ndst4* |
| *LRRC40* | *CNTN2* | *Dbi* | *Necab2* |
| *LRRC43* | *CNTN4* | *Dcc* | *Nefh* |
| *LRRN3* | *CNTN6* | *Dctd* | *Nefl* |
| *LRRTM2* | *CNTNAP3* | *Dcx* | *Nek2* |
| *LSP1P3* | *CNTNAP3B* | *Ddn* | *Nek7* |
| *MACROD2-AS1* | *COBL* | *Ddo* | *Nell1* |
| *MAEA* | *COBLL1* | *Ddr2* | *Neurod1* |
| *MAML3* | *COL11A1* | *Dgkd* | *Ngef* |
| *MAP4* | *COL11A2* | *Dgkz* | *Ngf* |
| *MAP7* | *COL16A1* | *Dhrs13* | *Nhsl1* |
| *MARCH7* | *COL1A2* | *Dhx33* | *Nkrf* |
| *MARK3* | *COL22A1* | *Dkk3* | *Nlk* |
| *MAST4* | *COL23A1* | *Dlat* | *Nmbr* |
| *MATK* | *COL5A2* | *Dlec1* | *Nmnat3* |
| *MATN1-AS1* | *COL7A1* | *Dleu7* | *Nostrin* |
| *MCTP2* | *COL8A1* | *Dlgap1* | *Npas4* |
| *MEF2C* | *COL9A1* | *Dlgap2* | *Npy1r* |
| *MEIS1* | *COMT* | *Dlgap3* | *Nr1d1* |
| *MEIS2* | *CORO1C* | *Dlk1* | *Nr4a1* |
| *MEX3B* | *CORO2B* | *Dlx1* | *Nrip3* |
| *MGAT4C* | *CPA4* | *Dlx2* | *Nrp2* |
| *MGC12916* | *CPLX2* | *Dlx5* | *Nrxn1* |
| *MGST1* | *CPNE4* | *Dlx6* | *Nt5dc3* |
| *MIAT* | *CPNE8* | *Dmtn* | *Ntng1* |
| *MIR1286* | *CPXM2* | *Dmxl2* | *Nucb2* |
| *MIR2054* | *CRABP2* | *Dnah1* | *Nudt4* |
| *MIR2116* | *CRB1* | *Dnah2* | *Nup93* |
| *MIR29A* | *CREB3L1* | *Dnah5* | *Nxph1* |
| *MIR3648* | *CRH* | *Dnah6* | *Oacyl* |
| *MIR3668* | *CRISPLD1* | *Dnah7b* | *Odf4* |
| *MIR3679* | *CRISPLD2* | *Dnaic1* | *Onecut2* |
| *MIR383* | *CRYM* | *Dnajb5* | *Oprk1* |
| *MIR3913-2* | *CSF1* | *Dnajc6* | *Otof* |
| *MIR3914-1* | *CSGALNACT1* | *Dner* | *Oxr1* |
| *MIR3935* | *CSMD2* | *Dnm1* | *Palm2* |
| *MIR421* | *CSNK1G1* | *Dnm3* | *Palmd* |
| *MIR4251* | *CSNK2A3* | *Doc2g* | *Paqr8* |
| *MIR4278* | *CSPG4* | *Dock10* | *Pard6b* |
| *MIR4280* | *CSPG5* | *Dock7* | *Pcdh19* |
| *MIR4295* | *CSRP1* | *Dock9* | *Pcdh20* |
| *MIR4318* | *CSRP2* | *Dok4* | *Pcdh8* |
| *MIR4322* | *CST3* | *Dpp10* | *Pcsk7* |
| *MIR4436A* | *CTGF* | *Dpysl5* | *Pde1b* |
| *MIR4462* | *CTNNAL1* | *Dr1* | *Pde2a* |
| *MIR4505* | *CTSC* | *Drc1* | *Per1* |
| *MIR4510* | *CTSO* | *Drd3* | *Phactr2* |
| *MIR4635* | *CTTNBP2* | *Dtnb* | *Phex* |
| *MIR4655* | *CXCL14* | *Dtnbp1* | *Phyh* |
| *MIR4715* | *CXCR4* | *Dtx4* | *Phyhip* |
| *MIR4764* | *CXXC4* | *Dusp26* | *Pid1* |
| *MIR4790* | *CYB561* | *Dusp3* | *Pip5k1b* |
| *MIR548A2* | *CYB5R2* | *Dusp5* | *Pkib* |
| *MIR548AI* | *CYGB* | *Dusp6* | *Pkp2* |
| *MIR548AP* | *CYP1B1* | *Dync1i1* | *Pla2g7* |

| | | | |
|---|---|---|---|
| *MIR548AR* | *CYP4V2* | *Dynll1* | *Plcb4* |
| *MIR548O2* | *CYSTM1* | *Dynlt1f* | *Plcd4* |
| *MIR551B* | *CYTH1* | *E030019B06Rik* | *Plch1* |
| *MIR5583-1* | *DAB2* | *Ebf3* | *Plcl1* |
| *MIR5702* | *DACH1* | *Ece2* | *Plcxd1* |
| *MIR573* | *DACT1* | *Ecel1* | *Plcxd2* |
| *MIR653* | *DACT2* | *Ednrb* | *Pld5* |
| *MIR663B* | *DAPL1* | *Eepd1* | *Pmepa1* |
| *MKNK1* | *DBX2* | *Efcab12* | *Pnoc* |
| *MLL3* | *DCBLD2* | *Efcab2* | *Pnp2* |
| *MMD* | *DCDC2* | *Efna5* | *Pou3f1* |
| *MMEL1* | *DCLK2* | *Efnb3* | *Ppargc1a* |
| *MREG* | *DDO* | *Efr3a* | *Ppargc1b* |
| *MRM1* | *DDX58* | *Efr3b* | *Ppfia2* |
| *MRPL45P2* | *DDX60L* | *Ehd3* | *Ppfibp1* |
| *MTRR* | *DENND2A* | *Ehd4* | *Ppm1e* |
| *MTSS1* | *DENND3* | *Eif1b* | *Ppm1l* |
| *MYADML* | *DEPDC1* | *Elavl2* | *Ppp1ca* |
| *MYO15A* | *DEPDC4* | *Elfn1* | *Ppp4r4* |
| *MYO16* | *DGKA* | *Elmo1* | *Prima1* |
| *MYOF* | *DGKD* | *Emilin2* | *Prkar2a* |
| *MYOM2* | *DGKH* | *Emx1* | *Prkg2* |
| *NACA2* | *DHH* | *Emx2os* | *Prr13* |
| *NAP1L3* | *DIO2* | *Enc1* | *Prr16* |
| *NAV3* | *DIRAS3* | *Enkur* | *Prrt4* |
| *NCF2* | *DLC1* | *Eno4* | *Ptch2* |
| *NCK2* | *DLG1* | *Enox2* | *Ptchd2* |
| *NCOA2* | *DLGAP1* | *Enpp1* | *Ptgds* |
| *NEFL* | *DLGAP1-AS1* | *Entpd7* | *Ptgs2* |
| *NEK4* | *DLGAP4* | *Epb4.1l4a* | *Ptpn3* |
| *NEO1* | *DLK1* | *Epdr1* | *Ptpn5* |
| *NFIA* | *DLL3* | *Epha4* | *Ptprg* |
| *NINJ2* | *DMD* | *Epha5* | *Pvalb* |
| *NLGN1* | *DNAJC1* | *Epha6* | *Pvrl1* |
| *NLGN3* | *DNAJC12* | *Epha7* | *Pvrl3* |
| *NRG1* | *DNAJC25* | *Ephb3* | *Pwwp2b* |
| *NRG2* | *DNAJC6* | *Ephb6* | *Qrfpr* |
| *NRXN3* | *DNASE2* | *Ephx4* | *Ralyl* |
| *NSUN6* | *DNER* | *Epn1* | *Ramp3* |
| *NTM* | *DNM3* | *Eps8* | *Rap1gap* |
| *NTRK2* | *DNMT3B* | *Erc2* | *Rarg* |
| *NUDT3* | *DOCK11* | *Errfi1* | *Rasd1* |
| *NUF2* | *DOCK4* | *Evc2* | *Rasd2* |
| *NUP35* | *DOCK5* | *Exoc3l4* | *Rasgef1b* |
| *NXF2B* | *DOCK9* | *Exoc6* | *Rasgrf2* |
| *OPHN1* | *DOK4* | *Exph5* | *Rasgrp2* |
| *OR4K2* | *DPF3* | *Extl1* | *Rbck1* |
| *OSMR* | *DPP10* | *F2rl2* | *Rbm38* |
| *OXR1* | *DPP4* | *Faah* | *Rbms1* |
| *P2RX5* | *DPP6* | *Fads2* | *Rcn1* |
| *PACRG* | *DPY19L1P1* | *Fam105a* | *Reln* |
| *PAPOLA* | *DPYD* | *Fam107a* | *Rem2* |
| *PARD6G-AS1* | *DSG2* | *Fam120b* | *Ret* |
| *PAX7* | *DUSP1* | *Fam131a* | *Rgs11* |
| *PCDHB1* | *DUSP10* | *Fam13c* | *Rgs6* |
| *PDCD11* | *DUSP15* | *Fam149a* | *Rgs9* |

| | | | |
|---|---|---|---|
| *PDCD6IP* | *DUSP23* | *Fam150b* | *Rhobtb2* |
| *PDE11A* | *DUSP4* | *Fam154b* | *Rhou* |
| *PDE4D* | *DUSP5* | *Fam174b* | *Ric8b* |
| *PDHA2* | *DYRK3* | *Fam179a* | *Rin1* |
| *PDK4* | *E2F8* | *Fam184a* | *Rnf115* |
| *PDLIM1* | *EBF4* | *Fam188a* | *Rpe65* |
| *PDZRN3* | *ECE1* | *Fam196b* | *Rps6ka4* |
| *PEBP1* | *ECI2* | *Fam198a* | *Rreb1* |
| *PHACTR1* | *ECM1* | *Fam19a1* | *Rundc1* |
| *PHF3* | *ECSCR* | *Fam19a2* | *Rxfp3* |
| *PHGR1* | *EDARADD* | *Fam212b* | *Rxrg* |
| *PHLPP1* | *EDN3* | *Fam216b* | *Ryr1* |
| *PHTF2* | *EDNRB* | *Fam220a* | *Scmh1* |
| *PID1* | *EEA1* | *Fam26e* | *Sdc4* |
| *PIFO* | *EEPD1* | *Fam49a* | *Sdf2l1* |
| *PIGF* | *EFCAB6* | *Fam65b* | *Sec14l1* |
| *PIK3CA* | *EFEMP1* | *Fam78a* | *Sec14l3* |
| *PIK3CB* | *EFHC2* | *Farp1* | *Sema3f* |
| *PIK3R1* | *EFNA1* | *Fat1* | *Serpinb1b* |
| *PIP4K2A* | *EFNA5* | *Fat4* | *Serpini1* |
| *PLEC* | *EGF* | *Fbxl16* | *Sertm1* |
| *PLEKHM3* | *EGFR* | *Fbxo17* | *Sez6* |
| *POC1B* | *EGR2* | *Fbxo34* | *Sez6l* |
| *PODN* | *EHBP1* | *Fbxo45* | *Sh2d5* |
| *PODXL* | *EHD1* | *Fbxw7* | *Shb* |
| *POLG* | *EHD3* | *Fem1c* | *Shf* |
| *POLR2D* | *EHD4* | *Fgd5* | *Shisa2* |
| *POTEA* | *EIF2AK4* | *Fgd6* | *Sipa1l2* |
| *POU3F2* | *EIF4EBP1* | *Fgf1* | *Slc17a6* |
| *POU5F1P4* | *ELAVL2* | *Fgf12* | *Slc1a3* |
| *POU6F2-AS1* | *ELAVL4* | *Fgf13* | *Slc26a5* |
| *PPM1H* | *ELF4* | *Fgf3* | *Slc2a1* |
| *PPP1R3B* | *ELK3* | *Fgf5* | *Slc38a5* |
| *PPP1R9A* | *ELL2* | *Fgfr1op2* | *Slc6a6* |
| *PPT1* | *ELMOD1* | *Fhdc1* | *Slc8a1* |
| *PRDM1* | *ELOVL2* | *Fhl1* | *Slc9a2* |
| *PRDM6* | *ELOVL6* | *Fhl2* | *Slc9a9* |
| *PRKCB* | *ELTD1* | *Fhod3* | *Slit2* |
| *PROS1* | *EML6* | *Fibcd1* | *Smg5* |
| *PRPF18* | *ENC1* | *Filip1* | *Smim3* |
| *PRRG3* | *ENG* | *Fkbp1b* | *Smpd3* |
| *PRSS35* | *ENHO* | *Flot1* | *Soga2* |
| *PSAT1* | *ENO1* | *Flot2* | *Sorcs2* |
| *PSMG3-AS1* | *ENO3* | *Flrt1* | *Sorl1* |
| *PTGR1* | *ENOX1* | *Flrt3* | *Sox17* |
| *PTPN4* | *ENPP2* | *Fmn1* | *Sox8* |
| *PTPRB* | *ENTPD1* | *Fmnl1* | *Spata2l* |
| *PTPRG-AS1* | *ENTPD6* | *Fnbp1l* | *Sphkap* |
| *PTPRO* | *EOGT* | *Fndc9* | *Spint1* |
| *PURG* | *EPAS1* | *Foxg1* | *Spp1* |
| *RAB11FIP2* | *EPB41L2* | *Foxn2* | *Spry2* |
| *RAPH1* | *EPB41L4A* | *Foxo6* | *Sptssb* |
| *RASSF8* | *EPB41L4B* | *Foxp1* | *Srm* |
| *RBFOX1* | *EPHA2* | *Frat2* | *Srrt* |
| *RBM47* | *EPHA3* | *Frrs1l* | *St8sia1* |
| *REEP3* | *EPHB1* | *Fry* | *St8sia2* |

| | | | |
|---|---|---|---|
| *REG3G* | *EPHB2* | *Frzb* | *St8sia3* |
| *RFC3* | *EPHX2* | *Fstl1* | *Stard10* |
| *RGS1* | *EPS15L1* | *Fxyd7* | *Stard8* |
| *RGS18* | *EPT1* | *Fzd1* | *Steap2* |
| *RGS7* | *ERAP2* | *Gaa* | *Stk32a* |
| *RIC3* | *ERBB3* | *Gabra3* | *Strn* |
| *RNU6-67* | *ERI1* | *Gabra5* | *Stxbp6* |
| *RPGRIP1L* | *ERLEC1* | *Gabrg1* | *Synj2* |
| *RSG1* | *ESPN* | *Gabrg3* | *Syt6* |
| *RTN4* | *ESRRA* | *Gad1* | *Tagln* |
| *RTP4* | *ESYT2* | *Gad2* | *Tanc1* |
| *RUNX2* | *ETNK2* | *Gadd45b* | *Tbc1d1* |
| *SAP30* | *ETS1* | *Gal* | *Tbc1d10c* |
| *SCML4* | *ETV3* | *Gal3st3* | *Tbc1d8* |
| *SDK1* | *ETV4* | *Galnt13* | *Tcerg1l* |
| *SENP5* | *F11R* | *Galnt18* | *Tesc* |
| *SEPN1* | *F2R* | *Galnt3* | *Tgfa* |
| *SERPINA13P* | *F2RL2* | *Gap43* | *Thbs3* |
| *SERPINI1* | *FABP3* | *Garem* | *Theg* |
| *SGCD* | *FABP5* | *Gcnt1* | *Tmem108* |
| *SGMS1* | *FABP7* | *Gcnt4* | *Tmem132c* |
| *SH2B2* | *FAM102A* | *Gfod1* | *Tmem181a* |
| *SH3KBP1* | *FAM117A* | *Gfra1* | *Tmem181b-ps* |
| *SH3PXD2A-AS1* | *FAM120C* | *Gfra2* | *Tmem181c-ps* |
| *SH3PXD2B* | *FAM129A* | *Ghr* | *Tmem191c* |
| *SHISA9* | *FAM129B* | *Glp1r* | *Tmem200a* |
| *SIX3* | *FAM134B* | *Glra2* | *Tmem200b* |
| *SLC10A7* | *FAM135A* | *Glra3* | *Tmem200c* |
| *SLC15A4* | *FAM13C* | *Glrx* | *Tmem215* |
| *SLC17A9* | *FAM162A* | *Gls* | *Tmem229a* |
| *SLC25A26* | *FAM171B* | *Gm10432* | *Tmem252* |
| *SLC25A37* | *FAM178A* | *Gm13152* | *Tmem65* |
| *SLC46A2* | *FAM181A* | *Gm14204* | *Tmprss9* |
| *SLC4A4* | *FAM189A1* | *Gm20751* | *Tox2* |
| *SLC8A1-AS1* | *FAM196A* | *Gm3002* | *Tpd52l1* |
| *SLC8A2* | *FAM198A* | *Gm3893* | *Tpst1* |
| *SLITRK1* | *FAM198B* | *Gm5089* | *Traip* |
| *SLITRK5* | *FAM19A5* | *Gm514* | *Trim11* |
| *SMOC2* | *FAM206A* | *Gm5607* | *Trim66* |
| *SMYD3* | *FAM211B* | *Gm6277* | *Tsc22d3* |
| *SNAPC1* | *FAM212B* | *Gm6537* | *Tshz2* |
| *SNHG5* | *FAM216A* | *Gm973* | *Ttc34* |
| *SNORA70B* | *FAM218A* | *Gmpr* | *Ttc39b* |
| *SNTB1* | *FAM21B* | *Gnal* | *Ubash3b* |
| *SNX13* | *FAM3C* | *Gnb4* | *Ube2e1* |
| *SORL1* | *FAM43A* | *Gng13* | *Ublcp1* |
| *SOX11* | *FAM46B* | *Gng4* | *Unc5d* |
| *SOX4* | *FAM47E* | *Golm1* | *Upp2* |
| *SOX9* | *FAM60A* | *Gpc1* | *Usp28* |
| *SPARCL1* | *FAM65B* | *Gpc3* | *Usp53* |
| *SPIN4* | *FAM69A* | *Gpd1* | *Utp14b* |
| *SPNS2* | *FAM69C* | *Gpd2* | *Vamp1* |
| *SPOPL* | *FAM76A* | *Gpr101* | *Vrk1* |
| *SPP2* | *FAM78B* | *Gpr115* | *Vsnl1* |
| *SPRY2* | *FAM81A* | *Gpr12* | *Vstm2a* |
| *SRC* | *FAM83D* | *Gpr133* | *Wdr54* |

| | | | |
|---|---|---|---|
| *SRPX* | *FAM83G* | *Gpr139* | *Wnt5a* |
| *SRRM3* | *FAM84B* | *Gpr153* | *Zbtb16* |
| *SRRT* | *FAM86DP* | *Gpr165* | *Zbtb7c* |
| *ST3GAL3* | *FAM86HP* | *Gpr22* | *Zbtb8a* |
| *ST3GAL4* | *FARP1* | *Gpr4* | *Zfhx2* |
| *ST8SIA2* | *FAT3* | *Gpr45* | *Zfp385b* |
| *STAB2* | *FBLIM1* | *Gpr56* | *Zfp467* |
| *STAC* | *FBLN1* | *Gpr63* | *Zfp536* |
| *STK3* | *FBLN2* | *Gpr68* | *Zfyve28* |
| *STOX2* | *FBLN7* | *Gprasp2* | |
| *SUPV3L1* | *FBN2* | *Gpsm1* | |
| *TAF4* | *FBXL17* | *Gpx3* | |
| *TBC1D1* | *FBXO27* | *Grasp* | |
| *TBC1D14* | *FBXO28* | *Grb10* | |
| *TBC1D26* | *FBXO32* | *Grid2* | |
| *TDRD12* | *FCGR2A* | *Grid2ip* | |
| *TEKT4P2* | *FCGRT* | *Grik1* | |
| *TENM1* | *FCHO1* | *Grik3* | |
| *TENM2* | *FCRL6* | *Grik4* | |
| *TEP1* | *FCRLB* | *Grik5* | |
| *TERF1* | *FDFT1* | *Grin2d* | |
| *TGFBR2* | *FERMT2* | *Grip2* | |
| *THBS1* | *FEZF2* | *Grk5* | |
| *THRB-AS1* | *FGF1* | *Grm4* | |
| *TIMP4* | *FGF13* | *Grm8* | |
| *TLX3* | *FGFBP2* | *Grtp1* | |
| *TM2D3* | *FGFBP3* | *Gtf2ird1* | |
| *TMCC1* | *FGFR2* | *Gyg* | |
| *TMEM114* | *FGFR4* | *Hap1* | |
| *TMEM132E* | *FGFRL1* | *Hapln4* | |
| *TMEM165* | *FHDC1* | *Hcn4* | |
| *TMEM30C* | *FHL1* | *Hdc* | |
| *TMLHE-AS1* | *FHL2* | *Heg1* | |
| *TMTC2* | *FHL3* | *Heph* | |
| *TNK2* | *FHOD1* | *Hfe2* | |
| *TPK1* | *FIBIN* | *Hipk2* | |
| *TPRG1* | *FJX1* | *Hivep2* | |
| *TPTE* | *FKBP11* | *Hk1* | |
| *TRABD2A* | *FLJ16779* | *Hkdc1* | |
| *TRAPPC5* | *FLJ35024* | *Hmgb3* | |
| *TRAPPC8* | *FLJ42875* | *Hmgcs2* | |
| *TREM2* | *FLJ46906* | *Hn1* | |
| *TRHDE-AS1* | *FLNC* | *Homer3* | |
| *TRIM44* | *FLVCR2* | *Hpca* | |
| *TRIM48* | *FMN2* | *Hpcal4* | |
| *TRIM49B* | *FMNL2* | *Hpdl* | |
| *TRPM1* | *FMNL3* | *Hrasls* | |
| *TRPM3* | *FNBP1* | *Hrh1* | |
| *TRPS1* | *FNDC5* | *Hrk* | |
| *TSSC1* | *FOS* | *Hs3st2* | |
| *TTC28* | *FOSL1* | *Hs3st4* | |
| *TTR* | *FOSL2* | *Hs3st5* | |
| *TTTY23* | *FOXJ1* | *Hs6st2* | |
| *TTTY3B* | *FOXN3* | *Htatip2* | |
| *TXNDC8* | *FOXN3-AS1* | *Htr1b* | |
| *UBE2H* | *FOXO3* | *Htr2c* | |

| | | | |
|---|---|---|---|
| *UBE2MP1* | *FOXP1* | *Htr3a* | |
| *UBXN10* | *FRAT1* | *Htr4* | |
| *UGT2B4* | *FRAT2* | *Htr6* | |
| *UNC5C* | *FREM2* | *Htr7* | |
| *UPK3BL* | *FRMD3* | *Htra3* | |
| *UTRN* | *FRMD4A* | *Icam5* | |
| *VENTXP7* | *FRRS1L* | *Id4* | |
| *VPREB1* | *FRYL* | *Idh2* | |
| *WISP2* | *FXYD7* | *Ifi203* | |
| *WNT2B* | *GAB1* | *Ifngr2* | |
| *WWC1* | *GABBR1* | *Igfbp4* | |
| *WWC2* | *GABBR2* | *Igfbpl1* | |
| *WWOX* | *GABPB2* | *Igsf1* | |
| *XIRP2* | *GABRB2* | *Igsf10* | |
| *XPNPEP1* | *GABRG3* | *Il13ra1* | |
| *XRCC6P5* | *GABRQ* | *Il16* | |
| *XYLT1* | *GAD1* | *Il17rd* | |
| *YIPF7* | *GAD2* | *Il1f9* | |
| *ZBTB40* | *GADD45A* | *Il34* | |
| *ZBTB7A* | *GADD45GIP1* | *Il4ra* | |
| *ZC3H6* | *GALC* | *Impact* | |
| *ZCWPW2* | *GALK1* | *Inadl* | |
| *ZFAT-AS1* | *GALNT15* | *Inf2* | |
| *ZFHX4* | *GALNT18* | *Inhba* | |
| *ZIC3* | *GALNT4* | *Inpp5j* | |
| *ZIC4* | *GALNT5* | *Insm1* | |
| *ZKSCAN2* | *GAP43* | *Iqcg* | |
| *ZNF141* | *GAPDH* | *Iqgap2* | |
| *ZNF146* | *GARNL3* | *Iqsec2* | |
| *ZNF226* | *GATA6* | *Isl1* | |
| *ZNF366* | *GATM* | *Islr2* | |
| *ZNF385D* | *GATS* | *Isoc1* | |
| *ZNF397* | *GBE1* | *Itga11* | |
| *ZNF407* | *GBP1* | *Itga7* | |
| *ZNF462* | *GBP3* | *Itga8* | |
| *ZNF507* | *GBX2* | *Itgbl1* | |
| *ZNF557* | *GCH1* | *Itih3* | |
| *ZNF620* | *GCNT1* | *Itih5* | |
| *ZNF645* | *GDNF* | *Itpkb* | |
| *ZNF706* | *GDPD1* | *Itpr3* | |
| *ZNF716* | *GEM* | *Iyd* | |
| *ZNF733P* | *GFAP* | *Jph1* | |
| *ZNF735* | *GFPT2* | *Jph3* | |
| *ZNF827* | *GFRA1* | *Jph4* | |
| *ZNF891* | *GGACT* | *Junb* | |
| | *GGT1* | *Kalrn* | |
| | *GGT8P* | *Kank4* | |
| | *GJA1* | *Kazn* | |
| | *GJB2* | *Kcna4* | |
| | *GLCCI1* | *Kcnab2* | |
| | *GLG1* | *Kcnc3* | |
| | *GLIS3* | *Kcnd2* | |
| | *GLRB* | *Kcng3* | |
| | *GNAL* | *Kcnh2* | |
| | *GNAO1* | *Kcnh3* | |
| | *GNG3* | *Kcnh6* | |

| | | | |
|---|---|---|---|
| | *GNG7* | *Kcnip1* | |
| | *GNL3* | *Kcnj12* | |
| | *GOLGA8B* | *Kcnj4* | |
| | *GPC2* | *Kcnj6* | |
| | *GPC6* | *Kcnk4* | |
| | *GPD1L* | *Kcnmb2* | |
| | *GPER* | *Kcnmb4* | |
| | *GPM6B* | *Kcnn3* | |
| | *GPNMB* | *Kcnq5* | |
| | *GPR137B* | *Kcns2* | |
| | *GPR139* | *Kcnt1* | |
| | *GPR155* | *Kcnv1* | |
| | *GPR158* | *Kctd17* | |
| | *GPR176* | *Kctd4* | |
| | *GPR19* | *Kctd6* | |
| | *GPR50* | *Khdrbs3* | |
| | *GPR88* | *Kif23* | |
| | *GPRC5B* | *Kif9* | |
| | *GPRIN1* | *Kit* | |
| | *GPX3* | *Klf10* | |
| | *GRAMD3* | *Klhdc8a* | |
| | *GRB10* | *Klhdc8b* | |
| | *GREM1* | *Klhl13* | |
| | *GRHL3* | *Klhl2* | |
| | *GRIA1* | *Klhl40* | |
| | *GRIA2* | *Klk10* | |
| | *GRIA4* | *Klk8* | |
| | *GRIK1* | *Krt73* | |
| | *GRIK4* | *Lama1* | |
| | *GRIN2A* | *Lama3* | |
| | *GRIN2B* | *Lancl1* | |
| | *GRIN2D* | *Lancl2* | |
| | *GRM7* | *Large* | |
| | *GRPR* | *Ldb2* | |
| | *GSTM1* | *Lfng* | |
| | *GSTM2* | *Lgi1* | |
| | *GSTO1* | *Lhfpl3* | |
| | *GSTO2* | *Lhfpl5* | |
| | *GSX2* | *Lhx8* | |
| | *GTF2E1* | *Lhx9* | |
| | *GTF2E2* | *Limd2* | |
| | *GTF2F2* | *Lin28b* | |
| | *GUCY1B3* | *Lin7a* | |
| | *GXYLT2* | *Lin7b* | |
| | *GYG2* | *Lingo1* | |
| | *GYPC* | *Lingo2* | |
| | *H19* | *Lingo3* | |
| | *H1F0* | *Lipg* | |
| | *HAP1* | *Lmo3* | |
| | *HAS2* | *Lmo4* | |
| | *HAS2-AS1* | *Lmo7* | |
| | *HAS3* | *Lphn2* | |
| | *HBEGF* | *Lpl* | |
| | *HCP5* | *Lrguk* | |
| | *HDAC9* | *Lrp11* | |
| | *HELLS* | *Lrp12* | |

| | | | |
|---|---|---|---|
| | *HEPACAM* | *Lrrc1* | |
| | *HEPH* | *Lrrc17* | |
| | *HERC3* | *Lrrc23* | |
| | *HERPUD1* | *Lrrc36* | |
| | *HES2* | *Lrrc4* | |
| | *HEY1* | *Lrrc48* | |
| | *HEY2* | *Lrrc9* | |
| | *HGF* | *Lrrn2* | |
| | *HGS* | *Lrrtm3* | |
| | *HIBADH* | *Lsm11* | |
| | *HIF1A* | *Ltk* | |
| | *HIST1H2AE* | *Lurap1l* | |
| | *HIST1H2BC* | *Luzp2* | |
| | *HIST1H2BD* | *Ly6e* | |
| | *HIST1H2BG* | *Lynx1* | |
| | *HIST1H2BH* | *Lypd1* | |
| | *HIST1H4H* | *Lzts1* | |
| | *HIVEP1* | *Mab21l1* | |
| | *HIVEP3* | *Madd* | |
| | *HK2* | *Magi1* | |
| | *HLA-B* | *Man1a* | |
| | *HLA-C* | *Map2k1* | |
| | *HLA-DMA* | *Map3k1* | |
| | *HLA-DMB* | *Map3k19* | |
| | *HLA-DOA* | *Mapk1* | |
| | *HLA-DOB* | *Mapk10* | |
| | *HLA-DPA1* | *Mapk15* | |
| | *HLA-DPB1* | *March3* | |
| | *HLA-DQA1* | *Mast3* | |
| | *HLA-DQA2* | *Mat2b* | |
| | *HLA-DQB1* | *Matk* | |
| | *HLA-DRA* | *Mboat7* | |
| | *HLA-DRB1* | *Mchr1* | |
| | *HLA-DRB5* | *Mctp1* | |
| | *HLA-DRB6* | *Mctp2* | |
| | *HLA-E* | *Mcur1* | |
| | *HLA-F* | *Mdga1* | |
| | *HLA-H* | *Mdh1b* | |
| | *HLA-L* | *Me3* | |
| | *HMGA1* | *Mef2a* | |
| | *HMGA2* | *Meg3* | |
| | *HMGN5* | *Megf11* | |
| | *HNF4G* | *Megf6* | |
| | *HNMT* | *Meig1* | |
| | *HOMER2* | *Meis1* | |
| | *HOPX* | *Meis2* | |
| | *HPCAL1* | *Mertk* | |
| | *HPRT1* | *Met* | |
| | *HPSE* | *Mfsd4* | |
| | *HR* | *Mgst1* | |
| | *HS3ST1* | *Mgst3* | |
| | *HS3ST3B1* | *Mical2* | |
| | *HS3ST4* | *Mid2* | |
| | *HS6ST1* | *Mir22hg* | |
| | *HS6ST2* | *Mir3070b* | |
| | *HSD17B11* | *Mis18a* | |

| | | | |
|---|---|---|---|
| | *HSD3B7* | *Mlc1* | |
| | *HSPA12A* | *Mlip* | |
| | *HSPA2* | *Mllt11* | |
| | *HTR1F* | *Mmd* | |
| | *HUNK* | *Mmp15* | |
| | *ICK* | *Mmp17* | |
| | *ICOSLG* | *Mndal* | |
| | *ID4* | *Mns1* | |
| | *IDO1* | *Mob3b* | |
| | *IER2* | *Mpp3* | |
| | *IER3* | *Mrap2* | |
| | *IFI44* | *Mrgpre* | |
| | *IFI44L* | *Msi2* | |
| | *IFIT2* | *Msra* | |
| | *IFITM1* | *Msrb2* | |
| | *IFNAR1* | *Mt2* | |
| | *IGF2* | *Mtfp1* | |
| | *IGFBP3* | *Mtmr12* | |
| | *IGFBP5* | *Mtss1* | |
| | *IGFBP6* | *Mttp* | |
| | *IGFBP7* | *Musk* | |
| | *IGFBPL1* | *Myadm* | |
| | *IGIP* | *Mybl1* | |
| | *IGLON5* | *Mycbpap* | |
| | *IGSF11* | *Myh7* | |
| | *IGSF9* | *Mylk* | |
| | *IL11* | *Myo10* | |
| | *IL13RA2* | *N28178* | |
| | *IL18BP* | *N4bp2* | |
| | *IL1RAP* | *Nab2* | |
| | *IL27RA* | *Nabp1* | |
| | *IL32* | *Nap1l5* | |
| | *IL33* | *Napb* | |
| | *IL4R* | *Nav3* | |
| | *INHBB* | *Nbeal2* | |
| | *INO80C* | *Nck2* | |
| | *INPP5D* | *Nckap1* | |
| | *IPCEF1* | *Ndn* | |
| | *IPO13* | *Ndnf* | |
| | *IQCK* | *Ndrg3* | |
| | *IQGAP1* | *Nebl* | |
| | *IQSEC2* | *Necab1* | |
| | *IRF1* | *Nefl* | |
| | *IRS1* | *Nek10* | |
| | *IRX3* | *Nell2* | |
| | *ISLR2* | *Neto1* | |
| | *ITGA2* | *Neu2* | |
| | *ITGA3* | *Neurl1b* | |
| | *ITGA5* | *Nfib* | |
| | *ITGAV* | *Nfix* | |
| | *ITGB4* | *Nfkbie* | |
| | *ITGB5* | *Ngb* | |
| | *ITK* | *Ngf* | |
| | *ITM2B* | *Nhs* | |
| | *ITPKB* | *Nid1* | |
| | *ITPR2* | *Nin* | |

| | | | |
|---|---|---|---|
| | *ITPR3* | *Ninl* | |
| | *ITPRIPL2* | *Nkd2* | |
| | *JAKMIP2-AS1* | *Nkx2-1* | |
| | *JAM2* | *Nog* | |
| | *JMJD7* | *Nos1ap* | |
| | *JPH1* | *Notch4* | |
| | *JRK* | *Nova1* | |
| | *JUN* | *Npas1* | |
| | *JUNB* | *Npas2* | |
| | *JUP* | *Npdc1* | |
| | *KAT2B* | *Nptx1* | |
| | *KBTBD7* | *Nptx2* | |
| | *KCNA3* | *Nptxr* | |
| | *KCNA6* | *Npy* | |
| | *KCNE4* | *Npy1r* | |
| | *KCNF1* | *Npy2r* | |
| | *KCNJ10* | *Nr2f1* | |
| | *KCNJ2* | *Nr3c2* | |
| | *KCNJ4* | *Nr4a1* | |
| | *KCNJ8* | *Nr4a3* | |
| | *KCNK10* | *Nrcam* | |
| | *KCNMA1* | *Nrg1* | |
| | *KCNMB1* | *Nrg3* | |
| | *KCNN2* | *Nrgn* | |
| | *KCNN4* | *Nrip2* | |
| | *KCNQ3* | *Nrip3* | |
| | *KCNQ5* | *Nrn1* | |
| | *KCTD9* | *Nrp1* | |
| | *KDR* | *Nrsn1* | |
| | *KHDRBS3* | *Nrsn2* | |
| | *KIAA0040* | *Nrxn1* | |
| | *KIAA0368* | *Nsf* | |
| | *KIAA0754* | *Nsmf* | |
| | *KIAA1107* | *Nt5dc3* | |
| | *KIAA1161* | *Ntn4* | |
| | *KIAA1199* | *Ntng1* | |
| | *KIAA1211L* | *Ntng2* | |
| | *KIAA1217* | *Ntrk1* | |
| | *KIAA1244* | *Ntrk2* | |
| | *KIAA1407* | *Nts* | |
| | *KIAA1524* | *Numbl* | |
| | *KIAA1549L* | *Nwd1* | |
| | *KIAA1598* | *Nxn* | |
| | *KIAA1755* | *Nxph1* | |
| | *KIAA1919* | *Nynrin* | |
| | *KIF20B* | *Ociad2* | |
| | *KIF26B* | *Ogfrl1* | |
| | *KIFAP3* | *Olfm1* | |
| | *KIFC3* | *Olfml2b* | |
| | *KIRREL3* | *Onecut2* | |
| | *KLF14* | *Oprd1* | |
| | *KLF15* | *Orai2* | |
| | *KLF2* | *Osbpl9* | |
| | *KLF5* | *Osr1* | |
| | *KLHL29* | *Otof* | |
| | *KLHL35* | *Otos* | |

| | | | |
|---|---|---|---|
| | *KLHL36* | *P2rx5* | |
| | *KLHL4* | *Pag1* | |
| | *KNDC1* | *Palmd* | |
| | *KNSTRN* | *Papln* | |
| | *KREMEN1* | *Parp1* | |
| | *KRT18* | *Parp6* | |
| | *KRT80* | *Pax6* | |
| | *L3HYPDH* | *Pbx3* | |
| | *L3MBTL1* | *Pcdh1* | |
| | *L3MBTL3* | *Pcdh15* | |
| | *L3MBTL4* | *Pcdh18* | |
| | *LAMA1* | *Pcdh20* | |
| | *LAMB1* | *Pcdhgb6* | |
| | *LAMB2* | *Pcdhgb7* | |
| | *LAMP5* | *Pcdhgc4* | |
| | *LCAT* | *Pcgf5* | |
| | *LDB2* | *Pclo* | |
| | *LDHA* | *Pcnxl2* | |
| | *LEF1* | *Pcsk2* | |
| | *LEPREL1* | *Pcsk6* | |
| | *LFNG* | *Pde1a* | |
| | *LGALS1* | *Pde1c* | |
| | *LGALS12* | *Pde3a* | |
| | *LGALS3* | *Pde9a* | |
| | *LGALS8* | *Pdgfra* | |
| | *LGI1* | *Pdxk* | |
| | *LGI2* | *Peg10* | |
| | *LGR4* | *Peg3* | |
| | *LHFPL3* | *Pfkl* | |
| | *LIF* | *Pgap1* | |
| | *LIMCH1* | *Pgbd5* | |
| | *LIMD2* | *Pgf* | |
| | *LIMK2* | *Pgm2l1* | |
| | *LIMS2* | *Pgm5* | |
| | *LINC00338* | *Pgrmc1* | |
| | *LINC00341* | *Phactr2* | |
| | *LINC00488* | *Phex* | |
| | *LINC00839* | *Phf20* | |
| | *LIPG* | *Phospho1* | |
| | *LIX1* | *Phyhip* | |
| | *LMCD1* | *Pik3r2* | |
| | *LMCD1-AS1* | *Pip4k2c* | |
| | *LMF1* | *Pip5k1a* | |
| | *LMNA* | *Pip5k1c* | |
| | *LMO2* | *Pipox* | |
| | *LMO3* | *Pitpnm3* | |
| | *LMO4* | *Pkm* | |
| | *LMOD1* | *Pkp2* | |
| | *LNX1* | *Plcb4* | |
| | *LOC100093631* | *Plcd4* | |
| | *LOC100127888* | *Plch1* | |
| | *LOC100130557* | *Plch2* | |
| | *LOC100130691* | *Plcxd1* | |
| | *LOC100130987* | *Pld5* | |
| | *LOC100131067* | *Pld6* | |
| | *LOC100134868* | *Plekha6* | |

| | | | |
|---|---|---|---|
| | *LOC100289495* | *Plekha7* | |
| | *LOC100505695* | *Plekhg5* | |
| | *LOC100506124* | *Plk2* | |
| | *LOC100506178* | *Pls3* | |
| | *LOC100506343* | *Plxna1* | |
| | *LOC100506385* | *Plxna3* | |
| | *LOC100506421* | *Plxna4* | |
| | *LOC100506990* | *Pm20d1* | |
| | *LOC100507194* | *Pnck* | |
| | *LOC100507577* | *Pnma3* | |
| | *LOC100527964* | *Pnoc* | |
| | *LOC100996291* | *Pop5* | |
| | *LOC155060* | *Popdc3* | |
| | *LOC283070* | *Por* | |
| | *LOC284998* | *Porcn* | |
| | *LOC338799* | *Postn* | |
| | *LOC389023* | *Pou3f1* | |
| | *LOC642852* | *Ppfia2* | |
| | *LOC643355* | *Ppfia3* | |
| | *LOC653160* | *Ppil6* | |
| | *LOC654433* | *Ppm1h* | |
| | *LOC728392* | *Ppp1cc* | |
| | *LOC728431* | *Ppp1r1a* | |
| | *LOC728463* | *Ppp1r32* | |
| | *LOC728730* | *Ppp3ca* | |
| | *LOC728743* | *Ppp3cb* | |
| | *LOC729683* | *Ppp3r1* | |
| | *LOC729970* | *Prdm16* | |
| | *LOC730101* | *Prdx4* | |
| | *LOC730183* | *Prickle2* | |
| | *LOX* | *Prkab2* | |
| | *LOXL1* | *Prkacb* | |
| | *LOXL1-AS1* | *Prkag2* | |
| | *LOXL4* | *Prkar2b* | |
| | *LPAR1* | *Prkca* | |
| | *LPAR2* | *Prkcd* | |
| | *LPAR4* | *Prkce* | |
| | *LPAR6* | *Prkcg* | |
| | *LPCAT2* | *Prkg2* | |
| | *LPHN2* | *Prokr2* | |
| | *LPIN1* | *Prrt2* | |
| | *LPIN2* | *Prrt3* | |
| | *LPL* | *Prss35* | |
| | *LPPR4* | *Prtn3* | |
| | *LPPR5* | *Psd* | |
| | *LRCH1* | *Ptch1* | |
| | *LRFN1* | *Ptch2* | |
| | *LRIG1* | *Ptchd1* | |
| | *LRIG3* | *Ptgfrn* | |
| | *LRP12* | *Ptgs2* | |
| | *LRP2* | *Ptk2b* | |
| | *LRP4* | *Ptn* | |
| | *LRP8* | *Ptpdc1* | |
| | *LRRC15* | *Ptpn5* | |
| | *LRRC3B* | *Ptpre* | |
| | *LRRC4C* | *Ptprt* | |

| | | | |
|---|---|---|---|
| | *LRRC56* | *Pvrl3* | |
| | *LRRC73* | *Pvrl4* | |
| | *LRRC8C* | *Pxdn* | |
| | *LRRCC1* | *Qpct* | |
| | *LRRTM2* | *R3hdm4* | |
| | *LRRTM3* | *Rab15* | |
| | *LRRTM4* | *Rab3d* | |
| | *LSP1* | *Rab3ip* | |
| | *LTBP2* | *Rab6b* | |
| | *LTBP3* | *Rabgap1l* | |
| | *LUZP2* | *Radil* | |
| | *LY6H* | *Rap1gap2* | |
| | *LYN* | *Rapgef3* | |
| | *LYNX1* | *Rapgef5* | |
| | *LYPD6B* | *Rapgefl1* | |
| | *LYST* | *Rara* | |
| | *MAEL* | *Rarres2* | |
| | *MAFB* | *Rasa4* | |
| | *MAGEL2* | *Rasal1* | |
| | *MAGI2* | *Rasgef1a* | |
| | *MAGI2-AS3* | *Rasgrp1* | |
| | *MALT1* | *Rasl11a* | |
| | *MAML3* | *Rasl11b* | |
| | *MAMLD1* | *Rassf9* | |
| | *MAOB* | *Raver2* | |
| | *MAP1B* | *Rbfox1* | |
| | *MAP1LC3A* | *Rbfox3* | |
| | *MAP1LC3C* | *Rbm20* | |
| | *MAP2K3* | *Rbms1* | |
| | *MAP2K5* | *Rbms3* | |
| | *MAP3K3* | *Rcan3* | |
| | *MAP3K5* | *Rcn1* | |
| | *MAP3K6* | *Rec8* | |
| | *MAP7D1* | *Rem2* | |
| | *MAPK8IP1* | *Resp18* | |
| | *MAPKAPK3* | *Ret* | |
| | *MARCH2* | *Rftn1* | |
| | *MARCH4* | *Rgag4* | |
| | *MARK1* | *Rgs10* | |
| | *MARVELD3* | *Rgs11* | |
| | *MASP1* | *Rgs14* | |
| | *MAST4* | *Rgs17* | |
| | *MB21D2* | *Rgs2* | |
| | *MBNL1-AS1* | *Rgs22* | |
| | *MBOAT1* | *Rgs3* | |
| | *MC1R* | *Rgs4* | |
| | *MCHR1* | *Rgs7bp* | |
| | *MCTP1* | *Rgs8* | |
| | *MCTP2* | *Rgsl1* | |
| | *MDFI* | *Rhpn1* | |
| | *ME3* | *Rimbp2* | |
| | *MED12L* | *Rims1* | |
| | *MEF2C* | *Rims3* | |
| | *MEGF9* | *Rit2* | |
| | *MESP1* | *Rltpr* | |
| | *METAP1* | *Rmst* | |

| | | | |
|---|---|---|---|
| | *METRNL* | *Rnf112* | |
| | *METTL7A* | *Rnf144b* | |
| | *METTL7B* | *Rnf152* | |
| | *MFAP2* | *Rnf165* | |
| | *MFAP3L* | *Rnf182* | |
| | *MFAP4* | *Rnf19a* | |
| | *MFAP5* | *Rnf207* | |
| | *MFI2* | *Robo1* | |
| | *MFRP* | *Robo2* | |
| | *MGARP* | *Rogdi* | |
| | *MGLL* | *Rprml* | |
| | *MGST1* | *Rps6ka2* | |
| | *MIAT* | *Rps6kl1* | |
| | *MICA* | *Rrad* | |
| | *MICAL2* | *Rspo1* | |
| | *MID1* | *Rspo2* | |
| | *MIF* | *Rspo3* | |
| | *MIF4GD* | *Rtn4r* | |
| | *MIPEPP3* | *Rtn4rl1* | |
| | *MIR210HG* | *Runx1t1* | |
| | *MITF* | *Runx2* | |
| | *MLC1* | *S100a10* | |
| | *MLLT11* | *Sall3* | |
| | *MMACHC* | *Samd14* | |
| | *MMP15* | *Samd4* | |
| | *MMP17* | *Sarm1* | |
| | *MN1* | *Scarf2* | |
| | *MOB3B* | *Scgn* | |
| | *MOK* | *Schip1* | |
| | *MORC4* | *Scn1b* | |
| | *MORN1* | *Scn8a* | |
| | *MOXD1* | *Scn9a* | |
| | *MPC1* | *Scrt2* | |
| | *MPP3* | *Scx* | |
| | *MRAP2* | *Sdc2* | |
| | *MRAS* | *Sdcbp* | |
| | *MREG* | *Sel1l3* | |
| | *MROH8* | *Sema3a* | |
| | *MRPL3* | *Sema3e* | |
| | *MSH5-SAPCD1* | *Sema3f* | |
| | *MSN* | *Sema4g* | |
| | *MT1X* | *Sema7a* | |
| | *MT2A* | *Sepp1* | |
| | *MT3* | *Sept3* | |
| | *MTFP1* | *Sept9* | |
| | *MTHFD2* | *Sepw1* | |
| | *MTM1* | *Serpina3n* | |
| | *MTSS1* | *Serpinb8* | |
| | *MTSS1L* | *Serpine2* | |
| | *MTTP* | *Sesn3* | |
| | *MTUS1* | *Sfrp2* | |
| | *MURC* | *Sgsm1* | |
| | *MXI1* | *Sh3bgrl3* | |
| | *MXRA5* | *Sh3bp5* | |
| | *MYC* | *Sh3gl2* | |
| | *MYCL1* | *Sh3rf1* | |

| | | | |
|---|---|---|---|
| | *MYL12A* | *Shisa6* | |
| | *MYLK* | *Sidt1* | |
| | *MYO10* | *Sipa1l3* | |
| | *MYO19* | *Six3* | |
| | *MYO1B* | *Six3os1* | |
| | *MYO1E* | *Skida1* | |
| | *MYO5B* | *Skil* | |
| | *MYO7A* | *Slc10a4* | |
| | *MYOF* | *Slc17a6* | |
| | *MZT1* | *Slc17a7* | |
| | *N4BP2L1* | *Slc17a8* | |
| | *NABP1* | *Slc1a3* | |
| | *NACC2* | *Slc20a2* | |
| | *NADKD1* | *Slc22a3* | |
| | *NAPEPLD* | *Slc24a2* | |
| | *NAT8L* | *Slc24a4* | |
| | *NAV1* | *Slc25a13* | |
| | *NAV2* | *Slc25a22* | |
| | *NBEAL2* | *Slc25a29* | |
| | *NCAM1* | *Slc25a34* | |
| | *NCAM2* | *Slc26a4* | |
| | *NCAPG* | *Slc2a6* | |
| | *NCEH1* | *Slc2a9* | |
| | *NCKAP5* | *Slc32a1* | |
| | *NCMAP* | *Slc35f1* | |
| | *NCR3LG1* | *Slc35g2* | |
| | *NDRG1* | *Slc37a1* | |
| | *NDRG2* | *Slc38a1* | |
| | *NDUFA9* | *Slc38a5* | |
| | *NDUFAF2* | *Slc44a5* | |
| | *NEDD4* | *Slc4a7* | |
| | *NEFH* | *Slc6a1* | |
| | *NEGR1* | *Slc6a11* | |
| | *NEK11* | *Slc6a15* | |
| | *NF2* | *Slc6a7* | |
| | *NFASC* | *Slc7a11* | |
| | *NFATC1* | *Slc7a14* | |
| | *NFE2L2* | *Slc7a3* | |
| | *NFIA* | *Slc7a4* | |
| | *NFKBIA* | *Slc7a8* | |
| | *NGEF* | *Slc8a2* | |
| | *NGFR* | *Slc8a3* | |
| | *NID1* | *Slc9a2* | |
| | *NIM1* | *Slc9a4* | |
| | *NIN* | *Slc9a5* | |
| | *NIPSNAP1* | *Slc9a6* | |
| | *NKAIN1* | *Slco2a1* | |
| | *NKAIN4* | *Slit3* | |
| | *NKD1* | *Slitrk3* | |
| | *NKX6-2* | *Slitrk5* | |
| | *NLGN3* | *Slitrk6* | |
| | *NLGN4X* | *Smoc1* | |
| | *NMB* | *Smoc2* | |
| | *NMNAT2* | *Smpd3* | |
| | *NMRK1* | *Sms* | |
| | *NNMT* | *Snap25* | |

| | | | |
|---|---|---|---|
| | *NOMO2* | *Snap91* | |
| | *NOS1* | *Snca* | |
| | *NOS1AP* | *Sncg* | |
| | *NOXA1* | *Snn* | |
| | *NPAS3* | *Snph* | |
| | *NPS* | *Sntb1* | |
| | *NPTXR* | *Snx8* | |
| | *NR2F1* | *Socs2* | |
| | *NR3C1* | *Sorcs1* | |
| | *NR4A1* | *Sort1* | |
| | *NRARP* | *Sox1* | |
| | *NRG2* | *Sox13* | |
| | *NRGN* | *Sox2* | |
| | *NRP1* | *Sp9* | |
| | *NRP2* | *Spata13* | |
| | *NRSN1* | *Spata18* | |
| | *NSG1* | *Spata2l* | |
| | *NT5DC3* | *Spats2l* | |
| | *NT5E* | *Spef2* | |
| | *NTM* | *Speg* | |
| | *NTSR1* | *Sphkap* | |
| | *NUPR1* | *Spint1* | |
| | *NXPE3* | *Spock1* | |
| | *NXPH1* | *Spon1* | |
| | *NXPH3* | *Spp1* | |
| | *OAF* | *Spred2* | |
| | *OCIAD2* | *Sprn* | |
| | *OCLN* | *Sptb* | |
| | *ODC1* | *Sptbn2* | |
| | *OGDHL* | *Srebf1* | |
| | *OGFRL1* | *Srgap1* | |
| | *OLFM1* | *Srl* | |
| | *OLFML2A* | *Ssh1* | |
| | *OLFML2B* | *Sspo* | |
| | *OLFML3* | *Sstr3* | |
| | *OLIG1* | *Ssx2ip* | |
| | *OLIG2* | *St18* | |
| | *OMG* | *St3gal5* | |
| | *ORC1* | *St6galnac5* | |
| | *OSBP2* | *Stac* | |
| | *OSBPL3* | *Stard5* | |
| | *OSBPL5* | *Stat5b* | |
| | *OTX2* | *Stim2* | |
| | *P2RX6* | *Strn4* | |
| | *P2RX7* | *Stx1a* | |
| | *P4HA2* | *Stxbp5* | |
| | *PABPC3* | *Stxbp5l* | |
| | *PABPC5* | *Sult4a1* | |
| | *PACRG* | *Susd2* | |
| | *PADI3* | *Sv2b* | |
| | *PAG1* | *Sv2c* | |
| | *PAK3* | *Syce2* | |
| | *PAK6* | *Syn1* | |
| | *PALM2* | *Syn2* | |
| | *PAPLN* | *Syna* | |
| | *PAPSS2* | *Syndig1* | |

| | | | |
|---|---|---|---|
| | *PAQR3* | *Synj1* | |
| | *PAQR6* | *Synm* | |
| | *PAQR8* | *Synpo* | |
| | *PAQR9* | *Synpr* | |
| | *PAR-SN* | *Syt1* | |
| | *PARD6A* | *Syt13* | |
| | *PARM1* | *Syt3* | |
| | *PARP12* | *Tacr1* | |
| | *PAWR* | *Tanc1* | |
| | *PAX6* | *Tbata* | |
| | *PCDH1* | *Tbc1d8b* | |
| | *PCDH10* | *Tbl1x* | |
| | *PCDH18* | *Tbr1* | |
| | *PCDH19* | *Tcerg1l* | |
| | *PCDH7* | *Tcf4* | |
| | *PCDH8* | *Tcfl5* | |
| | *PCDH9* | *Tcte1* | |
| | *PCDHA4* | *Tdrd5* | |
| | *PCDHAC1* | *Tec* | |
| | *PCDHGA3* | *Tecpr1* | |
| | *PCDHGC3* | *Tenm1* | |
| | *PCDHGC5* | *Tenm3* | |
| | *PCED1B* | *Tesc* | |
| | *PCK1* | *Tex40* | |
| | *PCP4* | *Tex9* | |
| | *PDE1C* | *Thbs2* | |
| | *PDE2A* | *Thbs4* | |
| | *PDE3A* | *Them6* | |
| | *PDE4B* | *Thra* | |
| | *PDE6B* | *Thrb* | |
| | *PDE8A* | *Thrsp* | |
| | *PDE8B* | *Thsd4* | |
| | *PDGFB* | *Timp2* | |
| | *PDGFRA* | *Tle1* | |
| | *PDGFRL* | *Tm4sf1* | |
| | *PDIA5* | *Tmco5* | |
| | *PDK1* | *Tmem130* | |
| | *PDLIM3* | *Tmem132c* | |
| | *PDLIM4* | *Tmem132e* | |
| | *PDP1* | *Tmem144* | |
| | *PDPN* | *Tmem151b* | |
| | *PDZD2* | *Tmem158* | |
| | *PEG10* | *Tmem163* | |
| | *PEG3* | *Tmem178* | |
| | *PERP* | *Tmem198* | |
| | *PFDN1* | *Tmem212* | |
| | *PFKFB2* | *Tmem232* | |
| | *PFKP* | *Tmem252* | |
| | *PGBD5* | *Tmem255a* | |
| | *PHKG1* | *Tmem42* | |
| | *PHLDA1* | *Tmem47* | |
| | *PHLDA2* | *Tmem59l* | |
| | *PHLDB2* | *Tmem67* | |
| | *PIEZO2* | *Tmem91* | |
| | *PIK3C2B* | *Tmie* | |
| | *PIK3R3* | *Tmsb10* | |

| | | | |
|---|---|---|---|
| | *PIM3* | *Tnfaip3* | |
| | *PIRT* | *Tnfaip8l1* | |
| | *PITPNM2* | *Tnfaip8l3* | |
| | *PITPNM3* | *Tnfrsf25* | |
| | *PKIB* | *Tnks1bp1* | |
| | *PKM* | *Tomm34* | |
| | *PLA2G4A* | *Tox* | |
| | *PLA2G5* | *Tox2* | |
| | *PLAC9* | *Tpd52l1* | |
| | *PLAU* | *Tppp3* | |
| | *PLAUR* | *Tprkb* | |
| | *PLB1* | *Trhde* | |
| | *PLCB4* | *Trim2* | |
| | *PLCE1* | *Trim66* | |
| | *PLCH1* | *Trnp1* | |
| | *PLCL2* | *Tro* | |
| | *PLD5* | *Trpc3* | |
| | *PLEKHA1* | *Trpc4* | |
| | *PLEKHA7* | *Trpc7* | |
| | *PLEKHF1* | *Trps1* | |
| | *PLEKHG4B* | *Tshz2* | |
| | *PLEKHG5* | *Tspan13* | |
| | *PLEKHH2* | *Tspan17* | |
| | *PLIN2* | *Tspan18* | |
| | *PLIN3* | *Tspan5* | |
| | *PLK1* | *Ttc39a* | |
| | *PLK2* | *Ttl* | |
| | *PLLP* | *Ttll3* | |
| | *PLOD2* | *Ttll8* | |
| | *PLP1* | *Tuba4a* | |
| | *PLS1* | *Tuba8* | |
| | *PLSCR4* | *Tyro3* | |
| | *PLXDC2* | *Uba7* | |
| | *PLXNA2* | *Ubash3b* | |
| | *PLXNA4* | *Ube2g2* | |
| | *PLXNB3* | *Ubxn10* | |
| | *PMAIP1* | *Ubxn11* | |
| | *PMEPA1* | *Unc13b* | |
| | *PML* | *Unc13c* | |
| | *PMP2* | *Unc5a* | |
| | *PNCK* | *Unc5c* | |
| | *PNP* | *Usp12* | |
| | *PNPLA3* | *Usp13* | |
| | *POC1B* | *Usp29* | |
| | *PODXL* | *Usp35* | |
| | *POLQ* | *Usp51* | |
| | *POLR1E* | *Usp6nl* | |
| | *POLR3G* | *Ust* | |
| | *POMT2* | *Vat1* | |
| | *POP1* | *Vat1l* | |
| | *POPDC3* | *Vill* | |
| | *POSTN* | *Vps37b* | |
| | *POU2F3* | *Vstm2l* | |
| | *PPAP2B* | *Vwa5b1* | |
| | *PPAP2C* | *Vwc2l* | |
| | *PPAPDC1A* | *Wasf1* | |

| | | | |
|---|---|---|---|
| | *PPARD* | *Wbscr17* | |
| | *PPARGC1A* | *Wdr6* | |
| | *PPL* | *Whrn* | |
| | *PPP1R14B* | *Wipf3* | |
| | *PPP1R14C* | *Wnt7b* | |
| | *PPP1R18* | *Xkr6* | |
| | *PPP1R1C* | *Xpr1* | |
| | *PPP1R2* | *Ypel1* | |
| | *PPP1R3B* | *Ywhah* | |
| | *PPP1R3E* | *Zbtb18* | |
| | *PPP2R5A* | *Zbtb7c* | |
| | *PRAF2* | *Zbtb8b* | |
| | *PRDM1* | *Zcchc12* | |
| | *PRDM16* | *Zdbf2* | |
| | *PRDX1* | *Zeb2* | |
| | *PRELID2* | *Zfhx3* | |
| | *PREP* | *Zfhx4* | |
| | *PRICKLE1* | *Zfp189* | |
| | *PRICKLE2* | *Zfp275* | |
| | *PRICKLE4* | *Zfp365* | |
| | *PRKAR2A* | *Zfp423* | |
| | *PRKAR2B* | *Zfp46* | |
| | *PRKCD* | *Zfp503* | |
| | *PRKCE* | *Zfp521* | |
| | *PRKCZ* | *Zfp697* | |
| | *PRKG1* | *Zfp783* | |
| | *PROCA1* | *Zfp811* | |
| | *PROCR* | *Zfp92* | |
| | *PRODH* | *Zfp941* | |
| | *PROKR1* | *Zfpm2* | |
| | *PROM1* | *Zfyve28* | |
| | *PROX1* | *Zic1* | |
| | *PRR16* | *Zic2* | |
| | *PRRX1* | *Zic3* | |
| | *PRSS23* | *Zic4* | |
| | *PSD3* | *Zim1* | |
| | *PSMA6* | *Zkscan16* | |
| | *PSRC1* | *Zkscan7* | |
| | *PSTPIP2* | *Zmat2* | |
| | *PTCHD1* | | |
| | *PTCHD2* | | |
| | *PTGDS* | | |
| | *PTGES* | | |
| | *PTGR1* | | |
| | *PTGS1* | | |
| | *PTHLH* | | |
| | *PTK2* | | |
| | *PTN* | | |
| | *PTP4A3* | | |
| | *PTPDC1* | | |
| | *PTPN3* | | |
| | *PTPN9* | | |
| | *PTPRE* | | |
| | *PTPRF* | | |
| | *PTPRN* | | |
| | *PTPRT* | | |

| | | | |
|---|---|---|---|
| | *PTPRU* | | |
| | *PTPRZ1* | | |
| | *PUSL1* | | |
| | *PVRL1* | | |
| | *PXMP4* | | |
| | *PXN* | | |
| | *PYGB* | | |
| | *QPCT* | | |
| | *RAB11FIP1* | | |
| | *RAB13* | | |
| | *RAB30* | | |
| | *RAB34* | | |
| | *RAB38* | | |
| | *RAB3B* | | |
| | *RAB3IL1* | | |
| | *RAD51D* | | |
| | *RADIL* | | |
| | *RAI14* | | |
| | *RALYL* | | |
| | *RAMP1* | | |
| | *RAP1GAP* | | |
| | *RAP1GAP2* | | |
| | *RAPGEF4* | | |
| | *RAPGEF5* | | |
| | *RARRES3* | | |
| | *RASD2* | | |
| | *RASEF* | | |
| | *RASGRF2* | | |
| | *RASGRP1* | | |
| | *RASGRP2* | | |
| | *RASL11B* | | |
| | *RASSF10* | | |
| | *RASSF8* | | |
| | *RBM24* | | |
| | *RBMS2* | | |
| | *RBPMS* | | |
| | *RCAN2* | | |
| | *RCBTB2* | | |
| | *RCL1* | | |
| | *RCOR2* | | |
| | *RDM1* | | |
| | *REEP1* | | |
| | *RELL1* | | |
| | *RENBP* | | |
| | *RFFL* | | |
| | *RFTN2* | | |
| | *RGMA* | | |
| | *RGMB* | | |
| | *RGR* | | |
| | *RGS10* | | |
| | *RGS11* | | |
| | *RGS16* | | |
| | *RGS3* | | |
| | *RGS4* | | |
| | *RGS5* | | |
| | *RGS7BP* | | |

| | | | |
|---|---|---|---|
| | *RGS8* | | |
| | *RHBDL1* | | |
| | *RHOU* | | |
| | *RHPN1* | | |
| | *RHPN2* | | |
| | *RIBC1* | | |
| | *RIN1* | | |
| | *RIPK2* | | |
| | *RNASE4* | | |
| | *RND1* | | |
| | *RND2* | | |
| | *RNF112* | | |
| | *RNF128* | | |
| | *RNF13* | | |
| | *RNF157* | | |
| | *RNF157-AS1* | | |
| | *RNF217* | | |
| | *RNF34* | | |
| | *ROBO2* | | |
| | *ROBO3* | | |
| | *RORB* | | |
| | *RPE65* | | |
| | *RPH3A* | | |
| | *RPL22L1* | | |
| | *RPL37A* | | |
| | *RPP25* | | |
| | *RPS6KA1* | | |
| | *RPS6KA5* | | |
| | *RPS6KL1* | | |
| | *RRAD* | | |
| | *RRAS2* | | |
| | *RRS1* | | |
| | *RSPH4A* | | |
| | *RTDR1* | | |
| | *RTN1* | | |
| | *RTN2* | | |
| | *RTN4R* | | |
| | *RXRA* | | |
| | *RXRB* | | |
| | *RYR3* | | |
| | *S100A10* | | |
| | *S100A16* | | |
| | *S100A2* | | |
| | *S100A3* | | |
| | *S100A4* | | |
| | *S100A6* | | |
| | *S100B* | | |
| | *S1PR1* | | |
| | *SALL1* | | |
| | *SAMD4A* | | |
| | *SAMD9* | | |
| | *SAPCD2* | | |
| | *SAT1* | | |
| | *SCG2* | | |
| | *SCG3* | | |
| | *SCG5* | | |

| | | | |
|---|---|---|---|
| | *SCGN* | | |
| | *SCN1A* | | |
| | *SCN3A* | | |
| | *SCN4B* | | |
| | *SCN9A* | | |
| | *SCNN1B* | | |
| | *SCNN1D* | | |
| | *SCPEP1* | | |
| | *SCRG1* | | |
| | *SCUBE1* | | |
| | *SCUBE2* | | |
| | *SDC1* | | |
| | *SDHAP2* | | |
| | *SDK1* | | |
| | *SDK2* | | |
| | *SEL1L3* | | |
| | *SELENBP1* | | |
| | *SELPLG* | | |
| | *SEMA4B* | | |
| | *SEMA5A* | | |
| | *SEMA5B* | | |
| | *SEMA6A* | | |
| | *SEMA6B* | | |
| | *SEMA6D* | | |
| | *SEMA7A* | | |
| | *SEMG1* | | |
| | *SENP3-EIF4A1* | | |
| | *SEPP1* | | |
| | *SEPSECS* | | |
| | *SEPT6* | | |
| | *SEPT7* | | |
| | *SERHL2* | | |
| | *SERINC2* | | |
| | *SERPINA3* | | |
| | *SERPINB8* | | |
| | *SERPINE1* | | |
| | *SERPINE2* | | |
| | *SERPING1* | | |
| | *SERTAD4* | | |
| | *SETD7* | | |
| | *SEZ6* | | |
| | *SFRP1* | | |
| | *SFT2D2* | | |
| | *SGK1* | | |
| | *SGSM1* | | |
| | *SH2B3* | | |
| | *SH3BGRL3* | | |
| | *SH3BP5* | | |
| | *SH3BP5-AS1* | | |
| | *SH3GL2* | | |
| | *SH3PXD2A* | | |
| | *SHISA9* | | |
| | *SHROOM4* | | |
| | *SIPA1* | | |
| | *SIPA1L2* | | |
| | *SKIL* | | |

| | | | |
|---|---|---|---|
| | *SLC10A4* | | |
| | *SLC13A5* | | |
| | *SLC15A3* | | |
| | *SLC18A1* | | |
| | *SLC18B1* | | |
| | *SLC1A1* | | |
| | *SLC1A3* | | |
| | *SLC1A4* | | |
| | *SLC24A3* | | |
| | *SLC25A27* | | |
| | *SLC25A33* | | |
| | *SLC26A2* | | |
| | *SLC2A1* | | |
| | *SLC2A10* | | |
| | *SLC2A5* | | |
| | *SLC2A8* | | |
| | *SLC31A2* | | |
| | *SLC32A1* | | |
| | *SLC35E4* | | |
| | *SLC35F2* | | |
| | *SLC37A1* | | |
| | *SLC38A1* | | |
| | *SLC39A10* | | |
| | *SLC39A14* | | |
| | *SLC43A3* | | |
| | *SLC47A2* | | |
| | *SLC48A1* | | |
| | *SLC4A10* | | |
| | *SLC4A4* | | |
| | *SLC6A20* | | |
| | *SLC6A9* | | |
| | *SLC7A1* | | |
| | *SLC7A11* | | |
| | *SLC7A5* | | |
| | *SLC9A3R1* | | |
| | *SLC9A7* | | |
| | *SLC9A9* | | |
| | *SLCO1C1* | | |
| | *SLCO4A1* | | |
| | *SLIT2* | | |
| | *SLITRK2* | | |
| | *SMAD7* | | |
| | *SMAGP* | | |
| | *SMAP2* | | |
| | *SMARCA2* | | |
| | *SMARCD2* | | |
| | *SMOC1* | | |
| | *SMOC2* | | |
| | *SMOX* | | |
| | *SMS* | | |
| | *SMTN* | | |
| | *SMURF2* | | |
| | *SMYD3* | | |
| | *SNAI2* | | |
| | *SNCAIP* | | |
| | *SNHG8* | | |

| | | | |
|---|---|---|---|
| | *SNORA76* | | |
| | *SNTB1* | | |
| | *SNTG1* | | |
| | *SNX10* | | |
| | *SOBP* | | |
| | *SOCS1* | | |
| | *SOGA2* | | |
| | *SOGA3* | | |
| | *SORBS1* | | |
| | *SORL1* | | |
| | *SORT1* | | |
| | *SOWAHC* | | |
| | *SOX1* | | |
| | *SOX13* | | |
| | *SOX2* | | |
| | *SOX21* | | |
| | *SOX3* | | |
| | *SOX5* | | |
| | *SOX6* | | |
| | *SOX9* | | |
| | *SP100* | | |
| | *SP140L* | | |
| | *SPARCL1* | | |
| | *SPATA13* | | |
| | *SPATA6* | | |
| | *SPC25* | | |
| | *SPEF2* | | |
| | *SPHK1* | | |
| | *SPOCD1* | | |
| | *SPOCK2* | | |
| | *SPP1* | | |
| | *SPRED3* | | |
| | *SPRY2* | | |
| | *SPSB1* | | |
| | *SPSB2* | | |
| | *SQRDL* | | |
| | *SRCIN1* | | |
| | *SRGAP1* | | |
| | *SRPX* | | |
| | *SSC5D* | | |
| | *SSFA2* | | |
| | *SSPN* | | |
| | *SSR3* | | |
| | *SST* | | |
| | *ST3GAL5* | | |
| | *ST6GAL1* | | |
| | *ST6GAL2* | | |
| | *ST7* | | |
| | *ST7-AS1* | | |
| | *ST8SIA1* | | |
| | *ST8SIA2* | | |
| | *ST8SIA3* | | |
| | *ST8SIA4* | | |
| | *STAC2* | | |
| | *STAMBPL1* | | |
| | *STAP2* | | |

| | | | |
|---|---|---|---|
| | *STARD13* | | |
| | *STARD4* | | |
| | *STARD8* | | |
| | *STAT2* | | |
| | *STC1* | | |
| | *STC2* | | |
| | *STEAP3* | | |
| | *STK10* | | |
| | *STK17A* | | |
| | *STK17B* | | |
| | *STK39* | | |
| | *STON1-GTF2A1L* | | |
| | *STOX1* | | |
| | *STPG1* | | |
| | *STRA6* | | |
| | *STX1A* | | |
| | *STX3* | | |
| | *STXBP5L* | | |
| | *SULF1* | | |
| | *SULF2* | | |
| | *SULT1C4* | | |
| | *SUSD5* | | |
| | *SUV420H2* | | |
| | *SYCE1L* | | |
| | *SYNE1* | | |
| | *SYNE3* | | |
| | *SYNJ2* | | |
| | *SYNM* | | |
| | *SYNPO* | | |
| | *SYNPR* | | |
| | *SYT11* | | |
| | *SYT12* | | |
| | *SYT17* | | |
| | *SYT6* | | |
| | *SYTL2* | | |
| | *TAB3* | | |
| | *TACC1* | | |
| | *TAF4B* | | |
| | *TAGLN2* | | |
| | *TAGLN3* | | |
| | *TALDO1* | | |
| | *TAOK3* | | |
| | *TAPT1* | | |
| | *TBC1D12* | | |
| | *TCEAL7* | | |
| | *TCEANC* | | |
| | *TCN2* | | |
| | *TDP1* | | |
| | *TENC1* | | |
| | *TENM1* | | |
| | *TENM2* | | |
| | *TESC* | | |
| | *TEX2* | | |
| | *TFEB* | | |
| | *TFPI* | | |
| | *TGFB2* | | |

| | | | |
|---|---|---|---|
| | *TGFBI* | | |
| | *TGFBR2* | | |
| | *TGIF1* | | |
| | *TGIF2* | | |
| | *THBS2* | | |
| | *THBS3* | | |
| | *THBS4* | | |
| | *THSD1* | | |
| | *TIAM1* | | |
| | *TIE1* | | |
| | *TIMP3* | | |
| | *TIMP4* | | |
| | *TINCR* | | |
| | *TLCD2* | | |
| | *TLE6* | | |
| | *TLN2* | | |
| | *TLR3* | | |
| | *TM4SF1* | | |
| | *TM4SF18* | | |
| | *TMCC3* | | |
| | *TMCO4* | | |
| | *TMED10* | | |
| | *TMED8* | | |
| | *TMEFF2* | | |
| | *TMEM108* | | |
| | *TMEM117* | | |
| | *TMEM132C* | | |
| | *TMEM132E* | | |
| | *TMEM154* | | |
| | *TMEM161B-AS1* | | |
| | *TMEM169* | | |
| | *TMEM170A* | | |
| | *TMEM170B* | | |
| | *TMEM173* | | |
| | *TMEM178A* | | |
| | *TMEM178B* | | |
| | *TMEM2* | | |
| | *TMEM200A* | | |
| | *TMEM205* | | |
| | *TMEM217* | | |
| | *TMEM229B* | | |
| | *TMEM231* | | |
| | *TMEM243* | | |
| | *TMEM255A* | | |
| | *TMEM27* | | |
| | *TMEM45A* | | |
| | *TMEM47* | | |
| | *TMEM51* | | |
| | *TMEM55A* | | |
| | *TMEM86A* | | |
| | *TMEM9B-AS1* | | |
| | *TMSB10* | | |
| | *TMTC1* | | |
| | *TMTC2* | | |
| | *TNC* | | |
| | *TNFAIP2* | | |

| | | | |
|---|---|---|---|
| | *TNFAIP3* | | |
| | *TNFRSF11B* | | |
| | *TNFSF4* | | |
| | *TNRC18* | | |
| | *TNS1* | | |
| | *TOMM34* | | |
| | *TOX2* | | |
| | *TP53I11* | | |
| | *TPBG* | | |
| | *TPCN1* | | |
| | *TPD52L1* | | |
| | *TPMT* | | |
| | *TPP1* | | |
| | *TPT1-AS1* | | |
| | *TRABD2B* | | |
| | *TRAM1L1* | | |
| | *TRAM2* | | |
| | *TRERF1* | | |
| | *TRH* | | |
| | *TRIB1* | | |
| | *TRIL* | | |
| | *TRIM14* | | |
| | *TRIM35* | | |
| | *TRIM46* | | |
| | *TRIP13* | | |
| | *TRMT6* | | |
| | *TRNP1* | | |
| | *TRPM8* | | |
| | *TSKU* | | |
| | *TSPAN12* | | |
| | *TSPAN13* | | |
| | *TSPAN7* | | |
| | *TTC21A* | | |
| | *TTC39A* | | |
| | *TUBA1C* | | |
| | *TUBA8* | | |
| | *TUBB3* | | |
| | *TUFT1* | | |
| | *TVP23A* | | |
| | *TWF2* | | |
| | *TYRO3* | | |
| | *UAP1L1* | | |
| | *UBN1* | | |
| | *UBXN11* | | |
| | *UCHL3* | | |
| | *UG0898H09* | | |
| | *UNC5D* | | |
| | *UNC93B1* | | |
| | *UPP1* | | |
| | *UQCC* | | |
| | *USP2* | | |
| | *USP53* | | |
| | *USP54* | | |
| | *UST* | | |
| | *UTRN* | | |
| | *VAMP1* | | |

| | | | |
|---|---|---|---|
| | *VAMP5* | | |
| | *VARS2* | | |
| | *VASH2* | | |
| | *VASN* | | |
| | *VAT1L* | | |
| | *VAV3* | | |
| | *VCAM1* | | |
| | *VEGFA* | | |
| | *VEPH1* | | |
| | *VGF* | | |
| | *VGLL3* | | |
| | *VIPR1* | | |
| | *VSIG10L* | | |
| | *VSNL1* | | |
| | *VSTM2L* | | |
| | *WASF3* | | |
| | *WBP5* | | |
| | *WBSCR17* | | |
| | *WDFY3-AS2* | | |
| | *WDR78* | | |
| | *WEE1* | | |
| | *WIPF3* | | |
| | *WLS* | | |
| | *WNK4* | | |
| | *WNT7B* | | |
| | *WWC2* | | |
| | *XYLB* | | |
| | *XYLT1* | | |
| | *YPEL2* | | |
| | *YRDC* | | |
| | *ZBTB47* | | |
| | *ZBTB7C* | | |
| | *ZCCHC12* | | |
| | *ZCCHC24* | | |
| | *ZDHHC13* | | |
| | *ZDHHC21* | | |
| | *ZDHHC22* | | |
| | *ZFAND6* | | |
| | *ZFHX4-AS1* | | |
| | *ZFP36* | | |
| | *ZFP69* | | |
| | *ZFPM2* | | |
| | *ZIC3* | | |
| | *ZMAT1* | | |
| | *ZNF185* | | |
| | *ZNF33B* | | |
| | *ZNF34* | | |
| | *ZNF37BP* | | |
| | *ZNF385D* | | |
| | *ZNF423* | | |
| | *ZNF436* | | |
| | *ZNF469* | | |
| | *ZNF483* | | |
| | *ZNF589* | | |
| | *ZNF665* | | |
| | *ZNF672* | | |

| | | | |
|---|---|---|---|
| | *ZNF774* | | |
| | *ZNF781* | | |
| | *ZNF782* | | |
| | *ZNF789* | | |
| | *ZNRF2* | | |

| Table 2.2. Overlaps between *Foxp1*$^{+/-}$ and *Foxp2*$^{+/-}$ STR target genes and D1+ and D2+ MSNs genes. | | | | | | | |
|---|---|---|---|---|---|---|---|
| ***Foxp2*$^{+/-}$ STR overlaps** | | | | ***Foxp1*$^{+/-}$ STR overlaps** | | | |
| **Upregulated** | | **Downregulated** | | **Upregulated** | | **Downregulated** | |
| **Drd1/*Foxp2*$^{+/-}$** | **Drd2/*Foxp2*$^{+/-}$** | **Drd1/*Foxp2*$^{+/-}$** | **Drd2/*Foxp2*$^{+/-}$** | **Drd1/*Foxp1*$^{+/-}$** | **Drd2/*Foxp1*$^{+/-}$** | **Drd1/*Foxp1*$^{+/-}$** | **Drd2/*Foxp1*$^{+/-}$** |
| *ATL3* | *1700019D03RIK* | *8430427H17RIK* | *4933432I03RIK* | *ADARB2* | *ATP1B1* | *AMZ1* | *1700001O22RIK* |
| *C1QL3* | *ADK* | *ARHGAP29* | *CLASP2* | *ANKRD29* | *FAM155A* | *DDIT4L* | *ARG2* |
| *CBLN1* | *ANKRD12* | *CACNG1* | *DGCR6* | *BC048546* | *FAM19A2* | *DMKN* | *DACH1* |
| *CCK* | *C230085N15RIK* | *CASP3* | *FAM20C* | *BHLHE22* | *GM13629* | *FAM105A* | *DBP* |
| *CMBL* | *CDC14A* | *FOXP2* | *FST* | *CALB2* | *HSPA1A* | *FANCB* | *GNB5* |
| *CPLX3* | *CNIH3* | *FZD3* | *GPR6* | *CBLN4* | *HTR7* | *NEK2* | *GPRIN3* |
| *DDHD1* | *ERLEC1* | *GEMIN5* | *ID4* | *CRH* | *NELL1* | *RYR1* | *GPX6* |
| *DSP* | *FAM173A* | *GPR26* | *MYH14* | *CRTAC1* | *NTNG1* | *SEC14L1* | *HPCA* |
| *EBF1* | *NCAPH2* | *IGFBP4* | *NTNG1* | *EFR3A* | *PRKAR2A* | *SERPINB1B* | *HRH3* |
| *EFR3A* | *PDCD4* | *KCNS2* | *PLXDC1* | *FGF12* | *RALYL* | | *KCNIP2* |
| *EYA1* | *QK* | *MAN1A* | *RIOK1* | *GNAI1* | *UNC5D* | | *KCNK2* |
| *FHL2* | *RABGAP1L* | *NCAM2* | *RIT2* | *GNG4* | | | *KLHL1* |
| *GNG2* | *SLITRK6* | *PCDH20* | *RPS9* | *HSPA12A* | | | *NGEF* |
| *KCNJ3* | *SMPD4* | *RASSF3* | *SLC1A1* | *ID2* | | | *NR4A1* |
| *MAPK11* | *TAOK3* | *RPS6KA5* | *SLC41A1* | *KCNJ3* | | | *NUCB2* |
| *MYH3* | *TMSB4X* | *RYR1* | *SYNPO2* | *LINGO2* | | | *PMEPA1* |
| *NAPB* | *ZCCHC7* | *SEC14L1* | *TBRG4* | *NRP2* | | | *RCN1* |
| *NCALD* | | | *TCF3* | *NRXN1* | | | *RHOBTB2* |
| *NEUROD2* | | | *ZHX3* | *PCDH20* | | | *SYT6* |
| *NEUROD6* | | | | *PKP2* | | | *VRK1* |
| *NOV* | | | | *PLCXD2* | | | |
| *NR4A2* | | | | *PPM1L* | | | |
| *NRG3* | | | | *RASGRF2* | | | |
| *NRN1* | | | | *SLC17A6* | | | |
| *NRXN1* | | | | *TTC39B* | | | |
| *OLFM1* | | | | *VSNL1* | | | |
| *PAK7* | | | | *VSTM2A* | | | |
| *PPP1R12B* | | | | | | | |
| *PRDM8* | | | | | | | |
| *PRSS12* | | | | | | | |
| *PSMB10* | | | | | | | |
| *RAI14* | | | | | | | |
| *RSPO2* | | | | | | | |
| *RTN4RL2* | | | | | | | |
| *SATB2* | | | | | | | |
| *SCYL3* | | | | | | | |
| *SFXN1* | | | | | | | |
| *SH3GL2* | | | | | | | |
| *TBR1* | | | | | | | |
| *USP14* | | | | | | | |
| *VIP* | | | | | | | |
| *VSNL1* | | | | | | | |
| *ZFP318* | | | | | | | |
| *ZFPM2* | | | | | | | |

| Table 2.3. GO categories of hNP ChIP-seq and RNA-seq datasets. | | | | | | | | |
|---|---|---|---|---|---|---|---|---|
| **RNA-seq** | | | **ChIP-seq** | | | **RNA-seq/ChIP-seq overlaps** | | |
| **GO term** | **Gene count** | **Benjamini p-value** | **GO term** | **Gene count** | **Benjamini p-value** | **GO term** | **Gene count** | **Benjamini p-value** |
| plasma membrane | 537 | 2.70E-19 | synapse | 24 | 1.40E-02 | synapse | 10 | 1.30E-02 |
| plasma membrane part | 345 | 6.60E-17 | cytoskeleton | 56 | 9.20E-02 | cell adhesion | 12 | 4.70E-01 |
| cell adhesion | 128 | 6.00E-09 | cell projection part | 15 | 2.70E-01 | biological adhesion | 12 | 2.70E-01 |
| biological adhesion | 128 | 3.30E-09 | actin binding | 18 | 9.80E-01 | carbohydrate biosynthetic process | 5 | 4.70E-01 |
| cell junction | 103 | 4.10E-09 | growth factor binding | 9 | 8.90E-01 | response to heat | 4 | 4.80E-01 |
| calcium ion binding | 151 | 6.80E-08 | cell projection | 30 | 4.30E-01 | dystrophin-associated glycoprotein complex | 3 | 2.30E-01 |
| synapse | 78 | 8.80E-09 | axon | 11 | 4.00E-01 | rhythmic process | 5 | 5.10E-01 |
| regulation of cell proliferation | 133 | 2.10E-07 | dystrophin-associated glycoprotein complex | 4 | 3.70E-01 | heart development | 6 | 5.00E-01 |
| enzyme linked receptor protein signaling pathway | 71 | 1.10E-06 | dendrite | 11 | 3.50E-01 | muscle contraction | 5 | 6.20E-01 |
| extracellular region part | 155 | 2.60E-07 | intracellular non-membrane-bounded organelle | 85 | 3.60E-01 | response to temperature stimulus | 4 | 6.20E-01 |
| extracellular matrix | 72 | 3.60E-07 | non-membrane-bounded organelle | 85 | 3.60E-01 | cell fraction | 13 | 3.70E-01 |
| cell morphogenesis involved in differentiation | 55 | 4.40E-06 | metal ion binding | 131 | 9.10E-01 | muscle system process | 5 | 6.50E-01 |
| cell morphogenesis | 71 | 4.50E-06 | cation binding | 132 | 8.40E-01 | response to abiotic stimulus | 7 | 6.20E-01 |
| neuron projection | 71 | 5.10E-07 | calmodulin binding | 10 | 8.00E-01 | glycogen metabolic process | 3 | 6.80E-01 |

| | | | | | | | | |
|---|---|---|---|---|---|---|---|---|
| response to hormone stimulus | 72 | 6.00E-06 | nerve terminal | 5 | 4.10E-01 | lung development | 4 | 6.50E-01 |
| response to endogenous stimulus | 77 | 6.40E-06 | ion binding | 133 | 7.80E-01 | glucan metabolic process | 3 | 6.30E-01 |
| response to organic substance | 118 | 5.90E-06 | cytoskeletal protein binding | 23 | 7.60E-01 | cellular glucan metabolic process | 3 | 6.30E-01 |
| proteinaceous extracellular matrix | 67 | 8.70E-07 | protein domain specific binding | 17 | 7.20E-01 | sarcomere | 4 | 4.30E-01 |
| neuron differentiation | 81 | 7.50E-06 | dendritic spine | 5 | 4.00E-01 | respiratory tube development | 4 | 6.20E-01 |
| integral to plasma membrane | 179 | 1.50E-06 | low-density lipoprotein binding | 4 | 7.20E-01 | memory | 3 | 6.40E-01 |
| intrinsic to plasma membrane | 182 | 1.50E-06 | asymmetric synapse | 3 | 4.60E-01 | synaptic transmission | 6 | 6.30E-01 |
| regulation of cell motion | 45 | 2.10E-05 | 4 iron, 4 sulfur cluster binding | 4 | 8.40E-01 | respiratory system development | 4 | 6.10E-01 |
| negative regulation of cell communication | 53 | 2.30E-05 | insulin-like growth factor binding | 4 | 8.40E-01 | cell junction | 8 | 4.20E-01 |
| negative regulation of signal transduction | 49 | 2.20E-05 | receptor complex | 8 | 5.60E-01 | polysaccharide metabolic process | 4 | 6.10E-01 |
| regulation of cell migration | 41 | 2.20E-05 | intrinsic to Golgi membrane | 5 | 5.30E-01 | learning or memory | 4 | 6.10E-01 |
| neuron projection development | 54 | 2.20E-05 | integral to plasma membrane | 42 | 5.10E-01 | gonad development | 4 | 6.00E-01 |
| insoluble fraction | 133 | 5.90E-06 | neuron projection | 16 | 4.90E-01 | regulation of system process | 6 | 6.00E-01 |
| regulation of locomotion | 44 | 3.40E-05 | insulin receptor substrate binding | 3 | 8.70E-01 | cell surface receptor linked signal transduction | 17 | 5.80E-01 |
| cell projection organization | 69 | 3.30E-05 | cell surface | 16 | 5.10E-01 | energy reserve metabolic process | 3 | 5.70E-01 |
| neuron development | 65 | 3.20E-05 | phosphoinositide 3-kinase complex | 3 | 5.10E-01 | myofibril | 4 | 4.00E-01 |

| | | | | | | | | |
|---|---|---|---|---|---|---|---|---|
| cellular component morphogenesis | 72 | 5.80E-05 | plasma membrane part | 70 | 5.20E-01 | polysaccharide biosynthetic process | 3 | 5.80E-01 |
| response to wounding | 89 | 6.60E-05 | intrinsic to plasma membrane | 42 | 5.10E-01 | contractile fiber part | 4 | 3.70E-01 |
| cell fraction | 161 | 1.60E-05 | cell junction | 21 | 5.30E-01 | response to drug | 5 | 6.00E-01 |
| cell surface | 67 | 1.50E-05 | glutamate receptor activity | 4 | 9.30E-01 | membrane fraction | 10 | 3.60E-01 |
| regulation of phosphorus metabolic process | 83 | 7.40E-05 | axon part | 5 | 5.40E-01 | Z disc | 3 | 3.40E-01 |
| regulation of phosphate metabolic process | 83 | 7.40E-05 | | | | tube development | 5 | 6.00E-01 |
| extracellular region | 269 | 1.50E-05 | | | | regulation of systemic arterial blood pressure by endothelin | 2 | 5.90E-01 |
| neuron projection morphogenesis | 46 | 7.60E-05 | | | | reproductive structure development | 4 | 5.90E-01 |
| synapse part | 52 | 1.80E-05 | | | | contractile fiber | 4 | 3.20E-01 |
| positive regulation of developmental process | 55 | 9.30E-05 | | | | development of primary sexual characteristics | 4 | 5.80E-01 |
| regulation of phosphorylation | 80 | 9.50E-05 | | | | insoluble fraction | 10 | 3.30E-01 |
| cell motion | 81 | 1.00E-04 | | | | cellular polysaccharide metabolic process | 3 | 6.10E-01 |
| positive regulation of cell proliferation | 73 | 1.00E-04 | | | | peptide metabolic process | 3 | 6.10E-01 |
| transmembrane receptor protein tyrosine kinase signaling pathway | 47 | 1.10E-04 | | | | cell-cell signaling | 8 | 6.20E-01 |
| membrane fraction | 126 | 2.50E-05 | | | | regulation of synaptic transmission | 4 | 6.10E-01 |
| intracellular signaling cascade | 174 | 1.10E-04 | | | | transmission of nerve impulse | 6 | 6.00E-01 |

| | | | | | | | | |
|---|---|---|---|---|---|---|---|---|
| positive regulation of transferase activity | 49 | 1.30E-04 | | | | response to mechanical stimulus | 3 | 6.00E-01 |
| extrinsic to membrane | 85 | 3.90E-05 | | | | neuron projection | 6 | 3.40E-01 |
| positive regulation of cell differentiation | 47 | 1.90E-04 | | | | plasma membrane | 28 | 3.20E-01 |
| regulation of system process | 58 | 1.90E-04 | | | | cell fate commitment | 4 | 6.00E-01 |
| vasculature development | 50 | 1.90E-04 | | | | negative regulation of transcription, DNA-dependent | 6 | 5.90E-01 |
| cell morphogenesis involved in neuron differentiation | 44 | 1.90E-04 | | | | leukocyte migration | 3 | 5.80E-01 |
| MHC protein complex | 20 | 5.00E-05 | | | | postsynaptic membrane | 4 | 3.10E-01 |
| blood vessel development | 49 | 2.10E-04 | | | | negative regulation of RNA metabolic process | 6 | 5.90E-01 |
| positive regulation of kinase activity | 47 | 2.10E-04 | | | | learning | 3 | 6.00E-01 |
| extracellular structure organization | 37 | 2.20E-04 | | | | regulation of transmission of nerve impulse | 4 | 6.00E-01 |
| blood vessel morphogenesis | 44 | 2.20E-04 | | | | sex differentiation | 4 | 6.10E-01 |
| negative regulation of response to stimulus | 27 | 2.30E-04 | | | | regulation of neurological system process | 4 | 6.20E-01 |
| cell projection | 110 | 6.30E-05 | | | | negative regulation of nucleobase, nucleoside, nucleotide and nucleic acid metabolic process | 7 | 6.20E-01 |
| regulation of response to external stimulus | 36 | 3.10E-04 | | | | skeletal muscle tissue development | 3 | 6.20E-01 |
| negative regulation of cell proliferation | 64 | 3.00E-04 | | | | skeletal muscle organ development | 3 | 6.20E-01 |

| | | | | | | | | |
|---|---|---|---|---|---|---|---|---|
| MHC class II receptor activity | 11 | 1.90E-03 | | | | ovulation cycle | 3 | 6.20E-01 |
| cell-cell signaling | 94 | 3.30E-04 | | | | negative regulation of nitrogen compound metabolic process | 7 | 6.20E-01 |
| cytoskeletal protein binding | 82 | 1.40E-03 | | | | | | |
| extracellular matrix part | 30 | 1.10E-04 | | | | | | |
| behavior | 77 | 5.10E-04 | | | | | | |
| regeneration | 21 | 5.10E-04 | | | | | | |
| wound healing | 40 | 5.30E-04 | | | | | | |
| response to extracellular stimulus | 44 | 5.70E-04 | | | | | | |
| axonogenesis | 40 | 6.60E-04 | | | | | | |
| regulation of transferase activity | 64 | 7.10E-04 | | | | | | |
| axon guidance | 27 | 7.10E-04 | | | | | | |
| regulation of kinase activity | 62 | 7.00E-04 | | | | | | |
| regulation of neurological system process | 34 | 7.20E-04 | | | | | | |
| positive regulation of protein kinase activity | 44 | 7.20E-04 | | | | | | |
| cell projection morphogenesis | 47 | 7.20E-04 | | | | | | |
| antigen processing and presentation | 23 | 7.10E-04 | | | | | | |

| | | | | | | | | |
|---|---|---|---|---|---|---|---|---|
| calmodulin binding | 32 | 3.00E-03 | | | | | | |
| postsynaptic membrane | 32 | 2.60E-04 | | | | | | |
| response to oxygen levels | 32 | 8.20E-04 | | | | | | |
| angiogenesis | 33 | 8.40E-04 | | | | | | |
| response to steroid hormone stimulus | 39 | 1.20E-03 | | | | | | |
| transmission of nerve impulse | 60 | 1.30E-03 | | | | | | |
| cell migration | 50 | 1.60E-03 | | | | | | |
| regulation of protein kinase activity | 59 | 1.60E-03 | | | | | | |
| basolateral plasma membrane | 41 | 7.00E-04 | | | | | | |
| cell part morphogenesis | 47 | 2.00E-03 | | | | | | |
| protein amino acid phosphorylation | 98 | 2.00E-03 | | | | | | |
| tube development | 42 | 2.20E-03 | | | | | | |
| antigen processing and presentation of peptide or polysaccharide antigen via MHC class II | 13 | 2.20E-03 | | | | | | |
| external side of plasma membrane | 36 | 8.00E-04 | | | | | | |
| regulation of synaptic transmission | 30 | 2.40E-03 | | | | | | |

| | | | | | | | | |
|---|---|---|---|---|---|---|---|---|
| response to drug | 41 | 3.00E-03 | | | | | | |
| cell motility | 53 | 3.00E-03 | | | | | | |
| localization of cell | 53 | 3.00E-03 | | | | | | |
| axon | 34 | 1.10E-03 | | | | | | |
| transmembrane receptor protein tyrosine kinase activity | 19 | 1.20E-02 | | | | | | |
| regulation of cell morphogenesis | 29 | 3.00E-03 | | | | | | |
| learning or memory | 26 | 3.00E-03 | | | | | | |
| positive regulation of locomotion | 24 | 2.90E-03 | | | | | | |
| protein kinase cascade | 61 | 2.90E-03 | | | | | | |
| protein dimerization activity | 82 | 1.10E-02 | | | | | | |
| response to mechanical stimulus | 17 | 3.20E-03 | | | | | | |
| cellular response to hormone stimulus | 29 | 3.70E-03 | | | | | | |
| response to nutrient | 30 | 3.70E-03 | | | | | | |
| regulation of transmission of nerve impulse | 31 | 3.70E-03 | | | | | | |
| MHC class II protein complex | 12 | 1.50E-03 | | | | | | |
| response to hypoxia | 29 | 4.10E-03 | | | | | | |

| | | | | | | | | |
|---|---|---|---|---|---|---|---|---|
| MAPKKK cascade | 36 | 4.20E-03 | | | | | | |
| PDZ domain binding | 15 | 1.80E-02 | | | | | | |
| regulation of cell adhesion | 29 | 5.90E-03 | | | | | | |
| actin binding | 54 | 1.90E-02 | | | | | | |
| response to glucocorticoid stimulus | 20 | 6.70E-03 | | | | | | |
| extracellular matrix organization | 24 | 6.70E-03 | | | | | | |
| response to vitamin | 18 | 7.00E-03 | | | | | | |
| positive regulation of cell motion | 23 | 7.20E-03 | | | | | | |
| response to corticosteroid stimulus | 21 | 7.10E-03 | | | | | | |
| growth factor binding | 24 | 2.10E-02 | | | | | | |
| response to inorganic substance | 38 | 7.70E-03 | | | | | | |
| positive regulation of multicellular organismal process | 43 | 8.40E-03 | | | | | | |
| antigen processing and presentation of peptide antigen | 11 | 8.80E-03 | | | | | | |
| chemical homeostasis | 76 | 9.00E-03 | | | | | | |
| anchored to membrane | 41 | 3.80E-03 | | | | | | |
| respiratory system development | 24 | 1.10E-02 | | | | | | |

| | | | | | | | | |
|---|---|---|---|---|---|---|---|---|
| skeletal system development | 52 | 1.20E-02 | | | | | | |
| phosphate metabolic process | 128 | 1.30E-02 | | | | | | |
| phosphorus metabolic process | 128 | 1.30E-02 | | | | | | |
| positive regulation of cell migration | 21 | 1.30E-02 | | | | | | |
| vesicle | 97 | 5.50E-03 | | | | | | |
| regulation of smooth muscle cell proliferation | 14 | 1.40E-02 | | | | | | |
| synaptic transmission | 49 | 1.40E-02 | | | | | | |
| growth | 34 | 1.50E-02 | | | | | | |
| cytoplasmic vesicle | 93 | 7.00E-03 | | | | | | |
| lung development | 22 | 2.00E-02 | | | | | | |
| placenta development | 16 | 2.00E-02 | | | | | | |
| response to abiotic stimulus | 57 | 2.00E-02 | | | | | | |
| response to molecule of bacterial origin | 20 | 2.10E-02 | | | | | | |
| cAMP metabolic process | 9 | 2.00E-02 | | | | | | |
| organ regeneration | 10 | 2.10E-02 | | | | | | |
| anchoring junction | 33 | 9.40E-03 | | | | | | |

| | | | | | | | | |
|---|---|---|---|---|---|---|---|---|
| response to insulin stimulus | 22 | 2.10E-02 | | | | | | |
| activation of protein kinase activity | 24 | 2.10E-02 | | | | | | |
| muscle organ development | 37 | 2.30E-02 | | | | | | |
| extracellular space | 97 | 1.10E-02 | | | | | | |
| intrinsic to membrane | 613 | 1.00E-02 | | | | | | |
| response to nutrient levels | 35 | 2.60E-02 | | | | | | |
| regulation of cell development | 36 | 2.60E-02 | | | | | | |
| cell-cell adhesion | 45 | 2.60E-02 | | | | | | |
| respiratory tube development | 22 | 2.60E-02 | | | | | | |
| cell-cell junction | 35 | 1.20E-02 | | | | | | |
| urogenital system development | 23 | 3.00E-02 | | | | | | |
| positive regulation of immune system process | 40 | 3.00E-02 | | | | | | |
| positive regulation of catalytic activity | 74 | 3.00E-02 | | | | | | |
| response to peptide hormone stimulus | 29 | 3.00E-02 | | | | | | |
| adherens junction | 30 | 1.30E-02 | | | | | | |
| multicellular organismal response to stress | 12 | 3.30E-02 | | | | | | |

| | | | | | | | | |
|---|---|---|---|---|---|---|---|---|
| negative regulation of cell differentiation | 37 | 3.20E-02 | | | | | | |
| regulation of myeloid cell differentiation | 17 | 3.20E-02 | | | | | | |
| positive regulation of cell communication | 51 | 3.30E-02 | | | | | | |
| membrane-bounded vesicle | 82 | 1.50E-02 | | | | | | |
| response to lipopolysaccharide | 18 | 3.40E-02 | | | | | | |
| regulation of MAP kinase activity | 27 | 3.50E-02 | | | | | | |
| cellular chemical homeostasis | 57 | 3.50E-02 | | | | | | |
| regulation of membrane potential | 26 | 3.60E-02 | | | | | | |
| regulation of behavior | 13 | 3.80E-02 | | | | | | |
| cellular ion homeostasis | 56 | 3.90E-02 | | | | | | |
| rhythmic process | 25 | 4.00E-02 | | | | | | |
| regulation of protein amino acid phosphorylation | 31 | 4.00E-02 | | | | | | |
| ion homeostasis | 60 | 4.20E-02 | | | | | | |
| response to cytokine stimulus | 18 | 4.20E-02 | | | | | | |
| cellular amino acid derivative metabolic process | 30 | 4.20E-02 | | | | | | |
| negative regulation of tissue remodeling | 6 | 4.50E-02 | | | | | | |

| | | | | | | | | |
|---|---|---|---|---|---|---|---|---|
| vasculogenesis | 12 | 4.40E-02 | | | | | | |
| positive regulation of cell adhesion | 15 | 4.70E-02 | | | | | | |
| ionotropic glutamate receptor complex | 7 | 2.40E-02 | | | | | | |
| postsynaptic density | 17 | 2.50E-02 | | | | | | |
| presynaptic membrane | 10 | 2.40E-02 | | | | | | |
| actin cytoskeleton | 44 | 2.40E-02 | | | | | | |
| cell-substrate junction | 23 | 2.40E-02 | | | | | | |
| basement membrane | 18 | 2.40E-02 | | | | | | |
| cell-substrate adherens junction | 22 | 2.60E-02 | | | | | | |
| cytoplasmic membrane-bounded vesicle | 78 | 2.60E-02 | | | | | | |
| cytoplasmic vesicle part | 33 | 2.70E-02 | | | | | | |
| receptor complex | 23 | 3.40E-02 | | | | | | |
| internal side of plasma membrane | 49 | 3.30E-02 | | | | | | |
| focal adhesion | 21 | 3.30E-02 | | | | | | |
| cell soma | 30 | 3.30E-02 | | | | | | |
| perinuclear region of cytoplasm | 45 | 4.10E-02 | | | | | | |

## REFERENCES FOR CHAPTER TWO


Ade KK, Wan Y, Chen M, Gloss B, Calakos N (2011) An Improved BAC Transgenic Fluorescent Reporter Line for Sensitive and Specific Identification of Striatonigral Medium Spiny Neurons. Frontiers in systems neuroscience 5:32.

Agmon A, Connors BW (1991) Thalamocortical responses of mouse somatosensory (barrel) cortex in vitro. Neuroscience 41:365-379.

Anders S, Pyl PT, Huber W (2014) HTSeq-a Python framework to work with high-throughput sequencing data. Bioinformatics.

Bacon C, Rappold GA (2012) The distinct and overlapping phenotypic spectra of FOXP1 and FOXP2 in cognitive disorders. Human genetics.

Bacon C, Schneider M, Le Magueresse C, Froehlich H, Sticht C, Gluch C, Monyer H, Rappold GA (2014) Brain-specific Foxp1 deletion impairs neuronal development and causes autistic-like behaviour. Molecular psychiatry.

Benjamini Y, Hochberg Y (1995) Controlling the false discovery rate: a practical and powerful approach to multiple testing. J R Stat Soc Ser B 57:289-300.

Centonze D, Rossi S, Mercaldo V, Napoli I, Ciotti MT, De Chiara V, Musella A, Prosperetti C, Calabresi P, Bernardi G, Bagni C (2008) Abnormal striatal GABA transmission in the mouse model for the fragile X syndrome. Biological psychiatry 63:963-973.

Chien WH, Gau SS, Chen CH, Tsai WC, Wu YY, Chen PH, Shang CY, Chen CH (2013) Increased gene expression of FOXP1 in patients with autism spectrum disorders. Molecular autism 4:23.

Curry T, Egeto P, Wang H, Podnos A, Wasserman D, Yeomans J (2013) Dopamine receptor D2 deficiency reduces mouse pup ultrasonic vocalizations and maternal responsiveness. Genes, brain, and behavior 12:397-404.

Darnell JC, Klann E (2013) The translation of translational control by FMRP: therapeutic targets for FXS. Nature neuroscience 16:1530-1536.

Darnell JC, Van Driesche SJ, Zhang C, Hung KY, Mele A, Fraser CE, Stone EF, Chen C, Fak JJ, Chi SW, Licatalosi DD, Richter JD, Darnell RB (2011) FMRP stalls ribosomal translocation on mRNAs linked to synaptic function and autism. Cell 146:247-261.

Deacon RM (2006) Assessing nest building in mice. Nat Protoc 1:1117-1119.

Ellegood J et al. (2015) Clustering autism: using neuroanatomical differences in 26 mouse models to gain insight into the heterogeneity. Molecular psychiatry 20:118-125.

Enard W et al. (2009) A humanized version of Foxp2 affects cortico-basal ganglia circuits in mice. Cell 137:961-971.

Feng X, Ippolito GC, Tian L, Wiehagen K, Oh S, Sambandam A, Willen J, Bunte RM, Maika SD, Harriss JV, Caton AJ, Bhandoola A, Tucker PW, Hu H (2010) Foxp1 is an essential transcriptional regulator for the generation of quiescent naive T cells during thymocyte development. Blood 115:510-518.

Ferland RJ, Cherry TJ, Preware PO, Morrisey EE, Walsh CA (2003) Characterization of Foxp2 and Foxp1 mRNA and protein in the developing and mature brain. The Journal of comparative neurology 460:266-279.

Fisher SE, Scharff C (2009) FOXP2 as a molecular window into speech and language. Trends in genetics : TIG 25:166-177.

Foeger NC, Norris AJ, Wren LM, Nerbonne JM (2012) Augmentation of Kv4.2-encoded currents by accessory dipeptidyl peptidase 6 and 10 subunits reflects selective cell surface Kv4.2 protein stabilization. The Journal of biological chemistry 287:9640-9650.

French CA, Jin X, Campbell TG, Gerfen E, Groszer M, Fisher SE, Costa RM (2012) An aetiological Foxp2 mutation causes aberrant striatal activity and alters plasticity during skill learning. Mol Psychiatry 17:1077-1085.
Gautier L, Cope L, Bolstad BM, Irizarry RA (2004) affy--analysis of Affymetrix GeneChip data at the probe level. Bioinformatics 20:307-315.
Gerfen CR, Surmeier DJ (2011) Modulation of striatal projection systems by dopamine. Annual review of neuroscience 34:441-466.
Geschwind DH, State MW (2015) Gene hunting in autism spectrum disorder: on the path to precision medicine. Lancet Neurol.
Gong S, Zheng C, Doughty ML, Losos K, Didkovsky N, Schambra UB, Nowak NJ, Joyner A, Leblanc G, Hatten ME, Heintz N (2003) A gene expression atlas of the central nervous system based on bacterial artificial chromosomes. Nature 425:917-925.
Grant LM, Richter F, Miller JE, White SA, Fox CM, Zhu C, Chesselet MF, Ciucci MR (2014) Vocalization deficits in mice over-expressing alpha-synuclein, a model of pre-manifest Parkinson's disease. Behavioral neuroscience 128:110-121.
Gross C, Yao X, Pong DL, Jeromin A, Bassell GJ (2011) Fragile X mental retardation protein regulates protein expression and mRNA translation of the potassium channel Kv4.2. The Journal of neuroscience : the official journal of the Society for Neuroscience 31:5693-5698.
Heiman M, Schaefer A, Gong S, Peterson JD, Day M, Ramsey KE, Suarez-Farinas M, Schwarz C, Stephan DA, Surmeier DJ, Greengard P, Heintz N (2008) A translational profiling approach for the molecular characterization of CNS cell types. Cell 135:738-748.
Heinz S, Benner C, Spann N, Bertolino E, Lin YC, Laslo P, Cheng JX, Murre C, Singh H, Glass CK (2010) Simple combinations of lineage-determining transcription factors prime cis-regulatory elements required for macrophage and B cell identities. Molecular cell 38:576-589.
Hernandez RN, Feinberg RL, Vaurio R, Passanante NM, Thompson RE, Kaufmann WE (2009) Autism spectrum disorder in fragile X syndrome: a longitudinal evaluation. American journal of medical genetics Part A 149A:1125-1137.
Hisaoka T, Nakamura Y, Senba E, Morikawa Y (2010) The forkhead transcription factors, Foxp1 and Foxp2, identify different subpopulations of projection neurons in the mouse cerebral cortex. Neuroscience 166:551-563.
Holy TE, Guo Z (2005) Ultrasonic songs of male mice. PLoS biology 3:e386.
Hu H, Wang B, Borde M, Nardone J, Maika S, Allred L, Tucker PW, Rao A (2006) Foxp1 is an essential transcriptional regulator of B cell development. Nature immunology 7:819-826.
Hu Z, Chang YC, Wang Y, Huang CL, Liu Y, Tian F, Granger B, Delisi C (2013) VisANT 4.0: Integrative network platform to connect genes, drugs, diseases and therapies. Nucleic acids research 41:W225-231.
Iossifov I et al. (2014) The contribution of de novo coding mutations to autism spectrum disorder. Nature 515:216-221.
Kaestner KH, Knochel W, Martinez DE (2000) Unified nomenclature for the winged helix/forkhead transcription factors. Genes & development 14:142-146.
Kang HJ et al. (2011) Spatio-temporal transcriptome of the human brain. Nature 478:483-489.
Kim J, Wei DS, Hoffman DA (2005) Kv4 potassium channel subunits control action potential repolarization and frequency-dependent broadening in rat hippocampal CA1 pyramidal neurones. J Physiol 569:41-57.
Klassen T, Davis C, Goldman A, Burgess D, Chen T, Wheeler D, McPherson J, Bourquin T, Lewis L, Villasana D, Morgan M, Muzny D, Gibbs R, Noebels J (2011) Exome sequencing of ion

channel genes reveals complex profiles confounding personal risk assessment in epilepsy. Cell 145:1036-1048.
Konopka G, Bomar JM, Winden K, Coppola G, Jonsson ZO, Gao F, Peng S, Preuss TM, Wohlschlegel JA, Geschwind DH (2009) Human-specific transcriptional regulation of CNS development genes by FOXP2. Nature 462:213-217.
Konopka G, Wexler E, Rosen E, Mukamel Z, Osborn GE, Chen L, Lu D, Gao F, Gao K, Lowe JK, Geschwind DH (2012) Modeling the functional genomics of autism using human neurons. Molecular psychiatry 17:202-214.
Lachmann A, Xu H, Krishnan J, Berger SI, Mazloom AR, Ma'ayan A (2010) ChEA: transcription factor regulation inferred from integrating genome-wide ChIP-X experiments. Bioinformatics 26:2438-2444.
Langfelder P, Horvath S (2008) WGCNA: an R package for weighted correlation network analysis. BMC bioinformatics 9:559.
Langfelder P, Luo R, Oldham MC, Horvath S (2011) Is my network module preserved and reproducible? PLoS Comput Biol 7:e1001057.
Langmead B, Trapnell C, Pop M, Salzberg SL (2009) Ultrafast and memory-efficient alignment of short DNA sequences to the human genome. Genome biology 10.
Lee H, Lin MC, Kornblum HI, Papazian DM, Nelson SF (2014) Exome sequencing identifies de novo gain of function missense mutation in KCND2 in identical twins with autism and seizures that slows potassium channel inactivation. Human molecular genetics 23:3481-3489.
Lein ES et al. (2007) Genome-wide atlas of gene expression in the adult mouse brain. Nature 445:168-176.
Li S, Weidenfeld J, Morrisey EE (2004) Transcriptional and DNA binding activity of the Foxp1/2/4 family is modulated by heterotypic and homotypic protein interactions. Molecular and cellular biology 24:809-822.
Li S, Wang Y, Zhang Y, Lu MM, DeMayo FJ, Dekker JD, Tucker PW, Morrisey EE (2012) Foxp1/4 control epithelial cell fate during lung development and regeneration through regulation of anterior gradient 2. Development 139:2500-2509.
Maloney SE, Rieger MA, Dougherty JD (2013) Identifying essential cell types and circuits in autism spectrum disorders. Int Rev Neurobiol 113:61-96.
Marshall CR et al. (2008) Structural variation of chromosomes in autism spectrum disorder. American journal of human genetics 82:477-488.
Maze I, Chaudhury D, Dietz DM, Von Schimmelmann M, Kennedy PJ, Lobo MK, Sillivan SE, Miller ML, Bagot RC, Sun H, Turecki G, Neve RL, Hurd YL, Shen L, Han MH, Schaefer A, Nestler EJ (2014) G9a influences neuronal subtype specification in striatum. Nature neuroscience 17:533-539.
Mortazavi A, Williams BA, McCue K, Schaeffer L, Wold B (2008) Mapping and quantifying mammalian transcriptomes by RNA-Seq. Nature methods 5.
Oldham MC, Konopka G, Iwamoto K, Langfelder P, Kato T, Horvath S, Geschwind DH (2008) Functional organization of the transcriptome in human brain. Nature neuroscience 11:1271-1282.
Ouwenga RL, Dougherty J (2015) Fmrp targets or not: long, highly brain-expressed genes tend to be implicated in autism and brain disorders. Molecular autism 6:16.
Parikshak NN, Gandal MJ, Geschwind DH (2015) Systems biology and gene networks in neurodevelopmental and neurodegenerative disorders. Nature reviews Genetics 16:441-458.

Parikshak NN, Luo R, Zhang A, Won H, Lowe JK, Chandran V, Horvath S, Geschwind DH (2013) Integrative functional genomic analyses implicate specific molecular pathways and circuits in autism. Cell 155:1008-1021.

Pietropaolo S, Delage P, Cayzac S, Crusio WE, Cho YH (2011) Sex-dependent changes in social behaviors in motor pre-symptomatic R6/1 mice. PloS one 6:e19965.

Pollard KS, Dudoit S, Laan MJ (2005) Multiple testing procedures: R multtest package and applications to genomics. N.Y.: Springer.

Robinson MD, McCarthy DJ, Smyth GK (2010) edgeR: a Bioconductor package for differential expression analysis of digital gene expression data. Bioinformatics 26:139-140.

Rogers DC, Fisher EM, Brown SD, Peters J, Hunter AJ, Martin JE (1997) Behavioral and functional analysis of mouse phenotype: SHIRPA, a proposed protocol for comprehensive phenotype assessment. Mamm Genome 8:711-713.

Rousso DL, Pearson CA, Gaber ZB, Miquelajauregui A, Li S, Portera-Cailliau C, Morrisey EE, Novitch BG (2012) Foxp-mediated suppression of N-cadherin regulates neuroepithelial character and progenitor maintenance in the CNS. Neuron 74:314-330.

Roy S, Watkins N, Heck D (2012) Comprehensive analysis of ultrasonic vocalizations in a mouse model of fragile X syndrome reveals limited, call type specific deficits. PloS one 7:e44816.

Salmon-Divon M, Dvinge H, Tammoja K, Bertone P (2010) PeakAnalyzer: genome-wide annotation of chromatin binding and modification loci. BMC bioinformatics 11:415.

Scattoni ML, Crawley J, Ricceri L (2009) Ultrasonic vocalizations: a tool for behavioural phenotyping of mouse models of neurodevelopmental disorders. Neuroscience and biobehavioral reviews 33:508-515.

Shu W, Lu MM, Zhang Y, Tucker PW, Zhou D, Morrisey EE (2007) Foxp2 and Foxp1 cooperatively regulate lung and esophagus development. Development 134:1991-2000.

Shu W, Cho JY, Jiang Y, Zhang M, Weisz D, Elder GA, Schmeidler J, De Gasperi R, Sosa MA, Rabidou D, Santucci AC, Perl D, Morrisey E, Buxbaum JD (2005) Altered ultrasonic vocalization in mice with a disruption in the Foxp2 gene. Proceedings of the National Academy of Sciences of the United States of America 102:9643-9648.

Sia GM, Clem RL, Huganir RL (2013) The human language-associated gene SRPX2 regulates synapse formation and vocalization in mice. Science 342:987-991.

Spiteri E, Konopka G, Coppola G, Bomar J, Oldham M, Ou J, Vernes SC, Fisher SE, Ren B, Geschwind DH (2007) Identification of the transcriptional targets of FOXP2, a gene linked to speech and language, in developing human brain. American journal of human genetics 81:1144-1157.

State MW, Sestan N (2012) Neuroscience. The emerging biology of autism spectrum disorders. Science 337:1301-1303.

Stein JL, de la Torre-Ubieta L, Tian Y, Parikshak NN, Hernandez IA, Marchetto MC, Baker DK, Lu D, Hinman CR, Lowe JK, Wexler EM, Muotri AR, Gage FH, Kosik KS, Geschwind DH (2014) A quantitative framework to evaluate modeling of cortical development by neural stem cells. Neuron 83:69-86.

Stroud JC, Wu Y, Bates DL, Han A, Nowick K, Paabo S, Tong H, Chen L (2006) Structure of the forkhead domain of FOXP2 bound to DNA. Structure 14:159-166.

Tang B, Becanovic K, Desplats PA, Spencer B, Hill AM, Connolly C, Masliah E, Leavitt BR, Thomas EA (2012) Forkhead box protein p1 is a transcriptional repressor of immune signaling in the CNS: implications for transcriptional dysregulation in Huntington disease. Hum Mol Genet 21:3097-3111.

Teramitsu I, Kudo LC, London SE, Geschwind DH, White SA (2004) Parallel FoxP1 and FoxP2 expression in songbird and human brain predicts functional interaction. The Journal of neuroscience : the official journal of the Society for Neuroscience 24:3152-3163.

Trapnell C, Pachter L, Salzberg SL (2009) TopHat: discovering splice junctions with RNA-Seq. Bioinformatics 25:1105-1111.

Vernes SC, Oliver PL, Spiteri E, Lockstone HE, Puliyadi R, Taylor JM, Ho J, Mombereau C, Brewer A, Lowy E, Nicod J, Groszer M, Baban D, Sahgal N, Cazier JB, Ragoussis J, Davies KE, Geschwind DH, Fisher SE (2011) Foxp2 regulates gene networks implicated in neurite outgrowth in the developing brain. PLoS genetics 7:e1002145.

Voineagu I, Wang X, Johnston P, Lowe JK, Tian Y, Horvath S, Mill J, Cantor RM, Blencowe BJ, Geschwind DH (2011) Transcriptomic analysis of autistic brain reveals convergent molecular pathology. Nature 474:380-384.

Wang B, Lin D, Li C, Tucker P (2003) Multiple domains define the expression and regulatory properties of Foxp1 forkhead transcriptional repressors. The Journal of biological chemistry 278:24259-24268.

Wang B, Weidenfeld J, Lu MM, Maika S, Kuziel WA, Morrisey EE, Tucker PW (2004) Foxp1 regulates cardiac outflow tract, endocardial cushion morphogenesis and myocyte proliferation and maturation. Development 131:4477-4487.

Wang L, Wang S, Li W (2012) RSeQC: quality control of RNA-seq experiments. Bioinformatics 28:2184-2185.

Xu X, Wells AB, O'Brien DR, Nehorai A, Dougherty JD (2014) Cell type-specific expression analysis to identify putative cellular mechanisms for neurogenetic disorders. The Journal of neuroscience : the official journal of the Society for Neuroscience 34:1420-1431.

Zhang B, Horvath S (2005) A general framework for weighted gene co-expression network analysis. Stat Appl Genet Mol Biol 4:Article17.

Zhang Y, Liu T, Meyer CA, Eeckhoute J, Johnson DS, Bernstein BE, Nusbaum C, Myers RM, Brown M, Li W, Liu XS (2008) Model-based analysis of ChIP-Seq (MACS). Genome biology 9:R137.

## CHAPTER THREE:

## FOXP1 IN FOREBRAIN PYRAMIDAL NEURONS CONTROLS GENE EXPRESSION REQUIRED FOR SPATIAL LEARNING AND SYNAPTIC ACTIVITY

Adapted From: **Araujo, D.J.**, Toriumi, K., Escamilla, C.O., Kulkarni, A., Anderson, A.G., Harper, M., Usui, N., Ellegood, J., Lerch, J.P., Birnbaum, S.G., Tucker, H.O., Powell, C.M., and Konopka, G. Foxp1 in forebrain pyramidal neurons controls gene expression required for spatial learning and synaptic plasticity. **Re-submitted to *The Journal of Neuroscience* for peer-review.**


### ABSTRACT

Genetic perturbations of the transcription factor *Forkhead Box P1* (*FOXP1*) are causative for severe forms of autism spectrum disorder that are often comorbid with intellectual disability. Recent work has begun to reveal an important role for FoxP1 in brain development, but the brain-region-specific contributions of Foxp1 to autism and intellectual disability phenotypes have yet to be fully determined. Here, we describe *Foxp1* conditional knockout (*Foxp1*$^{cKO}$) mice with loss of Foxp1 in the pyramidal neurons of the neocortex and the CA1/CA2 subfields of the hippocampus. *Foxp1*$^{cKO}$ mice exhibit behavioral phenotypes that are of potential relevance to autism spectrum disorder including hyperactivity, increased anxiety, communication impairments, and decreased sociability. In addition, *Foxp1*$^{cKO}$ mice have gross deficits in learning and memory tasks of relevance to intellectual disability. Using a genome-wide approach, we identified differentially expressed genes in the hippocampus of *Foxp1*$^{cKO}$ mice

associated with synaptic function and development. Furthermore, using magnetic resonance imaging, we uncovered a significant reduction in the volumes of both the entire hippocampus as well as individual hippocampal subfields of *Foxp1*$^{cKO}$ mice. Finally, we observed reduced maintenance of long-term potentiation in area CA1 of the hippocampus in these mutant mice. Together, these data suggest that proper expression of Foxp1 in the pyramidal neurons of the forebrain is important for regulating gene expression pathways that contribute to specific behaviors reminiscent of those seen in autism and intellectual disability. In particular, Foxp1 regulation of gene expression appears to be crucial for normal hippocampal development, CA1 physiology, and spatial learning.

## INTRODUCTION

Autism spectrum disorder (ASD) is often comorbid with intellectual disability (ID) (Geschwind and State, 2015; de la Torre-Ubieta et al., 2016). Delineating the brain circuits that contribute to distinct ASD and ID symptoms could be a major first step towards improved treatments for these disorders. ASD has a strong genetic component (Geschwind and State, 2015; de la Torre-Ubieta et al., 2016) that is shared in part with ID (Vissers et al., 2016). Numerous transcription factors coordinate the expression patterns of ASD- and ID-risk genes during early brain development (State and Sestan, 2012; de la Torre-Ubieta et al., 2016). Therefore, investigating the role of ASD- and ID-relevant transcription factors in a brain-region-specific manner could reveal circuit-based pathways that contribute to discrete behavioral phenotypes in the two disorders.

Heterozygous mutations and deletions in the transcription factor *FOXP1* are causative for ASD and ID (Bacon and Rappold, 2012; Le Fevre et al., 2013; Lozano et al., 2015; Vissers et al., 2016). Additionally, *FOXP1* has been classified as a high-confidence ASD- and ID-risk gene in several recent, large-scale sequencing studies (Iossifov et al., 2014; Sanders et al., 2015; Stessman et al., 2017). FOXP1 is a member of the Forkhead Box (FOX) transcription factor family, which is denoted by a unique nomenclature (uppercase for primates, title case for rodents, and mixed case for all other species or collection of species) (Kaestner et al., 2000).

Within the forebrain, Foxp1 expression is largely restricted to the pyramidal neurons of the neocortex and the CA1/CA2 hippocampal subfields as well the medium spiny neurons of the striatum (Ferland et al., 2003; Tamura et al., 2004; Hisaoka et al., 2010). Conditional-full-brain loss of *Foxp1* results in altered social behaviors, impaired learning and memory, and developmental aberrations in the striatum (Bacon et al., 2014). Neocortical knockdown of *Foxp1* disrupts neuronal migration and axon formation but the resultant behavioral phenotypes have not been assessed (Li et al., 2015). Finally, using a patient-relevant heterozygous *Foxp1* knockout mouse we have shown that Foxp1 regulates distinct, regional transcriptional profiles in the brain and that loss of *Foxp1* expression in the striatum strongly correlates with deficits in ultrasonic vocalization production (Araujo et al., 2015). While these studies have begun to shed light on the function of Foxp1 within the brain, the specific contributions of neocortical and hippocampal Foxp1 to ASD and ID phenotypes remain to be determined. Addressing this question is important, given that many changes to the anatomy,

transcriptional profiles, and physiology of the neocortex and hippocampus are observed in ASD and ID brains (Chen et al., 2015).

To investigate the regional contributions of Foxp1 expression to ASD- and ID-relevant phenotypes, we used an *Emx1.Cre* mouse line (Gorski et al., 2002) to generate a *Foxp1* conditional knockout (*Foxp1*$^{cKO}$) mouse with loss of Foxp1 in the pyramidal neurons of the neocortex and the hippocampus. In this study, we integrate behavioral profiling, electrophysiology, magnetic resonance imaging (MRI) analyses, and genomics. We show that loss of Foxp1 in the neocortex and hippocampus is sufficient to produce ASD- and ID-relevant behaviors such as hyperactivity, communication deficits, decreased sociability, and impaired spatial learning and memory. Additionally, we show that the ID-like learning and memory deficits observed in *Foxp1*$^{cKO}$ mice are likely due to alterations in hippocampal function, as behaviors involving broader cortical circuits are unaffected. Using RNA-sequencing (RNA-seq), we correlate these behavioral phenotypes to specific changes in the transcriptome of the *Foxp1*$^{cKO}$ hippocampus. We also employ MRI to demonstrate that loss of forebrain *Foxp1* expression leads to decreased hippocampal volumes. Finally, based on the genomic and morphological data, we assayed the electrophysiological properties of the *Foxp1*$^{cKO}$ hippocampus and found reduced CA1-dependent LTP maintenance. As a whole, our data suggest that certain behavioral consequences of *Foxp1* loss can be attributed to disrupted gene networks within distinct regions of the brain. Therefore, these data could lead to improved treatments for specific ASD and ID symptoms.

## MATERIALS AND METHODS

### Mice

Homozygous-floxed *Foxp1* (*Foxp1*$^{flox/flox}$) mice (Feng et al., 2010) were backcrossed with C57BL/6J mice for at least 10 generations to obtain congenic animals. Mice hemizygous for Cre recombinase expression under the control of the *Emx1* promoter (*Emx1.Cre*$^{+/-}$ mice) (Gong et al., 2003) were purchased from Jackson Laboratories (strain # 005628) and are congenic for the C57BL/6J background. Experimental animals were generated by crossing male *Emx1.Cre*$^{+/-}$*;Foxp1*$^{flox/flox}$ mice with female *Foxp1*$^{flox/flox}$ mice. Mice were kept in the animal facilities of UT Southwestern Medical Center under a 12-hour light-dark cycle and all behavioral testing occurred during the light cycle with the experimenter blind to genotype. Unless otherwise specified, all mice were given *ad libitum* access to food and water. All mouse studies were approved by the UT Southwestern Institutional Animal Care and Use Committee.

### Immunoblotting

Regional brain lysates from adult (>8 week) male mice were prepared and used in immunoblotting experiments as previously described (Araujo et al., 2015).

### Tissue Preparation

For immunohistochemistry, adult female and male mice were anesthetized with 80 – 100 mg/Kg Euthasol (UT Southwestern Medical Center Animal Resources Center Veterinary Drug Services), perfused with PBS containing 10 U/mL heparin (Sigma)

followed by fixative (4% PFA in PBS), and then immediately decapitated. Whole brains were removed and incubated in fixative for 24 hours at 4°C and then incubated in 30% sucrose (made in PBS with 0.02% sodium azide) for 24-48 hours at 4°C. Afterwards, brains were sectioned at 35-40 um on an SM2000 R sliding microtome (Leica). Sections were then stored in PBS containing 0.02% sodium azide until used in immunohistochemistry.

For magnetic resonance imaging, adult male mice were anesthetized with 80 – 100 mg/Kg Euthasol, perfused with PBS (without $Ca^{2+}$ and $Mg^{2+}$) containing 10 U/mL heparin and 2mM ProHance (Bracco Diagnostics), and then fixative (4% PFA in PBS without $Ca^{2+}$ and $Mg^{2+}$) containing 2mM ProHance. Afterwards, animals were immediately decapitated and the cartilaginous nose tip, eyes, skin, lower jar, ears, and zygomatic bones were removed. Brains (encased in the remaining skull structures) were then incubated in fixative containing 2mM ProHance and 0.02% sodium azide for 24 hours at 4°C and subsequently transferred to PBS (without $Ca^{2+}$ and $Mg^{2+}$) containing 2mM ProHance and 0.02% sodium azide for storage at 4°C.

**Immunohistochemistry**

Floating immunohistochemistry was performed according to standard procedures. Briefly, at room temperature, sections were first washed with TBS. Next, they were incubated with 3% hydrogen peroxide for 30 minutes, washed with TBS, treated with 0.3 M glycine for 30 minutes, and washed again with TBS. Sections were then incubated with primary antibodies diluted in TBS-T (0.4% Triton X-100) containing 1% bovine

serum albumin (BSA) and 3% normal donkey serum (NDS) overnight at 4°C. Next, sections were washed in TBS-T, incubated with secondary antibodies diluted in TBS-T containing 1% BSA and 3% NDS for 1 hour at room temperature, and then mounted onto microscope slides. Finally, slides were washed with TBS-T and allowed to dry overnight at room temperature, mounted with ProLong Diamond Antifade Mountant with DAPI (Thermo) and a coverslip, and allowed to set overnight at room temperature. Slides were imaged using a LSM 710 Confocal Microscope (Zeiss) connected to a computer running ZEN 2012 Software (Zeiss).

**Magnetic Resonance Imaging**

A multi-channel 7.0 Tesla MRI scanner (Agilent) was used to image the brains within skulls. 16 custom-built solenoid coils were used to image the brains in parallel (Bock et al., 2005; Lerch et al., 2011). A T2-weighted 3D Fast Spin Echo (FSE) sequence was used for the acquisition of the anatomical images. Parameters for the FSE sequence: TR of 350 milliseconds, and TEs of 12 milliseconds per echo for 6 echoes, two averages, field of view of 20 x 20 x 25 $mm^3$ and a matrix size of 504 x 504 x 630 giving an image with 40 um isotropic resolution. K-space was acquired with a cylindrical acquisition (Nieman et al., 2005). Total imaging time was 14 hours. To visualize and compare any changes in the mouse brains the images are linearly (6 parameter followed a 12 parameter) and non-linearly registered together. All scans were then resampled with the appropriate transform and averaged to create a population atlas representing the average anatomy of the study sample. The result of the registration is

to have all scans deformed into alignment with each other in an unbiased fashion. This allows for the analysis of the deformations needed to take each individual mouse's anatomy into this final atlas space, the goal being to model how the deformation fields relate to genotype (Nieman et al., 2006; Lerch et al., 2008). The Jacobian determinants of the deformation fields are then calculated as measures of volume at each voxel. Significant volume changes can then be calculated by warping a pre-existing classified MRI atlas onto the population atlas, which allows for the volume of 159 segmented structures encompassing cortical lobes, large white matter structures (i.e. corpus callosum), ventricles, cerebellum, brain stem, and olfactory bulbs to be assessed in all brains. This atlas is a combination of 3 separate atlases (Dorr et al., 2008; Ullmann et al., 2013; Steadman et al., 2014). In addition to the regional assessment, these images can be examined on a voxel-wise basis in order to localize the differences found within regions or across the brain. Multiple comparisons in this study were controlled for using the False Discovery Rate (Genovese et al., 2002).

**Antibodies**

The following antibodies were used for immunoblotting (IB) or immunohistochemistry (IHC): anti-Foxp1 ((Spiteri et al., 2007) (rabbit; 1:5000 (IB), 1:1000 (IHC))) and anti-GAPDH (mouse, Millipore; 1:5000 (IB)).

**RNA Processing**

RNA purification was performed on tissues dissected from P47 male mice and littermate controls as previously described (Araujo et al., 2015).

**qPCR**

qPCR was performed as previously described (Araujo et al., 2015). All primer sequences are available upon request.

**RNA-seq Library Preparation**

RNA-seq library preparation was performed according to previously published methods (Takahashi et al., 2015). Briefly, mRNA was isolated from 2 ug of total RNA (at RIN values $\geq$ 8.9) harvested from adult tissues via poly(A) selection. 15 PCR cycles were used for cDNA amplification. Pooled libraries, each at a final concentration of 2 nM, were sequenced on a NextSeq 500 sequencer (Illumina) by the McDermott Sequencing Core at UT Southwestern Medical Center to generate single-end 75 bp reads.

**RNA-seq Data Analysis**

Raw reads were first filtered for phred quality and adapters using FASTQC (Andrews, 2010) and Trimmomatic (Bolger et al., 2014). Filtered reads were then aligned to the reference mouse genome mm10 (https://genome.ucsc.edu) using STAR (Dobin et al., 2013) aligner. Uniquely mapped reads were used to obtain the gene counts using HTSeq package (Anders et al., 2015), and the read counts were normalized using the CPM (counts per million) method implemented in the edgeR package (Robinson et al.,

2010; McCarthy et al., 2012). For further analysis, we performed a sample-specific CPM filtering, considering genes with CPM values of 1.0 in all replicates for treatments or controls. DESeq (Anders and Huber, 2010; Love et al., 2014) was used to detect the differentially expressed genes (DEGs). We applied a filter of an adjusted p-value of $\leq$ 0.005 and absolute log fold change of $\geq$ 0.3 to identify DEGs.

**DEG Gene Ontology Analysis**

Gene Ontology (GO) analysis of the significant DEGs was carried out using ToppGene (https://toppgene.cchmc.org) and GO terms were reduced using REVIGO (Supek et al., 2011). GO categories were considered significant if they contained at least three genes and if they had a Benjamini and Hochberg corrected p-value, q-value, $\leq$0.05.

**Weighted Gene Co-expression Network Analysis**

Weighted gene co-expression network analysis (WGCNA) was carried out on 16 total RNA-seq samples (8 neocortical samples (4 control, 4 *Foxp1*$^{cKO}$) and 8 hippocampal samples (4 control, 4 *Foxp1*$^{cKO}$)). R package for WGCNA (Langfelder and Horvath, 2008) was used to build gene co-expression network using filtered CPM data (CPM >= 1 across all replicates of a condition). A signed network was constructed using *blockwiseModules* function of the WGCNA R package. A value of 10 was chosen as *Beta* with highest scale-free R square ($R^2$ = 0.8). For other parameters, we used *corType* = pearson, *maxBlockSize* = 15000, *reassignThreshold* = $1x10^{-6}$, *mergeCutHeight* = 0.1, *deepSplit* = 4, and *detectCutHeight* = 0.999. Visualization of

network plots were created using Cytoscape v3.4.0 (Shannon et al., 2003), representing the top 500 edges based on ranked weights.

**Hippocampal Electrophysiology**

An experimenter blind to genotype performed all electrophysiology studies. Juvenile (6-7 week old) male mice were anesthetized briefly with isoflurane (Baxter Healthcare Corporation) and rapidly decapitated to remove the brain, which was then submerged in ice-cold ACSF containing the following (in mM): 75 sucrose, 87 NaCl, 3 KCl, 1.25 $NaH_2PO_4$, 7 $MgSO_4$, 26 $NaHCO_3$, 20 dextrose, and 0.5 $CaCl_2$. Acute coronal hippocampal slices were cut 350 um thick using a VT 1000 S vibrating microtome (Leica). To reduce recurrent excitation of CA3 neurons, a cut was made between CA3 and CA1. Slices were allowed to recover at 34°C for 15 minutes in normal ACSF containing (in mM): 124 NaCl, 5 KCl, 1.25 $NaH_2PO_4$, 2 $MgCl_2$, 26 $NaHCO_3$, 10 dextrose, and 1 $CaCl_2$. Recovery continued for 45 minutes as slices were gradually cooled to room temperature for holding prior to recording. All solutions were pH 7.4 and saturated with 95% $O_2$/%5 $CO_2$.

All recordings were performed at 33°C ± 0.5°C in ACSF containing (in mM): 124 NaCl, 5 KCl, 1.25 $NaH_2PO_4$, 1 $MgCl_2$, 26 $NaHCO_3$, 10 dextrose, and 2 $CaCl_2$ saturated with 95% $O_2$/5% $CO_2$, and all data were collected using Clampex (pClamp Software Suite 10.2; Molecular Devices). Recordings were filtered at 1kHz and digitized at 10 kHz. CA3-CA1 synapses were stimulated by a 100$\mu$s biphasic pulse through custom-made nickel dichromate electrodes (A-M Systems) placed 400-500 um laterally from the

recording electrode and kept constant within this range for all experiments. Stimulation was controlled using a model 2200 stimulus isolator (A-M Systems). The recording electrode (1-3 MΩ) was filled with normal ACSF and placed in the stratum radiatum using a SZX7 dissecting microscope (Olympus) at 35X magnification. Sample size for all extracellular field recordings represents number of slices tested with two-four slices used per mouse. Response size was determined by fitting a straight line to the initial slope (10–40%) of the field EPSP (fEPSP) using automated analysis in Clampfit (pClamp Software Suite 10.2; Molecular Devices). For LTP, the stimulus intensity was set to generate ~50% of the maximum fEPSP, as determined by the I/O curve. LTP was induced with 2 trains of 100 Hz stimulation for 1 second separated by 1 minute. A 20-minute baseline was recorded before LTP induction and followed by at least 60 min of 0.05 Hz stimulation every 20 seconds.

**Novel Cage Activity Test**

Adult male and female mice were individually moved from their home cages into clean, plastic (18 cm x 28 cm) cages with minimal bedding. Each cage was then placed into a dark Plexiglas box. Movement was measured with Photobeam Activity System-Home Cage software (San Diego Instruments) for 2 hours for each mouse. The number of beam breaks were recorded every 5 minutes.

**Open Field Test**

The open field assay was performed on adult male and female mice as previously described (Araujo et al., 2015).

**Ultrasonic Vocalizations**

Ultrasonic vocalizations produced by adult male mice were assessed in a mating paradigm modified from previously published methods (Holy and Guo, 2005). Briefly, male mice were singly paired with age-matched C57BL/6J female mice for 1 week. Afterwards, female mice were removed from the cages and the males were singly-housed for 1 week. The next day (the test day), the male mice were allowed to habituate to the testing environment for 15 minutes. During habituation, food hoppers were removed and the cage lids were replaced with Styrofoam lids containing UltraSoundGate condenser microphones (Avisoft Bioacoustics) positioned at a fixed height. The condenser microphones were connected to UltraSoundGate416H hardware (Avisoft Bioacoustics) hooked up to a computer running Avisoft RECORDER software (Avisoft Bioacoustics). Next, habituated, age-matched C57BL/6J female mice were randomly placed into a cage containing a male. The resultant male songs were recorded for 3 minutes. No female was used in more than 2 recording sessions per day. Analyses of ultrasonic vocalization features were carried out as previously described (Araujo et al., 2015). Call duration reflects the average length of calls (in milliseconds), mean frequency denotes the average frequency of calls (in kilohertz), frequency range is the average difference between the maximum and minimum frequency at which calls are produced (in kilohertz), the fraction of calls with frequency jumps represents the

ratio of calls with and without frequency breaks, and the average slope of the call reflects modulation of call frequency over time (in hertz/milliseconds).

**Social Interaction Test**

Adult female and male mice were individually placed in an open field environment (44 cm x 44 cm, with walls 30 cm high) in a dimly lit room and allowed to explore for 5 minutes. Inside the open field arena, a small plastic chamber (the interaction box, 8.5 cm x 4.5 cm) was placed along one wall of the arena. After 5 minutes, the test mouse was removed and a novel, unfamiliar mouse (same sex and strain as the test mouse) was placed into the interaction box. Small holes in the interaction box allow the mice to see, hear and smell each other. The test mouse was returned to the open field environment and allowed to explore for another 5 minutes. The test mouse was monitored from above by a video camera connected to a computer running Ethovision 3.0 (Noldus). Both the amount of time the test mouse spent in the interaction zone immediately adjacent to the interaction chamber (within 8 cm) and the time spent in the four corners of the arena (9 cm x 9 cm each) were recorded.

**Nesting Behavior**

Nesting behavior was gauged in adult male and female mice as previously described (Araujo et al., 2015).

**Fear Conditioning**

Fear conditioning was conducted on adult female and male animals using boxes containing a grid metal floor attached to a scrambled shock generator. Mice were individually trained by placing them into the box for 2 minutes and giving them 3 separate tone-shock pairings (30s white noise, a 2 second, 0.5 mA shock, and 1 minute intervals between pairings). Context recall was assessed 24 hours later by placing the mice back into the original box and recording freezing for 5 minutes. Cue recall was assessed two days after training by placing the mice in the boxes altered with a plastic floor, an inverted roof, and a vanilla scent. Freezing was then measured for 3 minutes followed by the presentation of the white noise cue and measuring freezing for an additional 3 minutes with Video Freeze software (Med Associates).

**Morris Water Maze**

The Morris water maze was conducted on adult male mice using a 1.2 m diameter circular pool filled with opaque, tempera-paint dyed 23°C water. Stark visual cues were placed around the room containing the pool. Within the pool, a 10-cm circular plexiglass escape platform was submerged in one of the quadrants 1 cm below the water's surface. For training, mice were placed into the pool in one of four starting locations (north, south, east, or west, with the order being randomly determined) and allowed to swim until they located the escape platform. Upon finding the platform, mice were permitted to rest for 5 seconds before being removed. If they did not locate the platform within 60 seconds, mice were manually guided to the platform and given 5 seconds of rest before being removed. Mice received four training trials per day for 10 days and

were placed in temporary cages between the training trials of a particular day. On day 12, after a day of rest on day 11, a probe test was performed in which mice were allowed to swim in the pool for 60 seconds, with the escape platform removed. The movements of the animals were recorded by a video camera centered above the pool and tracked using ANY-Maze software (Stoelting). The latency to reach the escape platform was quantified for each mouse during the 10-day training period. For the probe test, the number of original platform crosses was analyzed for each mouse.

**T-maze**

The T-maze was constructed from gray polyvinyl, with the main array 40 cm long, the side arms 33 cm long, the walls 18.5 cm high, and the alleys 10 cm wide (Actimetrics). Before commencing any testing, adult female and male mice were subjected to food restriction until their body weight reached 85% of baseline. Then, for habituation to the T-maze, each mouse was placed into the apparatus, with all of the doors open and a food pellet (20 mg, Bio-Serv) placed in a cup at the end of each arm. This was carried out in four sessions, each 10-minutes long, for 2 days. After this habituation period, each mouse was used in ten test trials per day for 10 consecutive days. For the testing phase, each trial was composed of two different runs: the sample run and the test run. In the sample run, the pellet reward was placed randomly at one end of the arms, and the other arm was closed off. A mouse was then placed at the start position and allowed to travel freely to the end of the arm and consume the pellet. Immediately after consuming the pellet, the mouse was placed back in the start position, which was

closed off. While the mouse was isolated in the start position, the blocked arm was opened and the entire apparatus was wiped with 10% ethanol to remove olfactory cues. A food pellet was then placed in the arm opposite from the one containing the reward in the sample run. After a 30 second delay, the test run was started. In the test run, each mouse was allowed to travel to either arm. If the mouse chose the opposite arm that was rewarded in the sample run (a correct choice), it was allowed to consume the pellet. If the mouse chose the same arm as in the sample run (an incorrect choice), it was blocked in the arm for 30 seconds as punishment. Spatial working memory was evaluated by the average success rate for each day.

**Set-shifting Task**

With minor modifications, the set-shifting test was conducted as previously described (Cho et al., 2015). Before testing began, adult male and female mice were subjected to food restriction until their body weight reached 85% of baseline. Afterwards, animals were individually housed and then presented with two bowls in their home cage, until they began digging in one bowl. Each of these bowls contained a different odor and a different digging medium, and the odor-medium combinations were altered and counterbalanced from trial to trial. The digging media were white calcium sand and pine wood shavings, mixed with an odorant (ground garlic, or clove, 0.01% by volume) and peanut butter chip powder (0.1% by volume). The reward, a 5-10 mg piece of a peanut butter chip, was buried in the medium in both of the food bowls.

Testing began once mice reached their target weight. The testing procedure consisted of three phases (training, initial association, and rule-shift), with each phase lasting 1 day for a total of 3 consecutive days. On day 1 (the training day), mice were given ten consecutive trials in which they were allowed to dig amongst two bowls containing two different mediums, in order to learn that they could reliably find a food reward in only one of the bowls. On day 2 (the initial association day), mice learned that a specific cue (an odor or medium) predicted the presence of food reward, by being presented with different odor-medium combinations (which were switched and counterbalanced) during each trial. This predictive cue remained constant over the whole day, with each mouse being randomly assigned their own cue. On day 3 (the rule-shift day), the dimension (odor or medium) signaling the reward was changed. If the initial association paired a specific odor with the food reward, then the rule-shift phase paired a certain digging medium with reward and the mice needed to learn this new rule to obtain a reward.

In the initial association and the rule shift phases, the mice were considered to have learned the association between stimulus and reward if they made ten consecutive, correct choices. The phase ended when they met this criterion. When the mice made a correct choice on a trial, they were allowed to consume the food reward before the next trial. Between trials, mice were transferred from their home cage to a holding cage while new bowls were set up. After making an error on a trial, the mice were transferred to the holding cage for 1 minute as punishment. Additionally, in the rule-shift phase, two types of error were analyzed; perseverative errors, when a choice

was consistent with the rule of the initial association phase, and random errors, when a choice was inconsistent with both the rules of the initial association and the rule-shift phases.

**Experimental Design and Statistical Analysis**

All experiments reported in this study were designed to examine genotype-based effects between *Foxp1*$^{cKO}$ and littermate control mice. Effects on Foxp1 protein levels in the brain (Fig. 3.1A-C) were examined using adult (≥8 week old) male mice (3 mice/genotype). Effects on activity in a novel cage activity test (Fig. 3.2A,B) were tested using adult female and male mice (7-9 mice/genotype). Effects on activity and anxiety in an open field assay (Fig. 3.2C,D) were examined in adult male and female mice (8 mice/genotype). Adult male mice (12-15 mice/genotype) were used to test genotype-based effects on USV song production (Fig. 3.3A-F). Genotype-effects on nest building (Fig. 3.3G,H) were assessed in adult male and female mice (7-8 mice/genotype). Effects on sociability (Fig. 3.3I) were determined using adult female and male mice (12-16 mice/genotype). Adult male mice (10-12 mice/genotype) were used to evaluate effects on performance in the Morris water maze (Fig. 3.4A-C). Effects on performance in an alternating T-maze (Fig. 3.4D-F) were tested utilizing adult male and female mice (10 mice/genotype). Effects on performance in a fear conditioning test (Fig. 3.5A,B) were determined using adult female and male mice (12-16 mice/genotype). Adult male and female mice (9-10 mice/genotype) were used to examine effects on performance in a set-shifting task (Fig. 3.5C,D). Adult male mice (10 mice/genotype) were used to

determine the effects of genotype of relative regional brain volumes (Fig. 3.6A,B). Effects on hippocampal electrophysiological properties (Fig 3.8A-C) were determined using juvenile (6-7 week old) male mice (15-20 recordings/genotype). Effects on gene expression via qPCR (Figs. 3.7F, 8E) were tested using adult male mice (3/genotype). Except as noted for genomic analyses, Student's *t*-tests (2-tailed, type 2) were carried out for analyses of data in Figs. 3.1B, 2B,C,D, 3A,B,C,D,E,F,H,I, 4C,D,F, 5B, 6B, 7F, 8B,E and two-way ANOVAs (all with a Sidak's multiple comparison test) were carried out for analyses of data in Figs. 3.2A, 4A,E, 4A,C,D, and 5C. FDR was utilized for Fig. 3.6B. P-values were calculated using Prism 7 (GraphPad) and significance was assigned to values $\leq 0.05$. More detailed statistical information can be found in the Results section for each figure.

**GEO Accession Information**

The NCBI GEO accession number for the RNA-seq data reported in this study is GSE97181.

## RESULTS

Foxp1 is expressed within the pyramidal neurons of the neocortex and the CA1/CA2 hippocampal subfields (Ferland et al., 2003; Hisaoka et al., 2010). However, the distinct ASD and ID-related behavioral phenotypes governed by Foxp1 within these regions are undetermined. To examine the neocortical and hippocampal contributions of Foxp1 to ASD and ID-relevant behaviors, we characterized *Foxp1* conditional knockout

(*Emx1.Cre*$^{+/-}$;*Foxp1*$^{flox/flox}$) mice (hereafter called *Foxp1*$^{cKO}$ mice) in comparison to littermate control (*Foxp1*$^{flox/flox}$) mice.

There are four murine isoforms of Foxp1 and two of them (Foxp1A and Foxp1D) are highly expressed within the mouse brain (Wang et al., 2003; Araujo et al., 2015). Consistent with the forebrain expression pattern of Cre recombinase under the *Emx1* locus (Gorski et al., 2002), *Foxp1*$^{cKO}$ mice displayed near total loss of Foxp1 protein isoforms A and D in the neocortex (CTX) and hippocampus (HIP) (Fig. 3.1A,B; Student's t-test; CTX: $F_{(2,2)}$=4.21, **p=0.002; HIP: $F_{(2,2)}$=9.59 ***p=0.0002). As a negative control, we demonstrated that Foxp1 protein expression is preserved in the striatum (STR) of these animals (Fig. 3.1A,B; Student's t-test, $F_{(2,2)}$=2.67, p=0.7). In concordance with these results, we observed that Foxp1 expression is ablated in the projection neurons of the neocortex and the CA1/CA2 hippocampal subfields of *Foxp1*$^{cKO}$ mice (Fig. 3.1C). Because neuroglia and interneurons do not express Foxp1 (Hisaoka et al., 2010; Precious et al., 2016), we believe that this decrease in protein levels is due to a loss of *Foxp1* specifically in forebrain pyramidal neurons. Adult *Foxp1*$^{cKO}$ mice are viable, superficially healthy, and exhibit no differences in body weight (Student's t-test, $F_{(14,14)}$=2.45, p=0.96, n=15 mice/genotype). Thus, these animals represent a model with which to examine the neocortical and hippocampal-based contributions of Foxp1 to ASD and ID-relevant phenotypes.

Symptoms common between ASD and ID include hyperactivity and anxiety (van Steensel et al., 2011; Ageranioti-Belanger et al., 2012; Leitner, 2014; de la Torre-Ubieta et al., 2016). Therefore, we first assessed the baseline activity of adult (≥ 8 weeks old)

*Foxp1*$^{cKO}$ mice. *Foxp1*$^{cKO}$ mice exhibit sustained, increased activity over a two-hour period in a novel-cage (Fig. 3.2A; two-way ANOVA; genotype effect: $F_{(1,336)}$=163.6, ****p<0.0001; time effect: $F_{(23,336)}$=22.44, p<0.0001; interaction effect: $F_{(23,336)}$=2.2, p=0.001; and Fig. 3.2B; Student's t-test, $F_{(6,8)}$=3.6, **p=0.002). Additionally, in an open field assay *Foxp1*$^{cKO}$ mice cover more distance (Fig. 3.2C; Student's t-test, $F_{(7,7)}$=2.62, *p=0.02) and spend less time in the center of the arena with a corresponding increase in time spent around the border of the arena (Fig. 3.2D; Student's t-test; time in center: $F_{(7,7)}$=2.79, *p=0.02; time in border: $F_{(7,7)}$=2.7, *p=0.02). Together, these findings suggest a phenotype of hyperactivity and increased anxiety in *Foxp1*$^{cKO}$ mice, which are symptoms common to both ASD and ID.

As decreased social communication is one of the core features of ASD (Fakhoury, 2015; de la Torre-Ubieta et al., 2016; Park et al., 2016), we examined both the social and communicative behaviors of *Foxp1*$^{cKO}$ mice. The ultrasonic vocalizations (USVs) produced by adult male mice in response to the presence of female mice are a well-characterized form of mouse communication (Holy and Guo, 2005; Portfors and Perkel, 2014). We therefore assayed the USVs (known as "songs") produced by adult male *Foxp1*$^{cKO}$ mice during courtship encounters with age-matched females. *Foxp1*$^{cKO}$ mice produce fewer numbers of songs (Fig. 3.3A; Student's t-test, $F_{(14,12)}$=1.12, **p=0.002). Additionally, the songs of *Foxp1*$^{cKO}$ mice were shorter (Fig. 3.3B; Student's t-test, $F_{(12,13)}$=3.75, *p=0.01), covered a smaller frequency range (Fig. 3.3D; Student's t-test, $F_{(12,13)}$=1.94, *p=0.02), and were less complex as revealed by both a reduction in the number of songs with frequency jumps (Fig. 3.3E; Student's t-test, $F_{(12,14)}$=1.73,

*p=0.02) and an alteration in the average call slope (Fig. 3.3F; Student's t-test, $F_{(13,12)}$=1.72, ***p=0.0003). Notably, the mean frequency of *Foxp1*$^{cKO}$ songs was not altered (Fig. 3.3C; Student's t-test, $F_{(13,12)}$=1.52, p=0.45). (See the Materials and Methods section for details on call parameters.) We then tested nest building in *Foxp1*$^{cKO}$ mice because it is an important behavior for communal animals such as rodents (Deacon, 2006; Silverman et al., 2010). *Foxp1*$^{cKO}$ animals consistently produce low quality nests and in most cases never interact with the provided nesting material (Fig. 3.3G,H; Student's t-test, $F_{(6,7)}$=2.29, ****p<0.0001). In a social interaction paradigm, *Foxp1*$^{cKO}$ mice exhibited a social-retreat phenotype as indicated by their decreased time in the interaction zone (Fig. 3.3I; Student's t-test, $F_{(15,11)}$=1.91, **p<0.01) and their increased time in the corners of the testing arena (Fig. 3.3I, Student's t-test, $F_{(15,\ 11)}$=2.68, ***p<0.001). The increased preference for the corners of the sociability apparatus suggests that the decreased social interaction displayed by *Foxp1*$^{cKO}$ mice was not simply due to hyperactivity. Taken together, our results indicate that neocortical and hippocampal loss of Foxp1 protein expression is sufficient to lead to ASD-relevant deficits in communication and sociability.

Because both ASD patients and patients with *FOXP1* haploinsufficiency frequently present with ID (Le Fevre et al., 2013; Geschwind and State, 2015; Lozano et al., 2015; de la Torre-Ubieta et al., 2016), we next examined the learning and memory capabilities of *Foxp1*$^{cKO}$ mice. Over the course of 10 days of training in the Morris water maze, *Foxp1*$^{cKO}$ mice never learn to find the submerged platform (Fig. 3.4A; two-way ANOVA; genotype effect: $F_{(1,200)}$=199.6, ****p<0.0001; training day effect: $F_{(9,200)}$=6.98,

p<0.0001; interaction effect: $F_{(9,200)}$=3.25, p=0.001), indicating poor spatial learning (Vorhees and Williams, 2006). Additionally, on a probe day 48 hours after the last day of training, *Foxp1*$^{cKO}$ mice make fewer numbers of platform crosses (Fig. 3.4B,C; Student's t-test, $F_{(11,9)}$=2.78, **p=0.002). This was result was not unexpected, given that the *Foxp1*$^{cKO}$ mice showed no demonstrable learning. These deficits were not due to problems in visual acuity because *Foxp1*$^{cKO}$ mice are able to escape the maze just as quickly as control littermates on a visual probe day (Fig. 3.4D; Student's t-test, $F_{(11,9)}$=3.88, p=0.34). Moreover, these deficits are not due to changes in swim speeds, as *Foxp1*$^{cKO}$ mice show no differences in their average swimming velocity during training (two way-ANOVA, genotype effect: $F_{(1,120)}$=3.35 p=0.07). In a T-maze, *Foxp1*$^{cKO}$ mice do no better than chance during the course of a 10-day training period (Fig. 3.4E; two-way ANOVA; genotype effect: $F_{(1,170)}$=123.6, ****p<0.0001; training day effect: $F_{(9,170)}$=0.59, p=0.81; interaction effect: $F_{(9,170)}$=1.11, p=0.36; and Fig. 3.4F; Student's t-test, $F_{(8,9)}$=1.3, ****p<0.0001) implying deficits in spatial working memory in these animals (Shoji et al., 2012). Learning in the Morris water maze and the T-maze both rely on hippocampal function (Vorhees and Williams, 2006; Shoji et al., 2012; Yamamoto et al., 2014) and thus these results support altered hippocampal mechanisms in *Foxp1*$^{cKO}$ animals.

We next asked whether the decreased performance of *Foxp1*$^{cKO}$ mice in learning and memory tasks is due to impairment in broad circuits or if it is restricted to hippocampal-based spatial memory. We first employed cue/contextual fear conditioning, as it involves hippocampal, neocortical, and amygdala-based circuits in associative learning and memory (Puzzo et al., 2014; Tovote et al., 2015). We observed no

differences in the fear response of *Foxp1*$^{cKO}$ mice, as measured by their performance in a cue-dependent fear learning paradigm (Fig. 3.5A; two-way ANOVA; genotype effect: $F_{(1,52)}$=1.23, p=0.27; tone effect: $F_{(1,52)}$=242, p<0.0001; interaction effect: $F_{(1,52)}$=0.44, p=0.51). We also observed no differences in a context-dependent fear learning paradigm (Fig. 3.5B; Student's t-test, $F_{(11,15)}$=2.63, p=0.12). *Foxp1*$^{cKO}$ mice are able to hear the conditioned stimulus (the tone before the shock), as they demonstrated no differences in freezing when presented with the stimulus during training (p=0.77, two-way ANOVA). *Foxp1*$^{cKO}$ mice are also able to perceive the unconditioned stimulus (the shock itself) just as well as their littermate controls, because they showed no difference in the stimulus strengths needed to induce jumping, flinching, or vocalizing (Student's t-test; jumping: $F_{(11,15)}$=1.44, p=0.53; flinching: $F_{(11,15)}$=1.51, p=0.40; vocalizing: $F_{(11,15)}$=2.0, p=0.45). Given that contextual fear conditioning is heavily dependent on hippocampal function (Puzzo et al., 2014; Tovote et al., 2015), the intact context-dependent fear conditioning we observed in *Foxp1*$^{cKO}$ mice was surprising. This pointed to a specific deficit in complex hippocampal-based spatial tasks. To test this hypothesis, we examined the performance of *Foxp1*$^{cKO}$ animals in a set-shifting paradigm, which is a complex task that is largely reliant on prefrontal neocortical function (Cho et al., 2015; Heisler et al., 2015). We saw no differences in the behavior of *Foxp1*$^{cKO}$ mice compared to controls during the set-shifting task, as measured by the number of trials needed to reach criterion for training or the number of errors made during testing (Fig. 3.5C; two-way ANOVA; genotype effect: $F_{(1,9)}$=0.219, p=0.65; test phase effect: $F_{(1,9)}$=14.74, p=0.004; interaction effect: $F_{(1,9)}$=1.05, p=0.33; and Fig. 3.5D; two-way ANOVA;

genotype effect: $F_{(1,18)}$=0.65, p=0.43; error type effect: $F_{(1,18)}$=33.51, p<0.0001; interaction effect: $F_{(1,18)}$=0.11, p=0.74). Together, these results indicate that the learning and memory deficits seen in *Foxp1*$^{cKO}$ mice are restricted to complex, spatial, hippocampal-based processes.

The behavioral deficits we observed in *Foxp1*$^{cKO}$ mice are associated with many molecular mechanisms in the hippocampus (Lynch, 2004; Kumar, 2011). To determine the processes governing the behavioral phenotypes in *Foxp1*$^{cKO}$ mice, we ascertained transcriptional changes due to Foxp1 loss by carrying out RNA-seq on tissue samples from the neocortex and hippocampus of both *Foxp1*$^{cKO}$ mice and littermate controls. Differentially expressed genes (DEGs) were identified by applying an adjusted p-value of ≤0.005 and an absolute log fold change of ≥0.3 (see GEO Accession Information in Methods). By clustering the same number of top DEGs (based on fold change) in both the neocortex and hippocampus we found transcriptional signatures (gene clusters) that differentiated the two brain regions by genotype (Fig. 3.6A; Table 3.1). Additionally, these upregulated and downregulated gene clusters are enriched for specific gene ontology (GO) categories (https://toppgene.cchmc.org) (Fig. 3.6A; Extended Data Table 3.6-1). For the hippocampus, these GO categories include terms such as *reduced long term potentiation*, *abnormal synaptic transmission*, and *abnormal learning/memory/conditioning*, (Fig. 3.6A; Benjamini and Hochberg corrected p-value, q value; *reduced long term potentiation*, q=5.09x10$^{-4}$; *abnormal synaptic transmission*, q=5.64x10$^{-4}$, *abnormal learning/memory/conditioning*, q=8.57x10$^{-4}$).

To characterize the relevance of *Foxp1*$^{cKO}$ hippocampal and neocortical DEGs with regards to ASD pathophysiology, we overlapped these lists with those genes included on the Simons Foundation Autism Research Initiative (SFARI) website (843 genes) (https://sfari.org/resources/sfari-gene). The SFARI gene list represents ASD-risk genes that have been manually curated from the scientific literature. We found that both the neocortical and hippocampal *Foxp1*$^{cKO}$ DEGs significantly overlap with the ASD SFARI genes (Fig. 3.6B; hypergeometric test; overlap between *Foxp1*$^{cKO}$ CTX and SFARI ASD genes, $p=2.8x10^{-7}$; overlap between *Foxp1*$^{cKO}$ HIP and SFARI ASD genes, $p=3.8x10^{-9}$; Table 3.2). When we excluded ASD SFARI genes from categories 5 and 6 (*hypothesized* and *not supported*) from this analysis, we obtained a similar result (hypergeometric test; 17 genes (p=0.003) for *Foxp1*$^{cKO}$ hippocampal DEGs and 49 genes (p=0.0002) for *Foxp1*$^{cKO}$ neocortical DEGs). Finally, accounting for directional consistency, we found a significant overlap between the *Foxp1*$^{cKO}$ neocortical and hippocampal DEG datasets (Fig. 3.6B; hypergeometric test, overlap between *Foxp1*$^{cKO}$ HIP and *Foxp1*$^{cKO}$ CTX genes, $p=4.7x10^{-31}$). The genes included in this overlap are enriched for GO categories such as *potassium channel activity* (Benjamini and Hochberg corrected p-value, q value, $q=3.3x10^{-3}$) and *calcium ion transmembrane transporter activity* (Benjamini and Hochberg corrected p-value, q value, $q=2.6x10^{-2}$). Combined with our previous report (Araujo et al., 2015), these data suggest that while Foxp1 regulates distinct targets within different neuronal populations, it has an overall role in regulating the expression of ASD-risk genes and ion receptor genes throughout the brain.

Next, to understand the role of Foxp1 specifically within the hippocampus, we compared the transcriptional targets in the hippocampus of the *Foxp1*$^{cKO}$ mice with DEGs we previously identified in a whole-body heterozygous *Foxp1* knockout (*Foxp1*$^{+/-}$) mouse (Araujo et al., 2015). We were unable to compare neocortical data as there were no DEGs in the neocortex of the heterozygous *Foxp1* mice (Araujo et al., 2015). When we applied the same DEG cutoffs to these two datasets, we found a significant overlap of directionally consistent hippocampal target genes in these two *Foxp1* mouse models (Fig. 3.6C; hypergeometric test, $p=1.8x10^{-22}$; Table 3.3). This overlap represents ~20% of the *Foxp1*$^{cKO}$ DEGs, but only ~9% of the *Foxp1*$^{+/-}$ DEGs. That a relatively small proportion of *Foxp1*$^{+/-}$ hippocampal DEGs overlap with the DEGs in the *Foxp1*$^{cKO}$ mouse hippocampus is an important finding, as the only major behavioral phenotype seen in *Foxp1*$^{+/-}$ mice was an alteration in USV production and we therefore did not observe any spatial learning and memory deficits in the *Foxp1*$^{+/-}$ mice (Araujo et al., 2015). Taken together, these results indicate that complete and partial loss of *Foxp1* produce unique alterations in signaling pathways in the hippocampus. Moreover, these data suggest that the non-overlapping genes in the *Foxp1*$^{cKO}$ hippocampus are likely important for the observed learning and memory deficits seen in *Foxp1*$^{cKO}$ mice.

Next, we sought to determine the extent to which *Foxp1*$^{cKO}$ hippocampal DEGs affect signaling processes involved in hippocampal neuron identity. Specifically, we hoped to see if loss of *Foxp1* perturbs the expression of genes specific to CA1 pyramidal neurons. To accomplish this, we overlapped the *Foxp1*$^{cKO}$ hippocampal DEGs with CA1-specific genes identified by single-cell sequencing of the mouse CA1

(Zeisel et al., 2015). We found a significant overlap between these two gene expression datasets (Fig. 3.6D; hypergeometric test, $p=1.7x10^{-15}$; Table 3.4; Extended Data Table 3.6-2). The relatively small size of this overlap (~15% of the *Foxp1*$^{cKO}$ hippocampal DEGs) is most likely due to the fact that our RNA-seq data captured direct and indirect (as well as cell-autonomous and non-cell-autonomous) gene expression changes due to loss of *Foxp1* in both CA1 and CA2 neurons throughout the entirety of the hippocampus.

We then employed weighted gene co-expression network analysis (WGCNA) to further prioritize *Foxp1*$^{cKO}$ hippocampal DEGs with respect to ASD and ID (Langfelder and Horvath, 2008). WGCNA allows for the identification of networks (or modules) of genes with high co-expression. Three modules were genotype-specific (Fig. 3.6E; Extended Data Figure 3.6-1). One module (the "Dark Green" module), was hippocampus-specific (Fig. 3.6E) and contained several ASD-SFARI genes such as *Cadm2*, *Prkcb*, *Scn8a*, and *Syne1*. The Dark Green module also contained *Fmr1*, which when disrupted in humans leads to Fragile-X syndrome (Hernandez et al., 2009). Finally, a number of *Foxp1*$^{cKO}$ hippocampal DEGs that overlapped with each of the relevant gene lists discussed above (SFARI ASD genes and/or *Foxp1*$^{cKO}$ neocortical DEGs and/or *Foxp1*$^{+/-}$ hippocampal DEGs) were chosen at random and confirmed in independent *Foxp1*$^{cKO}$ hippocampal samples via qPCR (Fig. 3.6F; Student's t-test, $p<0.05$ for all genes). In summary, these genomic data identify transcriptional programs downstream of Foxp1 that may drive the regulation of hippocampal function.

The genomic data indicated a role for Foxp1 in the regulation of both neocortical and hippocampal development (Fig. 3.6A,D). To assess neuroanatomical alterations due to forebrain *Foxp1* loss that could explain the observed phenotypes, we analyzed the brains of *Foxp1*$^{cKO}$ mice via magnetic resonance imaging (MRI), which has been used on other ASD mouse models (Ellegood et al., 2015). We chose to focus our analyses on relative regional volumes (normalized to total volumes) as the there was a significant decrease in the overall volume of *Foxp1*$^{cKO}$ mouse brains (-12%, $p<0.0001$, Student's t-test and FDR<1%). In summary, we found reductions and increases in the relative volumes of numerous brain regions in *Foxp1*$^{cKO}$ mice (Fig 3.7A,B; $p<0.05$, Student's t-test, and FDR<0.05, for all regions; Extended Data Table 3.7-1). Brain regions with decreased relative volumes constituted neuronal populations expressing *Emx1* (including many neocortical areas) or white matter tracts originating from populations expressing *Emx1* (Fig. 3.7A,B; Extended Data Table 3.7-1). Interestingly, the most affected region (in terms of percent decrease) was the hippocampus (Fig. 3.7B). Moreover, hippocampal subfields and parahippocampal regions such as the dentate gyrus, stratum granulosum, and the pre-para subiculum were also significantly reduced in volume (Fig. 3.7A,B; Extended Data Table 3.7-1). Brain regions with increased relative volumes mostly constituted cerebellar nuclei, cerebellar white matter tracts, and subcortical nuclei (Fig. 3.7A; Extended Data Table 3.7-1). Taken as a whole, these data demonstrate that loss of *Foxp1* expression in the forebrain leads to alterations in regional volumes throughout the brain, with hippocampal structures being drastically affected.

The significant decrease in hippocampal volumes exhibited by *Foxp1*$^{cKO}$ mice suggested alterations in the functional properties of this region (Fig. 3.7A,B). Additionally, plasticity in general and long-term potentiation (LTP) in particular were GO categories enriched in *Foxp1*$^{cKO}$ HIP DEGs (Fig. 3.6A). LTP is a well-studied process by which excitatory synapses are strengthened in response to neuronal stimulation (Lynch, 2004; Kumar, 2011). Hippocampal LTP mediated by projections from CA3 pyramidal neurons to CA1 pyramidal neurons (Schaffer-collateral projections) is thought to underlie the encoding of spatial memory (Lynch, 2004; Kumar, 2011). Thus, we chose to examine hippocampal LTP in *Foxp1*$^{cKO}$ mice. Given that Foxp1 expression in the hippocampus is restricted to CA1/2 pyramidal neurons (Ferland et al., 2003), we recorded LTP in area CA1 in response to Schaffer collateral stimulation in *Foxp1*$^{cKO}$ mice. While the initial magnitude of CA1 LTP was normal in *Foxp1*$^{cKO}$ mice (arrows in Fig. 3.8A), the mean magnitude of LTP during the last 10 minutes of stimulation was significantly reduced (Fig. 3.8A,B; Student's t-test, $F_{(19,14)}$=2.16, ****p<0.0001), indicative of impaired plasticity maintenance. This result was not due to differential baseline synaptic transmission in the *Foxp1*$^{cKO}$ mice, as we found no difference in the fEPSP slope relative to current stimulation intensity (Fig. 3.8C; two-way ANOVA; genotype effect: $F_{(1,236)}$=0.23, p=0.63; time effect: $F_{(7,236)}$=11.97, p<0.0001; interaction effect: $F_{(7,236)}$=0.04, p>0.99). To characterize the *Foxp1*$^{cKO}$ hippocampal RNA-seq data with regards to genes involved in LTP maintenance, we overlapped our gene list with a dataset generated from microarrays performed on tetanized rodent hippocampal slices (Ryan et al., 2012). These two datasets significantly overlapped (Fig. 3.8D;

hypergeometric test, $p=2.32x10^{-4}$; Table 3.4). We tested all 12 of these overlapping genes (which included *Foxp1*) via qPCR and we were able to confirm differential expression for 9 of them in independent *Foxp1*$^{cKO}$ hippocampal samples (Fig. 3.8E; Student's t-test, $p<0.05$ for all genes except *Ccnd1*, *Dusp5*, and *Sorcs3*). Of the 12 genes overlapping between the LTP-maintenance dataset and the *Foxp1*$^{cKO}$ hippocampus dataset, 7 (*Ccnd1*, *Dsp*, *Gnb4*, *Grin3a*, *Rasd1*, *Runx1t1*, and *Sorcs3*) are not included in the *Foxp1*$^{+/-}$ hippocampus dataset (Araujo et al., 2015). These 7 genes therefore represent mechanisms that are uniquely disrupted in the *Foxp1*$^{cKO}$ hippocampus and which could explain the physiological and behavioral phenotypes displayed by *Foxp1*$^{cKO}$ mice. Indeed, several of these genes (*Rasd1*, *Gnb4*, and *Grin3a*) have been directly implicated in hippocampal-based learning and memory (de Quervain and Papassotiropoulos, 2006; Vilches et al., 2014; Carlson et al., 2016). These data suggest that control of genes involved in hippocampal LTP maintenance is disrupted in *Foxp1*$^{cKO}$ mice and that this may contribute to their learning and memory deficits.

## DISCUSSION

Elucidating molecular mechanisms important for learning and memory is an ambitious undertaking, especially in terms of connecting these mechanisms to disorders such as ASD and ID. Numerous genes have been linked to an increased risk for both of these disorders and this suggests common mechanisms between them (Santini and Klann, 2014; Plummer et al., 2016). However, only a few of these genes have been categorized as high-confidence risk genes (Iossifov et al., 2014; Sanders et al., 2015;

de la Torre-Ubieta et al., 2016; Mullins et al., 2016; Vissers et al., 2016; Stessman et al., 2017). *FOXP1* is among this list of high-confidence ASD-risk genes (Iossifov et al., 2014; Sanders et al., 2015; Vissers et al., 2016; Stessman et al., 2017), yet relatively little is known about the function of FOXP1 in the brain. We previously demonstrated that an ASD- and ID-patient-relevant haploinsufficient *Foxp1* mouse model exhibits vocalization deficits with alterations in striatal function and gene expression (Araujo et al., 2015). In addition, a mouse model with complete loss of *Foxp1* in the brain demonstrates a number of behavioral deficits and functional alterations in several brain regions (Bacon et al., 2014). Thus, these previously published data do not address the requirement for Foxp1 in specific brain regions and how such a requirement might be important for specific ASD- and ID-relevant phenotypes.

To investigate the functional role of Foxp1 in a brain-region-specific manner, we generated *Foxp1*$^{cKO}$ mice with complete loss of Foxp1 in the hippocampus and neocortex (Fig. 3.1A,B). We observe a number of striking behavioral deficits in these mice, most notably altered social interactions (Fig. 3.3I) and an almost total absence of spatial learning (Fig. 3.4A-F). Because the neural circuits for social behaviors are not fully understood, and because the hippocampus has been studied in depth for its relationship to learning and memory, we chose to focus on the potential role of Foxp1 in hippocampal-based functions in *Foxp1*$^{cKO}$ mice. Importantly, the majority of documented patients with ASD-causing mutations in *FOXP1* also have a diagnosis of ID (Le Fevre et al., 2013; Lozano et al., 2015; Vissers et al., 2016), making a mechanistic study of Foxp1 function in the hippocampus disease-relevant.

*Foxp1*$^{cKO}$ mice possess deficits in spatial learning, as they perform poorly in both the alternating T-maze and the Morris water maze (Fig. 3.4A-F). Conversely, *Foxp1*$^{cKO}$ mice have intact learning in contextual fear conditioning (Fig. 3.5A,B). Such results are seemingly in conflict with one another. However, when performed prior to testing, lesions of the hippocampus impair learning in the Morris water maze but preserve contextual fear conditioning in mice (Cho et al., 1999). Indeed, other mouse models of neuropsychiatric disorders have also shown that these two processes can be dissociated (Kubota et al., 2001; Huynh et al., 2009). Another explanation could be that hippocampal function in *Foxp1*$^{cKO}$ mice is sufficient to allow for the association of discrete, easily recognizable elements of the contextual-conditioning environment and the unconditioned stimulus (Maren, 2001). Finally, these conflicting results could be explained by the simple idea that *Foxp1*$^{cKO}$ mice might not be able to meet the cognitive load necessary for complex spatial tasks but that they are able to meet the cognitive load required for fear-based tasks, which involve more salient conditioning. The amygdala is critically involved in cue-based fear learning (Puzzo et al., 2014; Tovote et al., 2015) and there is limited expression of Foxp1 in the amygdala (Ferland et al., 2003). However, the intact cue-dependent fear conditioning in *Foxp1*$^{cKO}$ mice (Fig. 3.5A,B) suggests that the role the hippocampal-amygdala circuit plays in this task is spared with loss of Foxp1.

The intact set-shifting learning we observed in *Foxp1*$^{cKO}$ mice (Fig. 3.5C,D) suggests that while Foxp1 expression is almost completely absent in the neocortex of these animals, this expression loss does not affect other, broader types of learning.

Additionally, the spared shifting learning in *Foxp1*$^{cKO}$ mice (Fig. 3.5C,D) could represent compensation by subcortical circuits in which *Foxp1* expression is preserved. Regardless, these results need to be interpreted carefully, as we cannot fully rule out other learning defects due to neocortical loss of *Foxp1* that were not tested in this study. Together, our results suggest that *Foxp1*$^{cKO}$ mice exhibit a specific deficit in complex, hippocampal-based spatial tasks.

Mice with full-brain loss of *Foxp1* also display hyperactivity, impaired spatial learning, and impaired social behaviors (Bacon et al., 2014). Conversely, unlike the results presented here (Fig. 3.8A,B), hippocampal neuron excitability is reduced and hippocampal LTP is unaltered in full-brain *Foxp1* knockout mice (Bacon et al., 2014). However, the study on full-brain *Foxp1* knockout mice employed a weaker protocol for LTP induction (Bacon et al., 2014) and thus it is possible that such a protocol may not have recruited the same plasticity-maintenance mechanisms recruited in our study.

The *Foxp1*$^{cKO}$ hippocampus dataset possessed fewer DEGs than the *Foxp1*$^{+/-}$ hippocampus RNA-seq dataset (Fig. 3.6C). This result was surprising to us because we expected complete loss of *Foxp1* to yield greater disruptions to the hippocampus transcriptome than *Foxp1* haploinsufficiency. The larger number of hippocampal DEGs observed in *Foxp1*$^{+/-}$ mice could be explained by improper signaling to the hippocampus from subcortical regions that also experience reduced *Foxp1* levels. Using available single cell RNA-seq data (Zeisel et al., 2015), we find that *Foxp1*$^{cKO}$ hippocampal DEGs are most significantly enriched for genes expressed in CA1 and *Foxp1*$^{cKO}$ neocortical DEGs are most significantly enriched for genes expressed in pyramidal neurons of

somatosensory cortex (S1) (Extended Data Table 3.6-2). Therefore, our data suggest that loss of *Foxp1* leads to disruptions in the expression of genes important for cellular identity in both brain regions. The DEGs that result from loss of *Foxp1* in the hippocampus also indicate changes in pathways known to be important in hippocampal LTP, synaptic signaling, and spatial memory (Fig. 3.6A). We observed no differences in the basal synaptic transmission in the *Foxp1*$^{cKO}$ mouse hippocampus (Fig. 3.8C), suggesting that the diminished LTP-responses we recorded in the *Foxp1*$^{cKO}$ CA1 region (Fig. 3.8A,B) are due to dysregulation of downstream signaling networks and not alterations to the character of the synaptic input itself (Kotaleski and Blackwell, 2010). This is supported by the finding that our *Foxp1*$^{cKO}$ hippocampal RNA-seq dataset significantly overlapped with a hippocampal-maintenance gene list (Fig. 3.8D) (Ryan et al., 2012).

Future studies that directly test the involvement of genes regulated by Foxp1 in LTP-maintenance would be compelling, especially since synaptic signaling has a widely appreciated role in explaining the etiology of ASD and ID (Santini and Klann, 2014). However, it is unclear whether restoration of any one downstream gene (or combination of genes) would be sufficient to rescue both the physiological and behavioral deficits seen in *Foxp1*$^{cKO}$ mice. Conversely, the generation of additional brain-region-specific *Foxp1* knockout mice will address whether the expression of Foxp1 in the hippocampus is required for the observed behavioral deficits. Moreover, Foxp1 expression in the striatum is intact in the *Foxp1*$^{cKO}$ mice detailed here (Fig. 3.1A,B), yet there are robust striatal deficits in heterozygous *Foxp1* knockout mice (Araujo et al., 2015) and brain-

wide *Foxp1* knockout mice (Bacon et al., 2014). Thus, a *Foxp1* knockout mouse that primarily targets the striatum will be important for understanding the contributions of Foxp1 to the complex behavioral phenotypes associated with ASD and ID.

In summary, this study is an important step towards completing our understanding of the region-specific roles of FoxP1 within the brain. Since *FOXP1* is among the most salient ASD- and ID-genes, any knowledge of FOXP1 function should contribute to our understanding of ASD and ID pathophysiology. In-depth knowledge of the basic mechanisms of brain development and function, as it pertains to certain neurodevelopmental disease-relevant genes such as *FOXP1*, will be critical to designing effective therapeutics for the resultant conditions.

## FIGURES FOR CHAPTER THREE

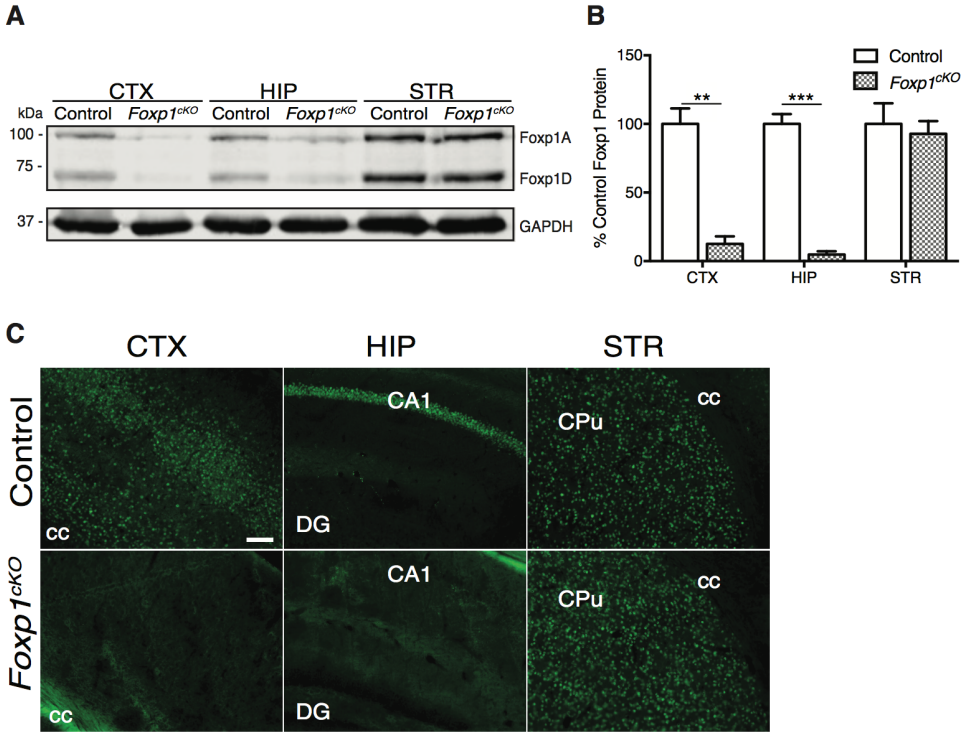


**Figure 3.1. Generation of *Foxp1$^{cKO}$* mice.** (A) Representative immunoblot displaying reduced Foxp1 protein levels in the neocortex (CTX) and hippocampus (HIP), but not the striatum (STR), of *Foxp1$^{cKO}$* mice, compared to littermate control mice. GAPDH is a loading control. (B) Quantification of Foxp1 expression in adult *Foxp1$^{cKO}$* mouse brains. Data are represented as means (± SEM). n=3 control mice, 3 *Foxp1$^{cKO}$* mice. **p=0.002; ***p=0.0002, Student's t-test, compared to control levels normalized to GAPDH. (C) Representative immunohistochemistry images showing that Foxp1 protein (white) expression is ablated in the projection neurons of the CTX, the CA1/CA2 subfields of the HIP, but preserved in the STR, of *Foxp1$^{cKO}$* mice. cc = corpus callosum, DG = dentate gyrus, CPu = caudate/putamen. Scale bars represent 100 um.

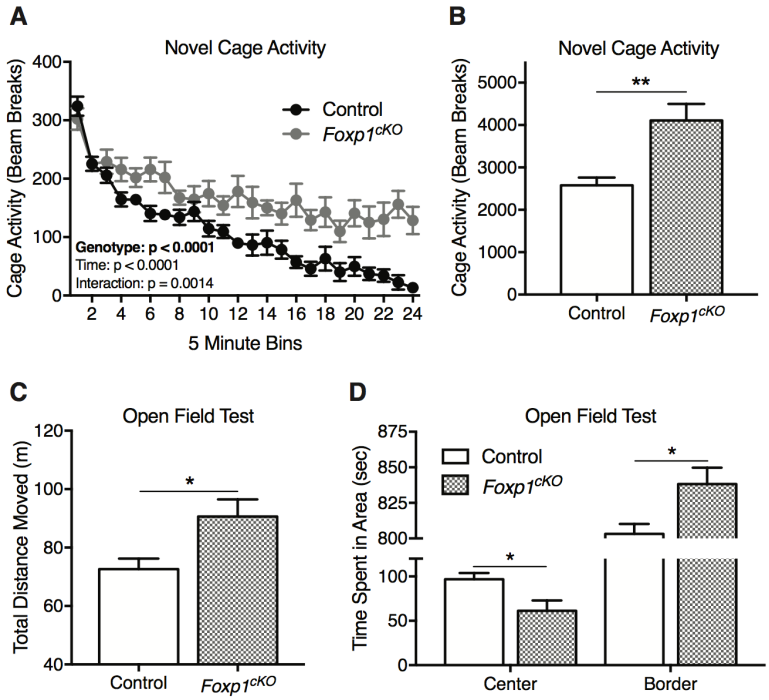


**Figure 3.2. *Foxp1*$^{cKO}$ mice display hyperactivity and anxiety-like behaviors.** (A,B) *Foxp1*$^{cKO}$ mice are hyperactive, as indicated by their increased activity in a novel cage environment. (A) *Foxp1*$^{cKO}$ mice display sustained, increased activity in a novel cage. Data are represented as means (± SEM). n=9 control mice, 7 *Foxp1*$^{cKO}$ mice. p<0.0001, two-way ANOVA, compared between genotypes. (B) As measured by their average activity over the course of two hours, *Foxp1*$^{cKO}$ mice are hyperactive. Data are represented as means (± SEM). n=9 control mice, 7 *Foxp1*$^{cKO}$ mice. **p=0.002, Student's t-test, compared between genotypes. (C) *Foxp1*$^{cKO}$ mice are hyperactive, as determined by their total distance moved in the open field test. Data are represented as means (± SEM). n=8 control animals, 8 *Foxp1*$^{cKO}$ animals. *p=0.02, Student's t-test, compared between genotypes. (D) *Foxp1*$^{cKO}$ mice are anxious, as determined by the

amount of time they spend in the center of the open field apparatus. Data are represented as means (± SEM). n=8 control animals, 8 *Foxp1*$^{cKO}$ animals. *p=0.02, Student's t-test, compared between genotypes.

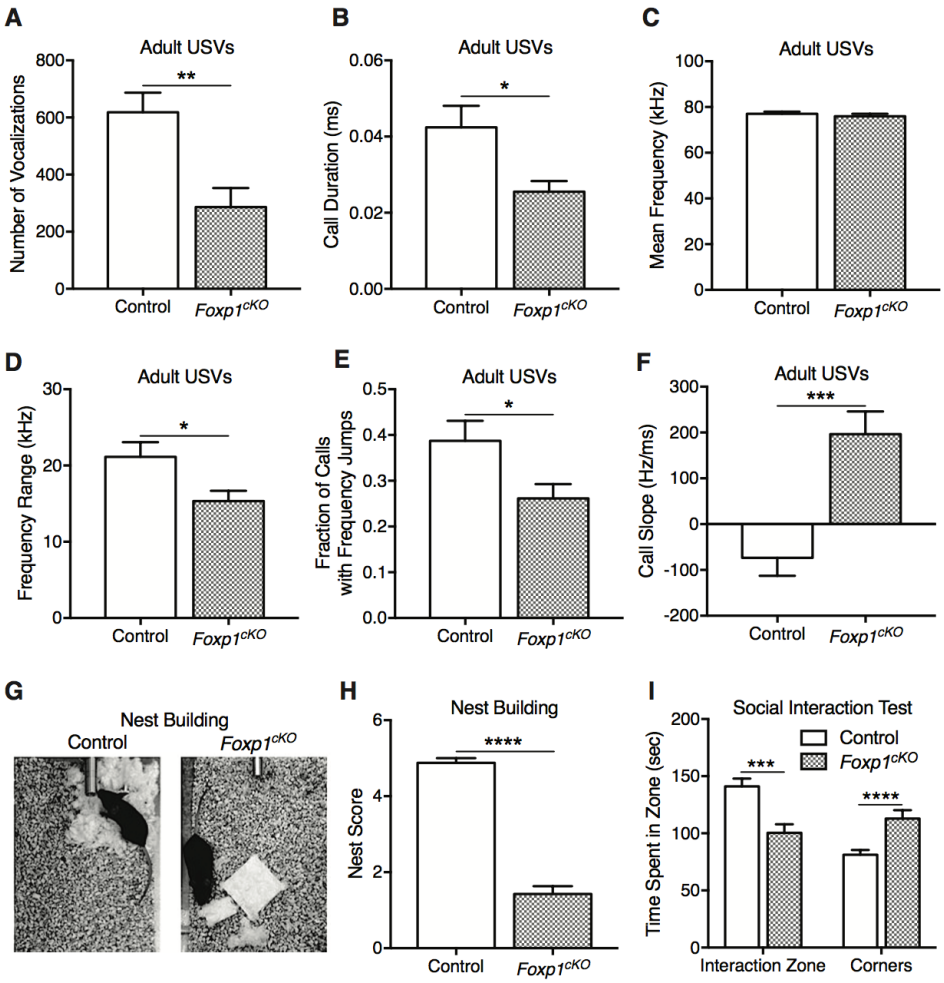


**Figure 3.3. Impaired social communication in *Foxp1$^{cKO}$* mice.** (A) Adult *Foxp1$^{cKO}$* male mice produce fewer total numbers of USV songs in a mating paradigm. Data are represented as means (± SEM). n=13 control mice and 15 *Foxp1$^{cKO}$* mice. **p=0.0019, Student's t-test, compared between genotypes. (B) *Foxp1$^{cKO}$* mice exhibit a significant reduction in their mean call duration. Data are represented as means (± SEM). n=13 controls mice, 14 *Foxp1$^{cKO}$* mice. *p=0.011, Student's t-test, compared between genotypes. (C) *Foxp1$^{cKO}$* mice show no differences in their mean call frequencies. Data are represented as means (± SEM). n=13 controls mice, 14

*Foxp1*$^{cKO}$ mice. p=0.45, Student's t-test, compared between genotypes. (D) Adult *Foxp1*$^{cKO}$ male mice produce USV with smaller frequency ranges. Data are represented as means (± SEM). n=13 control mice and 14 *Foxp1*$^{cKO}$ mice. *p=0.019, Student's t-test, compared between genotypes. (E) *Foxp1*$^{cKO}$ mice produce a smaller fraction of USVs with frequency jumps. Data are represented as means (± SEM). n=13 controls mice, 15 *Foxp1*$^{cKO}$ mice. *p=0.025, Student's t-test, compared between genotypes. (F) *Foxp1*$^{cKO}$ mice show a significant difference in the average slope of their songs. Data are represented as means (± SEM). n=13 controls mice, 14 *Foxp1*$^{cKO}$ mice. ***p=0.0003, Student's t-test, compared between genotypes. (G) Representative photographs of the nests produced by littermate control and *Foxp1*$^{cKO}$ mice. (H) *Foxp1*$^{cKO}$ produce poor quality nests. Data are represented as means (± SEM). n=8 control mice, 7 *Foxp1*$^{cKO}$ animals. ****p<0.0001, Student's t-test, compared between genotypes. (I) *Foxp1*$^{cKO}$ mice are less social than their littermate controls, as determined by the decreased time they spend interacting with a sex-matched conspecific (time in interaction zone). Data are represented as means (± SEM). n=16 control mice, 12 *Foxp1*$^{cKO}$ mice. **p<0.01, ***p<0.001, Student's t-test, compared between genotypes.

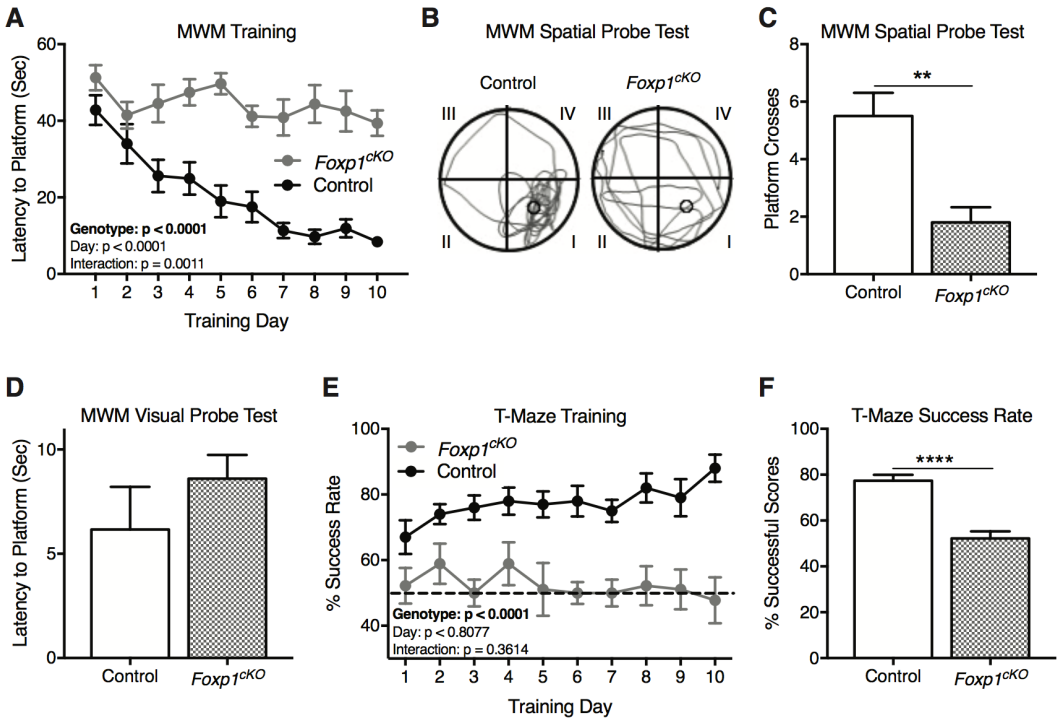


**Figure 3.4. *Foxp1*$^{cKO}$ mice display impairments in spatial learning.** (A) *Foxp1*$^{cKO}$ mice display poor learning via their escape latency in the training phase of the Morris water maze (MWM). Data are represented as means (± SEM). n=12 control animals, 10 *Foxp1*$^{cKO}$ animals. p<0.0001, two-way ANOVA, compared between genotypes. (B,C) *Foxp1*$^{cKO}$ show poor memory via the number of platform crosses they make during the MWM spatial probe. (B) Representative trace of swimming paths taken by *Foxp1*$^{cKO}$ and control littermate mice on a spatial probe day. Roman numerals designate different quadrants. The original location of the hidden platform is indicated by a circle in quadrant I. (C) Quantification of the number of platform crosses made by *Foxp1*$^{cKO}$ and control mice on a spatial probe day. Data are represented as means (± SEM). n=12 control animals, 10 *Foxp1*$^{cKO}$ animals. **p=0.002, Student's t-test, compared between genotypes. (D) *Foxp1*$^{cKO}$ mice display no difference in their ability to locate a raised

platform during a visual probe day in the MWM. Data are represented as means (± SEM). n=12 control animals, 10 *Foxp1*$^{cKO}$ animals. p=0.34, Student's t-test, compared between genotypes. (E) *Foxp1*$^{cKO}$ mice demonstrate poor learning and memory, as measured by their percentage of successful trials during training in the T-maze. Dashed line represents success based on chance. Data are represented as means (± SEM). n=10 control animals, 9 *Foxp1*$^{cKO}$ animals. p<0.0001, two-way ANOVA, compared between genotypes. (F) As measured by their average performance during training, *Foxp1*$^{cKO}$ mice display impaired learning in the T-maze. Data are represented as means (± SEM). n=10 control mice, 10 *Foxp1*$^{cKO}$ mice. ****p<0.0001, Student's t-test, compared between genotypes. The main effects for genotype and postnatal day, and their interactions, are presented within panels A and E.

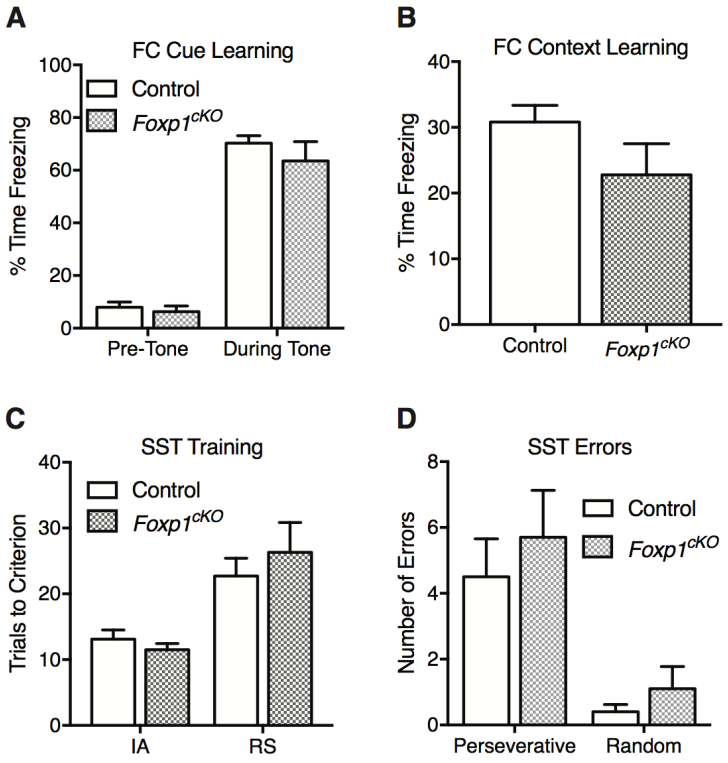


**Figure 3.5. *Foxp1*$^{cKO}$ mice do not display generalized learning and memory deficits.** (A,B) *Foxp1*$^{cKO}$ mice show no deficiencies in associative fear-memory tasks, as displayed by their performance in both the (A) cue and (B) context-dependent portions of a fear conditioning (FC) paradigm. Data are represented as means (± SEM). n=16 control mice, 12 *Foxp1*$^{cKO}$ mice. p=0.27, two-way ANOVA compared between genotypes (A), p=0.12, Student's t-test compared between genotypes (B). (C,D) *Foxp1*$^{cKO}$ show no deficits in cognitive flexibility, as measured by (C) the number of trials they need to reach criterion during both the initial association (IA) or the rule-shift (RS) portion of training for the set-shifting task (SST) or (D) the number of perseverative (Pers) or random (Rand) errors they make in the RS portion of the SST. Data are

represented as means (± SEM). n=10 control, 9 *Foxp1*$^{cKO}$ mice. p=0.65 (C), and p=0.43 (D), two-way ANOVA, compared between genotypes.

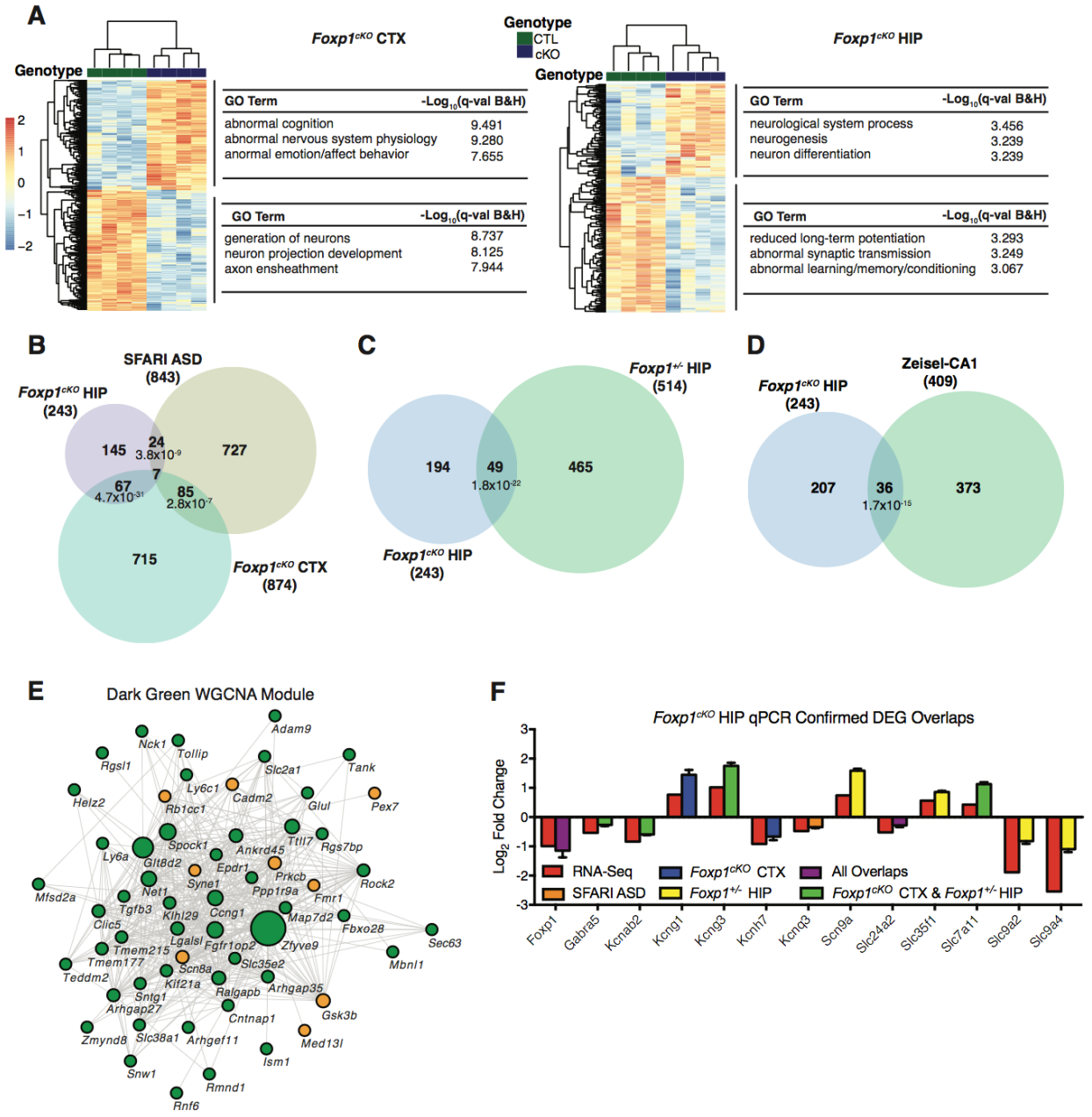


**Figure 3.6. Altered transcriptional programs in *Foxp1*$^{cKO}$ brains.** (A) Heatmap showing that based on the differentially expressed genes (DEGs) of either region, the neocortex (CTX) and hippocampus (HIP) segregate by genotype (*Foxp1*$^{cKO}$ (cKO) and control (CTL)). Significantly enriched gene ontology (GO) terms

(https://toppgene.cchmc.org; GO enrichment is the negative log of a Benjamini and Hochberg corrected p-value, q-value) associated with groups of genes are highlighted next to their respective DEG clusters. (B) Significant overlaps between DEGs in *Foxp1*$^{cKO}$ mouse CTX and HIP, and ASD-associated genes (SFARI ASD genes; https://sfari.org/resources/sfari-gene). 92 genes overlapped between *Foxp1*$^{cKO}$ CTX and SFARI ASD genes ($p=2.8x10^{-7}$; hypergeometric test), and 31 genes overlapped between *Foxp1*$^{cKO}$ HIP and SFARI ASD genes ($p=3.8x10^{-9}$; hypergeometric test). (C) Significant overlaps between *Foxp1*$^{cKO}$ HIP DEGs and heterozygous *Foxp1* knockout (*Foxp1*$^{+/-}$) HIP DEGs (Araujo et al., 2015). The *Foxp1*$^{+/-}$ HIP dataset was filtered using the same cutoffs for identifying DEGs (an adjusted p-value of $\leq 0.005$ and an absolute log fold change of $\geq 0.3$) that were applied to the *Foxp1*$^{cKO}$ datasets. 49 genes overlapped between *Foxp1*$^{+/-}$ HIP and *Foxp1*$^{cKO}$ HIP ($p=1.8x10^{-22}$; hypergeometric test). (D) Significant overlaps between *Foxp1*$^{cKO}$ HIP DEGs and CA1 pyramidal neuron single-cell sequencing data (Zeisel et al., 2015). 36 genes overlapped between *Foxp1*$^{cKO}$ HIP and Zeisel CA1 data ($p=1.7x10^{-15}$; hypergeometric test). (E) Visualization of the top 500 connections in the hippocampus-specific Dark Green module. ASD SFARI genes are highlighted in orange. (F) Confirmation of salient gene targets in independent *Foxp1*$^{cKO}$ hippocampal samples using qPCR. Data are represented as means (± SEM). n=3 control mice, 3 *Foxp1*$^{cKO}$ mice. With the exception of *Ccnd1*, *Dusp5*, and *Sorcs3*, all qPCR values are significant at $p<0.05$ (Student's t-test, compared to control levels, normalized to beta-actin).

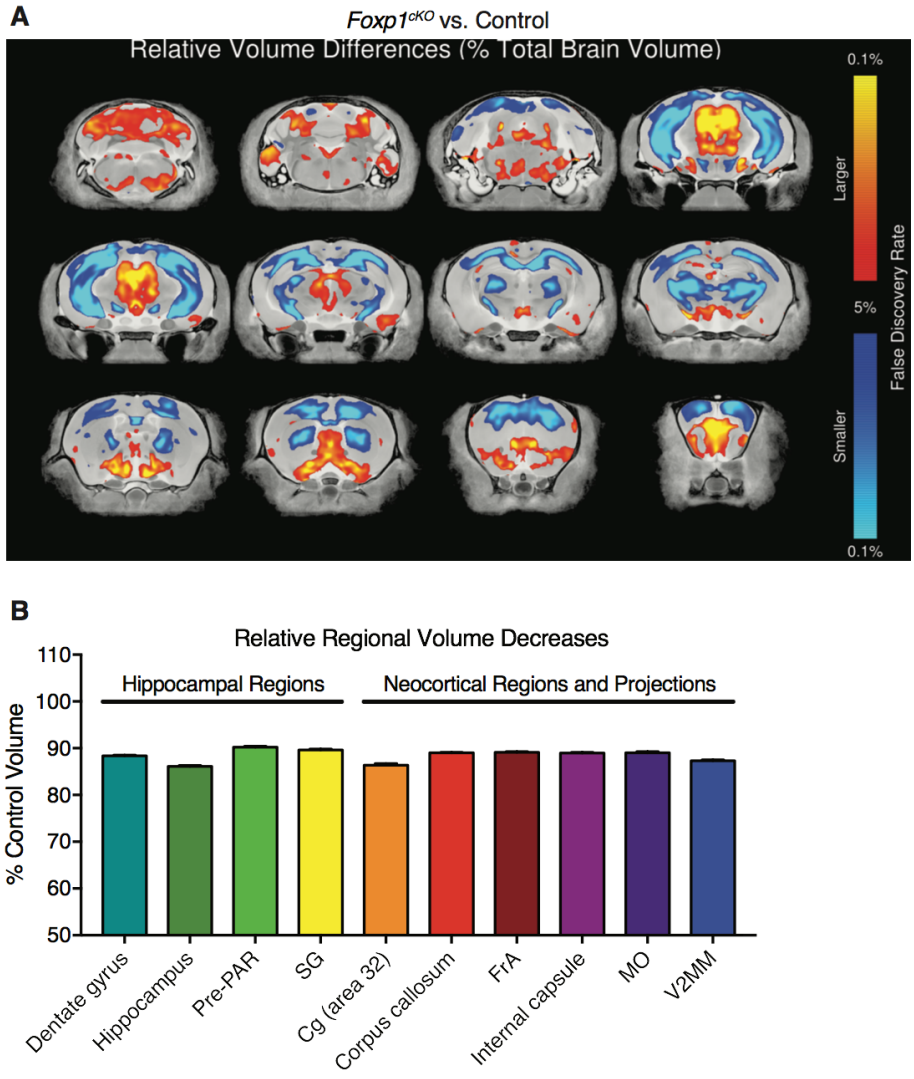


**Figure 3.7. Altered regional brain volumes in *Foxp1*$^{cKO}$ mice.** (A) Fly-through of representative coronal slices of the *Foxp1*$^{cKO}$ brain highlighting average, relative differences in regions with larger (red) or smaller (blue) volumes. (B) Representation of the average, relative volume decreases in several of the most significantly affected (in terms of percent decreases from control (100%) levels) hippocampal and neocortical areas in the *Foxp1*$^{cKO}$ mouse brain. Dashed line represents control levels. Data are represented as means (± SEM). All values are significant at $p<0.05$, Student's t-test,

and FDR<0.05. Cg = cingulate cortex, FrA = frontal association cortex, MO = medial orbital cortex, Pre-PAR = pre-para subiculum, and V2MM = secondary visual cortex-mediomedial area.

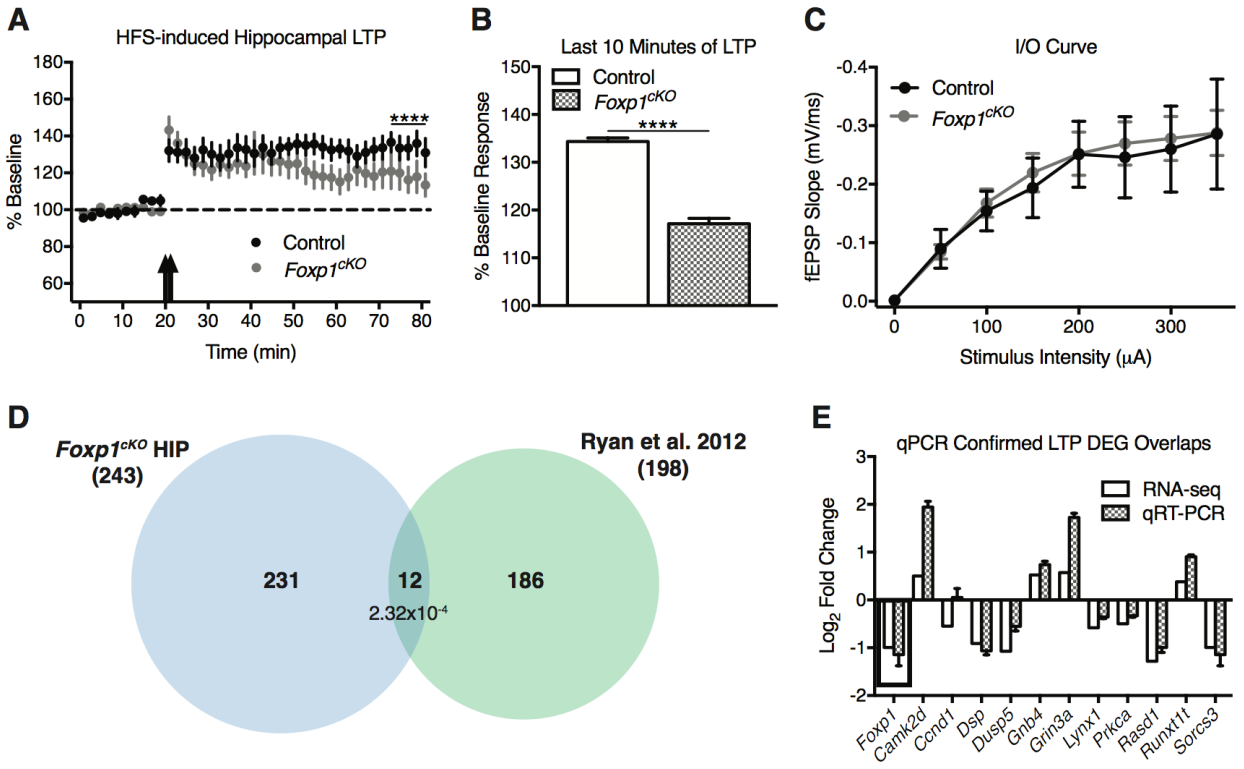


**Figure 3.8. Altered hippocampal synaptic plasticity in *Foxp1*$^{cKO}$ mice.** (A,B) In response to high-frequency stimulation (HFS), there is no difference in the initial magnitude of LTP in *Foxp1*$^{cKO}$ CA1 neurons (A), but there is a difference in the LTP response during the last 10 minutes of stimulation (B). Data are represented as means (± SEM). n = 15 control recordings, 20 *Foxp1*$^{cKO}$ recordings, Student's t-test, compared between genotypes. (C) Basal synaptic transmission is unchanged between *Foxp1*$^{cKO}$ and littermate control mice as measured by input/output curves comparing stimulus intensity to fEPSP slope in CA1 pyramidal neurons. Data are represented as means (± SEM). n=15 control recordings, 19 *Foxp1*$^{cKO}$ recordings. p=0.63, two-way ANOVA, compared between genotypes. (D) Significant overlaps between *Foxp1*$^{cKO}$ HIP DEGs and LTP-maintenance DEGs (Ryan et al., 2012). 12 genes overlapped between

*Foxp1*$^{cKO}$ HIP and LTP-maintenance dataset ($p=2.32x10^{-4}$; hypergeometric test). (E) Confirmation of genes that overlap between the *Foxp1*$^{cKO}$ hippocampal dataset and LTP-maintenance genes in independent *Foxp1*$^{cKO}$ hippocampal samples, using qPCR. Red bars indicate RNA-seq-based $log_2$-fold changes in expression. Colored bars represent the category of gene (SFARI ASD, and/or *Foxp1*$^{cKO}$ neocortex, and/or *Foxp1*$^{+/-}$ hippocampus) that these *Foxp1*$^{cKO}$ hippocampal DEGs overlap with. Data are represented as means (± SEM). n=3 control mice, 3 *Foxp1*$^{cKO}$ mice. All qPCR values are significant at $p<0.05$ (Student's t-test, compared to control levels, normalized to beta-actin).

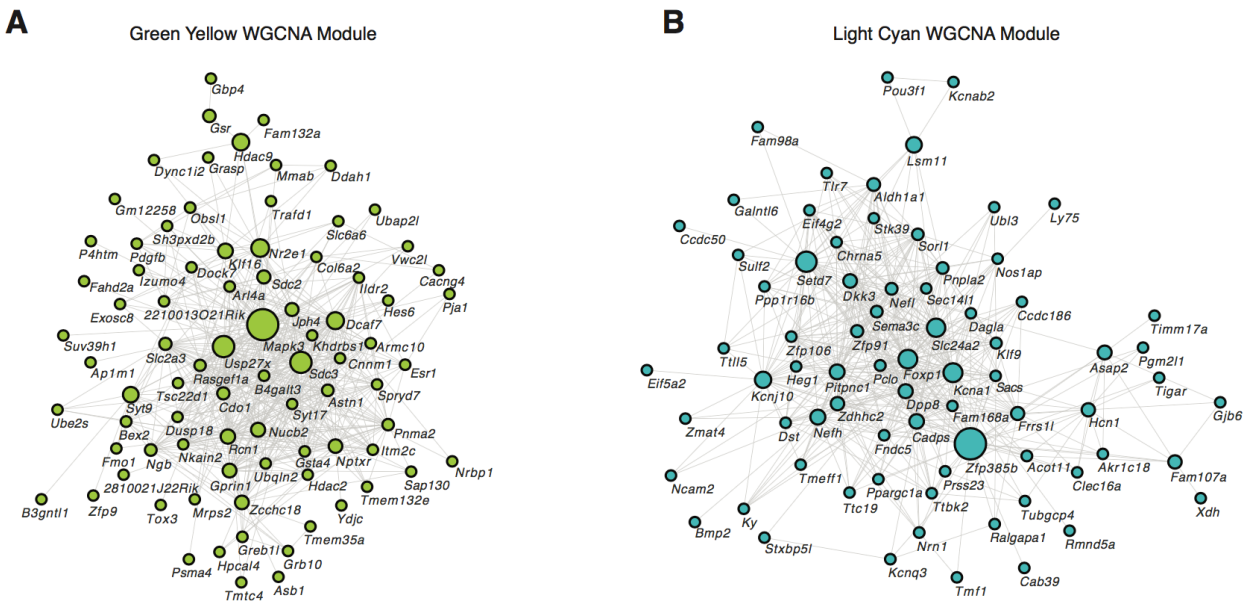


**Extended Data Figure 3.6-1. *Foxp1*$^{cKO}$ genotype-specific WGCNA modules.** (A) Visualization of the top 500 connections in the Green Yellow module. (B) Visualization of the top 500 connections in the Light Cyan module.

# TABLES FOR CHAPTER THREE

**Table 3.1. DEGs in the *Foxp1*$^{cKO}$ neocortex and hippocampus.**

| Hippocampus DEGs | | | Neocortex DEGs | | |
|---|---|---|---|---|---|
| **Gene ID** | **Log2 Fold Change** | **P-Value (adj.)** | **Gene ID** | **Log2 Fold Change** | **P-Value (adj.)** |
| *1700024P16Rik* | -3.06E+00 | 5.57E-26 | *1110032F04Rik* | -5.35E-01 | 2.91E-04 |
| *2810459M11Rik* | 7.05E-01 | 2.26E-03 | *1190002N15Rik* | -3.54E-01 | 3.07E-04 |
| *3110035E14Rik* | -4.76E-01 | 2.18E-05 | *1700019D03Rik* | -5.35E-01 | 1.17E-03 |
| *Adamtsl1* | 1.29E+00 | 4.51E-11 | *2700081O15Rik* | 4.33E-01 | 3.14E-03 |
| *Adcy1* | -4.38E-01 | 1.64E-03 | *2810459M11Rik* | 6.30E-01 | 1.80E-03 |
| *Adra2a* | 1.32E+00 | 1.66E-12 | *3110035E14Rik* | -4.90E-01 | 1.21E-11 |
| *Adrbk2* | 4.47E-01 | 2.06E-03 | *4932411E22Rik* | 1.10E+00 | 9.83E-04 |
| *Akap13* | -5.53E-01 | 1.01E-05 | *A730017C20Rik* | 4.30E-01 | 3.76E-03 |
| *Aldh1a1* | -8.95E-01 | 1.03E-07 | *A830010M20Rik* | -3.02E-01 | 1.69E-04 |
| *Ankrd33b* | -4.80E-01 | 1.14E-03 | *Abca2* | -3.35E-01 | 1.83E-03 |
| *Ankrd6* | 5.24E-01 | 4.62E-04 | *Abcb1a* | -3.97E-01 | 2.27E-03 |
| *Ar* | -6.09E-01 | 1.91E-06 | *Abcd2* | -8.83E-01 | 8.85E-25 |
| *Arhgap12* | -7.18E-01 | 1.44E-08 | *Abracl* | -1.02E+00 | 5.05E-08 |
| *Arhgap26* | -4.68E-01 | 2.18E-04 | *Ackr1* | 5.05E-01 | 2.99E-03 |
| *Arhgef6* | 5.92E-01 | 1.07E-04 | *Acot11* | -6.23E-01 | 1.09E-05 |
| *Arpc2* | -4.07E-01 | 3.73E-03 | *Acsl5* | -5.98E-01 | 9.04E-10 |
| *Arpp21* | 4.24E-01 | 2.03E-04 | *Acsl6* | -3.60E-01 | 2.83E-06 |
| *Asap2* | -4.90E-01 | 4.24E-03 | *Actn1* | 4.34E-01 | 8.75E-06 |
| *Atp2b1* | -5.06E-01 | 7.25E-05 | *Acvr2a* | 4.67E-01 | 5.35E-08 |
| *Atp2b4* | 5.90E-01 | 2.32E-04 | *Adam23* | -5.35E-01 | 6.95E-13 |
| *Bace2* | 1.41E+00 | 2.86E-05 | *Adamts2* | 9.57E-01 | 3.35E-04 |
| *Bmp3* | 8.16E-01 | 2.70E-04 | *Adcy2* | -3.38E-01 | 1.95E-04 |
| *Bmpr1b* | 4.55E-01 | 1.41E-03 | *Adcy8* | 5.71E-01 | 3.70E-04 |
| *Brinp1* | -4.53E-01 | 9.27E-04 | *Adcyap1* | 5.31E-01 | 2.03E-04 |
| *Btbd3* | -4.34E-01 | 2.49E-03 | *Adcyap1r1* | 4.19E-01 | 1.20E-05 |
| *Btg2* | 8.82E-01 | 9.00E-04 | *Adgrf5* | -3.58E-01 | 2.12E-03 |
| *C4b* | 9.02E-01 | 2.09E-05 | *Adgrg2* | 2.07E+00 | 2.80E-07 |
| *Cabp7* | -9.67E-01 | 5.65E-11 | *Adgrg6* | -1.00E+00 | 1.65E-04 |
| *Cacna1e* | -3.97E-01 | 2.40E-03 | *Adi1* | -5.03E-01 | 1.22E-03 |
| *Cadm2* | -4.26E-01 | 2.80E-03 | *Adipor2* | -5.09E-01 | 4.33E-06 |
| *Cadps* | -3.84E-01 | 4.84E-03 | *Adora1* | -5.81E-01 | 4.63E-14 |
| *Calb1* | 4.25E-01 | 2.93E-03 | *Adra1b* | -1.02E+00 | 1.22E-06 |
| *Calb2* | 2.51E+00 | 1.99E-62 | *Adra2a* | 7.61E-01 | 6.28E-05 |
| *Camk1d* | -4.96E-01 | 1.14E-04 | *Adssl1* | -9.30E-01 | 1.23E-04 |
| *Camk2b* | -4.04E-01 | 2.17E-03 | *Afap1l1* | -6.06E-01 | 4.22E-04 |
| *Camk2d* | 5.03E-01 | 3.74E-03 | *Agfg2* | 4.75E-01 | 6.99E-04 |
| *Car10* | 5.48E-01 | 2.28E-03 | *Ahnak* | -4.05E-01 | 1.75E-05 |
| *Car12* | 6.78E-01 | 5.03E-08 | *AI593442* | -4.11E-01 | 1.73E-08 |
| *Ccbe1* | -5.98E-01 | 9.42E-04 | *Aifm3* | -5.36E-01 | 1.41E-04 |
| *Ccnd1* | -5.49E-01 | 6.53E-05 | *Ajap1* | 5.65E-01 | 8.18E-07 |
| *Cd24a* | 1.02E+00 | 1.55E-11 | *Ak5* | 4.21E-01 | 1.45E-06 |
| *Cd36* | 2.62E+00 | 3.80E-24 | *Akap12* | -5.92E-01 | 3.78E-06 |
| *Cd44* | 1.37E+00 | 9.74E-11 | *Aldh1a1* | -1.16E+00 | 3.88E-21 |
| *Cdh12* | -8.70E-01 | 6.90E-08 | *Alox12b* | 2.00E+00 | 7.29E-10 |
| *Cdh8* | -4.42E-01 | 2.75E-03 | *Angpt1* | 6.83E-01 | 1.90E-04 |
| *Cdhr1* | 8.09E-01 | 1.64E-03 | *Ank1* | -7.97E-01 | 1.86E-12 |
| *Cds1* | -4.51E-01 | 3.62E-03 | *Ankrd29* | -4.25E-01 | 2.11E-04 |
| *Chgb* | -5.43E-01 | 2.65E-06 | *Ankrd34c* | -5.52E-01 | 3.08E-06 |
| *Chrm3* | -1.04E+00 | 4.80E-12 | *Ankrd40* | -3.33E-01 | 3.64E-04 |
| *Chst2* | -4.34E-01 | 2.35E-03 | *Ankrd45* | -3.16E-01 | 2.77E-03 |

| | | | | | |
|---|---|---|---|---|---|
| *Clvs2* | -6.59E-01 | 5.24E-06 | *Ankrd6* | 5.89E-01 | 3.85E-07 |
| *Cntnap2* | -4.24E-01 | 1.40E-03 | *Ankrd63* | 1.14E+00 | 1.69E-15 |
| *Cntnap5c* | -6.72E-01 | 1.85E-03 | *Ankub1* | -1.60E+00 | 1.89E-04 |
| *Coch* | 1.03E+00 | 2.24E-06 | *Anln* | -8.58E-01 | 1.55E-11 |
| *Col11a1* | -9.60E-01 | 4.99E-09 | *Ano4* | -6.49E-01 | 1.71E-05 |
| *Col12a1* | 7.74E-01 | 1.01E-03 | *Ap1s1* | 3.95E-01 | 4.58E-04 |
| *Col5a1* | 1.10E+00 | 2.19E-07 | *Ap3m2* | -3.30E-01 | 6.46E-04 |
| *Col5a2* | 7.66E-01 | 2.00E-03 | *Apaf1* | 5.83E-01 | 2.95E-03 |
| *Cpne4* | -5.19E-01 | 4.90E-05 | *Apln* | -7.47E-01 | 2.67E-07 |
| *Cpne7* | 4.46E-01 | 2.22E-03 | *Apod* | -4.99E-01 | 3.34E-06 |
| *Crim1* | -4.61E-01 | 2.53E-04 | *Arap2* | -4.73E-01 | 2.68E-09 |
| *Cryaa* | 5.94E+00 | 2.95E-06 | *Arc* | -5.11E-01 | 3.37E-06 |
| *Ctgf* | 7.85E-01 | 1.88E-03 | *Arhgap33* | 7.35E-01 | 1.35E-12 |
| *Dcn* | 6.63E-01 | 2.81E-05 | *Arhgap42* | -9.33E-01 | 9.25E-12 |
| *Dgkb* | -6.79E-01 | 6.34E-10 | *Arhgap6* | 1.34E+00 | 4.88E-20 |
| *Dgkh* | -6.88E-01 | 6.46E-05 | *Arhgef25* | -6.16E-01 | 2.86E-09 |
| *Dkk3* | -4.75E-01 | 4.89E-04 | *Arl15* | 3.31E-01 | 1.59E-03 |
| *Doc2a* | 1.31E+00 | 3.68E-07 | *Arl4a* | 5.36E-01 | 3.06E-09 |
| *Drd1* | 5.71E-01 | 4.36E-05 | *Arpp19* | -4.22E-01 | 4.20E-09 |
| *Drp2* | -6.59E-01 | 2.45E-07 | *Arpp21* | 5.09E-01 | 1.01E-13 |
| *Dsp* | -9.09E-01 | 7.63E-10 | *Arrdc2* | -9.97E-01 | 1.43E-03 |
| *Dusp5* | -1.07E+00 | 2.86E-05 | *Arsj* | 1.70E+00 | 6.69E-07 |
| *Dzip1* | -4.45E-01 | 9.18E-04 | *Asah2* | -5.28E-01 | 1.40E-04 |
| *Elovl4* | -4.59E-01 | 7.17E-04 | *Asap2* | -4.63E-01 | 1.06E-05 |
| *Endod1* | -4.92E-01 | 3.07E-03 | *Asb11* | -1.09E+00 | 2.46E-03 |
| *Enpp2* | 3.17E-01 | 3.74E-03 | *Aspa* | -9.98E-01 | 1.93E-08 |
| *Epha4* | -4.45E-01 | 1.40E-03 | *Astn1* | 3.77E-01 | 8.24E-07 |
| *Epha6* | -7.11E-01 | 6.62E-07 | *Astn2* | -9.86E-01 | 2.58E-13 |
| *Epha7* | -4.58E-01 | 2.15E-03 | *Atad2* | -4.66E-01 | 3.36E-03 |
| *Etv1* | 5.96E-01 | 3.03E-06 | *Atp10a* | -8.19E-01 | 2.59E-05 |
| *Fgf10* | -6.30E-01 | 3.74E-03 | *Atp1b3* | -3.05E-01 | 3.20E-03 |
| *Fibcd1* | -8.98E-01 | 2.19E-07 | *Atp2b2* | -4.37E-01 | 1.43E-10 |
| *Fibin* | 1.57E+00 | 5.58E-10 | *Atp2b4* | 9.66E-01 | 9.50E-46 |
| *Fmn1* | -5.85E-01 | 8.20E-04 | *Atp6ap1l* | 9.20E-01 | 1.36E-05 |
| *Fndc5* | -5.30E-01 | 2.14E-03 | *Auts2* | 3.88E-01 | 6.21E-06 |
| *Fos* | 9.77E-01 | 4.11E-03 | *AW551984* | 1.22E+00 | 7.21E-05 |
| *Foxp1* | -9.92E-01 | 2.29E-16 | *B230217C12Rik* | -4.22E-01 | 4.01E-05 |
| *Foxp2* | 6.22E-01 | 7.19E-05 | *B3galt5* | -8.17E-01 | 7.11E-10 |
| *Frrs1l* | -4.07E-01 | 1.80E-03 | *B3gat1* | 4.74E-01 | 4.78E-10 |
| *Gabra5* | -5.39E-01 | 1.02E-05 | *B3gat2* | 9.46E-01 | 8.31E-15 |
| *Glt8d2* | -1.01E+00 | 3.54E-05 | *B4galt3* | 4.73E-01 | 4.25E-03 |
| *Gm2115* | -9.81E-01 | 5.29E-16 | *Bace1* | 3.48E-01 | 3.92E-04 |
| *Gm765* | 3.26E+00 | 1.07E-06 | *Baz1a* | 1.15E+00 | 2.87E-06 |
| *Gnb4* | 5.23E-01 | 4.03E-03 | *BC030499* | 4.57E-01 | 5.74E-04 |
| *Gpr161* | -7.48E-01 | 3.35E-08 | *Bcas1* | -8.82E-01 | 3.89E-25 |
| *Gpr22* | -4.15E-01 | 4.10E-03 | *Bcat1* | -4.88E-01 | 2.75E-06 |
| *Gpr68* | -1.00E+00 | 2.03E-04 | *Bcr* | 3.12E-01 | 2.97E-03 |
| *Gpr88* | 3.90E-01 | 3.51E-06 | *Bdnf* | 5.09E-01 | 1.79E-06 |
| *Grem1* | -1.19E+00 | 2.09E-07 | *Bend6* | -4.60E-01 | 3.35E-09 |
| *Grin2a* | -4.48E-01 | 1.24E-03 | *Bex1* | 4.97E-01 | 1.27E-04 |
| *Grin3a* | 5.74E-01 | 6.11E-04 | *Bex4* | 6.47E-01 | 4.19E-03 |
| *Hectd2* | -5.64E-01 | 4.57E-05 | *Bhlhb9* | 3.17E-01 | 2.43E-03 |
| *Homer2* | -1.30E+00 | 1.36E-31 | *Bhlhe22* | 9.86E-01 | 6.35E-29 |
| *Hpca* | -6.86E-01 | 4.41E-09 | *Bhlhe40* | 4.02E-01 | 7.35E-06 |
| *Hpcal1* | 7.57E-01 | 3.02E-03 | *Blnk* | -9.61E-01 | 4.43E-05 |
| *Hrk* | 1.19E+00 | 4.73E-24 | *Bmp2* | -1.17E+00 | 3.47E-07 |

| | | | | | |
|---|---|---|---|---|---|
| *Hs3st4* | -4.90E-01 | 1.57E-03 | *Bmp3* | 4.58E-01 | 6.41E-06 |
| *Hspa1b* | 7.33E-01 | 3.09E-04 | *Bmper* | -8.42E-01 | 1.43E-03 |
| *Htr4* | -7.33E-01 | 7.58E-04 | *Btg2* | 1.27E+00 | 6.93E-14 |
| *Hunk* | -7.52E-01 | 7.01E-05 | *C1ql3* | 4.06E-01 | 5.82E-06 |
| *Il1r1* | -9.31E-01 | 2.84E-07 | *C2cd2l* | 5.45E-01 | 2.45E-08 |
| *Iqgap2* | -9.07E-01 | 7.57E-15 | *C2cd4c* | 8.18E-01 | 2.45E-03 |
| *Itgbl1* | 1.22E+00 | 1.36E-14 | *C77370* | 5.54E-01 | 1.56E-11 |
| *Itpr1* | -5.46E-01 | 4.32E-06 | *Cabp1* | -4.59E-01 | 6.25E-06 |
| *Kcnab2* | -8.37E-01 | 4.19E-13 | *Cacna1a* | -3.16E-01 | 2.53E-04 |
| *Kcnd2* | -5.73E-01 | 6.05E-06 | *Cacna1c* | 3.71E-01 | 5.88E-05 |
| *Kcng1* | 7.70E-01 | 1.16E-04 | *Cacna1i* | -7.49E-01 | 7.99E-12 |
| *Kcng3* | 1.02E+00 | 8.45E-07 | *Cacnb4* | -4.45E-01 | 2.18E-10 |
| *Kcnh7* | -9.18E-01 | 3.05E-17 | *Cacng2* | -3.27E-01 | 9.87E-05 |
| *Kcnq3* | -4.79E-01 | 2.80E-04 | *Cacng4* | 6.19E-01 | 3.31E-09 |
| *Kcnq5* | -5.82E-01 | 6.12E-07 | *Cadm1* | 3.33E-01 | 1.60E-05 |
| *Kirrel3* | 6.57E-01 | 2.28E-05 | *Cadm3* | 3.18E-01 | 9.20E-05 |
| *Klhl14* | 1.64E+00 | 6.47E-09 | *Cadps* | -4.42E-01 | 1.18E-08 |
| *Ksr1* | -6.25E-01 | 5.64E-05 | *Cadps2* | -5.73E-01 | 1.11E-11 |
| *Lct* | -1.16E+00 | 2.13E-09 | *Calb1* | 8.55E-01 | 2.36E-33 |
| *Lhx9* | -4.94E-01 | 9.56E-04 | *Caln1* | 5.31E-01 | 5.35E-13 |
| *Lifr* | -4.61E-01 | 1.64E-03 | *Camk2d* | 7.95E-01 | 1.55E-25 |
| *Lmo4* | 4.45E-01 | 1.39E-03 | *Camk2g* | -5.49E-01 | 3.66E-12 |
| *Lpl* | -1.37E+00 | 9.81E-31 | *Camk4* | -5.29E-01 | 2.10E-14 |
| *Lrp8* | 4.40E-01 | 7.55E-04 | *Camkv* | 4.28E-01 | 9.06E-07 |
| *Lrrc10b* | -7.90E-01 | 1.39E-03 | *Camta1* | -3.46E-01 | 3.43E-06 |
| *Lsm11* | -8.92E-01 | 4.69E-10 | *Capn2* | -3.37E-01 | 3.03E-03 |
| *Lynx1* | -5.83E-01 | 9.30E-06 | *Car8* | -5.73E-01 | 1.61E-04 |
| *Man1a* | -6.56E-01 | 8.00E-08 | *Casp3* | 5.68E-01 | 7.14E-04 |
| *Mapk10* | -4.04E-01 | 2.39E-03 | *Cbfa2t3* | 6.25E-01 | 2.56E-07 |
| *Matn2* | -6.77E-01 | 1.06E-05 | *Cbln2* | -7.72E-01 | 2.96E-11 |
| *Mc4r* | -1.36E+00 | 1.32E-04 | *Cbln4* | -8.11E-01 | 2.36E-09 |
| *Mef2c* | 4.70E-01 | 9.34E-04 | *Ccdc141* | -4.10E-01 | 3.26E-03 |
| *Meis2* | 3.40E-01 | 2.49E-03 | *Ccdc71l* | 4.25E-01 | 4.88E-03 |
| *Mfge8* | 6.23E-01 | 1.33E-03 | *Cckbr* | 5.45E-01 | 1.04E-06 |
| *Mmd* | -5.08E-01 | 1.47E-05 | *Ccnd1* | 3.86E-01 | 4.19E-04 |
| *Mndal* | 6.16E-01 | 1.17E-03 | *Ccnd2* | 4.09E-01 | 4.27E-07 |
| *Myo1b* | 4.84E-01 | 3.24E-03 | *Ccng1* | -4.15E-01 | 1.53E-07 |
| *Myo5b* | -4.22E-01 | 2.16E-03 | *Ccni* | -4.42E-01 | 2.46E-08 |
| *Ncald* | -5.32E-01 | 6.62E-07 | *Cd200* | 3.60E-01 | 1.13E-04 |
| *Ncdn* | -4.93E-01 | 6.67E-05 | *Cdc37l1* | -3.73E-01 | 3.16E-04 |
| *Ndst3* | -4.58E-01 | 1.61E-03 | *Cdh12* | -4.85E-01 | 5.17E-07 |
| *Ndst4* | -1.50E+00 | 1.48E-28 | *Cdh13* | 7.50E-01 | 1.80E-18 |
| *Necab1* | 9.73E-01 | 2.33E-20 | *Cdh19* | -8.03E-01 | 7.96E-09 |
| *Nectin1* | 4.94E-01 | 3.24E-03 | *Cdh20* | -6.67E-01 | 5.93E-05 |
| *Negr1* | 5.56E-01 | 1.44E-05 | *Cdh4* | 5.50E-01 | 1.73E-04 |
| *Neto1* | -5.55E-01 | 1.65E-06 | *Cdhr1* | 1.94E+00 | 1.82E-13 |
| *Neurod6* | -5.23E-01 | 1.44E-05 | *Cdk16* | -3.23E-01 | 2.35E-04 |
| *Nnat* | 4.52E-01 | 4.14E-03 | *Cdkn1c* | 6.57E-01 | 9.14E-04 |
| *Nov* | 6.05E-01 | 1.45E-05 | *Cdr2* | -1.10E+00 | 1.45E-06 |
| *Npr1* | 1.19E+00 | 2.67E-04 | *Celf3* | 4.00E-01 | 8.89E-04 |
| *Ntng1* | -8.01E-01 | 2.62E-08 | *Cep290* | -3.82E-01 | 2.32E-04 |
| *Olfml2b* | -6.61E-01 | 8.74E-04 | *Chga* | -5.92E-01 | 2.06E-07 |
| *Osbpl6* | -4.62E-01 | 7.88E-04 | *Chl1* | 5.57E-01 | 2.96E-15 |
| *Pcdh20* | -4.55E-01 | 2.96E-04 | *Chml* | -5.89E-01 | 2.43E-06 |
| *Pcp4* | 3.87E-01 | 4.07E-03 | *Chn2* | -7.16E-01 | 6.92E-12 |
| *Pcsk2* | -5.03E-01 | 2.09E-05 | *Chrm2* | -6.87E-01 | 1.41E-08 |

| | | | | | |
|---|---|---|---|---|---|
| *Pdyn* | 5.98E-01 | 9.80E-04 | *Ckb* | -3.71E-01 | 6.95E-05 |
| *Peak1* | -4.49E-01 | 1.16E-03 | *Cldn11* | -6.91E-01 | 5.50E-16 |
| *Penk* | 6.23E-01 | 5.58E-10 | *Clec18a* | 1.10E+00 | 4.18E-03 |
| *Pgr* | -4.68E-01 | 2.61E-03 | *Clic4* | -4.35E-01 | 1.58E-05 |
| *Phf20* | -4.34E-01 | 1.08E-03 | *Clstn2* | -4.98E-01 | 8.93E-09 |
| *Pirt* | -2.33E+00 | 4.66E-05 | *Cmpk2* | -5.78E-01 | 1.51E-04 |
| *Pkd2l1* | 3.57E+00 | 3.40E-24 | *Cnih3* | -5.02E-01 | 2.75E-04 |
| *Pla2g16* | 5.45E-01 | 2.24E-05 | *Cnnm1* | 4.03E-01 | 2.86E-06 |
| *Plagl1* | -6.40E-01 | 1.37E-08 | *Cnp* | -5.87E-01 | 1.04E-11 |
| *Plin4* | -1.13E+00 | 3.78E-03 | *Cntn2* | -3.95E-01 | 2.31E-04 |
| *Plk2* | -5.93E-01 | 1.16E-06 | *Cntn6* | 7.71E-01 | 1.04E-11 |
| *Plpp6* | -4.84E-01 | 9.50E-04 | *Cntnap1* | -4.17E-01 | 8.30E-06 |
| *Plxna1* | -5.30E-01 | 6.96E-05 | *Cntnap3* | 8.72E-01 | 2.31E-06 |
| *Plxnc1* | 5.95E-01 | 2.01E-05 | *Col11a1* | 4.77E-01 | 6.83E-04 |
| *Pou3f1* | -1.46E+00 | 1.45E-19 | *Col15a1* | -1.15E+00 | 4.53E-04 |
| *Ppm1e* | -5.99E-01 | 1.22E-07 | *Col23a1* | 1.17E+00 | 4.44E-09 |
| *Ppp1r1b* | 4.47E-01 | 7.07E-04 | *Col25a1* | -6.40E-01 | 4.39E-11 |
| *Prkar2b* | 4.97E-01 | 2.51E-04 | *Col5a1* | 1.01E+00 | 8.79E-15 |
| *Prkca* | -4.98E-01 | 1.11E-04 | *Col5a2* | 1.00E+00 | 1.67E-04 |
| *Prkcd* | -8.42E-01 | 1.33E-03 | *Col6a1* | 4.16E-01 | 9.51E-04 |
| *Prkcg* | -4.06E-01 | 1.64E-03 | *Col6a2* | 8.60E-01 | 3.05E-04 |
| *Prss35* | -1.03E+00 | 4.83E-06 | *Col8a1* | -8.76E-01 | 8.89E-04 |
| *Psat1* | 6.06E-01 | 4.13E-07 | *Comt* | 7.26E-01 | 7.11E-19 |
| *Ptgs2* | -7.76E-01 | 2.28E-07 | *Coro6* | -7.74E-01 | 1.18E-08 |
| *Ptpn14* | 8.15E-01 | 6.05E-06 | *Cpeb2* | -3.00E-01 | 1.00E-03 |
| *Rai14* | 7.42E-01 | 4.96E-04 | *Cplx1* | -5.91E-01 | 8.70E-15 |
| *Rapgef2* | -4.32E-01 | 9.80E-04 | *Cpm* | -6.64E-01 | 6.50E-04 |
| *Rasd1* | -1.28E+00 | 1.29E-10 | *Cpne4* | 4.56E-01 | 2.20E-07 |
| *Rasgrp1* | -4.57E-01 | 7.08E-04 | *Cpne6* | 1.19E+00 | 2.47E-26 |
| *Rasl11b* | -7.11E-01 | 9.50E-04 | *Cpne7* | 8.69E-01 | 2.86E-05 |
| *Rspo3* | 9.13E-01 | 5.14E-06 | *Crispld1* | 9.18E-01 | 9.91E-10 |
| *Runx1t1* | 3.79E-01 | 4.41E-03 | *Cryab* | -7.04E-01 | 7.49E-07 |
| *Ryr2* | -4.75E-01 | 7.30E-05 | *Csgalnact1* | 3.87E-01 | 7.13E-04 |
| *Sacs* | -4.55E-01 | 1.40E-03 | *Csmd3* | 3.20E-01 | 3.97E-03 |
| *Scn7a* | 8.95E-01 | 3.04E-05 | *Csrp1* | -4.36E-01 | 4.26E-06 |
| *Scn9a* | 7.44E-01 | 2.35E-03 | *Ctif* | -3.47E-01 | 2.67E-03 |
| *Sdk2* | 5.84E-01 | 1.17E-03 | *Ctnna1* | -3.72E-01 | 1.19E-03 |
| *Sel1l3* | -5.46E-01 | 2.16E-03 | *Ctsb* | -3.50E-01 | 1.73E-05 |
| *Sema3d* | 6.98E-01 | 1.91E-06 | *Cux2* | 3.64E-01 | 3.11E-05 |
| *Sema3e* | -1.11E+00 | 1.02E-22 | *Cwh43* | -1.04E+00 | 5.71E-04 |
| *Sfrp1* | 7.49E-01 | 7.88E-04 | *Cxcl12* | 4.19E-01 | 9.74E-06 |
| *Shisa2* | 1.04E+00 | 3.11E-04 | *Cxxc4* | -4.95E-01 | 7.78E-08 |
| *Shisa6* | -6.93E-01 | 1.86E-08 | *Cyld* | 5.17E-01 | 2.91E-12 |
| *Skida1* | -7.18E-01 | 3.46E-04 | *Cyp26b1* | -1.01E+00 | 2.24E-03 |
| *Slc17a6* | -5.29E-01 | 1.75E-05 | *Cyp39a1* | -1.45E+00 | 1.35E-05 |
| *Slc24a2* | -5.23E-01 | 5.04E-05 | *Cyr61* | 1.08E+00 | 2.75E-04 |
| *Slc2a1* | -5.92E-01 | 1.06E-04 | *D17Wsu92e* | -3.59E-01 | 4.16E-05 |
| *Slc35f1* | 5.63E-01 | 8.48E-06 | *D1Ertd622e* | -6.25E-01 | 3.34E-12 |
| *Slc4a10* | 3.76E-01 | 3.49E-03 | *D8Ertd82e* | 7.79E-01 | 1.73E-09 |
| *Slc5a7* | 7.08E-01 | 1.92E-04 | *Daam2* | -4.17E-01 | 4.00E-05 |
| *Slc7a11* | 4.30E-01 | 6.82E-04 | *Dach1* | 7.64E-01 | 6.94E-04 |
| *Slc9a2* | -1.89E+00 | 8.22E-32 | *Dagla* | -4.08E-01 | 6.46E-04 |
| *Slc9a4* | -2.54E+00 | 3.98E-42 | *Dapk1* | 3.21E-01 | 5.01E-04 |
| *Slitrk4* | -4.49E-01 | 8.20E-04 | *Dbpht2* | 6.04E-01 | 1.06E-12 |
| *Smtn* | 1.70E+00 | 1.82E-08 | *Dcaf6* | 3.17E-01 | 4.72E-04 |
| *Sorcs3* | -6.54E-01 | 1.92E-06 | *Dcaf7* | 4.78E-01 | 1.08E-08 |

| | | | | | |
|---|---|---|---|---|---|
| *Spink8* | -1.45E+00 | 1.29E-03 | *Dcbld2* | -3.59E-01 | 1.48E-03 |
| *Stac* | -2.62E+00 | 2.09E-05 | *Ddit4l* | -1.11E+00 | 1.59E-17 |
| *Stxbp5l* | -4.70E-01 | 3.02E-03 | *Ddn* | 5.62E-01 | 9.34E-17 |
| *Sult1a1* | -8.81E-01 | 4.23E-03 | *Deptor* | -1.70E+00 | 9.18E-58 |
| *Syndig1l* | 1.09E+00 | 1.73E-13 | *Dgkb* | 3.35E-01 | 1.45E-05 |
| *Tac1* | 5.07E-01 | 3.07E-03 | *Dgkg* | 8.70E-01 | 6.46E-16 |
| *Tcerg1l* | 9.22E-01 | 1.25E-06 | *Diaph1* | 4.53E-01 | 1.09E-05 |
| *Tead1* | 4.09E-01 | 1.56E-03 | *Diras2* | -3.41E-01 | 2.73E-05 |
| *Timp2* | 5.89E-01 | 2.34E-05 | *Dkk3* | -5.78E-01 | 1.82E-13 |
| *Tmem255a* | 5.50E-01 | 4.20E-03 | *Dkkl1* | -1.53E+00 | 1.24E-06 |
| *Tmem72* | 9.93E-01 | 1.92E-09 | *Dmp1* | -8.64E-01 | 1.95E-03 |
| *Tnc* | 7.11E-01 | 4.77E-03 | *Dnah14* | 1.25E+00 | 2.98E-06 |
| *Tox3* | 9.08E-01 | 4.13E-07 | *Dnah6* | 1.66E+00 | 2.05E-07 |
| *Trhde* | -6.89E-01 | 1.16E-06 | *Dnajb1* | 4.82E-01 | 2.15E-04 |
| *Trpc4* | -4.50E-01 | 4.91E-03 | *Dnajc21* | -5.63E-01 | 2.61E-09 |
| *Tshz3* | 8.19E-01 | 8.77E-05 | *Doc2b* | 1.33E+00 | 1.97E-20 |
| *Ttr* | 4.80E-01 | 4.87E-06 | *Dock5* | -8.42E-01 | 4.67E-05 |
| *Ust* | -5.32E-01 | 1.23E-03 | *Dpp4* | -1.07E+00 | 3.37E-06 |
| *Vat1l* | 5.37E-01 | 3.63E-05 | *Dpy19l1* | -5.81E-01 | 3.77E-11 |
| *Vgll3* | 1.86E+00 | 1.28E-21 | *Dpy19l3* | 7.83E-01 | 3.25E-15 |
| *Wbscr17* | -6.18E-01 | 2.86E-06 | *Dpysl3* | 3.79E-01 | 6.41E-04 |
| *Wipf3* | -7.89E-01 | 1.64E-11 | *Drd1* | 6.45E-01 | 3.90E-07 |
| *Zbtb16* | -5.37E-01 | 8.43E-05 | *Drd2* | 1.02E+00 | 1.47E-03 |
| *Zdhhc2* | -5.13E-01 | 8.53E-04 | *Dst* | -3.87E-01 | 5.97E-08 |
| *Zfp804a* | -5.65E-01 | 2.34E-05 | *Dusp18* | 6.98E-01 | 5.88E-12 |
| | | | *Dusp3* | -4.55E-01 | 2.60E-09 |
| | | | *Dusp4* | 1.12E+00 | 1.68E-06 |
| | | | *Dzip1* | -4.02E-01 | 3.55E-05 |
| | | | *E330009J07Rik* | -3.01E-01 | 1.21E-03 |
| | | | *Ebf2* | 1.35E+00 | 7.68E-04 |
| | | | *Efcab1* | 1.08E+00 | 9.89E-09 |
| | | | *Efhd2* | -4.64E-01 | 1.19E-06 |
| | | | *Efr3a* | -3.51E-01 | 2.16E-05 |
| | | | *Egr2* | 1.66E+00 | 8.07E-22 |
| | | | *Eif5a2* | -3.99E-01 | 2.88E-05 |
| | | | *Elavl4* | -5.08E-01 | 1.13E-11 |
| | | | *Ell2* | -5.86E-01 | 1.14E-09 |
| | | | *Enc1* | 3.95E-01 | 1.27E-07 |
| | | | *Endod1* | -3.60E-01 | 4.12E-04 |
| | | | *Epb41* | -6.67E-01 | 1.11E-13 |
| | | | *Epdr1* | -3.67E-01 | 5.81E-04 |
| | | | *Erbin* | -3.74E-01 | 2.92E-05 |
| | | | *Ermn* | -8.15E-01 | 1.89E-19 |
| | | | *Esr1* | 2.16E+00 | 5.35E-23 |
| | | | *Esrrg* | -7.82E-01 | 4.00E-14 |
| | | | *Etnppl* | -7.82E-01 | 6.21E-09 |
| | | | *Evc2* | 6.88E-01 | 1.02E-04 |
| | | | *Exd2* | 3.30E-01 | 2.68E-03 |
| | | | *Exoc6b* | -3.26E-01 | 4.96E-04 |
| | | | *Extl3* | -4.70E-01 | 3.55E-07 |
| | | | *Ezr* | -3.34E-01 | 1.78E-03 |
| | | | *Fa2h* | -6.14E-01 | 1.48E-03 |
| | | | *Fam101b* | 7.01E-01 | 1.32E-04 |
| | | | *Fam107a* | -5.77E-01 | 1.18E-15 |
| | | | *Fam124a* | 4.63E-01 | 3.63E-04 |
| | | | *Fam126a* | 5.78E-01 | 1.07E-05 |

| | | | | | |
|---|---|---|---|---|---|
| | | | *Fam13c* | 3.32E-01 | 5.00E-04 |
| | | | *Fam149a* | 3.79E-01 | 2.63E-03 |
| | | | *Fam19a1* | 7.92E-01 | 3.00E-16 |
| | | | *Fam3c* | -3.71E-01 | 8.24E-05 |
| | | | *Fam43a* | -9.32E-01 | 1.52E-04 |
| | | | *Fam65b* | 3.66E-01 | 3.20E-03 |
| | | | *Fap* | -1.02E+00 | 5.44E-05 |
| | | | *Fat3* | -5.01E-01 | 3.01E-11 |
| | | | *Fat4* | 6.30E-01 | 8.10E-06 |
| | | | *Fbxo10* | 6.10E-01 | 5.14E-05 |
| | | | *Fbxo32* | -1.17E+00 | 5.31E-19 |
| | | | *Fgd4* | 3.11E-01 | 2.44E-03 |
| | | | *Fgf10* | 8.59E-01 | 1.96E-06 |
| | | | *Fgfr3* | -4.35E-01 | 1.17E-03 |
| | | | *Fhad1* | -1.11E+00 | 5.97E-06 |
| | | | *Fhod3* | -4.95E-01 | 2.00E-06 |
| | | | *Filip1* | 6.41E-01 | 2.32E-03 |
| | | | *Flrt3* | 4.40E-01 | 7.61E-05 |
| | | | *Fmn1* | -7.04E-01 | 4.90E-12 |
| | | | *Fndc5* | -6.18E-01 | 2.12E-09 |
| | | | *Fndc9* | 1.45E+00 | 4.86E-04 |
| | | | *Fos* | 6.12E-01 | 1.56E-04 |
| | | | *Fosb* | 7.53E-01 | 1.13E-04 |
| | | | *Foxn3* | -6.61E-01 | 7.15E-06 |
| | | | *Foxo3* | -3.19E-01 | 1.89E-03 |
| | | | *Foxp1* | -1.36E+00 | 1.38E-67 |
| | | | *Fras1* | -5.59E-01 | 3.34E-05 |
| | | | *Frrs1l* | -3.09E-01 | 2.56E-05 |
| | | | *Fst* | 1.55E+00 | 3.74E-26 |
| | | | *Fstl4* | -3.99E-01 | 4.72E-03 |
| | | | *Fxyd6* | 8.00E-01 | 2.55E-09 |
| | | | *Fzd4* | -5.81E-01 | 1.35E-04 |
| | | | *Gaa* | 3.91E-01 | 1.40E-03 |
| | | | *Gabra2* | 4.27E-01 | 3.53E-08 |
| | | | *Gabra5* | -7.80E-01 | 3.32E-16 |
| | | | *Galntl6* | -5.23E-01 | 1.35E-05 |
| | | | *Gap43* | 4.24E-01 | 7.09E-08 |
| | | | *Gatm* | -4.11E-01 | 3.36E-05 |
| | | | *Gbp4* | 1.02E+00 | 2.92E-03 |
| | | | *Gbp9* | 8.05E-01 | 1.72E-04 |
| | | | *Gcnt4* | -5.43E-01 | 1.77E-04 |
| | | | *Gda* | 4.38E-01 | 8.13E-10 |
| | | | *Gfra2* | -1.36E+00 | 5.55E-41 |
| | | | *Git1* | -3.27E-01 | 4.05E-04 |
| | | | *Gjb6* | -6.23E-01 | 9.42E-09 |
| | | | *Gjc3* | -7.20E-01 | 6.30E-13 |
| | | | *Glp2r* | 1.82E+00 | 2.79E-08 |
| | | | *Glra3* | 2.31E+00 | 6.49E-141 |
| | | | *Glt8d2* | -1.04E+00 | 1.93E-11 |
| | | | *Glul* | -3.26E-01 | 1.60E-05 |
| | | | *Gm16485* | -9.47E-01 | 4.44E-17 |
| | | | *Gm19410* | 3.95E-01 | 3.09E-04 |
| | | | *Gm38393* | -4.34E-01 | 7.45E-06 |
| | | | *Gm765* | 1.54E+00 | 7.61E-32 |
| | | | *Gnb4* | 9.49E-01 | 2.25E-22 |
| | | | *Gng2* | 3.48E-01 | 4.67E-06 |

| | | | | | |
|---|---|---|---|---|---|
| | | | *Gng4* | 3.49E-01 | 3.22E-03 |
| | | | *Gng7* | 3.57E-01 | 1.04E-03 |
| | | | *Gpc3* | 9.95E-01 | 2.45E-03 |
| | | | *Gpc4* | 8.73E-01 | 1.49E-05 |
| | | | *Gpcpd1* | -4.38E-01 | 5.84E-08 |
| | | | *Gpr158* | -3.72E-01 | 2.15E-06 |
| | | | *Gpr37* | -6.65E-01 | 2.10E-07 |
| | | | *Gpr85* | 4.43E-01 | 3.49E-05 |
| | | | *Gpr88* | 9.21E-01 | 5.21E-37 |
| | | | *Gprc5b* | -4.04E-01 | 2.63E-04 |
| | | | *Gprin1* | 5.94E-01 | 9.91E-11 |
| | | | *Grb10* | 4.35E-01 | 5.17E-05 |
| | | | *Grem2* | 5.02E-01 | 1.57E-04 |
| | | | *Gria3* | 3.12E-01 | 3.14E-05 |
| | | | *Grin3a* | 5.40E-01 | 5.40E-08 |
| | | | *Grm1* | 3.96E-01 | 1.10E-04 |
| | | | *Grm2* | -1.38E+00 | 5.86E-13 |
| | | | *Grm5* | 3.68E-01 | 7.67E-07 |
| | | | *Grp* | 1.96E+00 | 2.54E-12 |
| | | | *Gsg1l* | 5.10E-01 | 5.77E-07 |
| | | | *Gspt2* | 4.29E-01 | 5.21E-04 |
| | | | *Gsta4* | 8.73E-01 | 1.24E-08 |
| | | | *Gucy1a3* | 1.02E+00 | 8.82E-49 |
| | | | *Gucy1b3* | 4.31E-01 | 3.52E-08 |
| | | | *Hap1* | 8.57E-01 | 2.25E-12 |
| | | | *Hapln2* | -9.06E-01 | 8.76E-04 |
| | | | *Hapln4* | -8.84E-01 | 3.51E-21 |
| | | | *Hcn1* | -4.79E-01 | 1.68E-10 |
| | | | *Hdac9* | 3.29E-01 | 1.43E-03 |
| | | | *Hdx* | -4.12E-01 | 1.31E-03 |
| | | | *Hecw1* | -3.01E-01 | 1.10E-04 |
| | | | *Heg1* | -5.16E-01 | 5.54E-07 |
| | | | *Hipk2* | -3.92E-01 | 9.84E-05 |
| | | | *Hlf* | -4.13E-01 | 1.50E-08 |
| | | | *Hr* | -1.11E+00 | 7.65E-14 |
| | | | *Hrh2* | 6.32E-01 | 1.27E-04 |
| | | | *Hrh3* | -7.36E-01 | 9.06E-07 |
| | | | *Hrk* | 6.51E-01 | 7.09E-08 |
| | | | *Hs3st2* | -1.16E+00 | 4.78E-18 |
| | | | *Hs6st2* | 3.15E-01 | 4.88E-03 |
| | | | *Hsbp1l1* | -2.36E+00 | 1.75E-08 |
| | | | *Hspa2* | 5.52E-01 | 1.70E-05 |
| | | | *Hspa4l* | -3.25E-01 | 1.73E-05 |
| | | | *Htr1f* | -8.95E-01 | 8.62E-05 |
| | | | *Htr2a* | -6.49E-01 | 1.04E-05 |
| | | | *Htr2c* | 1.17E+00 | 2.07E-26 |
| | | | *Htr7* | 7.78E-01 | 7.62E-05 |
| | | | *Htra1* | -4.28E-01 | 9.52E-06 |
| | | | *Igfn1* | 1.35E+00 | 3.28E-34 |
| | | | *Ikzf4* | 6.38E-01 | 1.83E-07 |
| | | | *Il1r1* | -9.69E-01 | 2.93E-05 |
| | | | *Il1rap* | -6.64E-01 | 7.49E-12 |
| | | | *Il1rapl1* | 3.43E-01 | 1.32E-03 |
| | | | *Il1rapl2* | -9.08E-01 | 3.43E-05 |
| | | | *Il33* | -7.43E-01 | 2.76E-10 |
| | | | *Ildr2* | 3.86E-01 | 7.39E-07 |

| | | | | | |
|---|---|---|---|---|---|
| | | | *Ina* | -3.84E-01 | 3.89E-07 |
| | | | *Inf2* | -7.63E-01 | 8.06E-12 |
| | | | *Inpp4b* | 4.82E-01 | 3.62E-03 |
| | | | *Inpp5j* | -5.27E-01 | 4.11E-03 |
| | | | *Iqsec1* | -4.57E-01 | 3.97E-09 |
| | | | *Iqsec3* | -4.82E-01 | 5.56E-07 |
| | | | *Itga4* | 1.60E+00 | 2.71E-69 |
| | | | *Itga8* | 8.60E-01 | 2.52E-08 |
| | | | *Itih3* | -6.88E-01 | 4.08E-03 |
| | | | *Itm2c* | 3.99E-01 | 3.18E-06 |
| | | | *Itpr1* | -3.46E-01 | 2.76E-06 |
| | | | *Jade3* | 6.05E-01 | 5.54E-05 |
| | | | *Jdp2* | -6.57E-01 | 1.73E-05 |
| | | | *Jph4* | 4.94E-01 | 7.89E-11 |
| | | | *Junb* | 6.79E-01 | 9.85E-06 |
| | | | *Kazn* | -5.20E-01 | 4.63E-07 |
| | | | *Kcna1* | -7.71E-01 | 1.49E-22 |
| | | | *Kcna2* | -5.38E-01 | 6.61E-15 |
| | | | *Kcnab2* | -3.63E-01 | 1.23E-05 |
| | | | *Kcnab3* | -1.64E+00 | 1.85E-42 |
| | | | *Kcnc1* | -3.50E-01 | 1.61E-04 |
| | | | *Kcnc3* | -7.78E-01 | 9.28E-18 |
| | | | *Kcnd3* | 3.25E-01 | 8.07E-04 |
| | | | *Kcnf1* | 5.39E-01 | 2.80E-08 |
| | | | *Kcng1* | 6.53E-01 | 6.41E-05 |
| | | | *Kcng3* | 7.28E-01 | 1.91E-03 |
| | | | *Kcng4* | -1.78E+00 | 9.11E-07 |
| | | | *Kcnh5* | -6.85E-01 | 7.18E-09 |
| | | | *Kcnh7* | -5.21E-01 | 6.13E-14 |
| | | | *Kcnip4* | 3.79E-01 | 7.45E-06 |
| | | | *Kcnj10* | -8.86E-01 | 1.21E-32 |
| | | | *Kcnk2* | -3.63E-01 | 2.12E-03 |
| | | | *Kcnmb4* | -5.66E-01 | 2.87E-04 |
| | | | *Kcnn3* | 5.06E-01 | 5.69E-05 |
| | | | *Kcnq5* | -3.91E-01 | 1.94E-06 |
| | | | *Kctd4* | 5.77E-01 | 2.77E-07 |
| | | | *Kif13b* | -6.40E-01 | 5.20E-05 |
| | | | *Kif26b* | 6.35E-01 | 2.72E-04 |
| | | | *Kirrel3* | 5.70E-01 | 1.83E-05 |
| | | | *Kit* | 3.91E-01 | 4.25E-03 |
| | | | *Klc2* | -4.02E-01 | 1.84E-04 |
| | | | *Klf16* | 6.60E-01 | 3.26E-05 |
| | | | *Klf9* | -4.76E-01 | 3.07E-11 |
| | | | *Klhdc7a* | -8.93E-01 | 8.72E-07 |
| | | | *Klhl13* | 5.06E-01 | 2.75E-05 |
| | | | *Kndc1* | -3.64E-01 | 6.94E-04 |
| | | | *Krt222* | -3.85E-01 | 1.33E-04 |
| | | | *Krt77* | 1.77E+00 | 1.03E-09 |
| | | | *Krt9* | 9.12E-01 | 1.39E-03 |
| | | | *Ky* | -1.92E+00 | 1.23E-05 |
| | | | *L1cam* | 4.00E-01 | 4.20E-06 |
| | | | *Lamb1* | 5.65E-01 | 4.73E-03 |
| | | | *Lamc2* | -7.45E-01 | 9.80E-04 |
| | | | *Lamp5* | 5.06E-01 | 1.19E-10 |
| | | | *Ldlrad4* | -4.65E-01 | 4.65E-04 |
| | | | *Lgi2* | -6.26E-01 | 3.32E-13 |

| | | | | | |
|---|---|---|---|---|---|
| | | | *Lgi3* | -5.24E-01 | 3.01E-04 |
| | | | *Lhfp* | -6.90E-01 | 2.74E-06 |
| | | | *Lhfpl3* | 6.25E-01 | 8.77E-09 |
| | | | *Lingo2* | 5.64E-01 | 2.41E-06 |
| | | | *Lix1* | 3.35E-01 | 1.22E-03 |
| | | | *Lmo3* | 3.05E-01 | 4.46E-04 |
| | | | *Lmo7* | 4.41E-01 | 9.67E-07 |
| | | | *Lpar1* | -4.59E-01 | 9.71E-04 |
| | | | *Lpgat1* | -3.70E-01 | 3.08E-07 |
| | | | *Lpl* | 1.58E+00 | 3.27E-60 |
| | | | *Lrch1* | -5.67E-01 | 3.03E-03 |
| | | | *Lrpap1* | 3.08E-01 | 4.77E-03 |
| | | | *Lrrc10b* | 9.38E-01 | 9.15E-04 |
| | | | *Lrrc55* | -8.10E-01 | 7.28E-13 |
| | | | *Lrrc58* | -3.39E-01 | 4.22E-05 |
| | | | *Lrrc8c* | -5.83E-01 | 2.06E-10 |
| | | | *Lrrn1* | -3.42E-01 | 2.64E-03 |
| | | | *Lrrn3* | -4.10E-01 | 1.71E-05 |
| | | | *Lrrtm4* | 8.21E-01 | 1.20E-17 |
| | | | *Lsm11* | -5.93E-01 | 1.49E-06 |
| | | | *Luzp1* | -5.33E-01 | 7.53E-12 |
| | | | *Lxn* | 5.33E-01 | 1.48E-04 |
| | | | *Ly6h* | 9.79E-01 | 2.95E-09 |
| | | | *Lynx1* | -7.95E-01 | 9.49E-22 |
| | | | *Lypd1* | 8.66E-01 | 1.77E-22 |
| | | | *Lyst* | -3.13E-01 | 1.29E-03 |
| | | | *Lzts1* | 4.80E-01 | 1.10E-06 |
| | | | *Mag* | -6.42E-01 | 2.79E-08 |
| | | | *Magi3* | 3.26E-01 | 2.61E-04 |
| | | | *Mal* | -7.96E-01 | 2.56E-25 |
| | | | *Mal2* | -3.52E-01 | 4.28E-06 |
| | | | *Man2a1* | -4.01E-01 | 5.41E-04 |
| | | | *Manea* | -3.00E-01 | 2.90E-03 |
| | | | *Map3k19* | 1.06E+00 | 1.80E-05 |
| | | | *Map9* | 3.12E-01 | 1.36E-04 |
| | | | *Mapk3* | 7.60E-01 | 4.39E-14 |
| | | | *Mapk4* | 4.46E-01 | 2.41E-06 |
| | | | *Mapk6* | -3.62E-01 | 4.26E-05 |
| | | | *March1* | 6.68E-01 | 7.75E-14 |
| | | | *March4* | 9.31E-01 | 6.12E-10 |
| | | | *Marcks* | 5.52E-01 | 4.63E-15 |
| | | | *Marcksl1* | 5.66E-01 | 1.76E-07 |
| | | | *Mas1* | 9.63E-01 | 6.03E-07 |
| | | | *Mb21d2* | -5.24E-01 | 8.46E-04 |
| | | | *Mblac2* | 3.23E-01 | 1.41E-03 |
| | | | *Mbp* | -8.03E-01 | 1.87E-30 |
| | | | *Mcf2* | -7.51E-01 | 1.14E-03 |
| | | | *Mdga1* | 1.06E+00 | 8.32E-09 |
| | | | *Medag* | -5.80E-01 | 3.18E-06 |
| | | | *Mef2c* | 3.10E-01 | 3.29E-05 |
| | | | *Mertk* | -3.78E-01 | 2.91E-04 |
| | | | *Mfge8* | 4.35E-01 | 5.22E-04 |
| | | | *Mgll* | -4.98E-01 | 5.06E-09 |
| | | | *Mink1* | 3.06E-01 | 7.04E-04 |
| | | | *Mobp* | -8.84E-01 | 6.21E-36 |
| | | | *Mog* | -6.53E-01 | 1.83E-06 |

| | | | | | |
|---|---|---|---|---|---|
| | | | *Moxd1* | 9.44E-01 | 1.92E-05 |
| | | | *Mtus1* | -5.40E-01 | 2.75E-06 |
| | | | *Mybl1* | -5.87E-01 | 1.63E-03 |
| | | | *Myl4* | -2.14E+00 | 1.58E-18 |
| | | | *Myo5a* | -3.92E-01 | 2.52E-08 |
| | | | *Myo5b* | 6.84E-01 | 8.20E-07 |
| | | | *Naaa* | 5.64E-01 | 4.08E-03 |
| | | | *Nat8l* | -4.09E-01 | 2.29E-06 |
| | | | *Nbeal1* | -3.38E-01 | 9.51E-04 |
| | | | *Ncam2* | -6.76E-01 | 4.35E-17 |
| | | | *Ndrg1* | -6.28E-01 | 9.67E-10 |
| | | | *Ndst4* | 1.41E+00 | 7.37E-18 |
| | | | *Nebl* | -3.46E-01 | 1.55E-04 |
| | | | *Necab1* | 4.02E-01 | 5.59E-08 |
| | | | *Necab2* | 9.73E-01 | 4.50E-07 |
| | | | *Nectin1* | 6.24E-01 | 5.59E-08 |
| | | | *Nectin3* | 4.98E-01 | 2.40E-07 |
| | | | *Nefh* | -1.11E+00 | 7.61E-32 |
| | | | *Nefl* | -3.94E-01 | 1.40E-07 |
| | | | *Nefm* | -8.56E-01 | 2.76E-31 |
| | | | *Nell2* | 4.93E-01 | 5.36E-11 |
| | | | *Net1* | -7.12E-01 | 1.11E-12 |
| | | | *Neurl1a* | 3.90E-01 | 1.95E-03 |
| | | | *Neurl1b* | 6.59E-01 | 1.06E-09 |
| | | | *Neurod1* | 4.31E-01 | 3.41E-04 |
| | | | *Nfic* | -6.91E-01 | 6.39E-15 |
| | | | *Nfkbia* | -4.29E-01 | 9.16E-04 |
| | | | *Ngb* | 2.46E+00 | 3.43E-04 |
| | | | *Nkain2* | 3.42E-01 | 2.11E-03 |
| | | | *Nlgn3* | 3.14E-01 | 5.07E-04 |
| | | | *Nnat* | 1.10E+00 | 2.54E-23 |
| | | | *Nol4l* | 3.53E-01 | 1.09E-03 |
| | | | *Nos1* | 9.11E-01 | 6.38E-19 |
| | | | *Nos1ap* | -4.32E-01 | 2.93E-04 |
| | | | *Nov* | 1.27E+00 | 3.27E-68 |
| | | | *Npnt* | -9.80E-01 | 8.99E-17 |
| | | | *Nptxr* | 4.01E-01 | 4.39E-08 |
| | | | *Nr2f2* | 5.40E-01 | 4.79E-05 |
| | | | *Nr3c2* | 4.29E-01 | 9.28E-05 |
| | | | *Nr4a2* | 1.19E+00 | 5.27E-47 |
| | | | *Nr4a3* | 7.21E-01 | 5.61E-14 |
| | | | *Nrarp* | 5.33E-01 | 9.62E-04 |
| | | | *Nrgn* | -3.48E-01 | 5.18E-06 |
| | | | *Nrn1* | -6.93E-01 | 1.44E-20 |
| | | | *Nrp2* | 8.72E-01 | 9.08E-15 |
| | | | *Nrsn1* | -5.71E-01 | 6.18E-15 |
| | | | *Nsg2* | 5.62E-01 | 7.06E-15 |
| | | | *Nsmaf* | -3.49E-01 | 3.45E-03 |
| | | | *Nt5c3* | -3.75E-01 | 1.39E-03 |
| | | | *Ntrk3* | 3.33E-01 | 2.33E-05 |
| | | | *Nudt4* | -7.07E-01 | 4.65E-20 |
| | | | *Nwd2* | 7.93E-01 | 1.61E-21 |
| | | | *Olfr78* | -2.62E+00 | 4.18E-16 |
| | | | *Onecut2* | -7.44E-01 | 6.16E-05 |
| | | | *Oprk1* | 8.10E-01 | 3.68E-11 |
| | | | *Osbp2* | -4.98E-01 | 2.95E-07 |

| | | | | | |
|---|---|---|---|---|---|
| | | | *Osbpl1a* | -3.18E-01 | 2.68E-05 |
| | | | *Osbpl3* | -1.01E+00 | 3.44E-25 |
| | | | *Otud1* | 5.11E-01 | 5.37E-05 |
| | | | *Otud7b* | -3.85E-01 | 4.36E-04 |
| | | | *Oxr1* | -3.91E-01 | 1.48E-07 |
| | | | *Oxtr* | 1.27E+00 | 2.57E-10 |
| | | | *Pacsin2* | -4.25E-01 | 3.90E-03 |
| | | | *Pak1* | -4.13E-01 | 9.42E-09 |
| | | | *Pak6* | 5.78E-01 | 3.99E-06 |
| | | | *Palmd* | 7.80E-01 | 1.64E-15 |
| | | | *Pam* | 4.20E-01 | 1.39E-07 |
| | | | *Pappa2* | -1.02E+00 | 2.14E-03 |
| | | | *Papss2* | 5.80E-01 | 1.57E-04 |
| | | | *Paqr4* | -7.23E-01 | 6.00E-07 |
| | | | *Paqr8* | -3.77E-01 | 7.05E-06 |
| | | | *Parm1* | -3.09E-01 | 3.25E-03 |
| | | | *Parva* | -5.14E-01 | 1.82E-08 |
| | | | *Pcdh1* | 3.04E-01 | 4.82E-03 |
| | | | *Pcdh15* | 3.94E-01 | 4.50E-05 |
| | | | *Pcdh19* | 7.16E-01 | 8.35E-15 |
| | | | *Pcdh20* | 5.04E-01 | 2.53E-06 |
| | | | *Pcdh7* | -6.04E-01 | 2.31E-18 |
| | | | *Pcdh8* | 1.23E+00 | 2.54E-15 |
| | | | *Pclo* | -3.24E-01 | 6.06E-06 |
| | | | *Pcp4* | -4.04E-01 | 5.89E-07 |
| | | | *Pdcd4* | 3.83E-01 | 7.26E-06 |
| | | | *Pde10a* | 5.87E-01 | 6.18E-13 |
| | | | *Pde1a* | -3.02E-01 | 2.50E-04 |
| | | | *Pde1b* | 3.86E-01 | 6.64E-04 |
| | | | *Pde2a* | 5.27E-01 | 6.04E-11 |
| | | | *Pde4a* | -5.19E-01 | 1.65E-08 |
| | | | *Pde5a* | -5.67E-01 | 6.55E-05 |
| | | | *Pde8a* | -6.40E-01 | 4.11E-05 |
| | | | *Pdgfc* | 6.32E-01 | 3.91E-03 |
| | | | *Pdzd4* | 4.36E-01 | 4.90E-06 |
| | | | *Pdzrn3* | 3.50E-01 | 4.15E-03 |
| | | | *Pea15a* | 4.99E-01 | 6.02E-12 |
| | | | *Peak1* | 6.88E-01 | 8.16E-14 |
| | | | *Penk* | 1.02E+00 | 2.49E-28 |
| | | | *Pex5l* | -4.47E-01 | 3.15E-08 |
| | | | *Pgr* | -7.71E-01 | 1.69E-16 |
| | | | *Pgrmc1* | 4.82E-01 | 1.58E-10 |
| | | | *Phactr2* | 5.27E-01 | 1.40E-07 |
| | | | *Pik3ca* | -3.22E-01 | 2.55E-04 |
| | | | *Pip4k2a* | -4.07E-01 | 4.22E-06 |
| | | | *Pip5k1c* | -3.66E-01 | 1.10E-05 |
| | | | *Pitpnc1* | -5.42E-01 | 1.75E-10 |
| | | | *Pkd2l1* | 5.24E+00 | 5.58E-20 |
| | | | *Plcxd2* | -7.03E-01 | 4.01E-19 |
| | | | *Pld5* | -1.04E+00 | 2.06E-07 |
| | | | *Plekha2* | -6.41E-01 | 3.76E-05 |
| | | | *Plekhb1* | -6.01E-01 | 1.62E-11 |
| | | | *Plekhg1* | -4.81E-01 | 3.63E-04 |
| | | | *Plekhh1* | -8.06E-01 | 3.33E-09 |
| | | | *Plin4* | -2.10E+00 | 1.58E-10 |
| | | | *Plk2* | 4.95E-01 | 5.34E-10 |

| | | | | | |
|---|---|---|---|---|---|
| | | | *Plp1* | -7.05E-01 | 6.97E-24 |
| | | | *Plppr1* | 1.03E+00 | 1.47E-05 |
| | | | *Plppr3* | 6.73E-01 | 4.40E-03 |
| | | | *Plppr4* | 3.53E-01 | 1.91E-06 |
| | | | *Plxdc1* | -9.45E-01 | 7.93E-05 |
| | | | *Plxnc1* | 4.46E-01 | 3.12E-06 |
| | | | *Pmp22* | -9.09E-01 | 7.80E-10 |
| | | | *Pnck* | 1.02E+00 | 2.78E-06 |
| | | | *Pnma2* | 4.45E-01 | 7.20E-06 |
| | | | *Pnmal2* | 6.73E-01 | 8.28E-17 |
| | | | *Pnrc2* | 3.46E-01 | 7.30E-04 |
| | | | *Postn* | -1.35E+00 | 8.40E-08 |
| | | | *Pou3f1* | -7.95E-01 | 2.14E-07 |
| | | | *Pou6f2* | -1.04E+00 | 1.04E-05 |
| | | | *Ppargc1a* | -3.15E-01 | 1.00E-03 |
| | | | *Ppat* | 4.58E-01 | 4.10E-04 |
| | | | *Ppfia2* | 3.94E-01 | 7.23E-07 |
| | | | *Ppfibp1* | 3.18E-01 | 2.99E-03 |
| | | | *Ppip5k1* | -3.52E-01 | 2.96E-04 |
| | | | *Ppip5k2* | -5.63E-01 | 6.57E-09 |
| | | | *Ppm1l* | -6.11E-01 | 9.31E-17 |
| | | | *Ppp1r16b* | -5.61E-01 | 9.59E-11 |
| | | | *Ppp1r1b* | 4.38E-01 | 2.60E-04 |
| | | | *Ppp1r36* | 1.61E+00 | 1.91E-03 |
| | | | *Ppp2r3a* | -3.48E-01 | 4.23E-04 |
| | | | *Prelp* | 6.44E-01 | 3.64E-03 |
| | | | *Prex1* | 3.68E-01 | 2.00E-04 |
| | | | *Prkcb* | -4.32E-01 | 1.20E-09 |
| | | | *Prkcz* | -3.09E-01 | 3.69E-04 |
| | | | *Prkg1* | 5.84E-01 | 3.18E-04 |
| | | | *Prkg2* | 1.02E+00 | 7.58E-18 |
| | | | *Prr16* | -1.57E+00 | 5.51E-20 |
| | | | *Prr18* | -7.83E-01 | 8.59E-08 |
| | | | *Prr5l* | -9.60E-01 | 2.65E-04 |
| | | | *Prrg1* | -1.00E+00 | 2.80E-08 |
| | | | *Prss23* | -1.30E+00 | 9.49E-22 |
| | | | *Psme4* | -3.46E-01 | 3.05E-04 |
| | | | *Ptgfrn* | -1.19E+00 | 8.51E-25 |
| | | | *Ptgs2* | 6.46E-01 | 1.14E-07 |
| | | | *Ptk2b* | 3.68E-01 | 2.01E-06 |
| | | | *Ptpn14* | 1.09E+00 | 9.19E-10 |
| | | | *Ptpn4* | -3.30E-01 | 1.86E-05 |
| | | | *Ptprb* | -3.82E-01 | 3.70E-04 |
| | | | *Ptprd* | -3.99E-01 | 4.47E-08 |
| | | | *Ptprm* | -4.22E-01 | 6.64E-04 |
| | | | *Ptpro* | 1.10E+00 | 8.55E-21 |
| | | | *Pvalb* | -1.15E+00 | 1.98E-19 |
| | | | *Pygl* | 1.26E+00 | 3.63E-04 |
| | | | *Pygm* | -6.70E-01 | 2.50E-04 |
| | | | *Qdpr* | -6.37E-01 | 9.33E-08 |
| | | | *Qk* | -3.62E-01 | 2.07E-06 |
| | | | *Qrfpr* | 2.02E+00 | 2.18E-12 |
| | | | *R3hdm1* | -3.63E-01 | 7.27E-07 |
| | | | *R3hdm2* | -4.15E-01 | 2.90E-08 |
| | | | *Ralgps2* | 3.38E-01 | 1.90E-03 |
| | | | *Rap1gds1* | -3.57E-01 | 2.96E-06 |

| | | | | | |
|---|---|---|---|---|---|
| | | | *Rapgef4* | -7.51E-01 | 2.88E-27 |
| | | | *Rapgefl1* | 3.03E-01 | 3.45E-03 |
| | | | *Rasgef1a* | 4.19E-01 | 1.73E-08 |
| | | | *Rasgef1c* | 6.49E-01 | 1.73E-04 |
| | | | *Rassf3* | -5.19E-01 | 9.76E-06 |
| | | | *Rassf4* | -9.26E-01 | 1.56E-03 |
| | | | *Rbfox3* | -3.34E-01 | 1.41E-05 |
| | | | *Rbm24* | 5.17E-01 | 1.91E-05 |
| | | | *Rcan2* | -4.07E-01 | 1.06E-07 |
| | | | *Rcn1* | 1.07E+00 | 1.47E-15 |
| | | | *Reln* | 5.25E-01 | 1.55E-08 |
| | | | *Rfx3* | 7.63E-01 | 3.80E-22 |
| | | | *Rgl1* | 3.14E-01 | 1.62E-03 |
| | | | *Rgs12* | 6.23E-01 | 4.33E-06 |
| | | | *Rgs14* | 7.67E-01 | 6.09E-06 |
| | | | *Rgs2* | 6.50E-01 | 9.19E-10 |
| | | | *Rgs4* | -3.69E-01 | 2.38E-07 |
| | | | *Rgs5* | -3.31E-01 | 1.07E-04 |
| | | | *Rgs9* | 6.60E-01 | 1.77E-06 |
| | | | *Rimklb* | 4.82E-01 | 4.20E-06 |
| | | | *Rims3* | -7.30E-01 | 1.13E-15 |
| | | | *Rin1* | 5.13E-01 | 2.48E-04 |
| | | | *Rin2* | -6.90E-01 | 3.52E-08 |
| | | | *Robo3* | -5.47E-01 | 2.46E-03 |
| | | | *Rorb* | -9.70E-01 | 6.41E-35 |
| | | | *Rps6ka2* | 6.18E-01 | 1.01E-06 |
| | | | *Rreb1* | 6.61E-01 | 8.14E-08 |
| | | | *Rsph4a* | 1.10E+00 | 4.20E-05 |
| | | | *Rxfp2* | -1.99E+00 | 2.44E-07 |
| | | | *Rxrg* | 1.12E+00 | 4.43E-05 |
| | | | *Ryr3* | 3.21E-01 | 4.84E-03 |
| | | | *S100b* | -4.25E-01 | 2.78E-05 |
| | | | *Sacs* | -3.93E-01 | 2.18E-07 |
| | | | *Sall2* | 4.32E-01 | 1.94E-03 |
| | | | *Samd14* | 8.33E-01 | 1.38E-03 |
| | | | *Samd3* | 1.91E+00 | 6.82E-09 |
| | | | *Samd4* | -3.98E-01 | 7.63E-04 |
| | | | *Satb1* | -3.84E-01 | 1.97E-06 |
| | | | *Scai* | -3.11E-01 | 1.56E-04 |
| | | | *Sccpdh* | -3.65E-01 | 2.07E-03 |
| | | | *Scd1* | -7.02E-01 | 9.43E-20 |
| | | | *Scn1a* | -9.49E-01 | 6.46E-41 |
| | | | *Scn1b* | -3.30E-01 | 5.38E-04 |
| | | | *Scn3a* | 3.82E-01 | 9.78E-05 |
| | | | *Scn3b* | 7.34E-01 | 1.74E-19 |
| | | | *Scn4b* | -4.78E-01 | 7.48E-06 |
| | | | *Scn5a* | 2.03E+00 | 4.66E-03 |
| | | | *Scrt1* | -8.44E-01 | 1.25E-17 |
| | | | *Scube1* | -6.08E-01 | 8.93E-09 |
| | | | *Sdc2* | 3.28E-01 | 3.04E-03 |
| | | | *Sdc3* | 3.98E-01 | 2.04E-05 |
| | | | *Sdc4* | -4.58E-01 | 8.81E-05 |
| | | | *Sdpr* | -6.19E-01 | 1.22E-04 |
| | | | *Sema3a* | 8.60E-01 | 1.95E-23 |
| | | | *Sema3c* | -7.81E-01 | 1.50E-14 |
| | | | *Sema7a* | -7.88E-01 | 1.05E-15 |

| | | | | | |
|---|---|---|---|---|---|
| | | | *Sepp1* | -3.02E-01 | 2.34E-04 |
| | | | *Sept4* | -5.45E-01 | 2.34E-07 |
| | | | *Sept6* | -3.07E-01 | 3.16E-03 |
| | | | *Sertad4* | -6.93E-01 | 1.95E-05 |
| | | | *Sertm1* | 9.22E-01 | 1.83E-13 |
| | | | *Setd7* | -4.90E-01 | 8.75E-11 |
| | | | *Sfrp1* | 5.49E-01 | 3.45E-03 |
| | | | *Sgk1* | -6.14E-01 | 8.52E-11 |
| | | | *Sgpp2* | -1.09E+00 | 1.04E-11 |
| | | | *Sh3bgrl2* | -5.61E-01 | 3.36E-05 |
| | | | *Sh3d19* | 5.72E-01 | 1.44E-05 |
| | | | *Sh3kbp1* | 3.29E-01 | 2.46E-03 |
| | | | *Sh3rf2* | 1.65E+00 | 2.91E-08 |
| | | | *Shisa7* | 4.61E-01 | 2.42E-08 |
| | | | *Sipa1l2* | -7.16E-01 | 9.13E-08 |
| | | | *Six3* | 9.91E-01 | 2.57E-03 |
| | | | *Slc12a2* | -4.33E-01 | 6.96E-07 |
| | | | *Slc16a2* | 6.32E-01 | 1.25E-09 |
| | | | *Slc16a6* | -5.75E-01 | 7.74E-05 |
| | | | *Slc17a6* | 4.69E-01 | 6.18E-05 |
| | | | *Slc22a3* | 2.05E+00 | 1.45E-07 |
| | | | *Slc24a2* | -6.36E-01 | 1.14E-21 |
| | | | *Slc29a4* | 1.86E+00 | 5.46E-04 |
| | | | *Slc2a1* | -6.37E-01 | 7.59E-12 |
| | | | *Slc2a3* | 3.28E-01 | 1.00E-03 |
| | | | *Slc30a1* | 3.78E-01 | 1.23E-03 |
| | | | *Slc30a10* | 5.93E-01 | 1.83E-05 |
| | | | *Slc35f4* | -7.57E-01 | 1.77E-05 |
| | | | *Slc36a4* | -3.45E-01 | 1.26E-03 |
| | | | *Slc38a2* | -5.79E-01 | 4.60E-13 |
| | | | *Slc39a12* | -4.30E-01 | 2.31E-04 |
| | | | *Slc44a1* | -3.79E-01 | 1.31E-04 |
| | | | *Slc44a5* | 6.26E-01 | 2.08E-04 |
| | | | *Slc7a11* | 3.98E-01 | 1.83E-05 |
| | | | *Slit2* | -3.30E-01 | 4.62E-03 |
| | | | *Smad3* | 6.65E-01 | 4.64E-11 |
| | | | *Smarca1* | 4.03E-01 | 1.86E-05 |
| | | | *Smarca2* | 4.48E-01 | 9.91E-10 |
| | | | *Smim3* | -9.01E-01 | 3.04E-03 |
| | | | *Smoc2* | 1.14E+00 | 1.32E-09 |
| | | | *Smtn* | 1.21E+00 | 2.12E-03 |
| | | | *Snap25* | -4.41E-01 | 9.07E-11 |
| | | | *Sobp* | 3.41E-01 | 2.70E-05 |
| | | | *Socs2* | -4.57E-01 | 2.95E-03 |
| | | | *Sorcs1* | -8.53E-01 | 9.55E-19 |
| | | | *Sorcs2* | 6.25E-01 | 2.46E-05 |
| | | | *Sorcs3* | 7.89E-01 | 2.23E-18 |
| | | | *Sorl1* | -4.98E-01 | 2.72E-12 |
| | | | *Sowaha* | 7.73E-01 | 1.01E-19 |
| | | | *Sox11* | 6.79E-01 | 2.52E-12 |
| | | | *Sox4* | 3.73E-01 | 4.87E-04 |
| | | | *Sox9* | 4.50E-01 | 3.36E-04 |
| | | | *Spock1* | -3.83E-01 | 3.53E-07 |
| | | | *Spock3* | 3.71E-01 | 1.41E-05 |
| | | | *Sptssb* | -1.75E+00 | 6.92E-05 |
| | | | *Ssbp2* | 3.04E-01 | 3.55E-03 |

| | | | | | |
|---|---|---|---|---|---|
| | | | *St6gal2* | -3.23E-01 | 1.69E-04 |
| | | | *Stac2* | -1.02E+00 | 3.20E-21 |
| | | | *Steap2* | -7.88E-01 | 2.10E-10 |
| | | | *Stk32c* | 4.32E-01 | 1.00E-03 |
| | | | *Stk39* | -3.15E-01 | 3.32E-03 |
| | | | *Stxbp6* | 5.16E-01 | 1.04E-11 |
| | | | *Sulf2* | -9.20E-01 | 3.10E-22 |
| | | | *Sult1a1* | -7.59E-01 | 9.98E-04 |
| | | | *Sult4a1* | -3.74E-01 | 2.19E-05 |
| | | | *Susd5* | -8.10E-01 | 4.43E-04 |
| | | | *Syndig1* | -4.98E-01 | 4.34E-03 |
| | | | *Syndig1l* | 1.39E+00 | 3.76E-18 |
| | | | *Synj2* | 4.78E-01 | 9.04E-07 |
| | | | *Synpr* | 6.09E-01 | 8.75E-11 |
| | | | *Syt16* | 3.85E-01 | 3.13E-05 |
| | | | *Syt17* | 9.63E-01 | 1.77E-20 |
| | | | *Syt2* | -1.10E+00 | 1.50E-23 |
| | | | *Tac1* | 5.74E-01 | 1.92E-04 |
| | | | *Tanc1* | -6.76E-01 | 4.98E-07 |
| | | | *Tbc1d4* | -5.41E-01 | 1.01E-03 |
| | | | *Tdo2* | 1.68E+00 | 2.61E-03 |
| | | | *Tenm3* | 3.39E-01 | 1.42E-03 |
| | | | *Tfcp2l1* | -8.05E-01 | 8.19E-05 |
| | | | *Tgfa* | 5.52E-01 | 8.41E-04 |
| | | | *Thra* | 5.17E-01 | 1.36E-11 |
| | | | *Tiam1* | 3.43E-01 | 2.15E-04 |
| | | | *Timp2* | 5.02E-01 | 3.38E-10 |
| | | | *Tle3* | 4.96E-01 | 9.75E-05 |
| | | | *Tlr7* | -8.41E-01 | 6.52E-04 |
| | | | *Tmeff1* | -3.71E-01 | 9.28E-05 |
| | | | *Tmem130* | 3.12E-01 | 4.18E-03 |
| | | | *Tmem132e* | 1.12E+00 | 3.90E-03 |
| | | | *Tmem150c* | 3.96E-01 | 2.71E-03 |
| | | | *Tmem158* | 4.32E-01 | 3.96E-05 |
| | | | *Tmem184c* | -3.21E-01 | 1.98E-04 |
| | | | *Tmem229a* | -4.30E-01 | 3.37E-06 |
| | | | *Tmem255a* | 1.36E+00 | 1.45E-24 |
| | | | *Tmem44* | -3.25E-01 | 3.13E-03 |
| | | | *Tmem88b* | -7.86E-01 | 3.32E-13 |
| | | | *Tmtc4* | 4.91E-01 | 3.52E-03 |
| | | | *Tns1* | -4.79E-01 | 1.52E-04 |
| | | | *Tox* | -7.19E-01 | 1.99E-08 |
| | | | *Tox3* | 8.58E-01 | 1.23E-08 |
| | | | *Trafd1* | 5.12E-01 | 1.91E-03 |
| | | | *Trp53i11* | 9.54E-01 | 1.24E-13 |
| | | | *Trp53inp1* | -4.88E-01 | 1.94E-05 |
| | | | *Trp53inp2* | -4.67E-01 | 5.97E-08 |
| | | | *Trpc3* | -9.50E-01 | 6.92E-09 |
| | | | *Trpc6* | 8.65E-01 | 1.11E-09 |
| | | | *Tsc22d3* | -7.42E-01 | 2.67E-13 |
| | | | *Tshz1* | -3.40E-01 | 2.46E-03 |
| | | | *Tspan2* | -7.67E-01 | 3.56E-23 |
| | | | *Tspan5* | -4.34E-01 | 1.14E-07 |
| | | | *Ttc19* | -3.39E-01 | 3.39E-04 |
| | | | *Ttc39b* | -6.12E-01 | 1.17E-14 |
| | | | *Ttll5* | -4.36E-01 | 7.14E-04 |

| | | | | | |
|---|---|---|---|---|---|
| | | | *Ttr* | 5.40E-01 | 2.75E-04 |
| | | | *Tubb2a* | 3.41E-01 | 2.74E-03 |
| | | | *Ube2e3* | 4.19E-01 | 2.40E-04 |
| | | | *Ublcp1* | -4.25E-01 | 8.68E-04 |
| | | | *Ubxn2a* | -4.50E-01 | 1.61E-06 |
| | | | *Ugt8a* | -6.03E-01 | 1.02E-10 |
| | | | *Unc5c* | -3.31E-01 | 1.60E-03 |
| | | | *Usp11* | 4.96E-01 | 6.77E-07 |
| | | | *Usp27x* | 6.70E-01 | 7.77E-05 |
| | | | *Usp54* | -4.91E-01 | 7.82E-07 |
| | | | *Vamp1* | -9.38E-01 | 6.61E-22 |
| | | | *Vat1l* | 9.06E-01 | 4.67E-18 |
| | | | *Vgf* | 3.63E-01 | 1.26E-03 |
| | | | *Vgll3* | -1.73E+00 | 1.79E-06 |
| | | | *Vmp1* | -3.85E-01 | 4.39E-05 |
| | | | *Vwc2l* | 7.29E-01 | 1.23E-05 |
| | | | *Wdr6* | 9.63E-01 | 1.01E-12 |
| | | | *Wfs1* | 1.16E+00 | 6.97E-24 |
| | | | *Whrn* | -1.01E+00 | 7.09E-08 |
| | | | *Xdh* | -1.24E+00 | 4.31E-05 |
| | | | *Ypel1* | 6.03E-01 | 8.91E-04 |
| | | | *Zbtb16* | -7.10E-01 | 1.54E-14 |
| | | | *Zbtb46* | 7.40E-01 | 4.10E-06 |
| | | | *Zcchc12* | 7.88E-01 | 1.21E-08 |
| | | | *Zcchc24* | -4.17E-01 | 1.10E-04 |
| | | | *Zdhhc15* | 5.40E-01 | 3.34E-04 |
| | | | *Zdhhc2* | -7.14E-01 | 1.86E-14 |
| | | | *Zfp365* | -3.24E-01 | 1.96E-05 |
| | | | *Zfp385a* | -5.86E-01 | 1.81E-03 |
| | | | *Zfp385b* | -5.26E-01 | 2.54E-07 |
| | | | *Zfp462* | 3.19E-01 | 2.71E-03 |
| | | | *Zfp57* | 5.32E-01 | 2.94E-03 |
| | | | *Zfp618* | 8.13E-01 | 3.73E-03 |
| | | | *Zfp697* | 4.73E-01 | 5.07E-06 |
| | | | *Zfp831* | 6.41E-01 | 1.57E-09 |
| | | | *Zkscan16* | 4.89E-01 | 8.25E-05 |
| | | | *Zmat4* | -1.18E+00 | 2.60E-38 |
| | | | *Zmiz2* | -3.95E-01 | 1.23E-04 |
| | | | *Zmym3* | 3.49E-01 | 9.74E-04 |
| | | | *Zscan18* | 5.06E-01 | 3.41E-03 |

| Table 3.2. Overlaps between *Foxp1*$^{cKO}$ DEGs and SFARI-ASD genes. | | | | | | | |
|---|---|---|---|---|---|---|---|
| Up-regulated *Foxp1*$^{cKO}$ DEGs | | | | Down-regulated *Foxp1*$^{cKO}$ DEGs | | | |
| **SFARI/CTX** | **SFARI/HIP** | **CTX/HIP** | **SFARI/CTX/HIP** | **SFARI/CTX** | **SFARI/HIP** | **CTX/HIP** | **SFARI/CTX/HIP** |
| *Arhgap33* | *C4b* | *2810459M11Rik* | *Drd1* | *1190002N15Rik* | *Ar* | *3110035E14Rik* | *Foxp1* |
| *Auts2* | *Cd44* | *Adra2a* | *Kirrel3* | *Astn2* | *Brinp1* | *Aldh1a1* | *Slc24a2* |
| *Bdnf* | *Foxp2* | *Ankrd6* | *Mef2c* | *Atp10a* | *Cacna1e* | *Asap2* | *Zbtb16* |
| *C77370* | *Mndal* | *Arpp21* | *Ppp1r1b* | *Atp2b2* | *Cadm2* | *Cadps* | |
| *Cacna1c* | *Scn7a* | *Atp2b4* | | *Bcas1* | *Cdh8* | *Cdh12* | |
| *Cadm1* | *Slc4a10* | *Bmp3* | | *Cacna1a* | *Chrm3* | *Dkk3* | |
| *Cntn6* | | *Btg2* | | *Cacna1i* | *Cntnap2* | *Dzip1* | |
| *Cntnap3* | | *Calb1* | | *Cadps2* | *Cntnap5c* | *Endod1* | |
| *Dapk1* | | *Camk2d* | | *Camk4* | *Epha6* | *Fmn1* | |
| *Drd2* | | *Cdhr1* | | *Camta1* | *Grin2a* | *Fndc5* | |
| *Egr2* | | *Col5a1* | | *Cep290* | *Kcnd2* | *Frrs1l* | |
| *Esr1* | | *Col5a2* | | *Dagla* | *Kcnq3* | *Gabra5* | |
| *Gap43* | | *Cpne7* | | *Dpp4* | *Lpl* | *Glt8d2* | |
| *Gda* | | *Fos* | | *Dst* | *Mc4r* | *Il1r1* | |
| *Gpr85* | | *Gm765* | | *Efr3a* | *Ntng1* | *Itpr1* | |
| *Grm1* | | *Gnb4* | | *Exoc6b* | *Ptgs2* | *Kcnab2* | |
| *Grm5* | | *Gpr88* | | *Gatm* | *Rasd1* | *Kcnh7* | |
| *Htr7* | | *Grin3a* | | *Gpr37* | *Zfp804a* | *Kcnq5* | |
| *Il1rapl1* | | *Hrk* | | *Hcn1* | | *Lsm11* | |
| *Itga4* | | *Kcng1* | | *Htr2a* | | *Lynx1* | |
| *Kit* | | *Kcng3* | | *Il1rapl2* | | *Pgr* | |
| *Lamb1* | | *Mfge8* | | *Kcnj10* | | *Plin4* | |
| *Lpl* | | *Necab1* | | *Kif13b* | | *Pou3f1* | |
| *Mapk3* | | *Nectin1* | | *Klc2* | | *Sacs* | |
| *Nlgn3* | | *Nnat* | | *Mal* | | *Slc2a1* | |
| *Nos1* | | *Nov* | | *Nefl* | | *Sult1a1* | |
| *Nr3c2* | | *Penk* | | *Nos1ap* | | *Zdhhc2* | |
| *Nrp2* | | *Pkd2l1* | | *Pde4a* | | | |
| *Ntrk3* | | *Plxnc1* | | *Prkcb* | | | |
| *Oxtr* | | *Ptpn14* | | *Ptprb* | | | |
| *Pcdh15* | | *Sfrp1* | | *Pvalb* | | | |
| *Pcdh19* | | *Slc7a11* | | *Rapgef4* | | | |
| *Pcdh8* | | *Smtn* | | *Rims3* | | | |
| *Pdzd4* | | *Syndig1l* | | *Scn1a* | | | |
| *Prex1* | | *Tac1* | | *Snap25* | | | |
| *Ptgs2* | | *Timp2* | | *Stk39* | | | |
| *Reln* | | *Tmem255a* | | *Zfp385b* | | | |
| *Rps6ka2* | | *Tox3* | | | | | |
| *Scn5a* | | *Ttr* | | | | | |
| *Sdc2* | | *Vat1l* | | | | | |
| *Sh3kbp1* | | | | | | | |
| *Slc29a4* | | | | | | | |
| *Smarca2* | | | | | | | |
| *Syt17* | | | | | | | |

| | | | | | | | |
|---|---|---|---|---|---|---|---|
| *Tdo2* | | | | | | | |
| *Thra* | | | | | | | |
| *Trpc6* | | | | | | | |
| *Zfp462* | | | | | | | |

| Table 3.3. Overlaps between *Foxp1*$^{cKO}$ HIP and *Foxp1*$^{+/-}$ HIP DEGs. | | | |
|---|---|---|---|
| **Up-regulated DEGs** | | **Down-regulated DEGs** | |
| ***Foxp1*$^{+/-}$ HIP DEGs** | ***Foxp1*$^{+/-}$ HIP/*Foxp1*$^{cKO}$ HIP** | ***Foxp1*$^{+/-}$ HIP DEGs** | ***Foxp1*$^{+/-}$ HIP/*Foxp1*$^{cKO}$ HIP** |
| *1700048O20Rik* | *Adra2a* | *1700017B05Rik* | *1700024P16Rik* |
| *4932411E22Rik* | *Atp2b4* | *1700024P16Rik* | *Akap13* |
| *5430417L22Rik* | *Calb2* | *2900026A02Rik* | *Camk1d* |
| *6430573F11Rik* | *Camk2d* | *4933426M11Rik* | *Camk2b* |
| *9430021M05Rik* | *Kcng3* | *6030419C18Rik* | *Ccbe1* |
| *A230065H16Rik* | *Meis2* | *9230009I02Rik* | *Chgb* |
| *Abat* | *Necab1* | *9630033F20Rik* | *Chrm3* |
| *Adcy7* | *Prkar2b* | *A330070K13Rik* | *Cpne4* |
| *Adcyap1r1* | *Scn9a* | *Aak1* | *Dusp5* |
| *Adra2a* | *Slc35f1* | *Acap3* | *Epha4* |
| *Agbl5* | *Tcerg1l* | *Acot3* | *Foxp1* |
| *Ahi1* | *Timp2* | *Acsl5* | *Gabra5* |
| *Amotl1* | *Tmem255a* | *Adam11* | *Gpr22* |
| *Angptl4* | | *Adamts3* | *Hpca* |
| *Ankrd34b* | | *Adamts8* | *Hs3st4* |
| *Ankrd34c* | | *Adora1* | *Htr4* |
| *Ankrd55* | | *AI115009* | *Kcnq5* |
| *Ankrd63* | | *Ak5* | *Lpl* |
| *Ankrd66* | | *Akap13* | *Lsm11* |
| *Ano1* | | *Amigo2* | *Lynx1* |
| *Ano2* | | *Amph* | *Mmd* |
| *Apold1* | | *Anxa11* | *Neto1* |
| *Arhgap36* | | *Ap2a2* | *Olfml2b* |
| *Arhgap6* | | *Arc* | *Pcdh20* |
| *Atp2b4* | | *Arg2* | *Pcsk2* |
| *Atp6ap1l* | | *Arhgef17* | *Plk2* |
| *Atp6v1c2* | | *Arhgef25* | *Prkca* |
| *AW551984* | | *Arhgef26* | *Prkcg* |
| *Baiap3* | | *Asb11* | *Prss35* |
| *BC005764* | | *Asph* | *Rasgrp1* |
| *BC089491* | | *Bcl11a* | *Rasl11b* |
| *Bex1* | | *Bsn* | *Sema3e* |
| *C130060K24Rik* | | *Cabp1* | *Slc24a2* |
| *C130074G19Rik* | | *Cacna2d3* | *Stxbp5l* |
| *Cacna1g* | | *Cacnb3* | *Wbscr17* |
| *Cacna2d2* | | *Camk1d* | *Wipf3* |
| *Cacng5* | | *Camk2a* | |
| *Calb2* | | *Camk2b* | |
| *Camk2d* | | *Camk4* | |
| *Cbln1* | | *Camta2* | |
| *Cdc42ep3* | | *Ccbe1* | |
| *Cdh13* | | *Ccdc3* | |
| *Cdh18* | | *Cd109* | |
| *Cdh22* | | *Cdc40* | |

| | | | |
|---|---|---|---|
| *Cdh4* | | *Cdk14* | |
| *Cdh6* | | *Cdkl2* | |
| *Cdh7* | | *Chgb* | |
| *Chn2* | | *Chn1* | |
| *Chrdl1* | | *Chrm3* | |
| *Chrm2* | | *Chrna7* | |
| *Cit* | | *Cidea* | |
| *Cited1* | | *Cldn22* | |
| *Clic4* | | *Cldn26* | |
| *Col15a1* | | *Clmp* | |
| *Col23a1* | | *Clstn2* | |
| *Col25a1* | | *Cnksr2* | |
| *Col26a1* | | *Col6a1* | |
| *Ctxn3* | | *Cpeb1* | |
| *Cxxc4* | | *Cplx2* | |
| *Ddo* | | *Cpne4* | |
| *Dlec1* | | *Cpne6* | |
| *Dlk1* | | *Crls1* | |
| *Dlx1* | | *Crmp1* | |
| *Dlx2* | | *Crym* | |
| *Dlx6* | | *Ctxn1* | |
| *Dnah1* | | *Cyp26b1* | |
| *Dnah7b* | | *Dnm1* | |
| *Dnm3* | | *Dock9* | |
| *Doc2g* | | *Dusp5* | |
| *Dpp10* | | *Dusp6* | |
| *Drd3* | | *Eepd1* | |
| *E030019B06Rik* | | *Enc1* | |
| *Ebf3* | | *Enox2* | |
| *Ece2* | | *Epdr1* | |
| *Ecel1* | | *Epha4* | |
| *Ednrb* | | *Erc2* | |
| *Efna5* | | *Exph5* | |
| *Eps8* | | *Faah* | |
| *Exoc3l4* | | *Fam13c* | |
| *F2rl2* | | *Fam19a1* | |
| *Fam107a* | | *Fam212b* | |
| *Fam196b* | | *Fbxl16* | |
| *Fam65b* | | *Fgf5* | |
| *Farp1* | | *Fhl2* | |
| *Fgd5* | | *Filip1* | |
| *Fgf1* | | *Flrt3* | |
| *Fgf3* | | *Foxg1* | |
| *Fnbp1l* | | *Foxp1* | |
| *Fndc9* | | *Frzb* | |
| *Fzd1* | | *Gabra5* | |
| *Gaa* | | *Gadd45b* | |
| *Gabra3* | | *Gal3st3* | |

| | | | |
|---|---|---|---|
| *Gabrg1* | | *Garem* | |
| *Gabrg3* | | *Golm1* | |
| *Gad1* | | *Gpc1* | |
| *Gad2* | | *Gpr22* | |
| *Gal* | | *Gpr45* | |
| *Galnt13* | | *Grik4* | |
| *Gap43* | | *Hapln4* | |
| *Gfra1* | | *Homer3* | |
| *Gfra2* | | *Hpca* | |
| *Ghr* | | *Hs3st4* | |
| *Glp1r* | | *Htr3a* | |
| *Glra2* | | *Htr4* | |
| *Glra3* | | *Htr6* | |
| *Gm14204* | | *Igfbp4* | |
| *Gm514* | | *Il16* | |
| *Gm5607* | | *Il34* | |
| *Gng4* | | *Islr2* | |
| *Gpc3* | | *Itga7* | |
| *Gpr101* | | *Itgbl1* | |
| *Gpr133* | | *Iyd* | |
| *Gpr153* | | *Kcnmb4* | |
| *Gpr165* | | *Kcnq5* | |
| *Gpr4* | | *Kcnv1* | |
| *Gprasp2* | | *Khdrbs3* | |
| *Gpx3* | | *Klf10* | |
| *Grb10* | | *Klhl2* | |
| *Grid2* | | *Klhl40* | |
| *Grid2ip* | | *Klk10* | |
| *Grik3* | | *Krt73* | |
| *Grin2d* | | *Large* | |
| *Grip2* | | *Lingo1* | |
| *Grk5* | | *Lmo3* | |
| *Grm4* | | *Lmo4* | |
| *Grm8* | | *Lpl* | |
| *Grtp1* | | *Lrrn2* | |
| *Hap1* | | *Lsm11* | |
| *Hfe2* | | *Ly6e* | |
| *Hrasls* | | *Lynx1* | |
| *Hs3st2* | | *Mctp1* | |
| *Hs6st2* | | *Mcur1* | |
| *Id4* | | *Mir22hg* | |
| *Igfbpl1* | | *Mmd* | |
| *Il13ra1* | | *Mmp17* | |
| *Il4ra* | | *Mpp3* | |
| *Isl1* | | *Msra* | |
| *Itih3* | | *Msrb2* | |
| *Itpr3* | | *Mtmr12* | |
| *Kank4* | | *Napb* | |

| | | | |
|---|---|---|---|
| *Kcng3* | | *Ndrg3* | |
| *Kcnh6* | | *Nefl* | |
| *Kcnip1* | | *Neto1* | |
| *Kcnn3* | | *Nkd2* | |
| *Kcnt1* | | *Nptx1* | |
| *Klhdc8a* | | *Npy2r* | |
| *Lama3* | | *Nr3c2* | |
| *Lhfpl3* | | *Nr4a1* | |
| *Lin28b* | | *Nr4a3* | |
| *Lrrc1* | | *Nrgn* | |
| *Lrrtm3* | | *Nrip3* | |
| *Luzp2* | | *Nsmf* | |
| *Lzts1* | | *Nt5dc3* | |
| *Mab21l1* | | *Numbl* | |
| *Magi1* | | *Ociad2* | |
| *Man1a* | | *Ogfrl1* | |
| *Mctp2* | | *Olfm1* | |
| *Megf6* | | *Olfml2b* | |
| *Meis2* | | *Osr1* | |
| *Met* | | *Otos* | |
| *Myh7* | | *Pcdh20* | |
| *Myo10* | | *Pcsk2* | |
| *Nap1l5* | | *Pde1a* | |
| *Ndnf* | | *Pfkl* | |
| *Necab1* | | *Pgbd5* | |
| *Ngb* | | *Pgm2l1* | |
| *Nhs* | | *Pip4k2c* | |
| *Notch4* | | *Pip5k1c* | |
| *Nova1* | | *Pkp2* | |
| *Nrsn2* | | *Plch2* | |
| *Ntng1* | | *Plk2* | |
| *Nts* | | *Ppp1r1a* | |
| *Otof* | | *Prickle2* | |
| *Pcdh15* | | *Prkca* | |
| *Pde3a* | | *Prkce* | |
| *Pde9a* | | *Prkcg* | |
| *Peg10* | | *Prrt2* | |
| *Peg3* | | *Prss35* | |
| *Pgap1* | | *Ptk2b* | |
| *Pipox* | | *Pvrl3* | |
| *Pitpnm3* | | *Pvrl4* | |
| *Plcb4* | | *R3hdm4* | |
| *Plch1* | | *Rab15* | |
| *Pld5* | | *Rab3d* | |
| *Plekha7* | | *Rapgef5* | |
| *Pnoc* | | *Rasgrp1* | |
| *Prdm16* | | *Rasl11a* | |
| *Prkar2b* | | *Rasl11b* | |

| | | | |
|---|---|---|---|
| *Prkg2* | | *Raver2* | |
| *Prokr2* | | *Rem2* | |
| *Ptch1* | | *Rgs14* | |
| *Ptch2* | | *Rnf112* | |
| *Ptchd1* | | *Rnf182* | |
| *Ptgfrn* | | *Rprml* | |
| *Rapgef3* | | *Scn1b* | |
| *Rasa4* | | *Sema3e* | |
| *Rbms1* | | *Sepw1* | |
| *Rbms3* | | *Serpina3n* | |
| *Rcan3* | | *Sh3gl2* | |
| *Rec8* | | *Slc17a8* | |
| *Resp18* | | *Slc24a2* | |
| *Ret* | | *Slc25a22* | |
| *Rgag4* | | *Slc2a6* | |
| *Rims3* | | *Slc4a7* | |
| *Rnf144b* | | *Slc6a15* | |
| *Rps6ka2* | | *Slc7a4* | |
| *Rrad* | | *Slc7a8* | |
| *Sall3* | | *Sms* | |
| *Scarf2* | | *Snap25* | |
| *Scn9a* | | *Snca* | |
| *Sesn3* | | *Sort1* | |
| *Sfrp2* | | *Speg* | |
| *Slc10a4* | | *Spock1* | |
| *Slc17a6* | | *Sprn* | |
| *Slc1a3* | | *Srl* | |
| *Slc22a3* | | *St6galnac5* | |
| *Slc25a34* | | *Stim2* | |
| *Slc32a1* | | *Stx1a* | |
| *Slc35f1* | | *Stxbp5l* | |
| *Slc6a11* | | *Sv2b* | |
| *Slc7a3* | | *Syce2* | |
| *Slc8a3* | | *Syn1* | |
| *Slitrk6* | | *Syn2* | |
| *Sorcs1* | | *Syndig1* | |
| *Sox1* | | *Tesc* | |
| *Sp9* | | *Tmem151b* | |
| *Spint1* | | *Tmem178* | |
| *Spp1* | | *Tmem252* | |
| *Srgap1* | | *Tmem59l* | |
| *Stac* | | *Tnfaip8l3* | |
| *Sv2c* | | *Trnp1* | |
| *Synm* | | *Ttl* | |
| *Tcerg1l* | | *Tuba8* | |
| *Tcfl5* | | *Unc5a* | |
| *Tec* | | *Unc5c* | |
| *Thrb* | | *Wasf1* | |

| | | | |
|---|---|---|---|
| *Thrsp* | | *Wbscr17* | |
| *Timp2* | | *Wipf3* | |
| *Tmem130* | | *Ywhah* | |
| *Tmem158* | | *Zbtb18* | |
| *Tmem163* | | *Zfp189* | |
| *Tmem255a* | | | |
| *Tmem91* | | | |
| *Tmie* | | | |
| *Tmsb10* | | | |
| *Tox* | | | |
| *Tox2* | | | |
| *Tpd52l1* | | | |
| *Trpc3* | | | |
| *Trpc7* | | | |
| *Unc13c* | | | |
| *Usp13* | | | |
| *Usp29* | | | |
| *Usp51* | | | |
| *Vat1* | | | |
| *Vill* | | | |
| *Vstm2l* | | | |
| *Vwc2l* | | | |
| *Wdr6* | | | |
| *Whrn* | | | |
| *Zbtb7c* | | | |
| *Zcchc12* | | | |
| *Zdbf2* | | | |
| *Zfhx3* | | | |
| *Zfp423* | | | |
| *Zfp503* | | | |
| *Zfp521* | | | |
| *Zfp92* | | | |
| *Zic1* | | | |
| *Zic2* | | | |
| *Zic3* | | | |
| *Zic4* | | | |
| *Zim1* | | | |

| Table 3.4. Overlaps between *Foxp1*$^{cKO}$ HIP DEGs and other datasets. | | | |
|---|---|---|---|
| **Overlaps with Zeisel et al., Science, 2015** | | **Overlaps with Ryan et al., PLoS ONE, 2012** | |
| **Up-regulated overlaps** | **Down-regulated overlaps** | **Up-regulated overlaps** | **Down-regulated overlaps** |
| *Dcn* | *Ar* | *Camk2d* | *Ccnd1* |
| *Etv1* | *Arpc2* | *Gnb4* | *Dsp* |
| *Itgbl1* | *Asap2* | *Grin3a* | *Dusp5* |
| *Plxnc1* | *Cacna1e* | *Runx1t1* | *Foxp1* |
| *Runx1t1* | *Cadm2* | | *Lynx1* |
| | *Cds1* | | *Prkca* |
| | *Epha6* | | *Rasd1* |
| | *Fgf10* | | *Sorcs3* |
| | *Gabra5* | | |
| | *Gpr161* | | |
| | *Grem1* | | |
| | *Grin2a* | | |
| | *Hectd2* | | |
| | *Htr4* | | |
| | *Hunk* | | |
| | *Kcnq3* | | |
| | *Ksr1* | | |
| | *Lct* | | |
| | *Matn2* | | |
| | *Mc4r* | | |
| | *Ndst3* | | |
| | *Ndst4* | | |
| | *Ntng1* | | |
| | *Osbpl6* | | |
| | *Plxna1* | | |
| | *Pou3f1* | | |
| | *Slc9a2* | | |
| | *Slc9a4* | | |
| | *Spink8* | | |
| | *Wbscr17* | | |
| | *Wipf3* | | |

| **Extended Data Table 3.6-1. Representative *Foxp1*$^{cKO}$ neocortex and hippocampus DEG REVIGO GO categories.** | | | | |
|---|---|---|---|---|
| ***Foxp1*$^{cKO}$ DEGs** | **Neocortex** | | | |
| | **Category ID** | **Name** | **p-value** | **q-value FDR (B&H)** |
| **Up-regulated categories** | MP:0002062 | abnormal associative learning | 1.69E-14 | 7.11E-11 |
| | MP:0002206 | abnormal CNS synaptic transmission | 1.93E-13 | 3.23E-10 |
| | MP:0003635 | abnormal synaptic transmission | 2.51E-13 | 3.23E-10 |
| | MP:0002063 | abnormal learning/memory/conditioning | 3.61E-13 | 3.23E-10 |
| | MP:0014114 | abnormal cognition | 3.84E-13 | 3.23E-10 |
| | MP:0003633 | abnormal nervous system physiology | 7.49E-13 | 5.25E-10 |
| | MP:0001462 | abnormal avoidance learning behavior | 1.87E-11 | 1.12E-08 |
| | MP:0002572 | abnormal emotion/affect behavior | 4.20E-11 | 2.21E-08 |
| | MP:0002065 | abnormal fear/anxiety-related behavior | 2.34E-10 | 1.10E-07 |
| | MP:0002799 | abnormal passive avoidance behavior | 1.31E-08 | 5.49E-06 |
| **Down-regulated categories** | GO:0022008 | neurogenesis | 2.62E-13 | 1.25E-09 |
| | GO:0048666 | neuron development | 9.35E-13 | 1.83E-09 |
| | GO:0048699 | generation of neurons | 1.15E-12 | 1.83E-09 |
| | GO:0031175 | neuron projection development | 6.26E-12 | 7.49E-09 |
| | GO:0007272 | ensheathment of neurons | 1.43E-11 | 1.14E-08 |
| | GO:0008366 | axon ensheathment | 1.43E-11 | 1.14E-08 |
| | GO:0030182 | neuron differentiation | 2.93E-11 | 2.00E-08 |
| | GO:0098916 | anterograde trans-synaptic signaling | 6.16E-11 | 2.95E-08 |
| | GO:0099537 | trans-synaptic signaling | 6.16E-11 | 2.95E-08 |
| | GO:0007268 | chemical synaptic transmission | 6.16E-11 | 2.95E-08 |
| ***Foxp1*$^{cKO}$ DEGs** | **Hippocampus** | | | |
| | **Category ID** | **Name** | **p-value** | **q-value FDR (B&H)** |
| **Up-regulated categories** | GO:0009628 | response to abiotic stimulus | 7.06E-09 | 1.19E-05 |
| | GO:0007610 | behavior | 7.74E-09 | 1.19E-05 |
| | GO:0044708 | single-organism behavior | 2.55E-07 | 2.61E-04 |
| | GO:0050877 | neurological system process | 4.56E-07 | 3.50E-04 |
| | GO:0010562 | positive regulation of phosphorus metabolic process | 8.45E-07 | 4.33E-04 |
| | GO:0045937 | positive regulation of phosphate metabolic process | 8.45E-07 | 4.33E-04 |
| | GO:0007611 | learning or memory | 1.30E-06 | 5.69E-04 |
| | GO:0022008 | neurogenesis | 1.73E-06 | 5.77E-04 |
| | GO:0030182 | neuron differentiation | 1.76E-06 | 5.77E-04 |
| | GO:0007612 | learning | 1.88E-06 | 5.77E-04 |
| | MP:0003633 | abnormal nervous system physiology | 5.11E-07 | 5.09E-04 |
| | MP:0001469 | abnormal contextual conditioning behavior | 6.21E-07 | 5.09E-04 |

| | | | | |
|---|---|---|---|---|
| **Down-regulated categories** | MP:0002062 | abnormal associative learning | 6.34E-07 | 5.09E-04 |
| | MP:0001473 | reduced long term potentiation | 7.58E-07 | 5.09E-04 |
| | MP:0003635 | abnormal synaptic transmission | 1.05E-06 | 5.64E-04 |
| | MP:0002063 | abnormal learning/memory/conditioning | 2.18E-06 | 8.57E-04 |
| | MP:0014114 | abnormal cognition | 2.23E-06 | 8.57E-04 |
| | MP:0001468 | abnormal temporal memory | 3.56E-06 | 1.19E-03 |
| | MP:0002696 | decreased circulating glucagon level | 3.97E-06 | 1.19E-03 |
| | MP:0002206 | abnormal CNS synaptic transmission | 6.36E-06 | 1.71E-03 |

**Extended Data Table 3.6-2. Overlaps between *Foxp1*$^{cKO}$ DEGs and cell-type-specific genes.**

| Cell-type-specific gene lists (Zeisel et al., 2015) | | ***Foxp1*$^{cKO}$ CTX DEGs** | | | | | |
|---|---|---|---|---|---|---|---|
| | | **Total** | | **Up-regulated** | | **Down-regulated** | |
| | | 874 | | 418 | | 456 | |
| **Cell type** | **Genes** | Overlap | p-value | Overlap | p-value | Overlap | p-value |
| **Astrocytes** | 240 | 15 | 5.83E-01 | 3 | 9.79E-01 | 12 | 1.09E-01 |
| **CA1** | 409 | 51 | **3.77E-06** | 40 | **8.56E-11** | 11 | 8.13E-01 |
| **Endothelial** | 353 | 25 | 3.35E-01 | 10 | 6.48E-01 | 15 | 2.07E-01 |
| **Ependymal** | 484 | 20 | 9.89E-01 | 17 | 3.20E-01 | 3 | 9.99E-01 |
| **Interneurons** | 365 | 43 | **8.35E-05** | 28 | **8.42E-06** | 15 | 2.44E-01 |
| **Microglia** | 436 | 10 | 9.99E-01 | 4 | 9.99E-01 | 6 | 9.97E-01 |
| **Mural cells** | 155 | 7 | 8.77E-01 | 3 | 8.59E-01 | 4 | 7.68E-01 |
| **Oligodendrocytes** | 453 | 50 | **1.20E-04** | 4 | 9.99E-01 | 46 | **1.67E-11** |
| **S1** | 294 | 60 | **5.90E-16** | 20 | **7.70E-04** | 40 | **3.29E-14** |
| **Cell-type-specific gene lists (Zeisel et al., 2015)** | | ***Foxp1*$^{cKO}$ HIP DEGs** | | | | | |
| | | **Total** | | **Up-regulated** | | **Down-regulated** | |
| | | 243 | | 99 | | 144 | |
| **Cell type** | **Genes** | Overlap | p-value | Overlap | p-value | Overlap | p-value |
| **Astrocytes** | 240 | 4 | 6.24E-01 | 2 | 5.24E-01 | 2 | 7.25E-01 |
| **CA1** | 409 | 36 | **1.66E-15** | 5 | 1.77E-01 | 31 | **2.93E-18** |
| **Endothelial** | 353 | 3 | 9.53E-01 | 1 | 9.26E-01 | 2 | 8.91E-01 |
| **Ependymal** | 484 | 9 | 4.99E-01 | 8 | 2.40E-02 | 1 | 9.94E-01 |
| **Interneurons** | 365 | 13 | **1.42E-02** | 10 | **3.10E-04** | 3 | 7.46E-01 |
| **Microglia** | 436 | 1 | 9.99E-01 | 1 | 9.60E-01 | 0 | 1.00 |
| **Mural cells** | 155 | 2 | 7.68E-01 | 1 | 6.79E-01 | 1 | 8.09E-01 |
| **Oligodendrocytes** | 453 | 3 | 9.88E-01 | 2 | 8.46E-01 | 1 | 9.92E-01 |
| **S1** | 294 | 14 | **8.37E-04** | 10 | **5.46E-05** | 4 | 3.78E-01 |

| Extended Data Table 3.7-1. Top 20 increases and decreases to regional brain volumes in *Foxp1*$^{cKO}$ mice. | | | | | |
|---|---|---|---|---|---|
| **Areas with decreased volumes** | | | **Areas with increased volumes** | | |
| **Brain Area** | **% Diff** | **FDR** | **Brain Area** | **% Diff** | **FDR** |
| Hippocampus | -13.88 | 1.64E-05 | Trunk of lobules 6 & 8 - white matter | 14.98 | 1.68E-03 |
| Cingulate cortex - area 32 | -13.63 | 2.13E-04 | Paraflocculus PFL | 14.48 | 1.94E-03 |
| Secondary visual cortex - mediomedial area | -12.68 | 4.63E-04 | Paramedian lobule | 14.28 | 7.10E-03 |
| Stria terminalis | -12.24 | 2.63E-06 | Lobule 8 - white matter | 13.63 | 1.50E-02 |
| Dentate gyrus | -11.65 | 1.53E-03 | Paraflocculus - white matter | 13.01 | 3.46E-03 |
| Secondary visual cortex - mediolateral area | -11.39 | 2.13E-04 | Lateral olfactory tract | 12.89 | 4.35E-04 |
| Internal capsule | -11.01 | 2.63E-06 | Copula - white matter | 12.83 | 1.03E-02 |
| Corpus callosum | -10.99 | 2.40E-05 | Lobule 6 - declive | 12.60 | 4.34E-03 |
| Medial orbital cortex | -10.98 | 1.34E-03 | Lobule 7 - tuber or folium | 12.48 | 9.67E-03 |
| Frontal association cortex | -10.88 | 7.18E-05 | Ventral tegmental decussation | 12.03 | 4.63E-04 |
| Stratum granulosum | -10.36 | 2.64E-03 | Subependymale zone/rhinocele | 11.63 | 2.40E-05 |
| Primary visual cortex - monocular area | -10.03 | 2.63E-03 | Lobules 4 & 5 - culmen ventral and dorsal | 11.61 | 2.63E-03 |
| Prepara subiculum | -9.79 | 4.56E-02 | Posterior commissure | 11.39 | 2.13E-04 |
| Cingulate cortex - area 29b | -9.24 | 4.54E-02 | Anterior lobule - white matter | 11.31 | 2.63E-03 |
| Primary visual cortex | -9.14 | 7.31E-03 | Crus 2 - white matter | 11.20 | 2.63E-03 |
| Primary somatosensory cortex - forelimb region | -8.84 | 9.85E-04 | Lobule 3 - white matter | 11.15 | 1.85E-02 |
| Primary auditory cortex | -8.70 | 1.76E-02 | Lobule 3 - central lobule dorsal | 11.08 | 2.11E-02 |
| Primary visual cortex - binocular area | -8.69 | 8.21E-04 | Anterior lobule - lobules 4 & 5 | 10.95 | 3.00E-03 |
| Primary somatosensory cortex - hindlimb region | -8.33 | 5.84E-04 | Lobules 4 & 5 - white matter | 10.79 | 3.45E-03 |
| Cingulate cortex area 24b | -8.28 | 6.19E-03 | Lobules 6 & 7 - white matter | 10.56 | 6.19E-03 |

## REFERENCES FOR CHAPTER THREE


Ageranioti-Belanger S, Brunet S, D'Anjou G, Tellier G, Boivin J, Gauthier M (2012) Behaviour disorders in children with an intellectual disability. Paediatr Child Health 17:84-88.

Anders S, Huber W (2010) Differential expression analysis for sequence count data. Genome biology 11:R106.

Anders S, Pyl PT, Huber W (2015) HTSeq--a Python framework to work with high-throughput sequencing data. Bioinformatics 31:166-169.

Andrews S (2010) FastQC: a quality control tool for high throughput sequence data. In.

Araujo DJ, Anderson AG, Berto S, Runnels W, Harper M, Ammanuel S, Rieger MA, Huang HC, Rajkovich K, Loerwald KW, Dekker JD, Tucker HO, Dougherty JD, Gibson JR, Konopka G (2015) FoxP1 orchestration of ASD-relevant signaling pathways in the striatum. Genes & development 29:2081-2096.

Bacon C, Rappold GA (2012) The distinct and overlapping phenotypic spectra of FOXP1 and FOXP2 in cognitive disorders. Human genetics 131:1687-1698.

Bacon C, Schneider M, Le Magueresse C, Froehlich H, Sticht C, Gluch C, Monyer H, Rappold GA (2014) Brain-specific Foxp1 deletion impairs neuronal development and causes autistic-like behaviour. Molecular psychiatry.

Bock NA, Nieman BJ, Bishop JB, Mark Henkelman R (2005) In vivo multiple-mouse MRI at 7 Tesla. Magnetic resonance in medicine 54:1311-1316.

Bolger AM, Lohse M, Usadel B (2014) Trimmomatic: a flexible trimmer for Illumina sequence data. Bioinformatics 30:2114-2120.

Carlson GC, Lin RE, Chen Y, Brookshire BR, White RS, Lucki I, Siegel SJ, Kim SF (2016) Dexras1 a unique ras-GTPase interacts with NMDA receptor activity and provides a novel dissociation between anxiety, working memory and sensory gating. Neuroscience 322:408-415.

Chen JA, Penagarikano O, Belgard TG, Swarup V, Geschwind DH (2015) The emerging picture of autism spectrum disorder: genetics and pathology. Annu Rev Pathol 10:111-144.

Cho KK, Hoch R, Lee AT, Patel T, Rubenstein JL, Sohal VS (2015) Gamma rhythms link prefrontal interneuron dysfunction with cognitive inflexibility in Dlx5/6(+/-) mice. Neuron 85:1332-1343.

Cho YH, Friedman E, Silva AJ (1999) Ibotenate lesions of the hippocampus impair spatial learning but not contextual fear conditioning in mice. Behavioural brain research 98:77-87.

de la Torre-Ubieta L, Won H, Stein JL, Geschwind DH (2016) Advancing the understanding of autism disease mechanisms through genetics. Nat Med 22:345-361.

de Quervain DJ, Papassotiropoulos A (2006) Identification of a genetic cluster influencing memory performance and hippocampal activity in humans. Proceedings of the National Academy of Sciences of the United States of America 103:4270-4274.

Deacon RM (2006) Assessing nest building in mice. Nat Protoc 1:1117-1119.

Dobin A, Davis CA, Schlesinger F, Drenkow J, Zaleski C, Jha S, Batut P, Chaisson M, Gingeras TR (2013) STAR: ultrafast universal RNA-seq aligner. Bioinformatics 29:15-21.

Dorr AE, Lerch JP, Spring S, Kabani N, Henkelman RM (2008) High resolution three-dimensional brain atlas using an average magnetic resonance image of 40 adult C57Bl/6J mice. NeuroImage 42:60-69.

Ellegood J et al. (2015) Clustering autism: using neuroanatomical differences in 26 mouse models to gain insight into the heterogeneity. Molecular psychiatry 20:118-125.

Fakhoury M (2015) Autistic spectrum disorders: A review of clinical features, theories and diagnosis. Int J Dev Neurosci 43:70-77.
Feng X, Ippolito GC, Tian L, Wiehagen K, Oh S, Sambandam A, Willen J, Bunte RM, Maika SD, Harriss JV, Caton AJ, Bhandoola A, Tucker PW, Hu H (2010) Foxp1 is an essential transcriptional regulator for the generation of quiescent naive T cells during thymocyte development. Blood 115:510-518.
Ferland RJ, Cherry TJ, Preware PO, Morrisey EE, Walsh CA (2003) Characterization of Foxp2 and Foxp1 mRNA and protein in the developing and mature brain. The Journal of comparative neurology 460:266-279.
Genovese CR, Lazar NA, Nichols T (2002) Thresholding of statistical maps in functional neuroimaging using the false discovery rate. NeuroImage 15:870-878.
Geschwind DH, State MW (2015) Gene hunting in autism spectrum disorder: on the path to precision medicine. Lancet Neurol.
Gong S, Zheng C, Doughty ML, Losos K, Didkovsky N, Schambra UB, Nowak NJ, Joyner A, Leblanc G, Hatten ME, Heintz N (2003) A gene expression atlas of the central nervous system based on bacterial artificial chromosomes. Nature 425:917-925.
Gorski JA, Talley T, Qiu M, Puelles L, Rubenstein JL, Jones KR (2002) Cortical excitatory neurons and glia, but not GABAergic neurons, are produced in the Emx1-expressing lineage. The Journal of neuroscience : the official journal of the Society for Neuroscience 22:6309-6314.
Heisler JM, Morales J, Donegan JJ, Jett JD, Redus L, O'Connor JC (2015) The attentional set shifting task: a measure of cognitive flexibility in mice. J Vis Exp.
Hernandez RN, Feinberg RL, Vaurio R, Passanante NM, Thompson RE, Kaufmann WE (2009) Autism spectrum disorder in fragile X syndrome: a longitudinal evaluation. American journal of medical genetics Part A 149A:1125-1137.
Hisaoka T, Nakamura Y, Senba E, Morikawa Y (2010) The forkhead transcription factors, Foxp1 and Foxp2, identify different subpopulations of projection neurons in the mouse cerebral cortex. Neuroscience 166:551-563.
Holy TE, Guo Z (2005) Ultrasonic songs of male mice. PLoS biology 3:e386.
Huynh DP, Maalouf M, Silva AJ, Schweizer FE, Pulst SM (2009) Dissociated fear and spatial learning in mice with deficiency of ataxin-2. PloS one 4:e6235.
Iossifov I et al. (2014) The contribution of de novo coding mutations to autism spectrum disorder. Nature 515:216-221.
Kaestner KH, Knochel W, Martinez DE (2000) Unified nomenclature for the winged helix/forkhead transcription factors. Genes & development 14:142-146.
Kotaleski JH, Blackwell KT (2010) Modelling the molecular mechanisms of synaptic plasticity using systems biology approaches. Nature reviews Neuroscience 11:239-251.
Kubota M, Murakoshi T, Saegusa H, Kazuno A, Zong S, Hu Q, Noda T, Tanabe T (2001) Intact LTP and fear memory but impaired spatial memory in mice lacking Ca(v)2.3 (alpha(IE)) channel. Biochem Biophys Res Commun 282:242-248.
Kumar A (2011) Long-Term Potentiation at CA3-CA1 Hippocampal Synapses with Special Emphasis on Aging, Disease, and Stress. Front Aging Neurosci 3:7.
Langfelder P, Horvath S (2008) WGCNA: an R package for weighted correlation network analysis. BMC bioinformatics 9:559.
Le Fevre AK, Taylor S, Malek NH, Horn D, Carr CW, Abdul-Rahman OA, O'Donnell S, Burgess T, Shaw M, Gecz J, Bain N, Fagan K, Hunter MF (2013) FOXP1 mutations cause intellectual disability and a recognizable phenotype. American journal of medical genetics Part A 161A:3166-3175.

Leitner Y (2014) The co-occurrence of autism and attention deficit hyperactivity disorder in children - what do we know? Front Hum Neurosci 8:268.
Lerch JP, Sled JG, Henkelman RM (2011) MRI phenotyping of genetically altered mice. Methods Mol Biol 711:349-361.
Lerch JP, Carroll JB, Spring S, Bertram LN, Schwab C, Hayden MR, Henkelman RM (2008) Automated deformation analysis in the YAC128 Huntington disease mouse model. NeuroImage 39:32-39.
Li X, Xiao J, Frohlich H, Tu X, Li L, Xu Y, Cao H, Qu J, Rappold GA, Chen JG (2015) Foxp1 regulates cortical radial migration and neuronal morphogenesis in developing cerebral cortex. PloS one 10:e0127671.
Love MI, Huber W, Anders S (2014) Moderated estimation of fold change and dispersion for RNA-seq data with DESeq2. Genome biology 15:550.
Lozano R, Vino A, Lozano C, Fisher SE, Deriziotis P (2015) A de novo FOXP1 variant in a patient with autism, intellectual disability and severe speech and language impairment. European journal of human genetics : EJHG 23:1702-1707.
Lynch MA (2004) Long-term potentiation and memory. Physiol Rev 84:87-136.
Maren S (2001) Neurobiology of Pavlovian fear conditioning. Annual review of neuroscience 24:897-931.
McCarthy DJ, Chen Y, Smyth GK (2012) Differential expression analysis of multifactor RNA-Seq experiments with respect to biological variation. Nucleic acids research 40:4288-4297.
Mullins C, Fishell G, Tsien RW (2016) Unifying Views of Autism Spectrum Disorders: A Consideration of Autoregulatory Feedback Loops. Neuron 89:1131-1156.
Nieman BJ, Flenniken AM, Adamson SL, Henkelman RM, Sled JG (2006) Anatomical phenotyping in the brain and skull of a mutant mouse by magnetic resonance imaging and computed tomography. Physiological genomics 24:154-162.
Nieman BJ, Bock NA, Bishop J, Sled JG, Josette Chen X, Mark Henkelman R (2005) Fast spin-echo for multiple mouse magnetic resonance phenotyping. Magn Reson Med 54:532-537.
Park HR, Lee JM, Moon HE, Lee DS, Kim BN, Kim J, Kim DG, Paek SH (2016) A Short Review on the Current Understanding of Autism Spectrum Disorders. Exp Neurobiol 25:1-13.
Plummer JT, Gordon AJ, Levitt P (2016) The Genetic Intersection of Neurodevelopmental Disorders and Shared Medical Comorbidities - Relations that Translate from Bench to Bedside. Front Psychiatry 7:142.
Portfors CV, Perkel DJ (2014) The role of ultrasonic vocalizations in mouse communication. Current opinion in neurobiology 28:115-120.
Precious SV, Kelly CM, Reddington AE, Vinh NN, Stickland RC, Pekarik V, Scherf C, Jeyasingham R, Glasbey J, Holeiter M, Jones L, Taylor MV, Rosser AE (2016) FoxP1 marks medium spiny neurons from precursors to maturity and is required for their differentiation. Exp Neurol 282:9-18.
Puzzo D, Lee L, Palmeri A, Calabrese G, Arancio O (2014) Behavioral assays with mouse models of Alzheimer's disease: practical considerations and guidelines. Biochem Pharmacol 88:450-467.
Robinson MD, McCarthy DJ, Smyth GK (2010) edgeR: a Bioconductor package for differential expression analysis of digital gene expression data. Bioinformatics 26:139-140.
Ryan MM, Ryan B, Kyrke-Smith M, Logan B, Tate WP, Abraham WC, Williams JM (2012) Temporal profiling of gene networks associated with the late phase of long-term potentiation in vivo. PloS one 7:e40538.
Sanders SJ et al. (2015) Insights into Autism Spectrum Disorder Genomic Architecture and Biology from 71 Risk Loci. Neuron 87:1215-1233.

Santini E, Klann E (2014) Reciprocal signaling between translational control pathways and synaptic proteins in autism spectrum disorders. Science signaling 7:re10.
Shannon P, Markiel A, Ozier O, Baliga NS, Wang JT, Ramage D, Amin N, Schwikowski B, Ideker T (2003) Cytoscape: a software environment for integrated models of biomolecular interaction networks. Genome research 13:2498-2504.
Shoji H, Hagihara H, Takao K, Hattori S, Miyakawa T (2012) T-maze forced alternation and left-right discrimination tasks for assessing working and reference memory in mice. J Vis Exp.
Silverman JL, Yang M, Lord C, Crawley JN (2010) Behavioural phenotyping assays for mouse models of autism. Nature reviews Neuroscience 11:490-502.
Spiteri E, Konopka G, Coppola G, Bomar J, Oldham M, Ou J, Vernes SC, Fisher SE, Ren B, Geschwind DH (2007) Identification of the transcriptional targets of FOXP2, a gene linked to speech and language, in developing human brain. American journal of human genetics 81:1144-1157.
State MW, Sestan N (2012) Neuroscience. The emerging biology of autism spectrum disorders. Science 337:1301-1303.
Steadman PE, Ellegood J, Szulc KU, Turnbull DH, Joyner AL, Henkelman RM, Lerch JP (2014) Genetic effects on cerebellar structure across mouse models of autism using a magnetic resonance imaging atlas. Autism Res 7:124-137.
Stessman HA et al. (2017) Targeted sequencing identifies 91 neurodevelopmental-disorder risk genes with autism and developmental-disability biases. Nature genetics.
Supek F, Bosnjak M, Skunca N, Smuc T (2011) REVIGO summarizes and visualizes long lists of gene ontology terms. PloS one 6:e21800.
Takahashi JS, Kumar V, Nakashe P, Koike N, Huang HC, Green CB, Kim TK (2015) ChIP-seq and RNA-seq methods to study circadian control of transcription in mammals. Methods Enzymol 551:285-321.
Tamura S, Morikawa Y, Iwanishi H, Hisaoka T, Senba E (2004) Foxp1 gene expression in projection neurons of the mouse striatum. Neuroscience 124:261-267.
Tovote P, Fadok JP, Luthi A (2015) Neuronal circuits for fear and anxiety. Nature reviews Neuroscience 16:317-331.
Ullmann JF, Watson C, Janke AL, Kurniawan ND, Reutens DC (2013) A segmentation protocol and MRI atlas of the C57BL/6J mouse neocortex. NeuroImage 78:196-203.
van Steensel FJ, Bogels SM, Perrin S (2011) Anxiety disorders in children and adolescents with autistic spectrum disorders: a meta-analysis. Clin Child Fam Psychol Rev 14:302-317.
Vilches N, Spichiger C, Mendez N, Abarzua-Catalan L, Galdames HA, Hazlerigg DG, Richter HG, Torres-Farfan C (2014) Gestational chronodisruption impairs hippocampal expression of NMDA receptor subunits Grin1b/Grin3a and spatial memory in the adult offspring. PloS one 9:e91313.
Vissers LE, Gilissen C, Veltman JA (2016) Genetic studies in intellectual disability and related disorders. Nature reviews Genetics 17:9-18.
Vorhees CV, Williams MT (2006) Morris water maze: procedures for assessing spatial and related forms of learning and memory. Nat Protoc 1:848-858.
Wang B, Lin D, Li C, Tucker P (2003) Multiple domains define the expression and regulatory properties of Foxp1 forkhead transcriptional repressors. The Journal of biological chemistry 278:24259-24268.
Yamamoto J, Suh J, Takeuchi D, Tonegawa S (2014) Successful execution of working memory linked to synchronized high-frequency gamma oscillations. Cell 157:845-857.
Zeisel A, Munoz-Manchado AB, Codeluppi S, Lonnerberg P, La Manno G, Jureus A, Marques S, Munguba H, He L, Betsholtz C, Rolny C, Castelo-Branco G, Hjerling-Leffler J,

Linnarsson S (2015) Brain structure. Cell types in the mouse cortex and hippocampus revealed by single-cell RNA-seq. Science 347:1138-1142.

# CHAPTER FOUR:

# CONCLUSIONS AND FUTURE DIRECTIONS

## OVERVIEW

Autism spectrum disorder (ASD) and intellectual disability (ID) are conditions with complex presentations and equally complex genetic architectures. Many genes implicated in ASD and ID are expressed during early brain development, a time-point thought to be critical in the pathogenesis of these disorders. Various transcription factors coordinate the expression of such genes. Therefore, discerning the brain-region-specific gene targets governed by transcription factors associated with ASD and ID could provide comprehensive and novel insights into the mechanisms responsible for these two disorders. *FOXP1* is a transcription factor that is enriched throughout the developing and mature brain and which has been recently identified as a high-confidence ASD- and ID-risk gene. This dissertation improves our understanding of the role that FoxP1 plays within the brain. Through my work, I demonstrate that Foxp1 controls distinct gene expression profiles in different brain regions and that Foxp1 and Foxp2 share gene targets within the striatum. I reveal an evolutionarily conserved function for FoxP1 in coordinating the expression of genes involved in striatal identity. I am the first to show that heterozygous loss of *Foxp1* differentially affects the physiological properties of medium spiny neurons (MSNs). I am also the first to show that *Foxp1* expression is necessary for proper ultrasonic vocalization (USV) production. Additionally, I have revealed that ablation of *Foxp1* specifically in the neocortex and

hippocampus is sufficient to produce behaviors reminiscent of ASD and ID such as hyperactivity, impaired communication, diminished social interactions, and learning and memory deficits. Finally, I have demonstrated that Foxp1 functions in regulating both hippocampal development and CA1-based long-term potentiation (LTP) maintenance. Taken together, these data point to a model in which reduced *Foxp1* levels compromise particular mechanisms in distinct neuronal subtypes and that, when disrupted together, these processes result in a recognizable ASD- and ID-like phenotype. This final chapter discusses additional unpublished data that I have collected, the implications of these data when integrated with my findings in Chapter 1 and Chapter 2, and suggestions for future experiments.

## MATERIALS AND METHODS

### AAV-injections

Stereotaxic injections were performed by the Neuro-Models Facility at UT Southwestern Medical Center. For injections, mice were anesthetized with isoflurane (4% induction, 2% maintenance) in a 70%/30% mix of nitrous oxide and oxygen. Afterwards, 0.5 or 1 uL of an AAV2-GFP virus (UNC Vector Core) ($3.4 \times 10^9$ viral genomes/uL) were injected bilaterally (with the right hemisphere receiving 1 uL and the left hemisphere receiving 0.5 uL), aiming at the CA1 region of the hippocampus (AP -2.1, ML +/-1.5, DV -1.4). The virus was delivered at a rate of 0.1 uL/minute (for 5 or 10 minutes/injection, depending on the hemisphere), followed by 5 minutes of rest before the needle was removed. To

ensure sufficient AAV2 infection of the hippocampus, mice were given a 2-week period before their brains were harvested for use in floating immunohistochemistry.

**Tissue Preparation**

For both floating immunohistochemistry and Nissl staining, adult female and male mice were anesthetized with 80 – 100 mg/Kg Euthasol (UT Southwestern Medical Center Animal Resources Center Veterinary Drug Services), perfused with PBS containing 10 U/mL heparin (Sigma) followed by fixative (4% PFA in PBS), and then immediately decapitated. Whole brains were removed and incubated in fixative for 24 hours at 4°C and then incubated in 30% sucrose (made in PBS with 0.02% sodium azide) for 24 – 48 hours at 4°C. Afterwards, brains were sectioned at 20 um on an SM2000 R sliding microtome (Leica). Sections were then stored in PBS containing 0.02% sodium azide until use in floating immunohistochemistry (**Chapter 2**) or Nissl staining.

**Nissl Staining**

Brain sections stored in PBS were mounted onto slides and allowed to dry for 24 – 48 hours. Sections were then rehydrated in PBS and then dehydrated with a series of immersions in ethanol at increasing concentrations: 70% ethanol for 3 minutes, 95% ethanol for 3 minutes, and then two separate immersions in 100% ethanol for 5 minutes each. Afterwards, sections were defatted with xylene for 5 minutes. The sections were then rehydrated by immersing them in the ethanol solutions, in the reverse order (3 minutes/treatment), followed by immersion in dd$H_2O$ for 2 minutes. Sections were then

stained with 0.1% cresyl violet for 4 minutes. Subsequently, sections were washed in $ddH_2O$ for 2 minutes and then again dehydrated with ethanol. The sections were then treated with Citrisolv (Thermo) for 5 minutes and then immediately covered with DPX mounting medium and allowed to dry overnight.

**Hippocampal CA1 Cell Density Estimations**

The Cavalieri volume estimation method (MicroBrightField) was used to estimate the density of the CA1/CA2 pyramidal cell layer. The CA1/CA2 region throughout both hippocampal formations (from approximately Bregma -1.400 mm to Bregma -2.700 mm) was visualized using the bright field setting on a BX51 microscope (Olympus) connected to a computer running Stereo Investigator 11.03 software (MicroBrightField). Afterwards, markers were placed (using a grid spacing of 50 um and a section evaluation interval of 10) over these regions. Total volumes were then determined using the built-in software estimator. All volume estimations possessed a Gundersen coefficient of error <0.10.

**Electro-convulsive Stimulation**

For each day of testing, approximately 15 minutes prior to electro-convulsive stimulation (ECS), ocular anesthesia (proparacaine 0.5% solution) (Henry Schein) was applied to the eyes of each mouse. Afterwards, each mouse received a series of ECS shocks via specialized ocular electrodes that made direct contact with the cornea. ECS was delivered at 4mA to every mouse on day 1 using an 7801 ECT Unit (UGO Basile), and

then the amperage was raised each day by 1mA until every mouse experienced a maximal seizure. The other ECS parameters were kept constant: 60Hz, 0.4ms pulse width, 0.2s total duration of shock. Afterwards, the electrodes were immediately removed and the mice were placed into a clean cage until visual signs of seizure stopped. The amperages that elicited both minimal and maximal seizures were recorded for each mouse. A minimal seizure involved loss of posture (mice fall over) and bilateral limb clonus (limbs on both sides spasm uncontrollably). A maximal seizure was defined by loss of posture, rigid straightening of the body, and bilateral tonic extension of hind limbs (hind limbs are extended and rigid). Most mice died upon experiencing a maximal seizure. However, if a mouse survived a maximal seizure, it was immediately sacrificed at the end of the test day. At the end of each testing day, mice were monitored for 30 minutes to ensure that they fully recovered and then given ophthalmic antibiotic eye drops (triple antibiotic containing bacitracin, neomycin, and polymyxin B (Bausch and Lomb) to prevent potential eye infections.

## CHAPTER 2 – FOXP1 ORCHESTRATION OF ASD RELEVANT SINGNALING PATHWAYS IN THE STRIATUM

### Discussion

Previous work has begun to shed light on the pathways governed by Foxp1 in the brain, with particular attention paid to the striatum (Tang et al., 2012; Bacon et al., 2014). However, whether Foxp1 controls specific gene targets in distinct brain regions, the level of conservation of these targets between murine and human neurons, and the

behavioral consequences of disrupting these particular mechanisms have yet to be determined. To answer these questions, we have utilized high-throughput sequencing techniques on human neural progenitors as well as patient-relevant *Foxp1*$^{+/-}$ mouse brains. We present data suggesting that Foxp1 orchestrates transcriptomes that are exclusive to the hippocampus and the striatum. Additionally, we demonstrate that Foxp1 and Foxp2 control unique gene targets in $D_1$ and $D_2$ receptor positive ($D_1$/$D_2$+) MSN subtypes. Specifically, Foxp2 appears to preferentially regulate genes in $D_1$+ MSNs while Foxp1 appears to have a broader role in regulating genes in both subtypes. We also present evidence that heterozygous deletion of *Foxp1* differentially impacts the intrinsic excitability of $D_1$+ and $D_2$+ MSNs. Indeed, loss of *Foxp1* led to a significant increase in $D_2$+ MSN excitability and a trend towards a decrease in $D_1$+ MSN excitability. We also show data indicating that Foxp1 influences the production of isolation-based postnatal USVs. Finally, we show evidence that Foxp1 has an evolutionarily conserved role in the control of genes involved in MSN identity. In summary, these data signify that loss of *Foxp1* may alter striatal-identity genes in a manner that upsets the balance of $D_1$+ and $D_2$+ MSN output that diminishes USV production (**Figure 4.1**). However, the data supporting this hypothesis are correlative in nature and further experimentation is needed to demonstrate causality.

**Remaining Questions and Future Directions**

*Is Foxp1 expression in striatal neurons necessary and sufficient for proper USV production?* Motivated by the strong expression of FoxP2 in MSNs (Ferland et al., 2003;

Frohlich et al., 2017), researchers have established the striatum as a critical region in the generation of vocalizations across species (Fisher and Scharff, 2009; Frohlich et al., 2017). Given that Foxp1 is able to heterodimerize with Foxp2 in the striatum (Frohlich et al., 2017), and that we have shown these two transcription factors share targets in this brain region, it is reasonable to assume that reduction of *Foxp1* specifically in the striatum is responsible for impaired USV production. What follows are two experiments that could demonstrate this conclusively.

I recommend rescuing the USV phenotype in *Foxp1*$^{+/-}$ mouse pups with virally-mediated expression of *Foxp1* in the striatum. Similar experiments have been carried out in mouse models of FXS and Parkinson's disease (Gombash et al., 2013; Gholizadeh et al., 2014). To accomplish this, injections of lentiviral-mediated *Foxp1* expression constructs could be directed at the postnatal day 0 (P0) *Foxp1*$^{+/-}$ mouse striatum. Well-established methods exist for this type of procedure (Osten et al., 2006; Davidson et al., 2010). Alternatively, HSV-1-mediated *Foxp1* expression constructs could be used for a greater infection spread (Berges et al., 2007). Afterwards, standard USV recordings of early postnatal mouse pups in a maternal-separation paradigm could be carried out to demonstrate that the behavioral phenotype has been rescued. As a control, it will be necessary to show that this treatment also results in wild-type Foxp1 levels exclusively in the striatum. Because the neocortex has been implicated in controlling the usage of call types (Hammerschmidt et al., 2015), it may be that rescuing striatal expression of *Foxp1* is sufficient to restore call numbers but not call features.

As an alternative to this experiment, I recommend examining the USVs of early postnatal mouse pups with deletion of *Foxp1* in MSNs. This could be accomplished by using commercially obtainable *Drd1a.Cre* and *Drd2.Cre* animals from the NIH MMRRC at UC Davis (strain numbers 030989-UCD and 032108-UCD, respectively) in combination with the *Foxp1*$^{flox/flox}$ mice detailed previously (**Chapter 3**) (Feng et al., 2010). Additionally, the availability of *Drd1a.Cre* and *Drd2.Cre* lines means that one could also investigate that the contributions of MSN subtypes to this behavior. Resolving these questions could lead to better pharmacological regimens in the management of the speech and language impairments seen in ASD and ID.

*Is it possible to disentangle the gene targets between Foxp1 and Foxp2 heterodimers and Foxp1 and Foxp2 homodimers?* Dimerization (either heterodimerization or homodimerization) is required for Foxp1 and Foxp2 to bind to DNA and properly regulate gene expression (Li et al., 2004; Lalmansingh et al., 2012; Sin et al., 2015; Mendoza and Scharff, 2017). Different homodimer and heterodimer combinations of Foxp1 and Foxp2 possess different regulatory capabilities (Sin et al., 2015). Moreover, my work has shown that Foxp1 and Foxp2 regulate common targets within the striatum. Still, disentangling the specific genes targeted by Foxp1 and Foxp2 heterodimers versus homodimers of Foxp1 and Foxp2 remains a challenge. This is because disrupting the capacity of Foxp1 to heterodimerize with Foxp2 will also inhibit Foxp1 from forming homodimers (Li et al., 2004; Frohlich et al., 2017). Until this technical limitation is overcome, the individual gene targets of Foxp1 and Foxp2 homodimers and heterodimers will remain unknown.

## CHAPTER 3 – FOXP1 IN FOREBRAIN PYRAMIDAL NEURONS CONTROLS GENE EXPRESSION REQUIRED FOR SPATIAL LEARNING AND SYNAPTIC PLASTICITY

### Discussion

Conditional, brain-specific homozygous loss of *Foxp1* leads to abnormal hippocampal and striatal morphology, altered striatal transcriptomes, and ASD-related behaviors (Bacon et al., 2014). Moreover, neocortical knock-down of *Foxp1* generates improper neocortical patterning but the resultant behavioral phenotypes have not been investigated (Li et al., 2015). Therefore, to understand if Foxp1 contributes to ASD- and ID-relevant behaviors in a brain-region-specific manner, we characterized mice with homozygous deletion of *Foxp1* exclusively in the pyramidal neurons of the neocortex and hippocampus. We show that these mice (called *Foxp1*$^{cKO}$ mice) exhibit ASD-like behaviors such as hyperactivity, anxiety, impaired communication, and decreased sociability. We also show that *Foxp1*$^{cKO}$ mice display ID-like behavioral phenotypes such as impaired spatial learning and memory. However, we also demonstrate that cognitive tasks reliant on broader circuits are unaffected. Correlated with these findings, we show that *Foxp1* mediates the expression of genes involved in hippocampal synaptic plasticity. Finally, we present evidence that suggests transcriptional dysregulation in the *Foxp1*$^{cKO}$ hippocampus leads to reduced hippocampal volumes as well as reduced long-term potentiation (LTP) maintenance in the CA1 pyramidal neurons of *Foxp1*$^{cKO}$ mice. Taken together, these data support the idea that loss of *Foxp1* specifically in forebrain pyramidal neurons is sufficient to phenocopy many of the hallmark features of ASD and

ID. Additionally, these data suggest that *Foxp1* loss in the hippocampus diminishes CA1-mediated LTP maintenance via disruptions in signaling networks downstream of synaptic input (**Figure 4.2**). Because generalized cognitive tasks are unimpaired in this mouse model, it is possible that preservation of Foxp1 in other brain regions is sufficient to spare non-spatial forms of learning and memory. Furthermore, it remains difficult to identify the exact contributions of either hippocampal and neocortical *Foxp1* to the described phenotypes. Thus, more experimentation will be needed to tackle these problems.

**Remaining Questions and Future Directions**

*Can we disentangle the contributions of neocortical and hippocampal Foxp1 to the behavioral phenotypes of Foxp1$^{cKO}$ mice?* Changes to the gene expression patterns, morphology, and physiology of the neocortex and hippocampus are typical of ASD and ID brains (Chen et al., 2015). In agreement with these observations, disruptions to overall neocortical development have been linked to the generation of impaired sociability and repetitive behaviors in ASD mouse models (Fang et al., 2014; Caubit et al., 2016). However, *Foxp1* is expressed throughout the neocortex and this region has been shown to influence many behavioral processes. In contrast, the hippocampus has a well-established role in spatial learning and memory. Therefore, we chose to focus on the spatial and learning impairments of *Foxp1$^{cKO}$* mice. Still, in order to definitively connect loss of hippocampal *Foxp1* to these deficiencies, I recommend attempting to rescue the expression of *Foxp1* in this region. This could be accomplished by injecting

virally-mediated expression constructs in the early postnatal hippocampus and assessing behaviors in adulthood (Davidson et al., 2010; Wang et al., 2013). Similar to the experiments described above, the P0 hippocampus could be targeted with AAV-mediated expression constructs for *Foxp1*. Animals could then be examined in either the T-maze or the Morris water maze, as detailed in our methods (**Chapter 3**).

We observed reduced CA1-dependent LTP maintenance in *Foxp1*$^{cKO}$ mice, which correlated with an enrichment of genes involved in the maintenance phase of LTP in our *Foxp1*$^{cKO}$ hippocampal dataset. Because we also detected no differences in basal synaptic plasticity, these data suggest that loss of *Foxp1* in CA1 pyramidal neurons leads to a disruption of signaling networks downstream of synaptic input. In order to test this hypothesis, I recommend rescuing the expression levels of DEGs involved in LTP maintenance, in the hippocampus of *Foxp1*$^{cKO}$ mice. Of the 12 genes that overlapped between the *Foxp1*$^{cKO}$ DEG list and an LTP-maintenance gene list, 7 were not included in the *Foxp1*$^{+/-}$ hippocampal DEG list. Of the 7 LTP-maintenance-phase DEGs exclusive to the *Foxp1*$^{cKO}$ hippocampus, 5 were confirmed via qPCR (*Dsp*, *Gnb4*, *Grin3a*, *Rasd1*, *Runx1t1*). Therefore, these 5 DEGs represent salient targets for expression-based rescue experiments with the methods detailed above. However, negative results from rescue experiments targeting any one differentially expressed LTP-maintenance gene would need to be interpreted carefully, as it is possible that normal expression of the entire hippocampal transcriptome is necessary for normal CA1-based LTP.

As stated earlier, the intact basal synaptic plasticity seen in the CA1 of *Foxp1*$^{cKO}$ mice suggests that differences in LTP-maintenance are not due to deficiencies in

synaptic input (i.e., synapse number, the amplitude of signals released, etc.). However, it will ultimately be necessary to test this idea. I attempted to test one aspect of this hypothesis by examining the spine density of apical dendrites of GFP-labeled CA1 neurons in *Foxp1*$^{cKO}$ mice. However, this experiment was hindered by a high background of GFP expression (due to widespread viral infection) in the stratum radiatum (where CA3 pyramidal neurons synapse onto CA1 neurons). Consequently, while the initial segments of CA1 apical dendrites could be identified (**Figure 4.3**), the spine-containing dendritic tufts in the stratum radiatum could not. Therefore, in order to successfully complete this experiment, I recommend diluting the viral stocks and/or reducing the injected volume.

If successful, the aforementioned experiments would beg the question of whether or not any behavior presented by *Foxp1*$^{cKO}$ mice could be tied to neocortical *Foxp1*. Interestingly, *Foxp1*$^{cKO}$ pups possess marked alterations to their postnatal USVs (**Figure 4.4**), when used in recording methods detailed previously (**Chapter 2**). This result, along with the corresponding deficit in *Foxp1*$^{cKO}$ adult USV production (**Chapter 3**), was surprising to us because we originally expected these animals to serve as a negative control for this behavior (expression of *Foxp1* in the striatum is preserved in *Foxp1*$^{cKO}$ mice). As both early postnatal pups and adults, *Foxp1*$^{cKO}$ mice not only produce fewer numbers of calls, they also produce calls that are shorter, less complex, and which cover a smaller frequency range (**Chapter 3; Figure 4.4**). A circuit connecting projection neurons from the motor cortex to the dorsal striatum has been proposed to control this behavior in mice (Arriaga et al., 2012; Arriaga and Jarvis,

2013). Thus, again, deficiencies in USV production by *Foxp1*$^{cKO}$ mice could be rescued with virally-mediated expression of *Foxp1* within the postnatal motor cortex. A major caveat to this proposition is the finding that many USV parameters are not affected after the developmental ablation of the entire neocortex (Hammerschmidt et al., 2015). However, that ablation of the neocortex doesn't affect USV production could be explained by a model in which the striatum regulates the generation of calls while the neocortex integrates sensory information important for determining when it is proper to produce calls. This idea is consistent with the hypothesis that postnatal USVs are produced in response to sensory cues that come with being separated from the nest (Scattoni et al., 2009; Portfors and Perkel, 2014). Finally, determining if the expression of *Foxp1* in other brain regions can affect performance of non-spatial tasks could be confronted by employing the *Drd1a/Drd2.Cre* animals mentioned previously.

The fact that both *Foxp1*$^{cKO}$ mouse pups and *Foxp1*$^{cKO}$ adult mice present with the same deficits in USV production is striking. This observation is consistent with the idea that mouse vocalizations are innate behaviors under strict control by cortical-striatal circuits involved in motor coordination (Portfors and Perkel, 2014). Additionally, these data suggest that proper expression of *Foxp1* in cortical-striatal may have a role in governing other motor behaviors. To test this hypothesis, I assessed the performance of adult *Foxp1*$^{cKO}$ mice in an accelerating rotarod test and a grip-strength test (methods detailed in **Chapter 2**). *Foxp1*$^{cKO}$ mice display reduced performance on an accelerating rotarod, as indicated by their decreased latency to fall, as well as reduced forelimb grip strength (**Figure 4.5**). This diminished performance in both an accelerating rotarod and

a grip-strength test could indicate that reduced *Foxp1* expression in the neocortex leads to either a reduction in proper signaling from the motor cortices to the spinal cord, abnormal striatal development due to a lack of normal input from the neocortex, or both. Testing these ideas via expression-based rescue or knock-down experiments would be extremely interesting, given that Foxp1 has been associated with Huntington's disease, which is also typified by improper motor coordination (Tang et al., 2012).

*Are the behaviors caused by loss of forebrain Foxp1 developmental in origin?* The endurance of a USV phenotype from early prenatal stages into adulthood in *Foxp1*$^{cKO}$ mice indicates that the other behavioral phenotypes of *Foxp1*$^{cKO}$ mice may also arise during early development. In accordance with this hypothesis, we have found a significant overlap of gene targets between P7 and adult *Foxp1*$^{cKO}$ neocortical and hippocampal RNA-sequencing datasets (**Figure 4.6; Table 4.1**). Additional evidence supporting this idea comes from the finding that P7 *Foxp1*$^{cKO}$ mouse pups display several of the same alterations in regional brain volumes seen in adult *Foxp1*$^{cKO}$ mice (**Figure 4.7; Table 4.2**). Thus, I recommend testing this notion with a tamoxifen-inducible *Cre* expression system (Feil et al., 2009). By inducing *Cre* expression at early postnatal and/or adult time points (via *Emx1.Cre-ER*$^{T2}$ mice – Jackson Laboratories strain # 027784), future experiments could determine if Foxp1 plays a developmental or operational role in orchestrating *Foxp1*$^{cKO}$ mouse phenotypes.

Experiments with an inducible *Emx1.Cre* mouse model could also answer whether Foxp1 operationally or developmentally regulates the neuroanatomical phenotypes seen in *Foxp1*$^{cKO}$ mice. Indeed, it could address the role of Foxp1 in

regulating the reduced CA1/2 pyramidal neuron density seen in both adult full-brain *Foxp1* knockout mice (Bacon et al., 2014) and adult *Foxp1*$^{cKO}$ mice (**Figure 4.8**). Lastly, this finding that *Foxp1*$^{cKO}$ pyramidal neurons of the CA1/2 region take up a larger volume is seemingly in conflict with the reduced *Foxp1*$^{cKO}$ hippocampal volumes revealed by MRI. However, our MRI experiments measured the total volume of the hippocampus whereas the stereology results detailed here only reflect the reduced compactness of pyramidal neurons in the CA1/2 region. Thus, while the CA1/2 pyramidal neuron layer takes up a larger volume, this likely reflects a laminarization deficit within a hippocampus that is reduced in size overall.

*Are the phenotypes exhibited by Foxp1*$^{cKO}$ *mice dose-dependent? Foxp1*$^{+/-}$ mice did not exhibit any observable deficits in spatial learning and memory (**Chapter 2**). Therefore, it is reasonable to predict that heterozygous *Foxp1*$^{cKO}$ mice (referred to as *Foxp1*$^{cKOHET}$ mice) would also not exhibit any learning and memory phenotypes, given that only one *Foxp1* allele is deleted in a restricted portion of the brain in these animals. To test this hypothesis, I examined the spatial learning and memory capabilities of adult *Foxp1*$^{cKOHET}$ mice in the Morris water maze. While *Foxp1*$^{cKOHET}$ mice display a delayed learning curve in the training portion of the maze, their learning did not differ significantly from littermate controls (**Figure 4.9**). Moreover, the number of platform crosses made by *Foxp1*$^{cKOHET}$ mice during a probe day 48 hours after training also did not differ significantly (**Figure 4.9**). Thus, it would appear that the spatial learning and memory capabilities of *Foxp1*$^{cKO}$ mice are not dose-dependent. I have also assayed the baseline activity of adult *Foxp1*$^{cKOHET}$ mice in a novel cage activity test. Interestingly, *Foxp1*$^{cKOHET}$

mice are slightly hypoactive (**Figure 4.9**). This suggests that affecting *Foxp1* expression in the neocortex and hippocampus is able to both increase and decrease levels of locomotor activity. Still, further testing is needed to yield greater confidence in these results due to the small sample size of *Foxp1*$^{cKOHET}$ mice used. This is especially true when one considers the variability of the *Foxp1*$^{cKOHET}$ data in the Morris water maze. With a larger sample size, the delayed learning curve exhibited by *Foxp1*$^{cKOHET}$ mice in the Morris water maze may become statistically significant. This is evidenced by the statistical significance seen in the novel cage activity, which utilized an even smaller number of *Foxp1*$^{cKOHET}$ mice.

It appears that *Foxp1* dosage affects the manifestation of neuroanatomical changes. This was determined by examining relative volume changes in distinct brain regions of adult *Foxp1*$^{+/-}$ mice using MRI. Specifically, *Foxp1*$^{+/-}$ mice possess both fewer and less severe regional volume changes than those seen in *Foxp1*$^{cKO}$ mice (**Figure 4.10**). Indeed, the vast majority of the brain regions affected in *Foxp1*$^{cKO}$ mice (the hippocampus, the dentate gyrus, the frontal association cortex, etc.) are spared in *Foxp1*$^{+/-}$ mice (**Figure 4.10**). There are a few relative volume changes in common between these two mouse models (affecting the internal capsule, the pre-para subiculum, the stratum granulosum, etc.) which suggests that *Foxp1* is especially critical in regulating the development of these regions. Taken together, these data indicate that loss of *Foxp1* affects the maturation of the brain in a dose-dependent manner.

At least one paper has found increased *FOXP1* levels to be correlated with a risk for ASD (Chien et al., 2013). While this increased expression of *FOXP1* was observed

in patient-derived lymphoblastoid cell lines, it suggests that *FOXP1* haploinsufficiency may not be able to explain the complete role of *FOXP1* in ASD and ID pathogenesis (Chien et al., 2013). Indeed, the production of ASD by increased levels of *FOXP1* could be explained with a model in which perturbing *FOXP1* levels affects the same gene networks within the brain, which in turn leads to similar behavioral consequences (**Chapter 2**) (**Figure 4.1**).

*Are Foxp1 mutant mice models of ASD and ID in general?* Hundreds of genes are linked to ASD and ID, but no single genetic mutation yields every symptom associated with the two disorders. For example, while epilepsy is a common symptom shared between ASD and ID (McGrother et al., 2006; Fakhoury, 2015), most *FOXP1* haploinsufficient patients do not regularly present with epilepsy or seizures in general (**Chapter 1**). This observation has been phenocopied in $Foxp1^{cKO}$ mice which, even with complete loss of *Foxp1* in the neocortex and hippocampus, show no special vulnerability to either maximal or minimal seizures when exposed to electro-convulsive stimulation (**Figure 4.11**). Therefore, results such as this should solidify the understanding that when studying either ASD and ID, we are dealing with a constellation of disorders and not a single condition.

## FINAL REMARKS

This dissertation advances our knowledge on the pathways directed by FoxP1 within the brain. First, I took advantage of a whole-body *Foxp1* heterozygous knockout mouse to determine the transcriptional program regulated by Foxp1 in the striatum. I also showed that disrupting this program is correlated with certain behavioral phenotypes

reminiscent of those seen in ASD. Second, I characterized a mouse with complete loss of *Foxp1* in the neocortex and hippocampus to show that Foxp1 contributes to ASD- and ID-relevant behaviors in a brain-region-specific manner. However, as is characteristic of science, these efforts have generated novel and exciting questions that remain to be answered. In the end, it is my hope that the work entailed in this dissertation will eventually lead to meaningful improvements in the lives of those confronting ASD and ID.

## FIGURES FOR CHAPTER FOUR

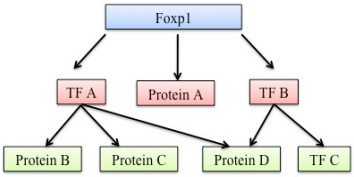


**Alterations to *Foxp1* levels perturbs striatal transcriptomes**

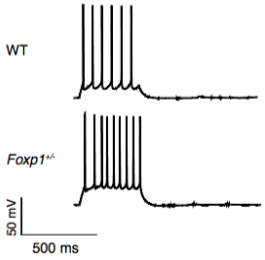


**Increased D2+ MSN excitability**

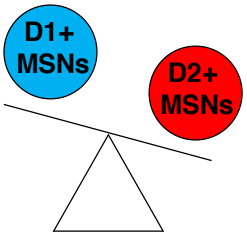


**Disruption of balance between D1+ and D2+ MSN output**

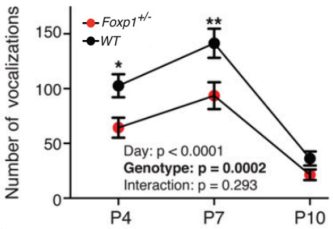


**Decreased USV production**

**Figure 4.1. Model connecting reduced striatal *Foxp1* expression to altered USVs.** Our data suggest that reduced *Foxp1* levels in the striatum leads to increased D2+ medium spiny neuron (MSN) excitability. In turn, this upsets the balance between D1+ and D2+ MSNs and leads to alterations in the generation of behaviors under striatal control such as ultrasonic vocalizations (USVs).

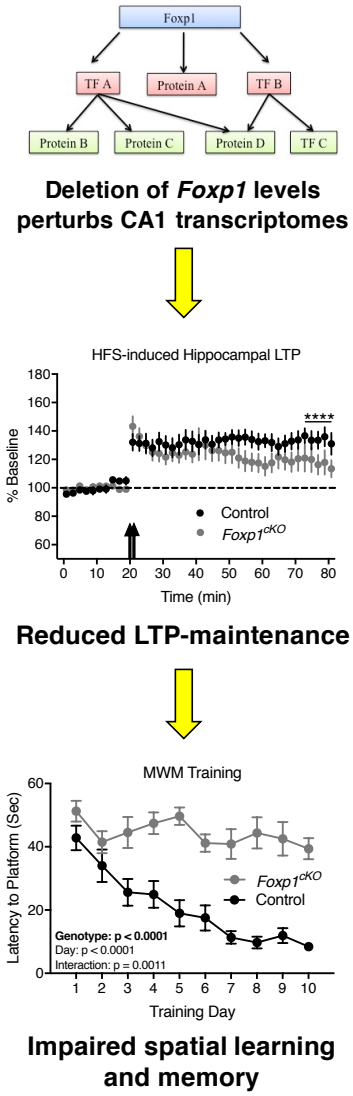


**Figure 4.2. Model connecting hippocampal *Foxp1* expression loss to impaired spatial learning and memory.** Our data indicate that loss of *Foxp1* in CA1 hippocampal neurons leads to improper expression of genes involved in the maintenance phase of CA1-dependent long-term potentiation (LTP). This is followed by diminished encoding of spatial learning and memory engrams in the hippocampus.

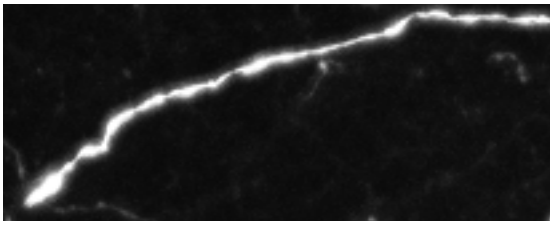

**Figure 4.3. Labeling of CA1 pyramidal neuron apical dendrites.** Representative image of the initial segment of a GFP-filled (white) apical dendrite from a CA1 pyramidal neuron. While apical dendrites could be individually identified, their spine-containing tufts could not, due to high GFP background in the stratum radiatum. Images were taken at 40X, using a LSM880 laser scanning microscope (Zeiss) connected to a computer running Zeiss software.

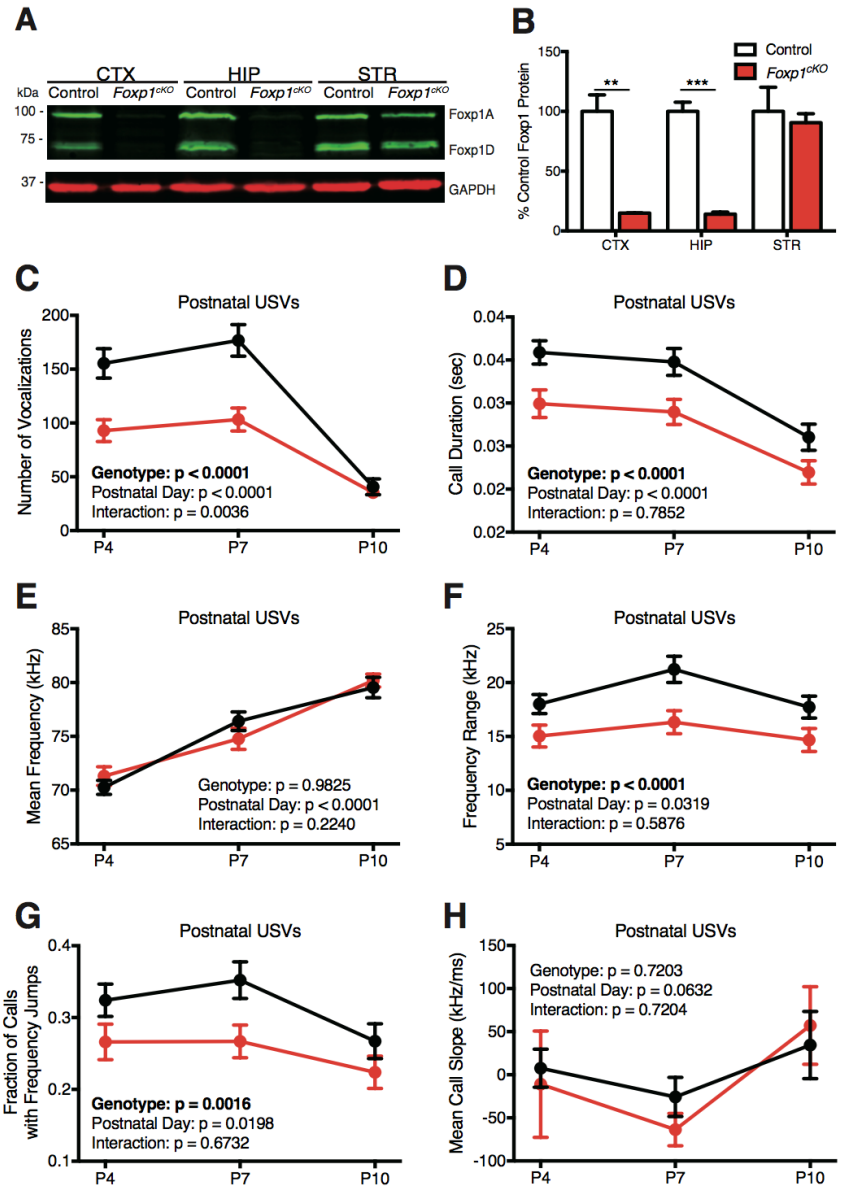


**Figure 4.4. Impaired USV production displayed by *Foxp1*$^{cKO}$ mouse pups.** (A) Representative immunoblot displaying reduced Foxp1 protein levels in the neocortex (CTX) and hippocampus (HIP), but not the striatum (STR), of postnatal day 7 (P7) *Foxp1*$^{cKO}$ mouse pups, compared to littermate control pups. GAPDH is a loading control. (B) Quantification of Foxp1 expression in P7 *Foxp1*$^{cKO}$ brains. Data are

represented as means (± SEM). n=3 control mice, 3 *Foxp1*$^{cKO}$ mice. **p=0.004; ***p=0.0004, Student's t-test, compared to control levels normalized to GAPDH. (C) *Foxp1*$^{cKO}$ mouse pups exhibit fewer total numbers of USVs, as a trend across all days. Data are represented as means (± SEM). n=51 control pups and 52 *Foxp1*$^{cKO}$ pups. p<0.0001, two-way ANOVA with a Sidak multiple comparison test, compared between genotypes. (D) *Foxp1*$^{cKO}$ mouse pups exhibit a significant reduction in their mean call duration, as a trend across all days. Data are represented as means (± SEM). n=45-51 controls pups, 50-52 *Foxp1*$^{cKO}$ pups. p<0.0001, two-way ANOVA with a Sidak multiple comparison test, compared between genotypes. (E) *Foxp1*$^{cKO}$ mouse pups show no differences in mean call frequency. Data are represented as means (± SEM). n=45-51 controls pups, 50-52 *Foxp1*$^{cKO}$ pups. p=0.98, two-way ANOVA with a Sidak multiple comparison test, compared between genotypes. (F) *Foxp1*$^{cKO}$ mouse pups exhibit calls with a smaller average frequency range, as a trend across all days. Data are represented as means (± SEM). n=45-51 controls pups, 50-52 *Foxp1*$^{cKO}$ pups. p<0.0001, two-way ANOVA with a Sidak multiple comparison test, compared between genotypes. (G) *Foxp1*$^{cKO}$ mouse pups display reduction in the fraction of calls with frequency jumps that they produce, as a trend across all days. Data are represented as means (± SEM). n=45-51 controls pups, 50-52 *Foxp1*$^{cKO}$ pups. p=0.0016, two-way ANOVA with a Sidak multiple comparison test, compared between genotypes. (H) *Foxp1*$^{cKO}$ mouse pups present with no significant difference in the average slope of their calls, as a trend across all days. n=45-51 controls pups, 50-52 *Foxp1*$^{cKO}$ pups. p=0.72, two-way ANOVA with a Sidak multiple comparison test,

compared between genotypes. The main effects for genotype and postnatal day, and the interactions between these two variables, are reported within each panel.

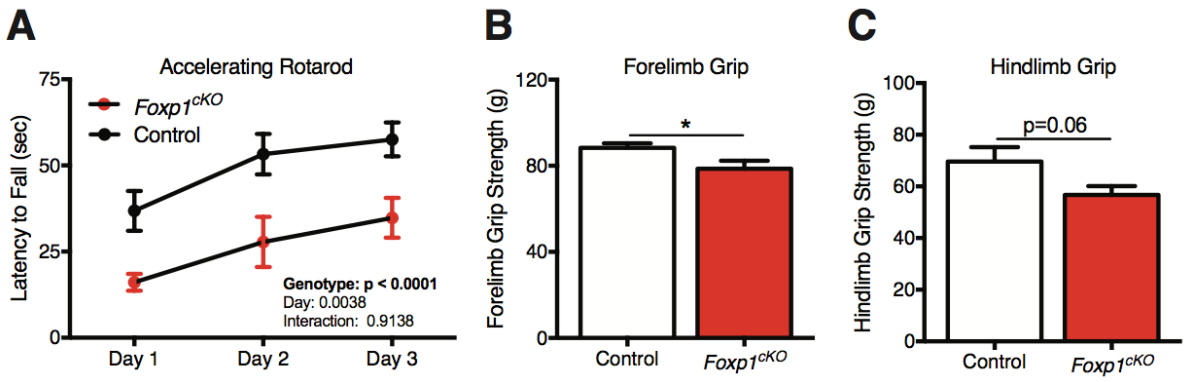


**Figure 4.5. Reduced performance by *Foxp1$^{cKO}$* mice in an accelerating rotarod and grip strength test.** (**A**) *Foxp1$^{cKO}$* mice exhibit deficits in motor coordination as measured by their decreased latency to fall during an accelerating rotarod test. Data are represented as means (± SEM). n=6 control mice, 7 *Foxp1$^{cKO}$* mice. p<0.0001, two-way ANOVA with a Sidak multiple comparison test, compared between genotypes. (**B**, **C**) *Foxp1$^{cKO}$* mice exhibit significant deficits in the grip strength of their fore limbs (**B**) but not their hind limbs (**C**). Data represented as means (± SEM). n=6 control mice, 7 *Foxp1$^{cKO}$* mice. *p=0.049, Student's t-test, compared between genotypes).

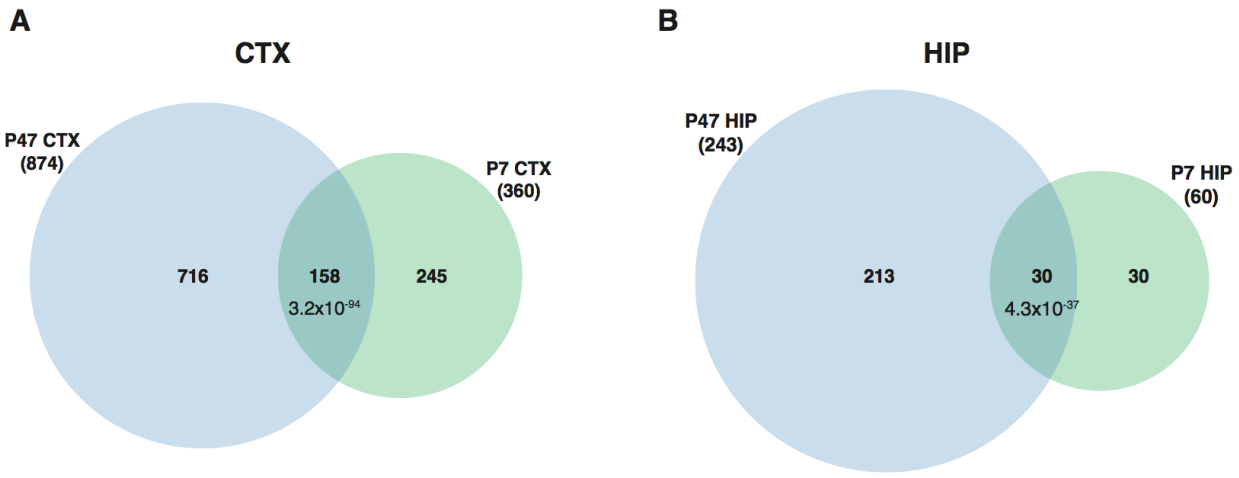


**Figure 4.6. Overlaps between P7 and adult *Foxp1*$^{cKO}$ neocortical and hippocampal DEGs.** (A) Significant overlap between the differentially expressed genes (DEGs) of P7 and adult (P47) *Foxp1*$^{cKO}$ mice in the neocortex. The same cutoffs for identifying DEGs (an adjusted p-value of ≤0.005 and an absolute log fold change of ≥0.3) were applied to both datasets. 158 directionally consistent DEGs overlapped between the P7 and P47 datasets ($p=3.2x10^{-94}$; hypergeometric test). (B) Significant overlap between the differentially expressed DEGs of P7 and adult *Foxp1*$^{cKO}$ mice in the hippocampus. 30 directionally consistent DEGs overlapped between the P7 and P47 datasets ($p=4.3x10^{-37}$; hypergeometric test).

**A**

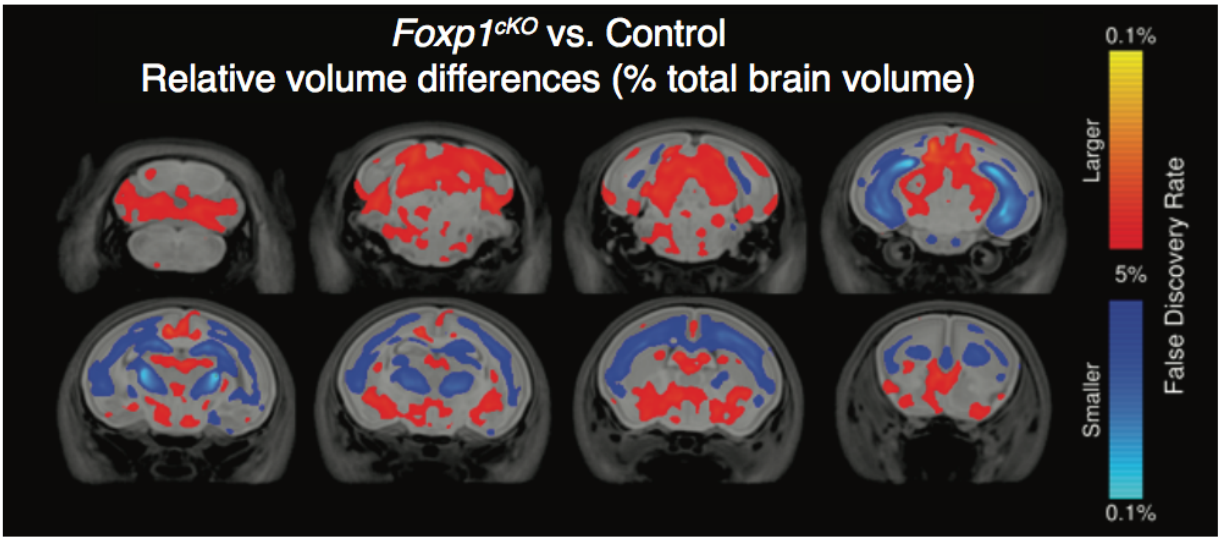


**B**

| Brain regions | Control Mean | Control SD | *Foxp1*cKO Mean | *Foxp1*cKO SD | %Diff | Effect | P-value | FDR | |
|---|---|---|---|---|---|---|---|---|---|
| hippocampus | 4.64 | 0.12 | 4.16 | 0.10 | -10.43 | -3.89 | 8.83E-14 | 4.94E-12 | *** |
| dentate gyrus of hippocampus | 0.67 | 0.02 | 0.62 | 0.02 | -7.58 | -2.84 | 2.02E-09 | 5.66E-08 | *** |
| corpus callosum | 3.16 | 0.07 | 3.01 | 0.05 | -4.66 | -2.07 | 1.06E-07 | 1.98E-06 | *** |
| cerebral cortex parieto temporal lobe | 20.52 | 0.32 | 19.86 | 0.35 | -3.17 | -2.01 | 4.92E-06 | 6.15E-05 | *** |
| cerebral cortex frontal lobe | 8.80 | 0.14 | 8.58 | 0.19 | -2.55 | -1.63 | 6.56E-04 | 2.45E-03 | *** |
| lateral olfactory tract | 0.09 | 0.00 | 0.10 | 0.00 | 4.25 | 1.37 | 1.61E-03 | 4.74E-03 | ** |
| fornix | 0.19 | 0.01 | 0.20 | 0.01 | 4.52 | 1.60 | 3.43E-04 | 1.71E-03 | *** |
| cerebral aqueduct | 0.03 | 0.00 | 0.04 | 0.00 | 4.61 | 0.97 | 1.24E-02 | 2.57E-02 | * |
| posterior commissure | 0.00 | 0.00 | 0.01 | 0.00 | 5.21 | 2.01 | 3.80E-04 | 1.71E-03 | *** |
| lateral septum | 1.06 | 0.03 | 1.11 | 0.03 | 5.40 | 2.05 | 5.49E-06 | 6.15E-05 | *** |

**Figure 4.7 Regional brain volumes in P7 *Foxp1*$^{cKO}$ mice.** (A) Fly-through of representative coronal brain slices of magnetic resonance images highlighting the relative volume differences in areas that are larger (in red) or smaller (in blue) in *Foxp1*$^{cKO}$ mice compared to controls (FDR<0.05). (B) Table of the brain regions with robust *Emx1* expression that demonstrate significantly altered volumes in *Foxp1*$^{cKO}$

mice at P7. Data are represented as means (with SD). n=15 control mouse pups, and 18 *Foxp1*$^{cKO}$ mouse pups. All regions are significant, with $p<0.05$, Student's test (*$p<0.05$, **$p<0.01$, ***$p<0.001$) and FDR<0.05, compared between genotypes. Modified from Usui et al., submitted to *Genes and Development*, 2017.

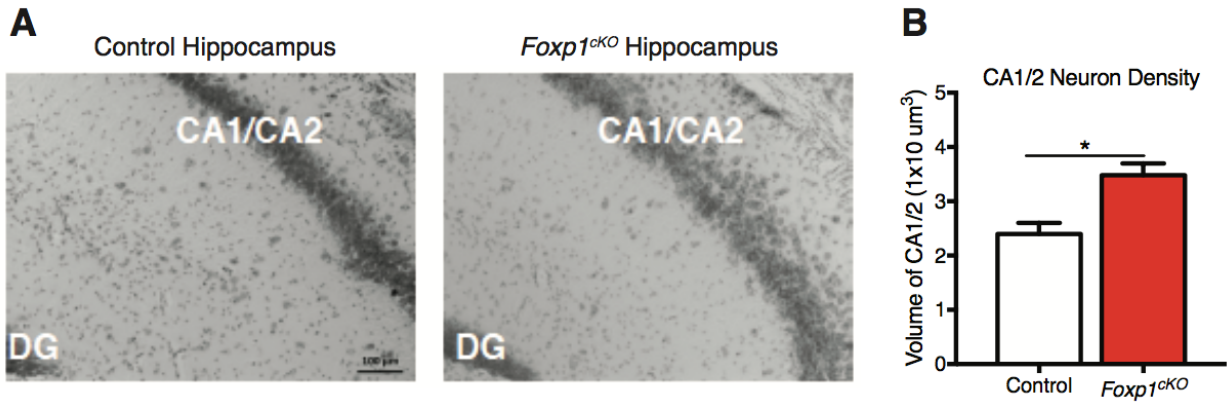


**Figure 4.8. *Foxp1*$^{cKO}$ mice possess decreased CA1/2 pyramidal neuron density.** (A) Representative image of Cresyl violet staining (dark grey) performed on adult coronal slices displaying reduced pyramidal neuron density in the CA1/2 area of the hippocampus. Scale bar represents 100 um. DG=dentate gyrus (B) Quantification of the decreased density of pyramidal neurons in CA1/CA2 hippocampal subfield of *Foxp1*$^{cKO}$ mice, as measured by the increased volume of space they occupy. Data are represented as means (± SEM). n=6 control sections, 6 *Foxp1*$^{cKO}$ sections. *p=0.022, Student's t-test, compared between genotypes.

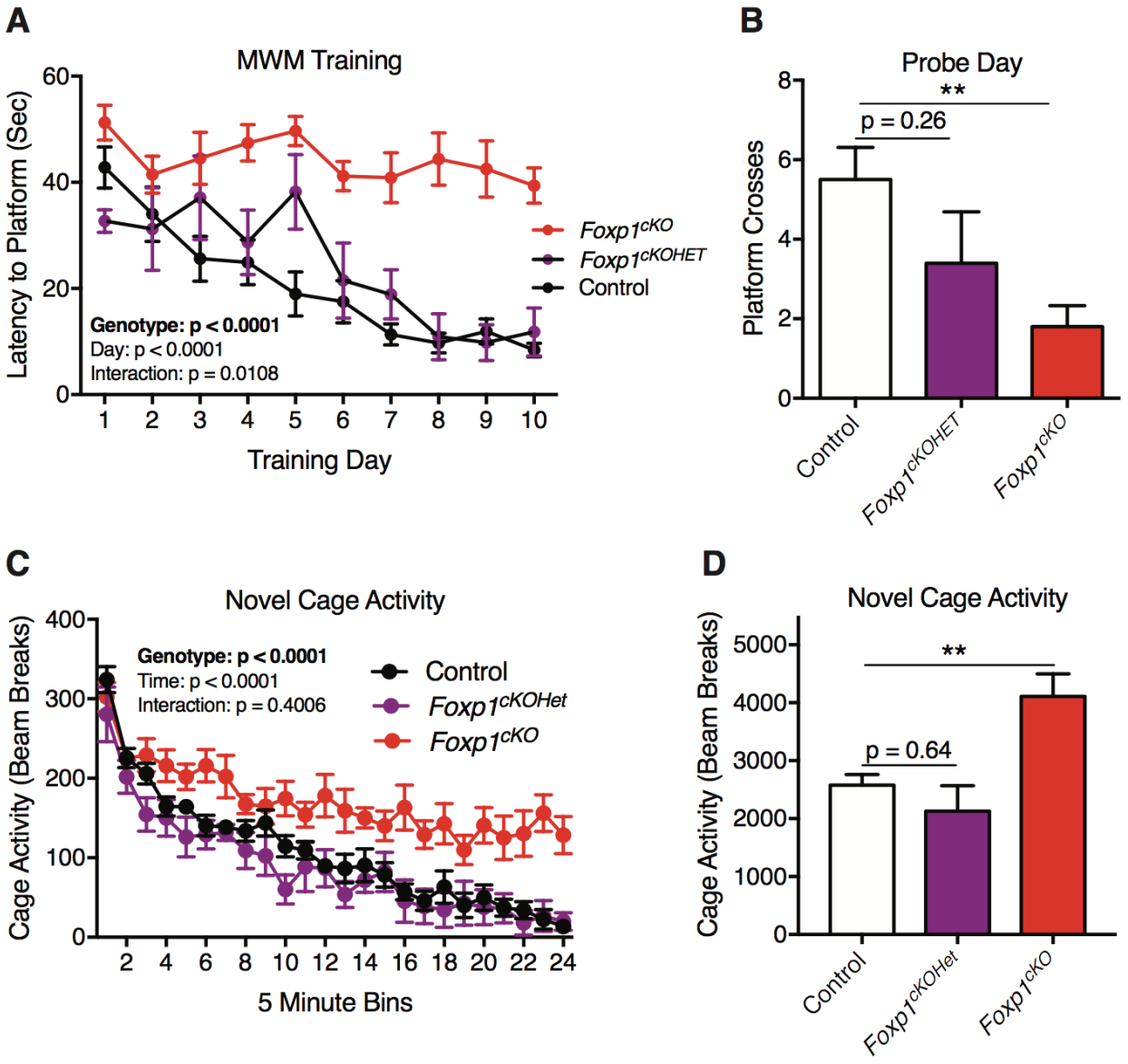


**Figure 4.9 General activity and spatial learning phenotypes of *Foxp1*$^{cKOHET}$ mice.** (A) *Foxp1*$^{cKOHET}$ mice display normal learning via their escape latency in the training phase of the Morris water maze (MWM). Data are represented as means (± SEM). n=12 control animals, 5 *Foxp1*$^{cKOHET}$, 10 *Foxp1*$^{cKO}$ animals. p=0.25, two-way ANOVA, compared between *Foxp1*$^{cKOHET}$ and control mice. (B) *Foxp1*$^{cKOHET}$ mice show normal memory via the number of platform crosses they make during the MWM spatial probe.

Data are represented as means (± SEM). n=12 control animals, 5 *Foxp1*$^{cKOHET}$, 10 *Foxp1*$^{cKO}$ animals. p=0.26, one-way ANOVA, compared between *Foxp1*$^{cKOHET}$ and control mice. **p=0.005, one-way ANOVA, compared between *Foxp1*$^{cKO}$ and control mice. (C,D) *Foxp1*$^{cKOHET}$ mice are slightly hypoactive, as indicated by their decreased activity in a novel cage environment. (C) *Foxp1*$^{cKOHET}$ mice display sustained, decreased activity in a novel cage. Data are represented as means (± SEM). n=9 control mice, 4 *Foxp1*$^{cKOHET}$, 7 *Foxp1*$^{cKO}$ mice. p=0.005, two-way ANOVA, compared between *Foxp1*$^{cKOHET}$ and control mice. (D) As measured by their average activity over the course of two hours, *Foxp1*$^{cKOHET}$ mice are slightly, but not significantly, hypoactive. Data are represented as means (± SEM). n=9 control mice, 4 *Foxp1*$^{cKOHET}$, 7 *Foxp1*$^{cKO}$ mice. p=0.64, one-way ANOVA, compared between *Foxp1*$^{cKOHET}$ and control mice. ***p=0.004, one-way ANOVA, compared between *Foxp1*$^{cKO}$ and control mice.

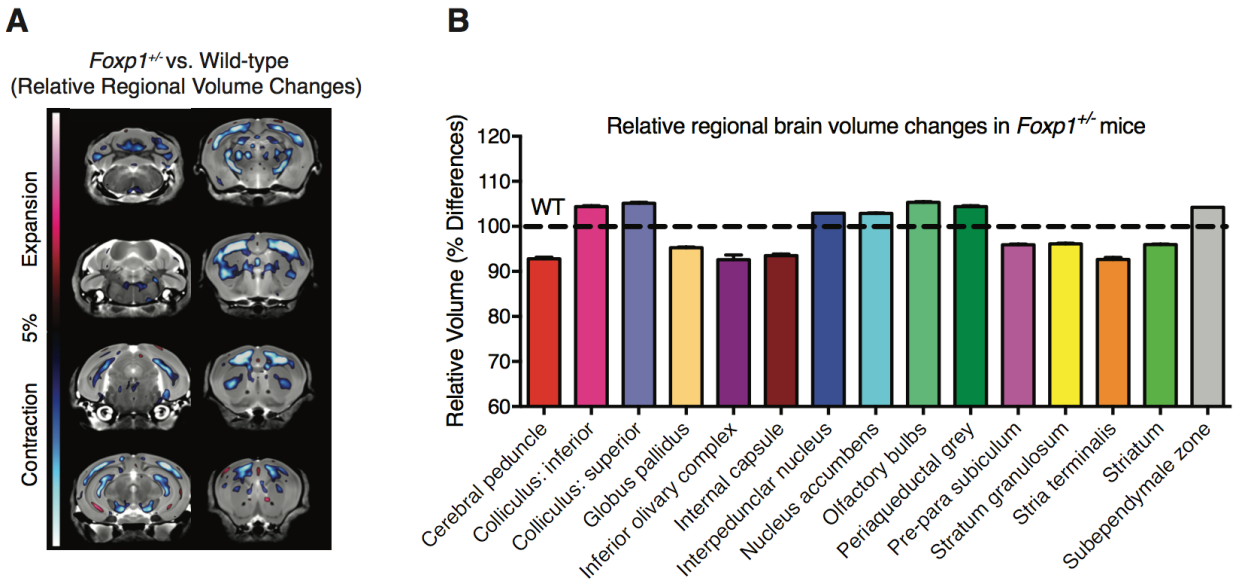


**Figure 4.10. Relative regional volume changes in the *Foxp1*$^{+/-}$ mouse brain.** (A) Fly-through of representative coronal images of the *Foxp1*$^{+/-}$ brain highlighting average, relative differences in regions with larger (red) or smaller (blue) volumes. (B) Representation of the average, relative volume decreases in all of the significantly affected (in terms of percent differences) areas in the *Foxp1*$^{+/-}$ mouse brain. Dashed line represents wild-type (WT) levels (100%). Data are represented as means (± SEM). All values are significant at $p<0.05$, Student's t-test, and FDR<0.10.

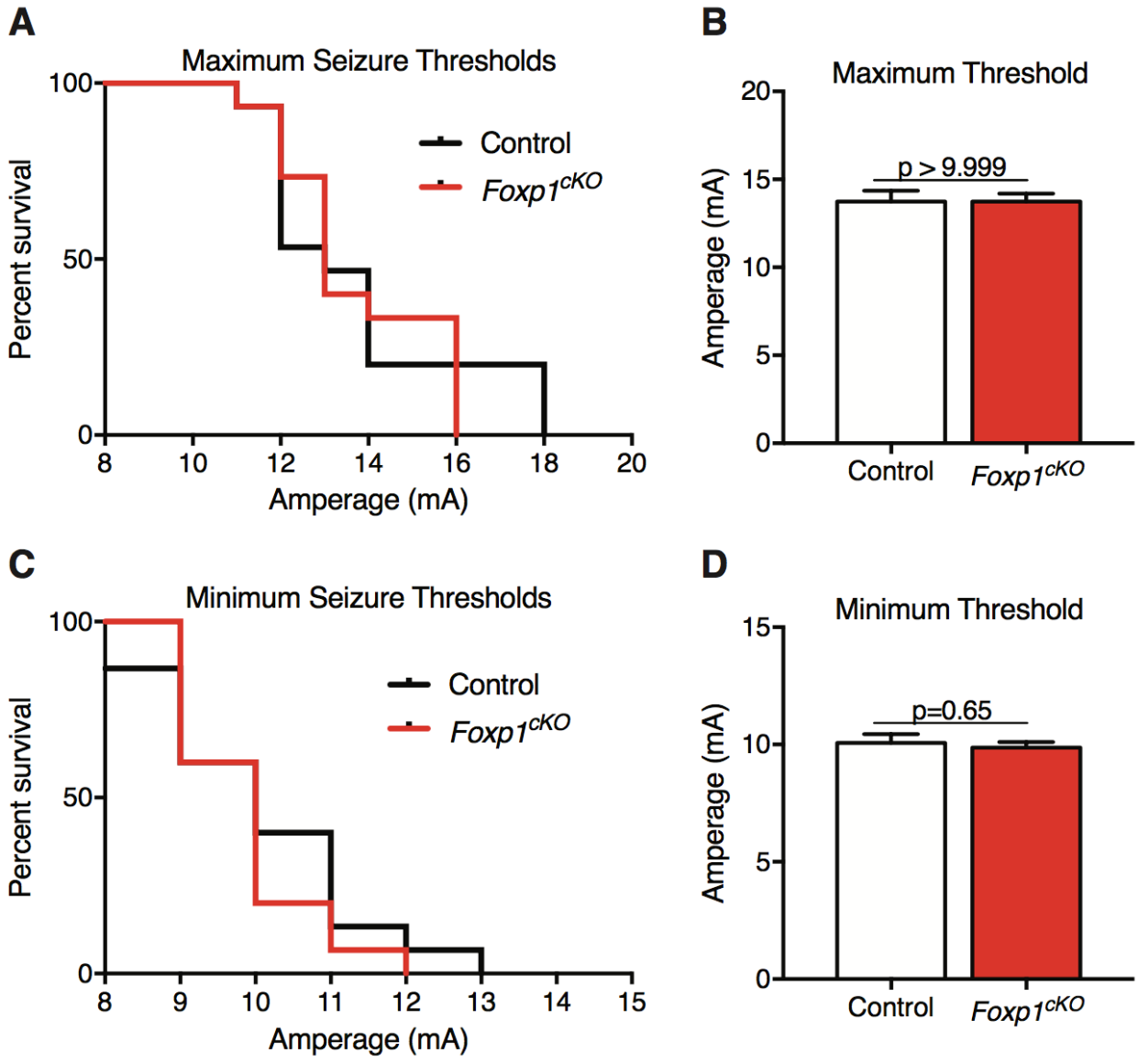


**Figure 4.11. *Foxp1*$^{cKO}$ mice are not especially vulnerable to seizure induction.** (A,B) The amperage needed to generate maximal seizures in *Foxp1*$^{cKO}$ mice is not significantly different, as measured by a survival curve in response to daily 1mA increases in amperage (A) or the average amperage needed to produce a maximal seizure (B). (C,D) The amperage needed to generate minimal seizures in *Foxp1*$^{cKO}$ mice is not significantly different, as measured by a survival curve in response to daily 1mA

increases in amperage (C) or the average amperage needed to produce a minimal seizure (D). (A,C) Data are represented as survival curves. n=15 control mice, 15 *Foxp1*$^{cKO}$ mice. p=0.75 (A), and p=0.73 (C), Gehan-Breslow-Wilcoxon chi-square test, compared between genotypes. (B, D) Data are represented as means (± SEM). n=15 control mice, 15 *Foxp1*$^{cKO}$ mice. p>0.999 (B), p=0.65 (D), Student's t-test, compared between genotypes.

# TABLES FOR CHAPTER FOUR

**Table 4.1. DEGs in the P7 *Foxp1*$^{cKO}$ neocortex and hippocampus.**

| P7 *Foxp1*$^{cKO}$ CTX DEGs | | | P7 *Foxp1*$^{cKO}$ HIP DEGs | | |
|---|---|---|---|---|---|
| **Gene ID** | **log2FoldChange** | **p-value (adj)** | **Gene ID** | **log2FoldChange** | **p-value (adj)** |
| *2900026A02Rik* | -3.69E-01 | 4.83E-05 | *Adgrl2* | 1.91E-03 | 5.76E-01 |
| *6430573F11Rik* | -6.79E-01 | 7.55E-08 | *Alcam* | 2.24E-03 | 3.93E-01 |
| *Abca9* | 4.05E-01 | 3.88E-04 | *Atp2b1* | 2.42E-05 | 3.37E-01 |
| *Abcd2* | -6.00E-01 | 1.75E-12 | *B3galt2* | 2.54E-03 | 6.15E-01 |
| *Acvr2a* | 3.50E-01 | 1.16E-08 | *Bcl11b* | 1.51E-08 | 6.06E-01 |
| *Adamts2* | 6.40E-01 | 1.13E-03 | *Bhlhe22* | 3.32E-05 | 5.14E-01 |
| *Adamts20* | -4.01E-01 | 1.05E-04 | *Cadm2* | 5.79E-13 | 5.84E-01 |
| *Adcy2* | -5.30E-01 | 8.18E-12 | *Calb1* | 2.90E-03 | 5.87E-01 |
| *Adcyap1* | 7.13E-01 | 3.51E-14 | *Camk1d* | 2.33E-04 | 5.30E-01 |
| *Adgra3* | -3.76E-01 | 1.24E-04 | *Cdh8* | 3.18E-03 | 6.24E-01 |
| *Adgrb1* | -6.77E-01 | 4.26E-17 | *Chl1* | 1.30E-11 | 5.01E-01 |
| *Adgrg2* | 4.91E-01 | 7.91E-04 | *Cntn4* | 2.47E-03 | 1.03E+00 |
| *Adora1* | -3.08E-01 | 3.30E-06 | *Dcn* | 3.96E-04 | 8.17E-01 |
| *AF529169* | -3.37E-01 | 9.86E-05 | *Ddx3y* | 2.61E-04 | 8.35E-01 |
| *Ak5* | 3.97E-01 | 1.91E-07 | *Edil3* | 2.01E-03 | 5.25E-01 |
| *Akap9* | 3.05E-01 | 2.07E-08 | *Enpp2* | 8.49E-04 | 4.55E-01 |
| *Aldh1a3* | 8.82E-01 | 6.92E-08 | *Fibin* | 1.30E-06 | 2.99E+00 |
| *Ankrd6* | 3.89E-01 | 3.05E-04 | *Fn1* | 3.06E-04 | 6.72E-01 |
| *Antxr2* | 7.09E-01 | 3.51E-04 | *Foxp1* | 1.41E-70 | 2.08E+00 |
| *Arhgap42* | -3.96E-01 | 7.66E-04 | *Gabra2* | 2.07E-05 | 5.21E-01 |
| *Arhgap44* | -3.80E-01 | 5.22E-06 | *Gpr26* | 2.02E-03 | 5.79E-01 |
| *Arntl* | -4.38E-01 | 4.80E-05 | *Grin3a* | 2.47E-03 | 4.53E-01 |
| *Asic2* | 3.97E-01 | 5.55E-05 | *Homer2* | 1.99E-04 | 6.11E-01 |
| *Astn2* | -8.00E-01 | 9.50E-12 | *Hrk* | 1.10E-03 | 8.05E-01 |
| *Atp1a1* | -4.76E-01 | 1.34E-14 | *Inpp5f* | 6.53E-05 | 4.23E-01 |
| *Atp2b2* | -4.08E-01 | 6.70E-13 | *Iqgap2* | 2.90E-03 | 8.34E-01 |
| *Atp2b4* | 5.27E-01 | 8.59E-23 | *Kcnd2* | 2.14E-06 | 6.43E-01 |
| *Atp8b1* | 6.08E-01 | 2.91E-03 | *Kcnq3* | 2.24E-03 | 3.76E-01 |
| *B3galt1* | -4.79E-01 | 2.56E-14 | *Kcnv1* | 6.73E-04 | 8.41E-01 |
| *Bace2* | -1.04E+00 | 5.99E-05 | *Ldb2* | 3.73E-04 | 7.62E-01 |
| *Bcl6b* | 4.44E-01 | 3.10E-03 | *Lpl* | 5.25E-50 | 1.34E+00 |
| *Bhlhe22* | 5.70E-01 | 4.45E-24 | *Mmd* | 4.67E-03 | 3.89E-01 |
| *Bmp2* | 5.84E-01 | 3.08E-06 | *Mndal* | 2.98E-03 | 8.84E-01 |
| *Boc* | -6.13E-01 | 3.07E-04 | *Mobp* | 3.15E-07 | 2.28E+00 |

| | | | | | |
|---|---|---|---|---|---|
| *Brinp1* | -3.00E-01 | 1.47E-06 | *Ndrg1* | 2.64E-04 | 8.13E-01 |
| *Btbd11* | 5.78E-01 | 2.28E-07 | *Ndst4* | 2.65E-20 | 2.48E+00 |
| *C1ql3* | 5.12E-01 | 1.36E-06 | *Necab1* | 8.35E-07 | 6.33E-01 |
| *C77080* | -8.38E-01 | 4.77E-03 | *Negr1* | 3.17E-06 | 4.94E-01 |
| *Cacnb2* | -4.25E-01 | 9.19E-05 | *Neurod1* | 1.22E-10 | 6.49E-01 |
| *Cadm1* | 3.65E-01 | 6.82E-11 | *Nfib* | 3.83E-04 | 3.21E-01 |
| *Cadm2* | -3.20E-01 | 1.76E-08 | *Nr4a2* | 2.86E-03 | 4.92E-01 |
| *Cadps* | -4.19E-01 | 6.17E-12 | *Nrp2* | 4.67E-03 | 3.84E-01 |
| *Cadps2* | -8.09E-01 | 7.56E-27 | *Nts* | 2.12E-04 | 1.08E+00 |
| *Calb1* | 4.39E-01 | 1.98E-08 | *Pcdh7* | 3.22E-04 | 4.65E-01 |
| *Calb2* | 9.17E-01 | 2.24E-13 | *Pcsk2* | 1.51E-08 | 9.62E-01 |
| *Camk2a* | -4.98E-01 | 1.80E-18 | *Pde1a* | 2.90E-03 | 4.10E-01 |
| *Camk2n1* | -5.18E-01 | 1.86E-20 | *Penk* | 2.61E-04 | 2.26E+00 |
| *Ccbe1* | 4.51E-01 | 1.08E-07 | *Pgm2l1* | 8.49E-06 | 3.69E-01 |
| *Cd44* | -8.66E-01 | 8.66E-16 | *Plp1* | 1.55E-09 | 1.31E+00 |
| *Cdh12* | -4.78E-01 | 2.04E-10 | *Plxnc1* | 4.67E-03 | 5.09E-01 |
| *Cdh13* | 5.01E-01 | 3.30E-19 | *Pou3f1* | 1.08E-04 | 9.80E-01 |
| *Cdh4* | 6.24E-01 | 3.88E-15 | *Rasgrp1* | 2.52E-10 | 7.69E-01 |
| *Cdh8* | -4.10E-01 | 2.94E-10 | *Scg2* | 6.32E-06 | 6.92E-01 |
| *Cdhr1* | 6.60E-01 | 4.34E-07 | *Sema3e* | 5.99E-04 | 7.29E-01 |
| *Cdk6* | 4.36E-01 | 1.89E-06 | *Shisa6* | 1.60E-08 | 6.33E-01 |
| *Cdkn1a* | 3.59E-01 | 1.34E-04 | *Slc17a6* | 1.36E-03 | 6.66E-01 |
| *Cdkn1c* | 3.98E-01 | 8.10E-04 | *Sptbn2* | 6.06E-05 | 5.44E-01 |
| *Cend1* | -3.07E-01 | 1.05E-04 | *Ssx2ip* | 1.71E-03 | 5.18E-01 |
| *Cep135* | -4.43E-01 | 4.03E-04 | *Ttr* | 1.92E-06 | 3.68E-01 |
| *Chgb* | -4.72E-01 | 4.00E-16 | *Vgll3* | 2.27E-03 | 1.74E+00 |
| *Chrm2* | -7.27E-01 | 4.80E-09 | | | |
| *Chst2* | 3.48E-01 | 2.00E-08 | | | |
| *Clec7a* | 1.13E+00 | 1.22E-03 | | | |
| *Clrn1* | 1.14E+00 | 1.39E-04 | | | |
| *Clstn2* | -4.80E-01 | 1.29E-13 | | | |
| *Cnih3* | -3.70E-01 | 6.91E-04 | | | |
| *Cntn3* | -3.72E-01 | 1.80E-06 | | | |
| *Coch* | -7.02E-01 | 2.22E-09 | | | |
| *Col11a1* | 4.24E-01 | 7.14E-07 | | | |
| *Col4a3* | -1.63E+00 | 8.72E-05 | | | |
| *Col4a4* | -7.17E-01 | 2.36E-03 | | | |
| *Col8a1* | -7.32E-01 | 2.16E-11 | | | |
| *Cplx1* | -4.79E-01 | 6.96E-11 | | | |

| | | | | | |
|---|---|---|---|---|---|
| *Cplx3* | -8.12E-01 | 4.47E-06 | | | |
| *Cpne2* | 3.58E-01 | 8.96E-04 | | | |
| *Cpne4* | 5.32E-01 | 5.84E-19 | | | |
| *Cpne7* | 7.88E-01 | 3.70E-12 | | | |
| *Cryab* | -8.47E-01 | 7.17E-08 | | | |
| *Cxxc4* | -3.56E-01 | 1.06E-08 | | | |
| *Cyp26b1* | -1.35E+00 | 1.32E-15 | | | |
| *Dbpht2* | 3.84E-01 | 7.29E-10 | | | |
| *Dcbld2* | -3.88E-01 | 2.37E-07 | | | |
| *Dcc* | -5.62E-01 | 4.43E-06 | | | |
| *Deptor* | -5.04E-01 | 1.79E-03 | | | |
| *Dgkb* | -4.60E-01 | 3.66E-09 | | | |
| *Dgkk* | 4.39E-01 | 3.13E-04 | | | |
| *Diaph3* | -7.64E-01 | 8.67E-05 | | | |
| *Diras2* | -3.42E-01 | 7.19E-08 | | | |
| *Dkk3* | -4.11E-01 | 1.08E-08 | | | |
| *Dmrtb1* | 9.33E-01 | 2.93E-03 | | | |
| *Dnah5* | 3.24E-01 | 3.15E-03 | | | |
| *Dnah8* | 1.09E+00 | 3.34E-10 | | | |
| *Doc2b* | 4.00E-01 | 2.45E-08 | | | |
| *Dock5* | -1.03E+00 | 1.00E-14 | | | |
| *Dok5* | 3.48E-01 | 1.14E-04 | | | |
| *Dpy19l1* | -3.20E-01 | 1.14E-03 | | | |
| *Drp2* | -4.53E-01 | 2.19E-09 | | | |
| *Ebf2* | 1.29E+00 | 2.83E-06 | | | |
| *Efna5* | 4.83E-01 | 1.07E-11 | | | |
| *Efnb2* | 3.21E-01 | 1.31E-06 | | | |
| *Epb41l4a* | 5.99E-01 | 5.57E-07 | | | |
| *Epha7* | -3.44E-01 | 7.14E-07 | | | |
| *Esr1* | 6.31E-01 | 9.58E-04 | | | |
| *Esrrg* | -7.97E-01 | 1.37E-16 | | | |
| *Etv1* | -3.94E-01 | 7.08E-08 | | | |
| *Etv6* | 5.87E-01 | 8.84E-14 | | | |
| *Exph5* | 9.71E-01 | 4.57E-04 | | | |
| *F2r* | 5.75E-01 | 1.75E-08 | | | |
| *Fam101b* | 3.68E-01 | 4.83E-05 | | | |
| *Fam126a* | 3.32E-01 | 1.24E-06 | | | |
| *Fam149a* | 3.67E-01 | 1.02E-05 | | | |
| *Fam184a* | 3.41E-01 | 4.23E-03 | | | |

| | | | | | |
|---|---|---|---|---|---|
| *Fam189a1* | -7.35E-01 | 4.98E-13 | | | |
| *Fam212b* | -4.29E-01 | 3.29E-03 | | | |
| *Fat3* | -3.20E-01 | 6.40E-07 | | | |
| *Fbxo32* | -9.08E-01 | 1.30E-07 | | | |
| *Fcrl5* | 2.96E+00 | 7.94E-04 | | | |
| *Fezf2* | -3.83E-01 | 2.47E-04 | | | |
| *Fgf10* | 8.62E-01 | 4.82E-18 | | | |
| *Fgfr2* | 4.10E-01 | 8.33E-06 | | | |
| *Flrt3* | 6.63E-01 | 3.02E-21 | | | |
| *Fndc5* | -4.50E-01 | 5.21E-05 | | | |
| *Fosl2* | -4.73E-01 | 2.39E-05 | | | |
| *Foxo1* | -6.63E-01 | 2.82E-16 | | | |
| *Foxp1* | -1.64E+00 | 2.33E-180 | | | |
| *Fras1* | -3.90E-01 | 1.78E-04 | | | |
| *Frmpd3* | -4.78E-01 | 1.82E-03 | | | |
| *Frmpd4* | -3.98E-01 | 2.24E-08 | | | |
| *Frzb* | 4.57E-01 | 3.46E-03 | | | |
| *Fst* | 1.23E+00 | 9.04E-13 | | | |
| *Fxyd7* | -5.64E-01 | 4.96E-04 | | | |
| *Gabrg3* | -3.68E-01 | 1.50E-06 | | | |
| *Galntl6* | -3.67E-01 | 2.31E-05 | | | |
| *Gatm* | 5.46E-01 | 5.84E-19 | | | |
| *Gfra2* | -6.23E-01 | 7.04E-09 | | | |
| *Gjd2* | 4.68E-01 | 6.78E-05 | | | |
| *Glis3* | 1.15E+00 | 9.38E-18 | | | |
| *Glp2r* | -1.77E+00 | 4.54E-13 | | | |
| *Glra3* | 1.31E+00 | 1.37E-56 | | | |
| *Gm11639* | 8.37E-01 | 2.24E-16 | | | |
| *Gm16485* | -6.03E-01 | 6.59E-04 | | | |
| *Gm765* | 2.54E+00 | 7.40E-10 | | | |
| *Gpc3* | 5.64E-01 | 1.01E-05 | | | |
| *Gpcpd1* | -3.17E-01 | 3.57E-07 | | | |
| *Gpnmb* | 1.16E+00 | 4.00E-06 | | | |
| *Gpr158* | -6.38E-01 | 1.34E-14 | | | |
| *Gpr161* | 3.19E-01 | 1.85E-05 | | | |
| *Gpr85* | 3.64E-01 | 8.22E-09 | | | |
| *Gprin3* | -5.08E-01 | 2.03E-12 | | | |
| *Greb1l* | 5.06E-01 | 2.36E-04 | | | |
| *Grem2* | 5.58E-01 | 6.33E-10 | | | |

| | | | | | |
|---|---|---|---|---|---|
| *Grid2* | -3.76E-01 | 2.24E-04 | | | |
| *Grm1* | 5.85E-01 | 4.61E-13 | | | |
| *Grm2* | -7.64E-01 | 3.42E-07 | | | |
| *Grm3* | -3.18E-01 | 1.56E-05 | | | |
| *Hap1* | 4.85E-01 | 6.60E-04 | | | |
| *Hcn1* | -3.71E-01 | 2.50E-08 | | | |
| *Hdac9* | 4.18E-01 | 1.81E-09 | | | |
| *Herc3* | -3.16E-01 | 7.97E-06 | | | |
| *Hlf* | -3.17E-01 | 2.37E-05 | | | |
| *Hnmt* | -4.61E-01 | 3.79E-05 | | | |
| *Hpca* | -4.90E-01 | 3.04E-12 | | | |
| *Hpgd* | 1.04E+00 | 6.28E-10 | | | |
| *Hr* | -6.49E-01 | 3.07E-05 | | | |
| *Hrasls* | -7.58E-01 | 2.24E-04 | | | |
| *Hs3st2* | -8.94E-01 | 1.26E-16 | | | |
| *Hs3st4* | -4.08E-01 | 1.62E-07 | | | |
| *Hs3st5* | -5.09E-01 | 1.24E-03 | | | |
| *Hsd11b1* | -9.63E-01 | 2.92E-05 | | | |
| *Htr7* | 7.54E-01 | 3.25E-12 | | | |
| *Id2* | 7.28E-01 | 1.22E-38 | | | |
| *Id4* | 3.01E-01 | 4.05E-03 | | | |
| *Igfbp5* | 3.90E-01 | 1.85E-12 | | | |
| *Igsf10* | 3.63E-01 | 4.83E-03 | | | |
| *Il1rap* | -6.24E-01 | 1.01E-10 | | | |
| *Il1rapl2* | -7.45E-01 | 7.76E-10 | | | |
| *Inhbb* | -7.11E-01 | 6.83E-07 | | | |
| *Ipcef1* | -3.74E-01 | 2.82E-08 | | | |
| *Itgb3* | -1.03E+00 | 5.07E-10 | | | |
| *Jade1* | -4.71E-01 | 8.00E-07 | | | |
| *Kcnh5* | -9.69E-01 | 3.91E-17 | | | |
| *Kcnj10* | -3.50E-01 | 3.73E-07 | | | |
| *Kcnj3* | -3.04E-01 | 3.14E-05 | | | |
| *Kcnj9* | -7.59E-01 | 4.31E-13 | | | |
| *Kcnk2* | -3.57E-01 | 3.81E-05 | | | |
| *Kcnq5* | -3.30E-01 | 2.28E-07 | | | |
| *Kcnt2* | -3.60E-01 | 6.81E-07 | | | |
| *Khdrbs2* | 4.33E-01 | 2.46E-05 | | | |
| *Kirrel3* | 4.97E-01 | 1.36E-08 | | | |
| *Klf9* | -3.67E-01 | 2.36E-09 | | | |

| | | | | | |
|---|---|---|---|---|---|
| *Klhl1* | 7.50E-01 | 3.03E-20 | | | |
| *Klhl4* | 4.11E-01 | 1.44E-05 | | | |
| *Lbh* | -3.82E-01 | 2.89E-04 | | | |
| *Lclat1* | -3.13E-01 | 2.65E-04 | | | |
| *Lgi2* | -5.24E-01 | 1.32E-15 | | | |
| *Lhfp* | -6.83E-01 | 6.77E-13 | | | |
| *Lhx2* | 4.59E-01 | 6.08E-09 | | | |
| *Limch1* | 3.60E-01 | 6.84E-09 | | | |
| *Lmo3* | -3.09E-01 | 8.09E-06 | | | |
| *Lmo7* | 3.32E-01 | 6.23E-07 | | | |
| *Lmod3* | -1.25E+00 | 4.87E-04 | | | |
| *Lpl* | -3.02E-01 | 3.25E-06 | | | |
| *Lynx1* | -7.66E-01 | 4.17E-11 | | | |
| *Lypd6* | -5.75E-01 | 3.27E-09 | | | |
| *Lypd6b* | -4.06E-01 | 1.27E-03 | | | |
| *March1* | 4.16E-01 | 1.63E-12 | | | |
| *Masp1* | -9.77E-01 | 1.26E-07 | | | |
| *Mb21d2* | -8.01E-01 | 1.36E-14 | | | |
| *Mc4r* | 1.58E+00 | 2.56E-21 | | | |
| *Mdga1* | 3.41E-01 | 1.78E-05 | | | |
| *Mex3a* | 3.14E-01 | 4.73E-06 | | | |
| *Mgat5* | 3.17E-01 | 2.36E-06 | | | |
| *Mical2* | -4.27E-01 | 1.85E-09 | | | |
| *Mmp17* | -3.75E-01 | 2.91E-03 | | | |
| *Ncam2* | -6.60E-01 | 1.82E-27 | | | |
| *Nebl* | -3.21E-01 | 1.38E-04 | | | |
| *Nedd9* | 3.35E-01 | 4.95E-03 | | | |
| *Nefh* | -8.36E-01 | 1.31E-08 | | | |
| *Nefl* | -6.70E-01 | 2.28E-30 | | | |
| *Nefm* | -7.67E-01 | 5.23E-34 | | | |
| *Neurod1* | 6.80E-01 | 1.74E-22 | | | |
| *Ngef* | -6.63E-01 | 6.31E-12 | | | |
| *Nipal3* | 3.20E-01 | 4.87E-03 | | | |
| *Nov* | 7.50E-01 | 2.81E-40 | | | |
| *Npr3* | 3.36E-01 | 1.75E-03 | | | |
| *Npy1r* | 3.65E-01 | 4.80E-04 | | | |
| *Nr1d1* | -4.37E-01 | 2.93E-03 | | | |
| *Nr2f2* | 4.07E-01 | 4.23E-08 | | | |
| *Nr4a2* | 3.38E-01 | 8.11E-07 | | | |

| | | | | | |
|---|---|---|---|---|---|
| *Nrip1* | 4.94E-01 | 9.41E-19 | | | |
| *Nrp2* | 3.29E-01 | 7.20E-05 | | | |
| *Nrsn1* | -4.20E-01 | 2.50E-08 | | | |
| *Ntsr1* | 6.47E-01 | 2.12E-11 | | | |
| *Nudt4* | -6.41E-01 | 2.56E-31 | | | |
| *Osbpl3* | -8.05E-01 | 7.47E-20 | | | |
| *Ostn* | -2.91E+00 | 7.31E-09 | | | |
| *Oxtr* | 7.92E-01 | 1.85E-09 | | | |
| *Parm1* | -5.40E-01 | 3.83E-08 | | | |
| *Pax6* | 4.41E-01 | 4.75E-03 | | | |
| *Pcdh8* | 7.04E-01 | 2.03E-10 | | | |
| *Pcdh9* | -3.01E-01 | 3.58E-07 | | | |
| *Pde1a* | 3.70E-01 | 2.87E-08 | | | |
| *Pdzrn3* | 3.69E-01 | 1.75E-06 | | | |
| *Peg10* | 4.69E-01 | 8.90E-07 | | | |
| *Penk* | 8.94E-01 | 1.36E-09 | | | |
| *Pex5l* | -7.08E-01 | 4.88E-20 | | | |
| *Pgr* | -5.76E-01 | 1.39E-06 | | | |
| *Piezo2* | 6.70E-01 | 1.69E-03 | | | |
| *Pitpnc1* | -4.46E-01 | 2.84E-13 | | | |
| *Plagl1* | 7.01E-01 | 1.51E-19 | | | |
| *Plb1* | -1.77E+00 | 2.92E-13 | | | |
| *Plcxd2* | -5.82E-01 | 2.14E-24 | | | |
| *Plcxd3* | 3.80E-01 | 1.31E-03 | | | |
| *Pld5* | -1.38E+00 | 1.61E-05 | | | |
| *Plxnc1* | 3.51E-01 | 2.36E-07 | | | |
| *Plxnd1* | -6.46E-01 | 3.90E-18 | | | |
| *Postn* | -4.81E-01 | 6.34E-05 | | | |
| *Ppargc1a* | -3.80E-01 | 1.62E-07 | | | |
| *Ppat* | 3.73E-01 | 4.82E-05 | | | |
| *Ppfibp1* | 4.00E-01 | 1.15E-09 | | | |
| *Ppm1k* | -4.12E-01 | 1.20E-05 | | | |
| *Ppm1l* | -4.61E-01 | 1.36E-14 | | | |
| *Prdm8* | 3.48E-01 | 5.43E-07 | | | |
| *Prex1* | 4.30E-01 | 6.87E-09 | | | |
| *Prickle1* | -4.25E-01 | 4.08E-07 | | | |
| *Prkcg* | -4.82E-01 | 1.65E-12 | | | |
| *Prox1* | 3.12E-01 | 2.30E-03 | | | |
| *Ptgfrn* | -4.98E-01 | 3.43E-11 | | | |

| | | | | | |
|---|---|---|---|---|---|
| *Ptprn2* | -3.24E-01 | 2.31E-05 | | | |
| *Ptpru* | 7.97E-01 | 9.04E-13 | | | |
| *Rap1gds1* | -3.02E-01 | 2.23E-06 | | | |
| *Rasgrp1* | -5.43E-01 | 1.84E-16 | | | |
| *Rasl11b* | -6.24E-01 | 9.19E-05 | | | |
| *Rbm24* | 3.91E-01 | 8.72E-05 | | | |
| *Rcn1* | 5.19E-01 | 9.86E-12 | | | |
| *Rfx3* | 6.35E-01 | 8.09E-31 | | | |
| *Rgs9bp* | -1.65E+00 | 1.92E-10 | | | |
| *Rhpn2* | 1.01E+00 | 8.62E-04 | | | |
| *Rnf152* | -5.54E-01 | 4.77E-16 | | | |
| *Rora* | -1.02E+00 | 5.77E-43 | | | |
| *Rorb* | -1.60E+00 | 5.52E-143 | | | |
| *Rprm* | -1.07E+00 | 1.66E-26 | | | |
| *Rps6ka2* | 4.27E-01 | 9.39E-05 | | | |
| *Rreb1* | -5.05E-01 | 3.29E-03 | | | |
| *Rsad1* | -3.55E-01 | 3.14E-03 | | | |
| *Rxfp1* | -3.51E-01 | 2.93E-08 | | | |
| *Rxfp2* | -2.24E+00 | 2.16E-11 | | | |
| *Ryr2* | -3.87E-01 | 9.63E-10 | | | |
| *Scd1* | -3.38E-01 | 1.91E-06 | | | |
| *Scrt1* | -4.41E-01 | 4.48E-05 | | | |
| *Scube1* | -8.30E-01 | 5.46E-19 | | | |
| *Sema3a* | 5.47E-01 | 9.49E-18 | | | |
| *Sema7a* | -6.24E-01 | 4.77E-16 | | | |
| *Sfrp2* | 5.52E-01 | 2.25E-03 | | | |
| *Sh3pxd2a* | 3.21E-01 | 2.65E-03 | | | |
| *Shc4* | 4.80E-01 | 1.55E-03 | | | |
| *Shisa3* | 1.35E+00 | 1.96E-11 | | | |
| *Shisa6* | -6.84E-01 | 1.40E-22 | | | |
| *Slc16a2* | 6.25E-01 | 1.28E-22 | | | |
| *Slc17a6* | 3.50E-01 | 7.89E-08 | | | |
| *Slc17a7* | -3.87E-01 | 2.81E-09 | | | |
| *Slc17a8* | -3.36E-01 | 2.89E-03 | | | |
| *Slc24a2* | -6.63E-01 | 3.76E-28 | | | |
| *Slc2a13* | -4.67E-01 | 7.00E-10 | | | |
| *Slc30a3* | -1.64E+00 | 4.10E-10 | | | |
| *Slc6a7* | -6.10E-01 | 6.78E-08 | | | |
| *Slc9a7* | -5.00E-01 | 6.90E-04 | | | |

| | | | | | |
|---|---|---|---|---|---|
| *Slit2* | -4.20E-01 | 2.66E-06 | | | |
| *Smarca2* | 3.85E-01 | 1.58E-11 | | | |
| *Snap25* | -3.17E-01 | 1.71E-08 | | | |
| *Snx7* | -3.42E-01 | 2.26E-05 | | | |
| *Sorcs1* | -8.61E-01 | 6.78E-38 | | | |
| *Sorcs3* | -3.46E-01 | 3.67E-03 | | | |
| *Sorl1* | -4.81E-01 | 8.11E-13 | | | |
| *Sox11* | 4.18E-01 | 1.41E-15 | | | |
| *Spon1* | -4.24E-01 | 2.61E-07 | | | |
| *Spp1* | 1.26E+00 | 3.43E-40 | | | |
| *St8sia2* | 3.47E-01 | 1.19E-08 | | | |
| *St8sia5* | -6.18E-01 | 2.78E-03 | | | |
| *Stac* | 7.35E-01 | 6.04E-05 | | | |
| *Stxbp6* | 3.32E-01 | 6.16E-07 | | | |
| *Sulf2* | -5.56E-01 | 1.01E-17 | | | |
| *Susd5* | -1.05E+00 | 6.27E-11 | | | |
| *Syndig1* | -8.75E-01 | 1.82E-09 | | | |
| *Syne1* | -3.07E-01 | 3.32E-06 | | | |
| *Synj2* | 5.35E-01 | 1.22E-06 | | | |
| *Synm* | 3.07E-01 | 1.45E-05 | | | |
| *Syt17* | 8.42E-01 | 1.02E-12 | | | |
| *Tbata* | -1.39E+00 | 2.86E-03 | | | |
| *Tcf24* | 1.48E+00 | 4.99E-04 | | | |
| *Tcf7l2* | 1.04E+00 | 1.89E-14 | | | |
| *Tes* | 4.57E-01 | 3.74E-03 | | | |
| *Tgfbr1* | -4.04E-01 | 1.47E-07 | | | |
| *Thbs3* | 5.31E-01 | 4.43E-04 | | | |
| *Tmem132d* | -4.97E-01 | 4.53E-04 | | | |
| *Tmem255a* | 8.27E-01 | 4.02E-10 | | | |
| *Tmtc1* | -3.32E-01 | 1.06E-05 | | | |
| *Tnc* | 4.02E-01 | 8.80E-10 | | | |
| *Tnfrsf11a* | -6.24E-01 | 1.34E-04 | | | |
| *Tox* | -3.06E-01 | 4.52E-03 | | | |
| *Tox3* | 5.28E-01 | 3.29E-06 | | | |
| *Trpa1* | -8.76E-01 | 1.86E-13 | | | |
| *Trpc3* | -4.71E-01 | 5.42E-05 | | | |
| *Trpc4* | -3.25E-01 | 3.44E-04 | | | |
| *Trpc5* | -4.12E-01 | 1.34E-04 | | | |
| *Trpm3* | -4.17E-01 | 2.23E-10 | | | |

| | | | | | |
|---|---|---|---|---|---|
| *Tshr* | 4.74E-01 | 7.56E-04 | | | |
| *Tuba4a* | -4.09E-01 | 3.22E-06 | | | |
| *Unc5d* | -3.15E-01 | 1.09E-05 | | | |
| *Vcan* | 4.91E-01 | 3.60E-21 | | | |
| *Vgll3* | -1.32E+00 | 3.69E-07 | | | |
| *Vit* | 7.53E-01 | 1.99E-05 | | | |
| *Vstm2l* | -7.50E-01 | 2.49E-07 | | | |
| *Vwc2l* | 4.83E-01 | 7.21E-09 | | | |
| *Whrn* | -1.04E+00 | 3.21E-09 | | | |
| *Wnt4* | 5.71E-01 | 6.11E-05 | | | |
| *Wscd1* | 5.19E-01 | 3.29E-05 | | | |
| *Zfp385b* | -5.02E-01 | 4.02E-07 | | | |
| *Zic1* | 5.62E-01 | 5.59E-10 | | | |
| *Zmat4* | -4.62E-01 | 3.68E-04 | | | |

**Table 4.2. Relative regional brain volumes in P7 *Foxp1*$^{cKO}$ mice.**

| Brain region | Control | | *Foxp1*$^{cKO}$ | | Statistics | | |
|---|---|---|---|---|---|---|---|
| | Mean | SD | Mean | SD | %Diff | p-value | FDR |
| amygdala | 3.41 | 5.76E-02 | 3.49 | 6.02E-02 | 2.34 | 5.26E-04 | 2.10E-03 |
| arbor vita of cerebellum | 0.01 | 2.92E-04 | 0.01 | 3.53E-04 | 3.78 | 1.58E-02 | 3.05E-02 |
| basal forebrain | 1.44 | 3.80E-02 | 1.50 | 3.15E-02 | 4.43 | 9.91E-06 | 9.25E-05 |
| cerebellar cortex | 6.95 | 2.62E-01 | 7.35 | 2.83E-01 | 5.75 | 2.23E-04 | 1.39E-03 |
| cerebral aqueduct | 0.03 | 1.64E-03 | 0.04 | 1.78E-03 | 4.61 | 1.24E-02 | 2.57E-02 |
| cerebral cortex frontal lobe | 8.80 | 1.37E-01 | 8.58 | 1.92E-01 | -2.55 | 6.56E-04 | 2.45E-03 |
| cerebral cortex occipital lobe | 1.63 | 7.59E-02 | 1.70 | 5.65E-02 | 3.86 | 1.03E-02 | 2.22E-02 |
| cerebral cortex parieto temporal lobe | 20.52 | 3.25E-01 | 19.86 | 3.48E-01 | -3.17 | 4.92E-06 | 6.15E-05 |
| cerebral peduncle | 0.14 | 3.54E-03 | 0.14 | 3.19E-03 | -2.74 | 2.70E-03 | 6.86E-03 |
| colliculus inferior | 1.35 | 5.23E-02 | 1.41 | 5.86E-02 | 4.08 | 8.11E-03 | 1.82E-02 |
| colliculus superior | 2.67 | 7.75E-02 | 2.83 | 1.07E-01 | 6.16 | 2.41E-05 | 1.93E-04 |
| corpus callosum | 3.16 | 7.12E-02 | 3.01 | 5.18E-02 | -4.66 | 1.06E-07 | 1.98E-06 |
| dentate gyrus of hippocampus | 0.67 | 1.79E-02 | 0.62 | 1.70E-02 | -7.58 | 2.02E-09 | 5.66E-08 |
| fasciculus retroflexus | 0.04 | 1.31E-03 | 0.04 | 9.97E-04 | 3.47 | 2.59E-03 | 6.86E-03 |
| fornix | 0.19 | 5.30E-03 | 0.20 | 6.57E-03 | 4.52 | 3.43E-04 | 1.71E-03 |
| fourth ventricle | 0.14 | 7.19E-03 | 0.14 | 6.45E-03 | 3.71 | 3.79E-02 | 6.64E-02 |
| fundus of striatum | 0.08 | 3.02E-03 | 0.09 | 3.13E-03 | 3.61 | 8.01E-03 | 1.82E-02 |
| hippocampus | 4.64 | 1.24E-01 | 4.16 | 9.55E-02 | -10.43 | 8.83E-14 | 4.94E-12 |
| hypothalamus | 3.75 | 7.69E-02 | 3.86 | 8.02E-02 | 2.91 | 3.96E-04 | 1.71E-03 |
| lateral olfactory tract | 0.09 | 2.95E-03 | 0.10 | 3.63E-03 | 4.25 | 1.61E-03 | 4.74E-03 |
| lateral septum | 1.06 | 2.78E-02 | 1.11 | 3.13E-02 | 5.40 | 5.49E-06 | 6.15E-05 |
| medial septum | 0.17 | 6.85E-03 | 0.18 | 5.84E-03 | 5.88 | 6.44E-05 | 4.51E-04 |
| midbrain | 4.65 | 8.87E-02 | 4.82 | 1.46E-01 | 3.73 | 3.37E-04 | 1.71E-03 |
| nucleus accumbens | 0.83 | 2.18E-02 | 0.85 | 2.19E-02 | 3.04 | 2.39E-03 | 6.69E-03 |
| olfactory tubercle | 0.82 | 2.63E-02 | 0.85 | 2.49E-02 | 4.11 | 7.02E-04 | 2.46E-03 |
| periaqueductal grey | 1.03 | 2.83E-02 | 1.07 | 3.90E-02 | 3.61 | 4.30E-03 | 1.05E-02 |
| pons | 4.01 | 9.28E-02 | 4.10 | 1.14E-01 | 2.33 | 1.58E-02 | 3.05E-02 |
| posterior commissure | 0.00 | 1.26E-04 | 0.01 | 2.16E-04 | 5.21 | 3.80E-04 | 1.71E-03 |
| stria medullaris | 0.09 | 2.32E-03 | 0.10 | 3.05E-03 | 3.67 | 1.18E-03 | 3.67E-03 |
| superior olivary complex | 0.18 | 6.27E-03 | 0.19 | 6.24E-03 | 2.51 | 4.28E-02 | 7.27E-02 |
| third ventricle | 0.39 | 1.40E-02 | 0.40 | 9.65E-03 | 2.49 | 2.54E-02 | 4.58E-02 |
| medial preoptic area | 0.08 | 4.01E-03 | 0.09 | 3.10E-03 | 5.44 | 1.04E-03 | 3.41E-03 |
| paraventricular hypothalamic nucleus | 0.03 | 1.02E-03 | 0.03 | 8.40E-04 | 3.09 | 1.65E-02 | 3.09E-02 |

## REFERENCES FOR CHAPTER FOUR


Arriaga G, Jarvis ED (2013) Mouse vocal communication system: are ultrasounds learned or innate? Brain and language 124:96-116.

Arriaga G, Zhou EP, Jarvis ED (2012) Of mice, birds, and men: the mouse ultrasonic song system has some features similar to humans and song-learning birds. PloS one 7:e46610.

Bacon C, Schneider M, Le Magueresse C, Froehlich H, Sticht C, Gluch C, Monyer H, Rappold GA (2014) Brain-specific Foxp1 deletion impairs neuronal development and causes autistic-like behaviour. Molecular psychiatry.

Berges BK, Wolfe JH, Fraser NW (2007) Transduction of brain by herpes simplex virus vectors. Mol Ther 15:20-29.

Caubit X et al. (2016) TSHZ3 deletion causes an autism syndrome and defects in cortical projection neurons. Nature genetics 48:1359-1369.

Chen JA, Penagarikano O, Belgard TG, Swarup V, Geschwind DH (2015) The emerging picture of autism spectrum disorder: genetics and pathology. Annu Rev Pathol 10:111-144.

Chien WH, Gau SS, Chen CH, Tsai WC, Wu YY, Chen PH, Shang CY, Chen CH (2013) Increased gene expression of FOXP1 in patients with autism spectrum disorders. Molecular autism 4:23.

Davidson S, Truong H, Nakagawa Y, Giesler GJ, Jr. (2010) A microinjection technique for targeting regions of embryonic and neonatal mouse brain in vivo. Brain research 1307:43-52.

Fakhoury M (2015) Autistic spectrum disorders: A review of clinical features, theories and diagnosis. Int J Dev Neurosci 43:70-77.

Fang WQ, Chen WW, Jiang L, Liu K, Yung WH, Fu AK, Ip NY (2014) Overproduction of upper-layer neurons in the neocortex leads to autism-like features in mice. Cell Rep 9:1635-1643.

Feil S, Valtcheva N, Feil R (2009) Inducible Cre mice. Methods Mol Biol 530:343-363.

Feng X, Ippolito GC, Tian L, Wiehagen K, Oh S, Sambandam A, Willen J, Bunte RM, Maika SD, Harriss JV, Caton AJ, Bhandoola A, Tucker PW, Hu H (2010) Foxp1 is an essential transcriptional regulator for the generation of quiescent naive T cells during thymocyte development. Blood 115:510-518.

Ferland RJ, Cherry TJ, Preware PO, Morrisey EE, Walsh CA (2003) Characterization of Foxp2 and Foxp1 mRNA and protein in the developing and mature brain. The Journal of comparative neurology 460:266-279.

Fisher SE, Scharff C (2009) FOXP2 as a molecular window into speech and language. Trends in genetics : TIG 25:166-177.

Frohlich H, Rafiullah R, Schmitt N, Abele S, Rappold GA (2017) Foxp1 expression is essential for sex-specific murine neonatal ultrasonic vocalization. Human molecular genetics 26:1511-1521.

Gholizadeh S, Arsenault J, Xuan IC, Pacey LK, Hampson DR (2014) Reduced phenotypic severity following adeno-associated virus-mediated Fmr1 gene delivery in fragile X mice. Neuropsychopharmacology : official publication of the American College of Neuropsychopharmacology 39:3100-3111.

Gombash SE, Manfredsson FP, Kemp CJ, Kuhn NC, Fleming SM, Egan AE, Grant LM, Ciucci MR, MacKeigan JP, Sortwell CE (2013) Morphological and behavioral impact of AAV2/5-mediated overexpression of human wildtype alpha-synuclein in the rat nigrostriatal system. PloS one 8:e81426.

Hammerschmidt K, Whelan G, Eichele G, Fischer J (2015) Mice lacking the cerebral cortex develop normal song: insights into the foundations of vocal learning. Sci Rep 5:8808.
Lalmansingh AS, Karmakar S, Jin Y, Nagaich AK (2012) Multiple modes of chromatin remodeling by Forkhead box proteins. Biochim Biophys Acta 1819:707-715.
Li S, Weidenfeld J, Morrisey EE (2004) Transcriptional and DNA binding activity of the Foxp1/2/4 family is modulated by heterotypic and homotypic protein interactions. Molecular and cellular biology 24:809-822.
Li X, Xiao J, Frohlich H, Tu X, Li L, Xu Y, Cao H, Qu J, Rappold GA, Chen JG (2015) Foxp1 regulates cortical radial migration and neuronal morphogenesis in developing cerebral cortex. PloS one 10:e0127671.
McGrother CW, Bhaumik S, Thorp CF, Hauck A, Branford D, Watson JM (2006) Epilepsy in adults with intellectual disabilities: prevalence, associations and service implications. Seizure 15:376-386.
Mendoza E, Scharff C (2017) Protein-Protein Interaction Among the FoxP Family Members and their Regulation of Two Target Genes, VLDLR and CNTNAP2 in the Zebra Finch Song System. Front Mol Neurosci 10:112.
Osten P, Dittgen T, Licznerski P (2006) Lentivirus-Based Genetic Manipulations in Neurons In Vivo. In: The Dynamic Synapse: Molecular Methods in Ionotropic Receptor Biology (Kittler JT, Moss SJ, eds). Boca Raton (FL).
Portfors CV, Perkel DJ (2014) The role of ultrasonic vocalizations in mouse communication. Current opinion in neurobiology 28:115-120.
Scattoni ML, Crawley J, Ricceri L (2009) Ultrasonic vocalizations: a tool for behavioural phenotyping of mouse models of neurodevelopmental disorders. Neuroscience and biobehavioral reviews 33:508-515.
Sin C, Li H, Crawford DA (2015) Transcriptional regulation by FOXP1, FOXP2, and FOXP4 dimerization. J Mol Neurosci 55:437-448.
Tang B, Becanovic K, Desplats PA, Spencer B, Hill AM, Connolly C, Masliah E, Leavitt BR, Thomas EA (2012) Forkhead box protein p1 is a transcriptional repressor of immune signaling in the CNS; implications for transcriptional dysregulation in Huntington disease. Human molecular genetics.
Wang XD, Su YA, Wagner KV, Avrabos C, Scharf SH, Hartmann J, Wolf M, Liebl C, Kuhne C, Wurst W, Holsboer F, Eder M, Deussing JM, Muller MB, Schmidt MV (2013) Nectin-3 links CRHR1 signaling to stress-induced memory deficits and spine loss. Nature neuroscience 16:706-713.

## VITAE

Daniel John Araujo ("D.J.") matriculated into St. Mary's University (StMU) of San Antonio, TX, in 2007. However, it wasn't until Daniel met his college mentor Dr. Timothy Raabe that he considered pursuing a career in scientific research. With Dr. Raabe's encouragement, Daniel participated in the Summer Undergraduate Research Fellowship (SURF) Program at UT Southwestern Medical Center (UTSW) in Dallas, TX, in the summer of 2009. In the SURF Program, Daniel worked in the laboratory of Dr. Adrian Rothenfluh and subsequently became hooked on research. Daniel graduated from StMU in the spring of 2011 and entered the Graduate School of Biomedical Sciences at UTSW that fall. Since then, Daniel has focused on studying the genetic underpinnings of autism in the laboratory of Dr. Genevieve Konopka. Upon graduation from UTSW, Daniel will join the laboratory of Dr. Kairo Saijo at UC Berkeley as a postdoctoral investigator. In Dr. Saijo's laboratory, Daniel will examine the role of endocannabinoid signaling in neuroinflammatory disorders.